

Institut für Organische Chemie und Biochemie
der Technischen Universität München

**Design and Synthesis of Selective Ligands for the $\alpha 5\beta 1$ Integrin Receptor
and
Cyclic Peptides as Affinity Ligands for Factor VIII Purification**

Dominik Heckmann

Vollständiger Abdruck der von der Fakultät für Chemie der Technischen Universität
München zur Erlangung des akademischen Grades eines

Doktors der Naturwissenschaften

genehmigten Dissertation.

Vorsitzender: Univ.-Prof. Dr. Steffen J. Glaser

Prüfer der Dissertation:

1. Univ.-Prof. Dr. Dr. Horst Kessler
2. Hon.-Prof. Dr. Reinhard Fässler
Ludwig-Maximilians-Universität München
3. Univ.-Prof. Dr. Johannes Buchner

Die Dissertation wurde am 17.04.2007 bei der Technischen Universität München eingereicht
und durch die Fakultät für Organische Chemie und Biochemie am 09.07.2007 angenommen.

SCIENCE: A way of finding things out and then making them work. Science explains what is happening around us the whole time. So does RELIGION, but science is better because it comes up with more understandable excuses when it is wrong. There is a lot more Science than you think.

-- From A Scientific Encyclopedia for the Enquiring Young Nome by Angalo de Haberdasheri (Terry Pratchett, Wings)

Die vorliegende Arbeit wurde in der Zeit von Juli 2003 bis März 2007 am Institut für Organische Chemie und Biochemie der Technischen Universität München unter Anleitung von Herrn Prof. Dr. Horst Kessler angefertigt.

Meinem Lehrer, Herrn Prof. Dr. Horst Kessler, danke ich für die interessanten Themenstellungen, die einzigartig guten Arbeitsbedingungen und die weitreichenden Freiheiten bei der Ausgestaltung der Themen.

Mein weiterer Dank gilt:

- Meinem Laborkollegen Lucas Doedens und Janine Eckardt für das prima Arbeitsklima. Timo Weide, Eric Biron, Jörg Auernheimer, Armin Modlinger, Axel Meyer, Timo Huber, Florian Manzenrieder, Florian Opperer und Monika Lopez-Garcia für alles zwischen fachliche Diskussionen und Freizeitgestaltung.
- Der ganzen NMR-Gruppe und besonders Dr. Rainer Hässner für das Beantworten einer Menge Fragen und der Hilfe bei großen und kleinen Spektrometer- und Computerproblemen.
- Georg Voll und Martin Sukopp für die Hilfe bei der Strukturaufklärung des Peptides und Luciana Marinelli für ihre Unterstützung und konstante Begeisterung.
- Mona Wolff, Maria Kranawetter und Burkhard Cordes für die Unterstützung der praktischen Arbeit – ob Synthese, HPLC oder MS.
- Dr. Grit Zahn und Dr. Roland Stragies von der Jerini AG, Berlin für zuverlässige biologische Testungen und wertvolle Anregungen zum Thema Integrinliganden.
- Michael Leiss und Prof. Reinhard Fässler für die fruchtbare Kooperation und wertvolle Diskussionen über die Welt der Biochemie und der knock-out Mäuse.
- Prof. Evgueni Saenko und Dr. Alexsey Khrenov für die Testungen und die gute Kooperation auf dem Gebiet der Faktor VIII bindenden Peptide.

- Allen ungezählten Praktikanten / Hiwis, besonders Jessie Zheng Zhang, Julia Braunagel, Christiane Müller, Timo Korfmann, Pierre Göppert, Christian Kutruff, Markus Bollinger als Bachelor und Praktikant, Bele Boeddinghaus und Elke Steinhardt, die mich bei der Arbeit unterstützt und Farbe ins Labor gebracht haben.
- Ilka Varnay für engagiertes Schlagzeugspielen und die Möglichkeit, den Laborfrust in Musik umzusetzen (gleiches gilt für Andreas Zander und Wilbert Snijders). Außerdem dem AK-Kessler Karting Team.
- Meinem Freund Guido Clever für gute Nachbarschaft, Clubbesuche, Bier und Gespräche; außerdem allen Heidelbergern, deren Türen immer offenstehen.
- Julia Braunagel und Timo Huber für's Korrekturlesen der Arbeit.
- Julia, meiner wichtigsten Entdeckung an der TU - auch wenn sie nicht im Experimentalteil vorkommt... für alles.
- Meiner ganzen Familie, besonders meinen Eltern, Tobias und Sabine für die unablässige Unterstützung.

Index

I. Introduction.....	1
II. General Section	3
II.1 Basics of Medicinal Chemistry	3
II.1.1 Pharmacological relevance of peptides and peptidomimetics.....	3
II.1.2 Optimization of lead structures.....	4
II.2 Integrins as Targets in Medicinal Chemistry	6
II.2.1 Integrin structure	7
II.2.2 Mechanisms of integrin activation	10
II.2.3 Ligand binding to integrins	13
II.2.4 Integrin ligands.....	14
II.2.5 The $\alpha 5\beta 1$ homology model	18
II.2.6 Integrin-mediated signal transduction	21
II.2.7 Antiangiogenic cancer therapy.....	24
II.2.8 Role of integrins $\alpha v\beta 3$ and $\alpha 5\beta 1$	27
II.3 Biological Relevance of Blood Coagulation Factor VIII.....	28
II.3.1 The blood coagulation cascade	29
II.3.2 Structure of Factor VIII	31
II.3.3 Purification of Factor VIII.....	32
II.3.4 Optimization of the lead sequence.....	33
III Results and Discussion	35
III.1 Rational Design of Selective Integrin Ligands	35
III.1.1 Synthesis of integrin ligands based on the tyrosine scaffold.....	35
III.1.2 Design of $\alpha 5\beta 1$ selective ligands	43
III.1.3 Design of $\alpha v\beta 3$ selective ligands.....	56
III.1.4 Impact of different basic moieties on $\alpha 5\beta 1$ / $\alpha v\beta 3$ affinity	59
III.1.5 Introduction of constraints into tyrosine-based ligands	63
III.1.6 Introduction of linker-spacer systems to tyrosine based $\alpha 5\beta 1$ ligands	68
III.1.7 Synthesis of $\alpha 5\beta 1$ -ligands based on the <i>aza</i> -glycine scaffold.....	72
III.1.8 Hydroxamic acids as aspartic acid substitutes.....	78
III.1.9 Biological studies with $\alpha 5\beta 1$ / $\alpha v\beta 3$ selective ligands.....	81

III.2	Cyclic Peptides as Affinity Ligands for FVIII purification	90
III.2.1	Alanine scan of the most active cyclic hexapeptide sequences	90
III.2.2	Mutational analysis of P2	91
III.2.3	<i>N</i> -Methyl scan of peptide P2	93
III.2.4	Structure determination and binding analysis of P2	95
III.2.5	Outlook	99
IV	Experimental Section	101
IV.1	Materials and Methods	101
IV.2	General Procedures	102
IV.3	Compound Preparation and Analytical data	110
IV.4	Preparation of Cyclic Peptides	209
IV.4.1	NMR-structure of P2	213
V.	Summary	216
VI.	References	220
VII.	Appendix (Curriculum Vitae)	232

– Abbreviations

Å	Ångstrom, 10^{-10} m
Ac	Acetyl-
CAN	Acetonitrile
ADDP	Azodicarboxylic dipiperidide
ADME	Absorption, distribution, metabolism, excretion
ADMIDAS	Adjacent metal induced adhesion site
Bn	Benzyl-
Boc	<i>tert</i> -Butyloxycarbonyl-
br.	Broad
Bu	Butyl
^t Bu	<i>tert</i> -Butyl
CAM	cell adhesion molecule
Cbz	Benzyloxycarbonyl-
Conc.	Concentrated
COSY	correlated spectroscopy
d	Doublet or days
δ	Chemical shift
1D, 2D, 3D	One / two / three- dimensional
DCM	Dichloromethane
dd	Dublett of dubletts
dest.	Distilled
DIAD	Diisopropylazodicarboxylate
DIEA	Diisopropylethylamine
DMA	<i>N,N</i> -Dimethylacetamide
DMAP	4-Dimethylaminopyridine
DMF	<i>N,N</i> -Dimethylformamide
DMSO	Dimethylsulfoxide
DPPA	Diphenylphosphoric acid azide
ECM	Extracellular matix
ESI-MS	electrospray ionization mass spectrometry
Et	Ethyl-
FAK	Focal adhesion kinase
FV-XIII	Blood coagulation factors V-XIII
Fmoc	9-Fluorenylmethoxycarbonyl
Fn	Fibronectin
GC-MS	gas chromatography mass spectroscopy
h	Hour
HATU	<i>O</i> -(7-Azabenzotriazol-1-yl)- <i>N,N,N',N'</i> -tetramethyluronium-hexafluorophosphat

HMBC	heteronuclear multiple bond correlation
HMQC	heteronuclear multiple quantum coherence
HMQC-COSY	heteronuclear multiple quantum coherence with COSY-pulse sequence
HOAc	Acetic acid
HOAt	1-Hydroxy-7-azabenzotriazol
HOBt	1-Hydroxybenzotriazol
HPLC	high performance liquid chromatography
HSQC	heteronuclear single quantum coherence
Hz	Hertz
H-Tic-OH	Tetrahydroisoquinolin-3-carboxylic acid
IC	inhibitory capacity
<i>J</i>	Scalar coupling constants
kDa	Kilodalton
KHMDS	Potassium hexamethyldisilazid
LC-MS	liquid chromatography mass spectrometry
LIMBS	Ligand-induced metal ion dependent binding site
Ln	Laminin
m	Multiplett
M	Molar
Me	Methyl-
MeOH	Methanol
MHz	Megahertz
MIDAS	Metal ion dependent site
min.	Minutes
mL	Milliliter
mmol	Millimol
MS	Mass spectroscopy
MW	Molecular weight
ⁿ <i>J</i>	Scalar coupling over n-bonds
N	Normal
NMM	<i>N</i> -Methylmorpholine
NMP	<i>N</i> -Methylpyrrolidone
NMR	nuclear magnetic resonance
NOESY	nuclear Overhauser enhancement spectroscopy
PBS	phosphate buffered saline
Ph	Phenyl
ppm	parts per million
q	Quartett
R _f	Retention faktor
ROESY	rotating frame nuclear Overhauser and exchange spectroscopy

R _t	Retention time
RT	Room temperatur
s	Singulett
sat.	Saturated
SPPS	<i>solid phase peptide synthesis</i>
t	Triplet
TBAF	Tributylammoniumfluorid
TBDPS	<i>Tert.</i> butyldiphenylsilyl
TBTU	O-(1H-Benzotriazol-1-yl)- <i>N,N,N',N'</i> -tetramethyluronium-tetrafluoroborat
TCP	Tritylchlorid-Polystyrene-resin
TEA	Triethylamine
TFA	Trifluoroacetetic acid
TFE	Trifluoroethanol
THF	Tetrahydrofurane
TIPS	Triisopropylsilane
TMS	Trimethylsilyl-
TOCSY	total correlation spectroscopy
UV	Ultraviolett
Vn	Vitronectin
vWF	<i>von Willebrand</i> Factor

I. Introduction

The directed design of an appropriate drug to fight disease has always been a dream of mankind. In the rise of the first cultures, curative agents were mostly provided by plants and were strongly connected to spirituality. With the rise of modern science and especially organic chemistry, it was possible for the first time to identify and synthesize natural and artificial compounds and to use those compounds as drugs. The development of constitutional formulas in chemistry allowed the directed synthesis of new compounds and led to a rapid expansion of modern organic chemistry. It was now possible for the first time to conclude chemical properties from the molecular structure, which later allowed the establishment of *structure-activity-relationships* (SAR) in medicinal chemistry.^[1] In the last century, the rapidly expanding knowledge about biochemical pathways from enzymes to the sequencing of the genome provided insights to the mechanisms of drug activity as well as the prospect to design new bioactive compounds on a molecular level. The *key-lock-principle* stated by Emil Fischer and Paul Ehrlich is commonly regarded as a milestone in chemical biology.^[2, 3] Based on the principles of molecular recognition, medicinal chemistry tries to design molecules which interfere with pathologic pathways in order to cure diseases. But how to find the right “key” molecule considering the fact, that the so-called “chemical space” for molecules with a weight of less than 500 exceeds the staggering number of 10^{60} ?^[4] Since the early 20th century, many approaches have been established to tackle this challenge. Such approaches are for example *combinatorial chemistry*^[5], which allows the synthesis of highly diverse libraries of compounds, *high-throughput-screenings* (HTS)^[6] for the rapid identification of new lead structures, the use of biotechnology compounds (such as *antibodies* or *antisense molecules*)^[7] and the so-called *rational design* of bioactive molecules. The rapid increase in computational power and the development of automated processes such as HTS and the solid phase synthesis of peptides^[8, 9], nucleic acids^[10, 11] and sugars^[12] allow an exponential increase in compounds, which can be biologically evaluated with minimal time effort. On the other hand, the progress in molecular biology, *genomics*^[13] and *proteomics*^[14] yields an abundance of proteins as new potential drug targets. Parallel, the knowledge about the structure of the targets, e.g. proteins increases and deepens by means of more sophisticated

methods such as X-ray structures and structure determination by *nuclear magnetic resonance* (NMR). With a detailed image of the target's structure, the rational approach gets more and more important for pharmaceutical research. Computational methods include the *de-novo-design* ^[15] as well as *virtual screenings* and *docking* experiments. ^[16, 17] Computational methods are also useful for the prediction of protein structure. In case of receptor families with a high degree of homology and one structurally determined member, the so-called *homology modeling* ^[18] is used to gather structural information, which can be used in the optimization of lead structures.

The work published in this thesis concentrates on two topics:

- The design of selective ligands for integrins $\alpha 5\beta 1$ and $\alpha v\beta 3$ for the use in antiangiogenic cancer therapy using rational and combinatorial methods.
- Synthesis and structural properties of cyclic peptides as affinity ligands for the purification of blood coagulation Factor VIII.

II. General Section

II.1 Basics of Medicinal Chemistry

II.1.1 Pharmacological relevance of peptides and peptidomimetics

Biologically active peptides are the product of gene transcription and interact – after synthesis *in vivo* – with proteins or protein conjugates. The ubiquitous control and modulation of cellular functions, the cellular signaling pathways and the immune response are mostly the result of *non-covalent* protein-protein or peptide-protein interactions.^[19-21] In the last 30 years, many biologically active peptides such as *somatostatin*, *substance P*, *cholecystokinin*, *endorphin*, *enkephalin*, *angiotensin II* or *endothelin* have been discovered and characterized.^[22-24] As neurotransmitters, neuronal modulators or hormones, they bind to membrane-bound receptors to facilitate cell-cell communication, control metabolism, respiration and immune response. This large variety of vitally important functions makes peptides important targets for drug discovery.^[25] For that reason, the number of native or modified peptides used in the treatment of disease is continuously increasing. However, the use of peptides as drugs is strictly limited by following factors:

- 1) The poor metabolic stability of peptides as they are subjected to proteolytic degradation in the gut and the serum.
- 2) A poor bioavailability due to the high molecular mass and a lack of active transporters.
- 3) A moderate or extensive clearance by liver and kidneys.
- 4) Adverse effects based on interactions with multiple receptors.

To overcome these disadvantages, great effort has been made to turn native peptides into more drug-like molecules. The integration of a recognition motif into a cyclic peptide is a feasible way to restrict the conformational space of the amino acid sequence and was demonstrated to show an impact on binding affinity and receptor specificity.^[26] Restriction in conformational freedom may increase binding affinity to a receptor, but only if the biologically active conformation is included in the allowed conformational space (*matched case*). The resulting activity gain is owed to the decrease in conformational entropy which is lost upon binding and a pre-induced

strain towards adoption of the binding conformation. In the *mismatched case*, where the peptide is not able to adopt a biologically active conformation, the affinity towards the target receptor is lost. Especially backbone-cyclized penta- and hexapeptides are known to stabilize distinct conformations by adaptation of turn-like structures.^[26-28] A “spatial screening”^[29a-e, 30] of different conformations (keeping the chemical nature of the side chains unchanged) of a cyclized peptide sequence can be achieved either by variation of the chirality of selected amino acids, alterations of ring size sequence reversion (*retro-inverso* peptides)^[31,32] or incorporation of structural templates^[33]. A library of both, active and inactive peptides with assigned conformation allows detailed structure-activity relationships. An important structural modification of peptides turned out to be the incorporation of *N*-methylated amino acids into the sequence, which has already proved to be a valuable tool in structure-activity-relationship studies.^[34] This modification often induces a *cis* *N*-methylated peptide bond, a change in the lipophilicity profile and induces sterical hindrance. This also results in an increased proteolytic stability for *N*-methylated peptides.^[35] The concept of *N*-methylation has been applied successfully on the peptidic integrin ligands and led to the compound *cyclo(-RGDfN-MeVal-)*, now developed by MERCK KGaA, Darmstadt, under the name Cilengitide^[36], which is in phase III of clinical investigation.

A peptidomimetic is defined as a substance having a secondary structure as well as other structural features analogues to that of the original peptide which allows it to displace the original peptide from receptors or enzymes.^[25] They may offer advantages over physiologically active linear peptides by improving oral bioavailability and better stability against enzymatic degradation within the organism.

II.1.2 Optimization of lead structures

The process of simplification – from a complex protein to a small molecule – is not an achievement of modern chemical research. During evolution, nature has always sampled and modified small molecules to mimic protein - protein interactions. Many of them initially developed as toxins are widely used in medicine. A prominent example is morphine, which acts as a natural peptide mimetic for β -endorphin.^[37, 38] It shows all features of a peptidomimetic drug: The functionalities of the amino acid

side chains originally involved in the binding event are fixed on a rigid scaffold in the correct three-dimensional arrangement. The modern medicinal chemist uses a variety of strategies to imitate and speed up this process.^[25, 39, 40] As long as no structure of the target protein is available, the development of drug candidates concentrates on more or less biased screening methods and, if a hit could be identified, an optimization of the lead structure. This approach is called “ligand-oriented drug design”.^[41] The determination of the target’s 3D-structure by means of X-ray spectroscopy or NMR allows switching to “structure-based drug design”, a method that streamlines the process of drug development. It depends on an iterative procedure of design, chemical synthesis and subsequent biological evaluation of specific compounds. However, there is still a large gap between known protein sequences and 3D-structure. To date, the most successful theoretical approach to bridge this gap is homology modeling. It is possible to construct an approximate 3D-model of a structural unknown protein if the sequence homology to the known 3D-structure of the reference protein is higher than 40%. Such a homology modeled structure is suitable for rational drug design.^[18] Despite all benefits of structure-based design, an *ab initio* design of a bioactive molecule has not been achieved yet. Still, a highly diverse synthesis of compound libraries is needed to find a suitable lead structure, which then can be optimized using rational methods. It has to be highlighted here, that a high receptor affinity alone is not sufficient for the development of a drug. Considering the complexity of biological processes, the activity *in vivo* may differ a lot from the activity measured *in vitro*. In order to reach its destination, an active agent has to interact with both aqueous (cytoplasm) and lipophilic (membranes) environments. Only substances with medium lipophilicity are water soluble and able to cross membrane barriers. The lipophilicity is commonly expressed by the logP value, where P is the *partition coefficient* between octan-1-ol and water (Equation II-1).^[42]

$$P = \frac{[c]_{\text{octanol}}}{[c]_{\text{water}} * (1 - \alpha)}$$

Equation II-1. Calculation of the partition coefficient P. α is the degree of dissociation in water.

II. General Section

An analysis of ~2200 orally available drugs by *Lipinsky et al.* at *Pfizer Inc.* revealed a number of common properties. These features, known as “*Pfizer’s rule of five*” matched 90% of all examined drugs: ^[43, 44]

- 1) LogP < 5
- 2) Molecular weight < 500 g/mol
- 3) Number of hydrogen-bond donors < 5
- 4) Number of hydrogen-bond acceptors < 10
- 5) One rule may be violated

However, examples like the orally available immune suppressant *cyclosporine*, which violates each of the five rules indicate, that those points should be considered as guidelines rather than rules. Another approach represents the “*Veber rules*”: They postulate a favorable oral bioavailability for molecules with less than 10 rotatable bonds and a polar surface of less than 140 Å² (which corresponds to < 12 H-bond donors / acceptors). ^[45] Although the *rules of five* may provide information about “drug likeness” in terms of oral bioavailability, they are not able to predict the metabolic stability of the compounds. Most drugs which are too small to be recognized by the immune system are transformed into more polar metabolites by non-specific enzymes (e.g. cytochrome P460). The metabolites are cleared from the body via kidneys, bile or feces. The factors, which account for the pharmacological profile of a compound, are summarized as ADMET-parameters. They describe the absorption, distribution, metabolism, elimination and toxicity. ^[41] During the process of drug development, all those parameters have to be taken into account and be constantly optimized.

II.2 Integrins as Targets in Medicinal Chemistry

In order to fulfill their functions in tissues and organisms, cells must sense their surrounding environment and rapidly adapt to changes. ^[46] The *extracellular matrix* (ECM) provides a physical scaffold for cell positioning and an instructive interface, which allows cells to communicate in a very precise manner over short distances. Cell surface receptors of the integrin family are essential mediators and integrators of ECM-dependent communication. This function is highly conserved during evolution

from metazoas to mammals, thereby demonstrating their essential role in multicell organisms. ^[47] Adhesion receptors of this family were initially identified in the 1980s by scientists working in different fields of biomedical research. They were identified as being involved in cell adhesion to the ECM as well as platelet aggregation, homing of leucocytes and the immune response. The identification of fibronectin as an ECM protein which is strongly involved in cell adhesion led to identification of the arginine-glycine-aspartic acid (RGD) sequence as crucial recognition motif, ^[48] and facilitated the identification and purification of the fibronectin / vitronectin receptors by affinity chromatography. ^[49, 50] Due to its appearance in many ECM proteins such as Fibronectin, Vitronectin, Fibrinogen, Laminin, Osteopontin, etc., it was initially but prematurely named “universal recognition motif”. Up to now, many different recognition sequences from several natural integrin ligands have been discovered. ^[51, 52] Molecular cloning and sequencing joined these receptors together with other adhesion receptors such as the platelet fibrinogen receptor, the *very late antigens* (VLAs) and *leucocyte-function associated antigen* (LFA) to form one family of adhesion receptors. ^[53] The term “integrin” was introduced by *Tamkun* and *Hynes* to denote the role of these proteins as an integral membrane complex involved in the transmembrane association between the extracellular matrix and the cytoskeleton. ^[54] As far as integrins are important for a variety of biological processes, they are also involved in various pathological processes such as inflammation, vascular homeostasis, thrombosis, restenosis, bone resorption, cardiovascular disorders, cancer invasion, metastasis and tumor angiogenesis. ^[55-58] As the field of integrin structure, function and medicinal application is very broad, this introduction will concentrate on the integrins $\alpha\text{IIb}\beta\text{3}$, $\alpha\text{v}\beta\text{3}$, $\alpha\text{5}\beta\text{1}$ and $\alpha\text{v}\beta\text{5}$, which all recognize the common recognition motif RGD.

II.2.1 Integrin structure

Integrins are $\alpha\beta$ heterodimeric, type I transmembrane proteins with large extracellular and short cytoplasmic domains of 700-1100 and 30-50 residues respectively, which are linked by a short, transmembrane region. ^[59] In mammals, 18 different α and 8 β subunits are known, which can assemble non-covalently to form 24 dimers. An overview over the possible combinations of α and β subunits is given in (Figure II-1).

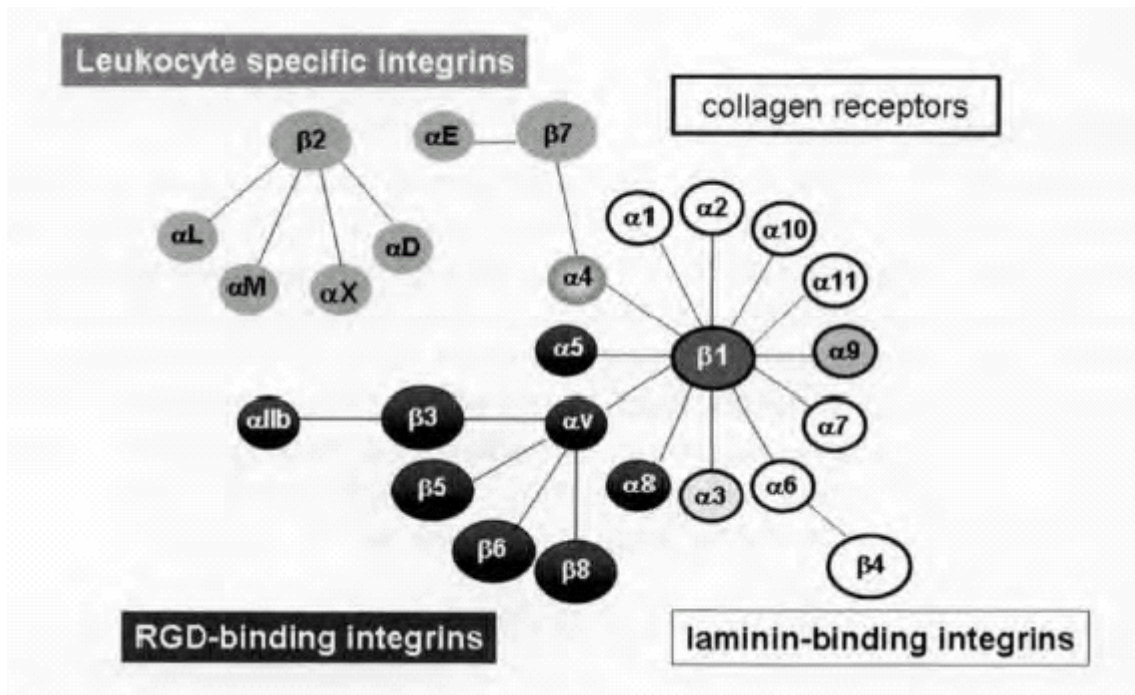


Figure II-1. *The integrin family:* Combinations of α and β subunits, which have been identified on cells up to now.

The structure of integrins was primarily investigated by electron microscopy, which revealed for $\alpha 5\beta 1$ a 28 nm long molecule consisting of a 8 x 12 nm globular head region and two 2 x 20 nm rod-like tails.^[60] Structure examinations were continued employing various methods such as mutagenesis or monoclonal antibody epitope mapping.^[59] A major breakthrough was the first crystal structure of the $\alpha v\beta 3$ headgroup^[61], shortly followed by the crystal structure of the headgroup in association with Cilengitide.^[62] As visible in the X-ray structure, both integrin subunits have a recognizable domain structure (Figure II-2). The two subunits assemble in an ovoid-like shape consisting of a 9 x 6 x 4.5 nm head and two almost parallel tails. In a subset of integrins – not in $\alpha v\beta 3$ or other RGD-dependent integrins – a ~200-residue module homologous with the cation-binding A-domain of *von Willebrand factor* is found (called αA -domain or αI -domain, for *inserted domain*), which is inserted into a seven-blade β -propeller (438 residues in αv). An A-domain-like polypeptide segment is also found in the β -subunit ($\beta 1$, 243 residues in $\beta 3$), which is looping out from a unique immunoglobulin (Ig)-like “hybrid” domain (133 residues in $\beta 3$). The tail of the αv -subunit is composed of three β -sandwich domains: one Ig-like “thigh” domain and two very similar domains that form the “calf” module. The $\beta 3$ -tail consists of a PSI module which is found in several protein families (plexins, semaphorins and

integrins)^[63], four cysteine-rich, epidermal-growth-factor (EGF)-like domains and a β -tail domain (β TD). The ribbon drawing of $\alpha v\beta 3$ in Figure II-2 is a straightened model of the originally obtained structure, where the tails of both subunits are folded back at a $\sim 135^\circ$ angle, resulting in a V-shape with a kink between the thigh-domain and the calf module of αv . In case of an integrin anchored inside the cell membrane, this would result in a head-group pointing back to the membrane. The resulting hypothesis of a *switchblade*-mechanism of integrin activation is still under investigation.^[64] As the binding site of the RGD ligand is located at the interface of the β -propeller domain of the αv subunit and the β I-domain of the $\beta 3$ -subunit, the two participating domains should be further outlined:

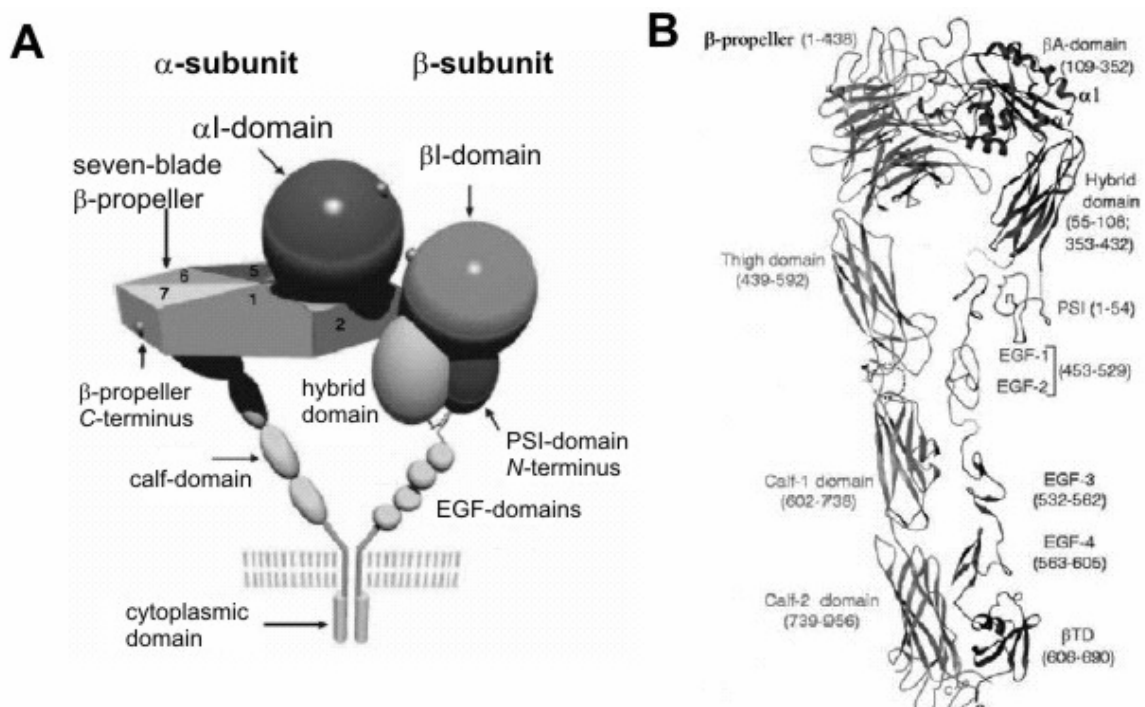


Figure II-2. *Integrin structure:* Comparison of the schematic domain structure **A** with the ribbon drawing of the X-ray structure of $\alpha v\beta 3$.^[61] **B** shows a straightened model. The α I-domain is not present in $\alpha v\beta 3$.

The β -propeller is formed from the amino terminal, seven fold ~ 60 residue sequence repeats of αv and consists of seven radially arranged “blades”, each formed from a four-stranded antiparallel sheet. Each of the seven blades reveals a unique consensus sequence with three aromatic residues per blade, all pointing towards the center of the propeller, thus forming a “cage”-like, hydrophobic cavity. The space is

occupied by the Arg²⁶¹ of the β -subunit, stabilizing the $\alpha\beta$ -heterodimer by cation- π -interaction.

The β I-domain is inserted into the B-C-loop of the β 3-hybrid domain and adapts a so-called *Rossmann fold* structure, which is also found in G-proteins (G β) as nucleotide binding motif.^[65] It consists of a central six-stranded β -sheet surrounded by eight helices. Furthermore, it contains three binding sites for divalent cations (Ca²⁺, Mg²⁺, Mn²⁺, etc.), dependent on the used buffer. A *metal ion dependent adhesion site* (MIDAS) motif is set in a cleft at the top of the central β -strand. In contrast to the unbound, inactive $\alpha\nu\beta$ 3, it is only occupied by a metal ion in the protein-ligand complex. In the corresponding X-ray structure, it is occupied by a Mn²⁺ ion, which essentially contributes to ligand binding by coordination of Mn²⁺ with the aspartic acid carboxyl function. The MIDAS is flanked by the ADMIDAS (*adjacent MIDAS*), which is occupied by a metal ion in both bound and unbound state. In addition, the conformational change induced by the binding event unfolds another metal ion binding site, the LIMBS (*ligand induced metal binding site*). Binding of a metal ion to the LIMBS may stabilize the ligand-bound conformation of the integrin.^[62] In the published structures of the α IIb β 3 integrin, however, all three binding sites are occupied by Ca²⁺ ions.^[66] There is still much discussion about the effect of the nature of the divalent ions and their effects. It seems that Mg²⁺ and particularly Mn²⁺ have a strong agonistic effect on the activity of integrin α 5 β 1 and $\alpha\nu\beta$ 3, while Ca²⁺ reveals antagonistic effects.^[67] However, Ca²⁺ was not found to be inhibitory in α IIb β 3.

II.2.2 Mechanisms of integrin activation

The recent results gave rise to several theories concerning the mode of activation and the conformational changes of the heterodimer on the way of ligand-binding. *Springer et al.* describe the different states of the integrin α IIb β 3 on the basis of X-ray structures as shown in Figure II-3:^[66, 68] The integrin is found in a resting state, which adapts the bent conformation **A**. The head region is pointing back towards the cell membrane and the affinity for ligands is low. The equilibrium with the extended, high-affinity state **B** is controlled by proteins binding to the intracellular domains of

the integrin and is crucial for the *inside-out* signaling. On binding of an extracellular ligand, the heterodimer undergoes a second conformational change. It results in an outward swing of the β -hybrid domain of $\sim 60^\circ$ relative to the ligand-binding β I-domain.

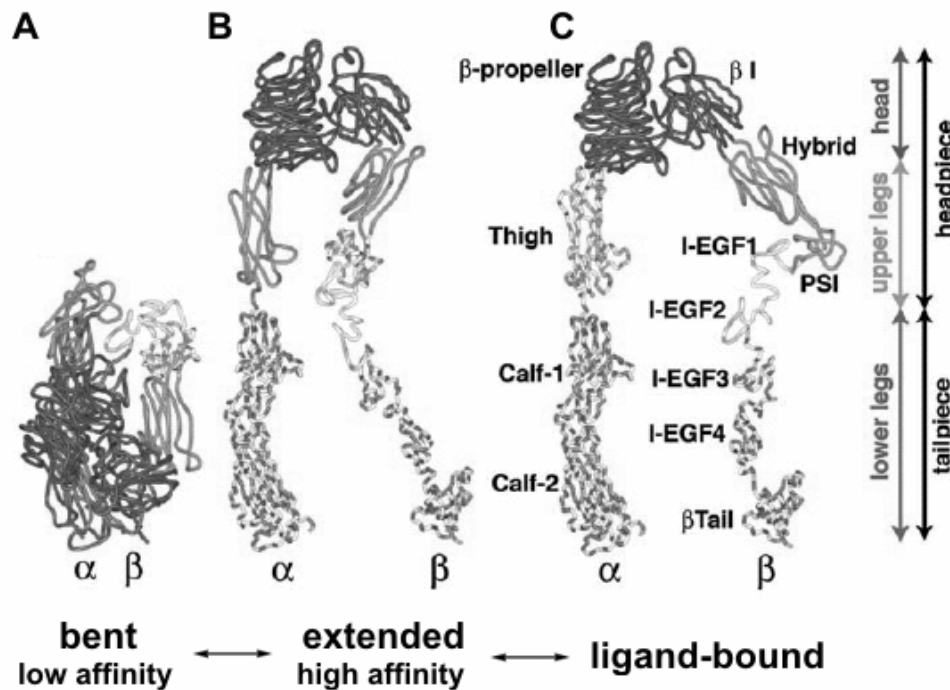


Figure II-3. Mechanism of integrin activation according to Springer et al. (so-called “switch-blade mechanism”):^[66] The ribbon drawings of the extracellular region of α IIb β 3 are based on crystallographic data and are in accordance with electron microscopy.

The PSI-domain, positioned below the hybrid domain, acts as a rigid connecting rod that translates the swing of the hybrid-domain into a separation of the leg regions **C**. This change may act as induction of the *outside-in* signaling as a result of ligand-binding. The postulated separation of the leg regions is in contradiction to the observations of Adair and Yeager made by means of electron cryoscopy.^[69] The electron density map indicated an association of the transmembrane helices of both α - and β - subunit. This interaction may be stabilized by a salt-bridge ((α IIb)Arg⁹⁹⁵ and (β 3)Asp⁷²³), as indicated by mutagenesis studies.^[70] With the observation, that isolated α IIb- and β 3- subunits tend to form dimers and trimers respectively, it was suggested that these mechanisms of integrin subunit assembly and clustering also play a role in integrin activation and signal transduction.^[71, 72] It could be shown that cells show extensive activation of FAK on integrin clustering, which indicates active

outside-in signaling. As the spatial segregation of both subunits is unlikely in the ligand bound state – the ligand binds to the interface between α and β subunit – the assembly of integrins has been reproduced using computational methods. ^[73]

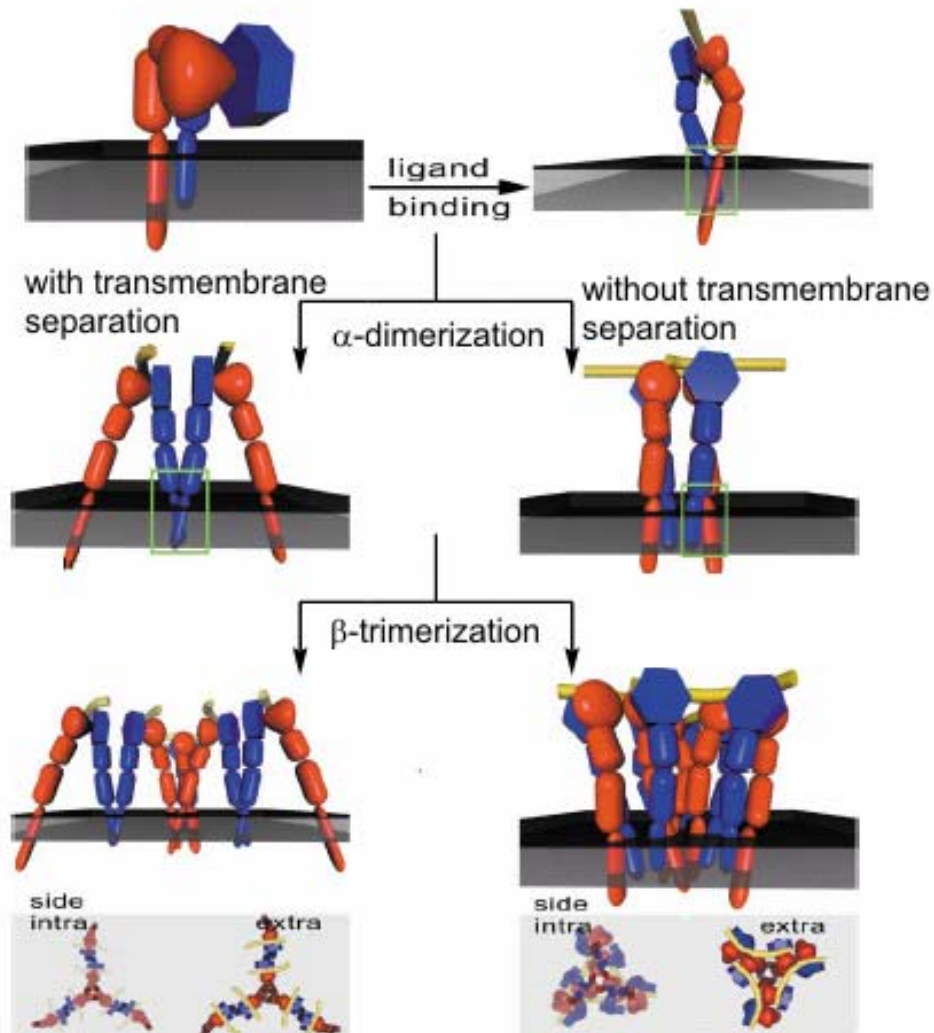


Figure II-4. Model of integrin clustering according to Gottschalk and Kessler:^[73] On integrin activation and ligand binding, α subunits (blue) and β subunits (red) cluster by dimerization and trimerization, respectively. Both transmembrane separation and association are possible in this model.

The highly homologue transmembrane regions of different integrins all contain a GpA-like structure, which is known to associate. ^[74] In the model shown in Figure II-4, it is ambiguous, whether the integrin clusters form hetero- or homo- transmembrane complexes. The total size of an integrin cluster is not fixed, but very likely to form larger complexes as found in *focal adhesion points*.

II.2.3 Ligand binding to integrins

In integrins without I-domain, such as $\alpha 5\beta 1$, $\alpha v\beta 3$, $\alpha v\beta 5$ and $\alpha IIb\beta 3$, the ligand binding site is located between the β -propeller of the α -subunit and the βI -domain of the β -subunit. Figure II-5 shows the binding modes of the RGD-peptide Cilengitide in integrin $\alpha v\beta 3$ and the binding mode of Tirofiban in $\alpha IIb\beta 3$ based on crystallographic data. [62, 66]

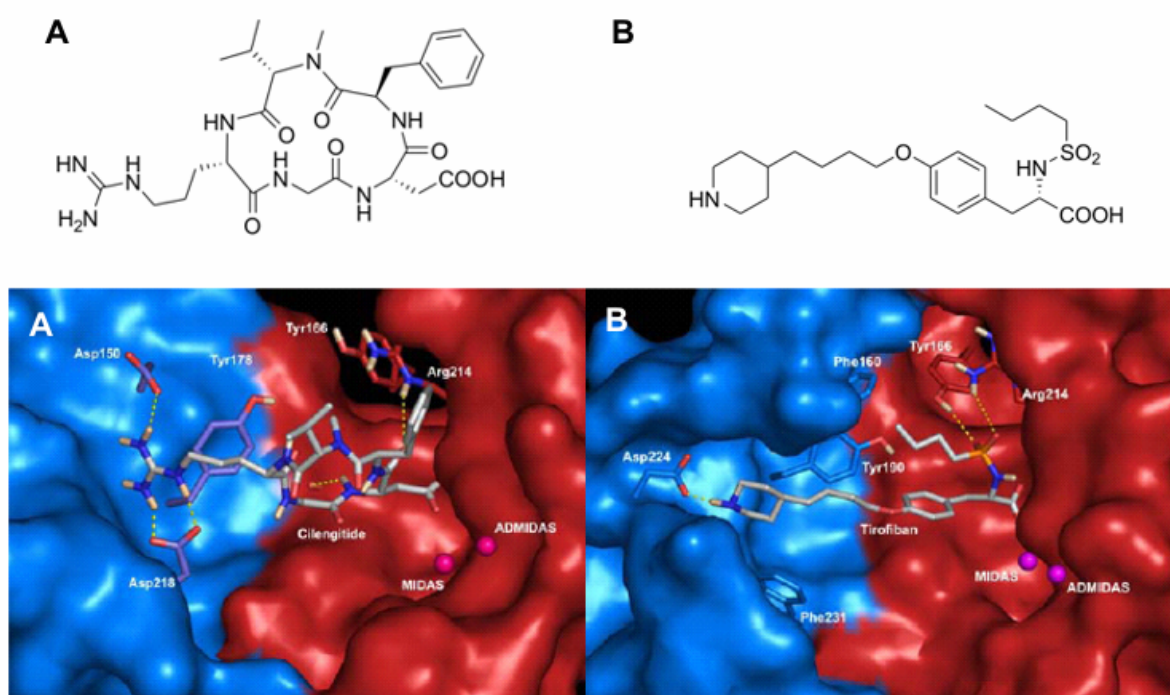


Figure II-5. Comparison of ligand binding in $\alpha v\beta 3$ and $\alpha IIb\beta 3$. Binding modes of Cilengitide in $\alpha v\beta 3$ (A) and Tirofiban in $\alpha IIb\beta 3$ as derived from crystal structures. Visible is the Connolly surface of the integrin (α -subunit blue and β -subunit red). Important residues are assigned, hydrogen bonds shown in yellow. Metal cations are shown as purple spheres.

The guanidinium group of *cyclo*(-RGDfN-MeVal-) is fixed inside a narrow groove formed by the D3-A3- and D4-A4-loops of the β -propeller of αv by a bidentate salt bridge to (αv)-Asp²¹⁸ at the bottom of the groove and by an additional salt bridge with (αv)-Asp¹⁵⁰ at the rear. Contacts between the Asp of the ligand and the βI -domain primarily involve the Asp carboxylate group, which protrudes into a cleft between the βI loops A'- $\alpha 1$ and C'- $\alpha 3$. The carboxylate function coordinates a Mn²⁺ ion at the

MIDAS in $\beta 1$ and is also involved in a hydrogen bond with the backbone amide proton of $(\beta 3)\text{-Asn}^{215}$ (not shown in Figure II-5). Further hydrogen bonds are formed with the backbone carbonyl of $(\beta 3)\text{Arg}^{216}$ and the side-chain of $(\beta 3)\text{Arg}^{214}$. The D-Phe residue contributes to the binding by a weak $\pi\text{-}\pi$ interaction with $(\beta 3)\text{Tyr}^{122}$. The glycine introduces the formation of a γ -turn in the cyclic peptide but doesn't interact with the receptor itself. Due to extensive SAR studies, the optimal distance between the Arg-C^{ξ} and the Asp-C^{β} of Cilengitide has been determined to be ~ 14 Å.^[75] The binding mode of Tirofiban to $\alpha\text{IIb}\beta 3$ is basically analog. The carboxylic function of the tyrosine scaffold coordinates the metal ion at the MIDAS, while the basic piperidine moiety is engaged in a salt bridge with the $(\alpha\text{IIb})\text{Asp}^{224}$. In contrast to the αv subunit, the responsible aspartic acid residue is more immersed in the receptor leading to a longer groove in the β -propeller. An αIIb -ligand therefore requires an elongation to reach both anchoring points. The optimal length for a $\alpha\text{IIb}\beta 3$ -ligand is ~ 16 Å, an observation that has been extensively utilized in the design of selective compounds. The $(\alpha v)\text{Asp}^{218}$ is replaced by $(\alpha\text{IIb})\text{Phe}^{231}$, which, together with $(\alpha\text{IIb})\text{Phe}^{160}$ and $(\alpha\text{IIb})\text{Tyr}^{190}$, results in a significantly more hydrophobic environment compared to αv . This hydrophobic cleft is occupied by the *n*-butyl-side chain of the sulfonamide, that itself is positioned by two hydrogen bonds with the $(\beta 3)\text{Tyr}^{166}$ -hydroxyl function and the guanidine group of $(\beta 3)\text{Arg}^{214}$.

II.2.4 Integrin ligands

Due to their biological relevance in many pathological processes, integrins have been a promising target for medicinal chemistry over the past decades. The research effort, fueled by the resolution of X-ray structures enabling structure-based design, yields a continuously increasing number of artificial integrin ligands – from antibodies to small molecules. While the monoclonal antibodies target a certain epitope on the receptor, the peptides and small-molecule ligands aim at the mimicry of the natural ligands (e.g. RGD containing fibronectin).^[76] The following chapter gives a brief overview over natural and artificial integrin ligands keeping the focus on $\alpha 5\beta 1$ and $\alpha v\beta 3$.

II.2.4.1 Natural integrin ligands

The most abundant class of integrin ligands are the extracellular matrix proteins like *fibronectin*, *vitronectin* and *fibrinogen*. Due to its biological relevance, the protein fibronectin should be further elucidated. It is widely expressed by multiple cell types and is critically important in vertebrate development, as demonstrated by the early embryonic lethality of mice with targeted inactivation of the Fn-gene.^[77] Fn usually exists as a dimer of two nearly identical ~250 kDa subunits linked covalently near their C-termini by a pair of disulfide bridges. Each monomer consists of three types of repeating units (termed Fn-repeats): Fn-I, Fn-II and Fn-III. Fn contains 12 type I repeats, 2 type II repeats and 15-17 type III repeats, which totally account for 90% of the Fn sequence.

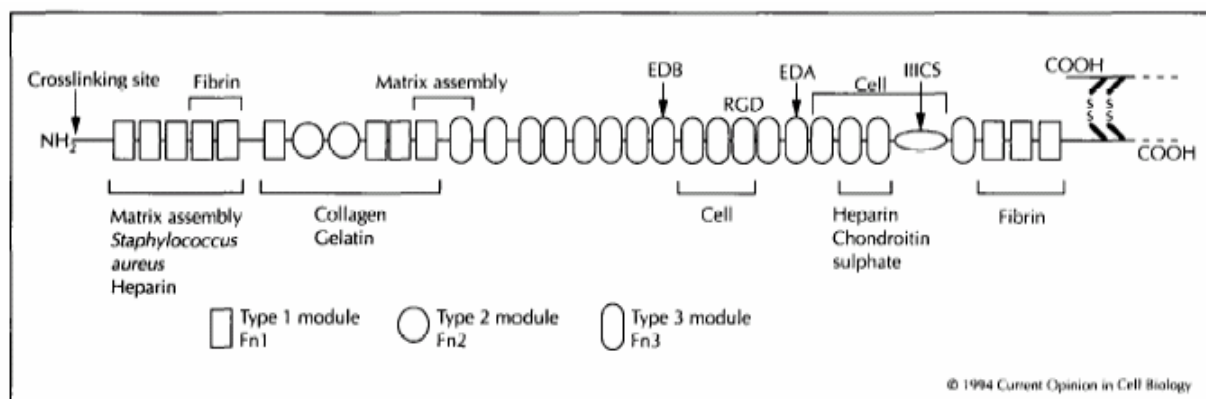


Figure II-6. Modular structure of fibronectin. Binding sites are assigned by brackets.^[78]

All three types of Fn-repeats are also found in other molecules suggesting that Fn evolved through exon shuffling. Fn is an abundant soluble constituent of plasma and other body fluids. Assembly of soluble fibronectin on cell surfaces results in insoluble, associated fibronectin, which becomes a part of the ECM. The process, referred to as *fibronectin fibrillogenesis*, depends on the self-association of Fn molecules directed by multiple binding sites along the molecule.^[78, 79] Integrins, especially $\alpha 5\beta 1$ have been found critical for this process, as it can be inhibited by anti- $\alpha 5\beta 1$ antibodies as well as other antagonists. The binding site of Fn has been tracked down by mutagenesis studies to the RGD sequence, which is presented in a loop on the Fn-III₁₀ repeat. This recognition sequence is mainly responsible for fibronectin binding and assembly, but not the only binding sequence. For instance, a 'synergy site' PHSRN has been identified in Fn-III₉, which promotes specific binding of $\alpha 5\beta 1$,

apparently via interaction with the $\alpha 5$ subunit. Further $\alpha 5\beta 1$ binding sites could be identified in the *N*-terminal region of Fn, which seem to be distinct from those generated in response to ligation with the RGD sequence. [77]

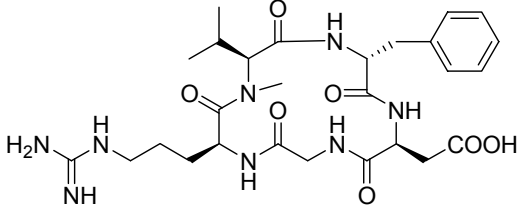
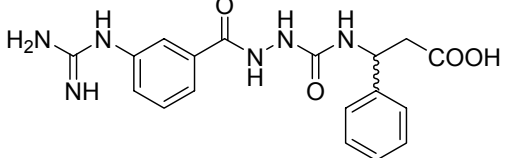
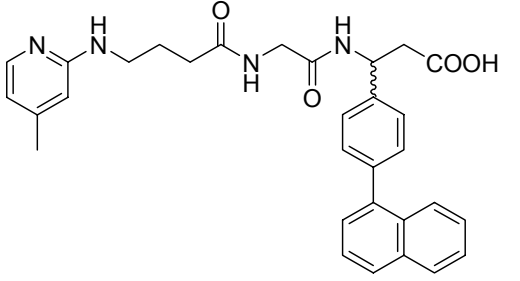
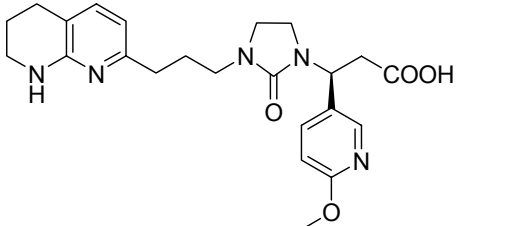
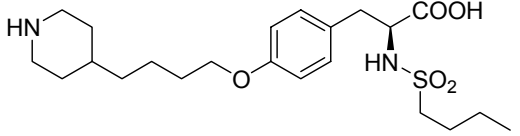
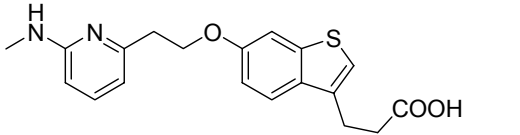
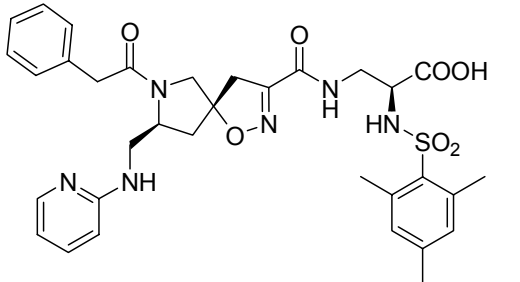
Another soluble, endogenous ligand for integrin $\alpha 5\beta 1$ is endostatin. It was discovered shortly after its analogue angiostatin (binding $\alpha v\beta 3$) as an endogenous inhibitor of angiogenesis. Endostatin was identified as fragment of collagen XVIII, which is cleaved from the collagen matrix by matrix metalloproteases, which are predominantly secreted by activated endothelial cells. The production of endostatin as an antagonist of $\alpha 5\beta 1$ may be part of a negative feedback and serve as regulatory element in angiogenesis.

II.2.4.2 Synthetic integrin ligands

Most of the effort spent on design of integrin ligands concerns the integrins $\alpha IIb\beta 3$ and $\alpha v\beta 3$. Inhibition of the platelet receptor $\alpha IIb\beta 3$ is a promising way to inhibit fibrinogen-dependent platelet aggregation useful for the treatment of thrombosis. The main target of antiangiogenic cancer therapy was – up to now – $\alpha v\beta 3$. The prospect of strong adverse effects by non-selective ligands pointed out the importance of receptor-selectivity in the process of integrin ligand design. The progress in structure determination of the different receptors generally accelerated the process of ligand design. With $\alpha 5\beta 1$ being drawn into the focus of research, the challenges to design a selective ligands are multiplying.

Table II-1 shows a selection of different ligands, their structure and their activity on the integrin subtypes tested. It should be stressed that IC_{50} values of different published ligands refer to different testing systems and are comparable to a certain limit.

Table II-1. Structures and activities of selected integrin ligands.

Entry	Structure	IC_{50} [nM]	Reference
1 Cilengitide		0.5 ($\alpha v \beta 3$) 70 ($\alpha v \beta 5$) 860 ($\alpha IIb \beta 3$)	[36]
2		2.6 ($\alpha v \beta 3$) 280 ($\alpha v \beta 5$) 8300 ($\alpha IIb \beta 3$)	[80]
3		8 ($\alpha v \beta 3$) 5170 ($\alpha v \beta 5$) 4230 ($\alpha IIb \beta 3$)	[81]
5		0.1 ($\alpha v \beta 3$) 10 ($\alpha v \beta 5$) 35000 ($\alpha IIb \beta 3$)	[82]
6 Tirofiban		36 ($\alpha IIb \beta 3$)	[83]
7		30 ($\alpha v \beta 3$) 140 ($\alpha v \beta 5$) 7800 ($\alpha 5 \beta 1$) >20000 ($\alpha IIb \beta 3$)	[84]
8 SJ749		49 ($\alpha v \beta 3$) >100000 ($\alpha IIb \beta 3$) 0.2 ($\alpha 5 \beta 1$)	[85]

The comparison of the different ligands outlines the general similarities: A basic moiety mimicking the arginine side chain of RGD and a carboxyl group representing the aspartic acid are attached to a more or less rigid scaffold that arranges them in the appropriate three-dimensional way. In most cases, an aromatic residue in the vicinity of the carboxylate improves the binding properties by additional interactions with the receptor. The nature of the scaffold is of minor importance.

The α IIb β 3 inhibitor Tirofiban (Aggrastat[®])^[83] is an authorized drug for the treatment of *angina pectoris* and *myocardial infarct*. Another authorized drug targeting α IIb β 3 is Abciximab (ReoPro[®]), a fragment of a chimeric, monoclonal antibody against α IIb β 3. It shows higher receptor affinity as Tirofiban, but lacks selectivity.^[86] The α v β 3 antagonist Cilengitide is currently in clinical phase III trials in patients with *glioblastoma multiforme*, *metastatic prostate cancer* and *lymphoma* (<http://www.clinicaltrials.gov/ct/search?term=cilengitide>). According to the growing interest in α 5 β 1 antagonists, the first compounds will be in clinical trials in the near future.

II.2.5 The α 5 β 1 homology model

The lack of reliable structural data in the past excluded α 5 β 1 as target for structure-based drug design. However, the high homology between the different integrin subtypes makes them promising targets for homology modeling, which has already been achieved in our group for α v β 5 integrin.^[87] The model of α 5 β 1 was created by Axel Meyer and is described in greater detail in his PhD thesis.^[88, 89] Homology modeling of proteins is considered to be possible for a homology of 40% or greater.^[18] This precondition is met by the integrins α v β 3 and α 5 β 1 with 53% homology for α v/ α 5 and 55% for β 3/ β 1. The sequence of the integrin subunits was determined and compared using the program BLAST. Highly homologue sequences (>65%) were aligned using CLUSTALX. The sequence comparison gave a particularly low homology in the SDL (*specificity determining loop*), a short (CZDMKTTC) loop, stabilized by a disulfide bridge located in the β 3-subunit of α v β 3.

The SDL is considered important for the $\alpha v\beta 3$ specificity towards natural ligands.^[90] Considering small-molecule ligands, the SDL is supposed to be rather unimportant for selectivity as it is located too far away from the binding site.^[87] The metal ion binding sites MIDAS, ADMIDAS and LIMBS were found to be highly conserved, which is in good agreement with the importance of metal ion coordination for ligand binding. Interestingly, the $(\beta 3)\text{Arg}^{261}$, which stabilizes the heterodimer by π -cation interaction with the aromatic residues of the αv - β propeller is mutated to a lysine. Based on this aligned sequences and using the *comparative protein modeling method* of the program MODELLER, ten different homology models have been created and evaluated for stereochemical quality using PROCHECK. To obtain a reliable model for docking experiments, the homology models were optimized by adjusting the binding site of the receptor model to a highly active ligand. Due to the fact, that the biological relevance of integrin $\alpha 5\beta 1$ has just recently been drawn into the focus of research – with the finding, that $\alpha 5\beta 1$ is the only unambiguously proangiogenic integrin – the number of $\alpha 5\beta 1$ ligands is quite limited. Considering the structural similarities of both receptors, many known $\alpha v\beta 3$ antagonists are most likely to be biselective on both integrins. Apart from some published cyclic peptides with mostly micromolar activity, the most active $\alpha 5\beta 1$ ligands up to date are a series of spirocyclic isoxazolines with an IC_{50} of 0.2 nM towards $\alpha 5\beta 1$ and a 200 fold selectivity against $\alpha v\beta 3$ synthesized by Smallheer *et al.*^[85] Docking of the most potent ligand SJ749 into the optimized homology model and superposition with the corresponding $\alpha v\beta 3$ head group derived from the X-ray structure reveals a number of differences:

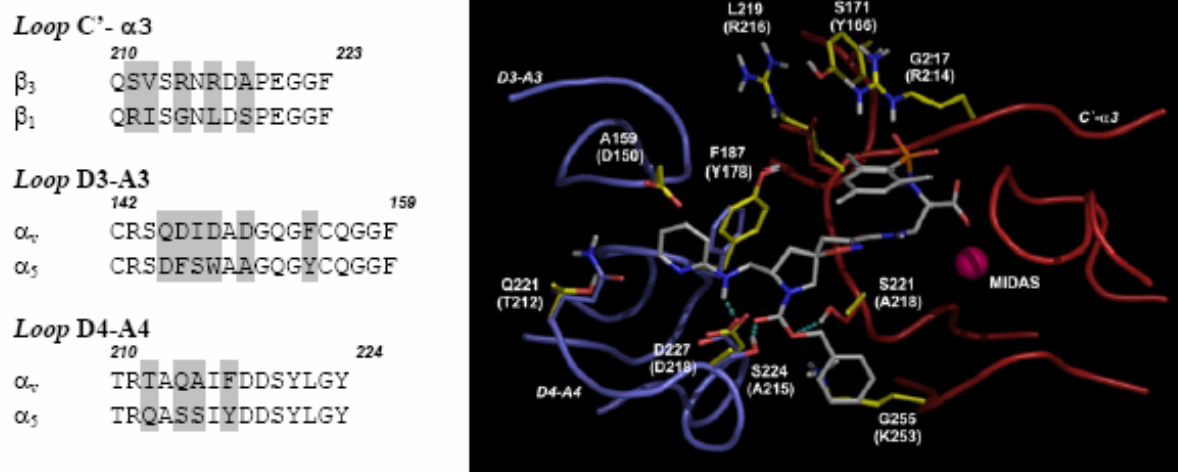


Figure II-7. Comparison of the binding pockets of $\alpha 5\beta 1$ and $\alpha v\beta 3$. Mutations in the sequence are marked gray. Ribbon drawing of $\alpha 5\beta 1$ ($\alpha 5$ in blue, $\beta 1$ in red). Analog amino acids of $\alpha v\beta 3$ are shown in yellow. Binding mode of SJ749 was calculated with AutoDock.

Firstly, SJ749 binds the integrin in a manner similar to other RGD peptides / mimetics (Figure II-5): The carboxylic function coordinates the metal ion located in the MIDAS, while the basic aminopyridinyl moiety is inserted into a narrow groove between the D3-A3 and the D4-A4 loop of the ($\alpha 5$)-propeller, forming a hydrogen bond to the highly conserved ($\alpha 5$)Asp²²⁷ (Asp²¹⁸ in αv). It is noteworthy, that a second (αv)Asp¹⁵⁰, that also can participate in binding is mutated to an alanine ($\alpha 5$)Ala¹⁵⁹. On the other hand, in the $\alpha 5$ subunit, the groove is terminated by a ($\alpha 5$)Gln²²¹ (Thr²¹² in αv) resulting in a slightly shortened binding pocket. On the one hand, a more hydrophobic pocket should favor more lipophilic and basic moieties in $\alpha 5$, while, on the other hand, the fact that the pocket is shorter could be an important issue to induce selectivity *against* $\alpha 5\beta 1$ by employing bulkier basic groups. In the β -subunit, the most obvious difference between the two receptors is the C'-a3 loop, were the ($\beta 3$)Arg²¹⁴, that forms a hydrogen bond with the sulfonamide of SJ749 (Figure II-7) is lacking in $\beta 1$ (Gly²¹⁷). In addition to that, the residues ($\beta 3$)Arg²¹⁶ and ($\beta 3$)Tyr¹⁶⁶ are replaced by ($\beta 1$)Leu²¹⁹ and ($\beta 1$)Ser¹⁷¹ respectively, which are less sterical demanding and open a new relatively hydrophobic cleft in $\beta 1$. A promising approach towards $\alpha 5\beta 1$ -selective ligands could be to directly address this hydrophobic cavity by a bulky aromatic group that would result in a clash with ($\beta 3$)Arg²¹⁴ thus disabling binding in $\alpha v\beta 3$. An additional feature of the ligand SJ749 is the benzyl carbamate that forms an additional interaction with the ($\alpha 5$)Ser²²⁴ and the ($\beta 1$)Ser²²¹ which are both replaced

by alanine in $\alpha v\beta 3$ (Ala²¹⁵ and Ala²¹⁸, respectively). This substitution pattern increases affinity towards $\alpha 5\beta 1$ without hampering binding towards $\alpha v\beta 3$.

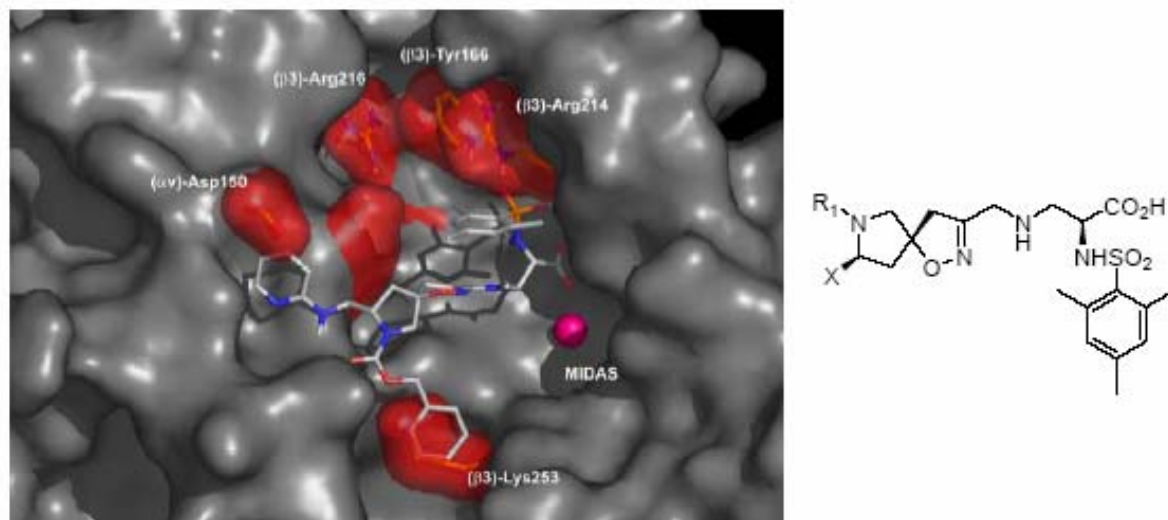


Figure II-8. Docking of the spiroisoxazolin (SJ749) into the homology model of $\alpha 5\beta 1$. Shown is the superposition of the Connolly-surfaces of $\alpha 5\beta 1$ (gray) and $\alpha v\beta 3$ (transparent red).

To design a new $\alpha 5\beta 1$ ligand with improved selectivity, a scaffolding molecule has to be found, that arranges the crucial functionalities (basic moiety and carboxyl function) in the appropriate distance and allows attachment of other potential selectivity-inducing groups. It is important to keep the balance between rigidity - providing better binding energies in the *matched case* - and flexibility, which increases the probability of active ligands. Further requirements for the synthesis of a compound library are easy synthetic accessibility and high variability. In this thesis, different scaffolding structures are presented which more or less meet these requirements.

II.2.6 Integrin-mediated signal transduction

Beside their adhesive function, which allows cells to spread on the ECM, integrins are vitally important as an interface used for bidirectional signaling processes.^[46] Figure II-9 shows the major functional pathways dependent on integrin activation which are known up to now.

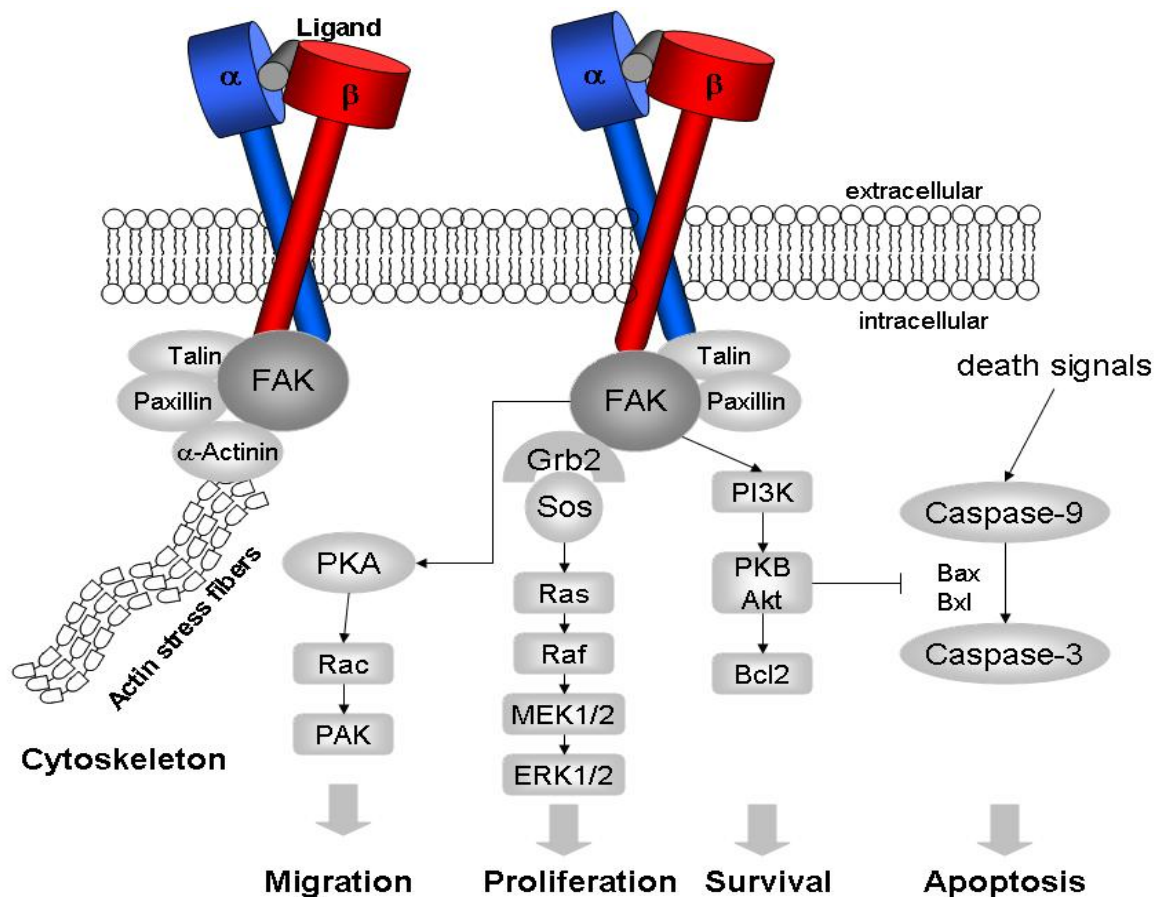


Figure II-9. *Integrin-dependent signaling pathways (excerpt).* ^[91]

Although their intracellular domains are relatively small, they are able to recruit a high number of different proteins involved in the construction and anchorage of the cytoskeleton (actin stressfibers) and in various signaling pathways. The clustering of active integrins in focal adhesion points induces binding of the proteins talin, paxillin and vinculin, which connect the integrins to the actin cytoskeleton. Furthermore, the integrin clusters bind and activate various tyrosine kinases such as FAK (focal adhesion kinase), Fyn or ILK (integrin-linked kinase). The most prominent of them is the non-receptor tyrosine kinase FAK, as it is activated by almost all integrins. Upon ligation of integrins with the ECM, FAK undergoes autophosphorylation at Tyr³⁹⁷ and thus is able to bind other kinases such as Src, which themselves phosphorylate FAK at further tyrosine residues. This signaling complex accommodates a high number of proteins, some of them acting as kinases or scaffolds while some of them are not yet fully understood. This is the starting point for different signaling pathways: Binding of the Grb2-Sos-complex activates the Ras-cascade leading to activation of the ERKs (extracellular regulated kinases). They are known to activate transcription factors which regulate progression through the G₁ phase of the cell cycle and contribute to

cell growth. FAK also activates the serine / threonine kinase PKB (also known as Akt) via phosphatidylinositol-3-kinase. PKB itself phosphorylates and thus inactivates proapoptotic molecules such as Bad, Bax and caspase-9. On loss of attachment to the matrix, cells undergo apoptosis, a phenomenon referred to as “anoikis” (homelessness). It is very important for the integrity of tissue as it prevents cells that have lost contact with their surrounding to establish themselves at inappropriate locations. The nuclear factor κ B (NF- κ B) is a key transcription factor for the regulation of the immune and inflammatory response. It also promotes cell survival by inducing the expression of anti-apoptotic molecules.^[92] The exact mechanism of its activation by integrins is still under investigation. On the other hand, there is also evidence for the active recruitment of pro-apoptotic molecules such as caspase-8 by unligated integrins (IMD, integrin-mediated death).^[93] As another function, integrins can activate the Rho GTPases (Rho, Rac and Cdc42), which act as molecular switches that provoke change in the organization of the actin cytoskeleton. For example is Rac involved in the formation of lamellipodia, the formation of new focal adhesion points as well as their disassembly, which are all crucial factors for cell migration. The mechanisms of signal transductions mentioned above all contribute to the *outside-in* signaling, which allows the cells to react on changes in binding to the ECM. For the corresponding *inside-out* signaling, the mechanisms are still a matter of debate. However, there is strong evidence that the state of integrin activation is at least partly regulated by GTPases such as Ras and Rap-1.^[94, 95] Furthermore, recent results demonstrate that interactions between different integrins that are present on the cell surface can strongly influence the adhesive functions of individual receptors. This effect, referred to as integrin “cross-talk”, has been demonstrated in a number of systems.^[96]

II.2.7 Antiangiogenic cancer therapy

To elucidate the functions of integrins *in vivo*, many *knock-out* studies have been performed in various models. The phenotypes of selected integrin knockouts is shown in Table II-2:

Table II-2. Phenotypes of mice with constitutive gene deletion. ^[46, 52]

Gene deleted	Heterodimers affected	Major ligand	ECM	Knockout phenotype
$\beta 1$	$\alpha 1\beta 1$, $\alpha 2\beta 1$, $\alpha 10\beta 1$, $\alpha 11\beta 1$, $\alpha 9\beta 1$, $\alpha 7\beta 1$, $\alpha 6\beta 1$, $\alpha 3\beta 1$, $\alpha 8\beta 1$, $\alpha v\beta 1$, $\alpha 5\beta 1$, $\alpha 4\beta 1$	Fn, Vn, Ln, Co		Lethal at E5.5 Failure of organizing the embryonic inner mass.
$\beta 3$	$\alpha 11b\beta 3$, $\alpha v\beta 3$	Fb, Vn, Fn, Ln, OPN, vWF, Fibrin		Viable, bleeding disorders (<i>Glanzmann's thrombasthenia</i>). Osteoclast functional defects in bones. Extensive Angiogenesis
αv	$\alpha v\beta 1$, $\alpha v\beta 3$, $\alpha v\beta 5$, $\alpha v\beta 6$, $\alpha v\beta 8$	Vn, Fn, Ln, Fb, vWF, OPN, Fibrin		8% die at E10.5-12.5. 92% die soon after birth due to brain hemorrhages (malformation of cerebral vasculature)
$\alpha 5$	$\alpha 5\beta 1$	Fn		Lethal at E10. Vasculogenesis but no maturation / angiogenesis
$\alpha 11b$	$\alpha 11b\beta 3$	Fb		Viable, bleeding disorders (<i>Glanzmann's thrombasthenia</i>).

The phenotypes of the gene deletions highlight the importance of integrins for embryogenesis. Embryonic lethality is thereby mostly the result of an impaired formation of the vasculature. These findings are the basis of antiangiogenic therapy. Angiogenesis, the formation and differentiation of new blood vessels from pre-existing ones by recruitment of endothelial progenitor cells plays a key role during embryonic development, also in wound healing and in the female reproductive system.^[91] In adults, the vascular network is quiescent and angiogenesis is triggered only locally and transiently. Under certain abnormal conditions, the fine balance between local inhibitory control and pro-angiogenetic signals is deregulated leading to pathological neovascularization, detected in a variety of diseases like diabetic retinopathy, restenosis, adipositas, rheumatoid arthritis, psoriasis and tumor growth.^[97] In order to initiate the angiogenetic process endothelial cells have to dissociate from neighboring cells and degrade the underlying basement membrane, before they invade the underlying tissue. During invasion and migration, the interaction of endothelial cells with the ECM is mediated by integrins^[98], which are also involved in final stages of the angiogenic process, including the construction of capillary loops and the determination of the polarity of the endothelial cells, allowing lumen formation of new vessels. The formation of a tumor-associated vasculature (tumor angiogenesis) has been observed already over 100 years ago, but it was not until the 1970s, thanks to the pioneering work of *Judah Folkman*, that the biological relevance of tumor angiogenesis to tumor biology was broadly recognized and investigated within the cancer research community.^[99] Since then, tumor angiogenesis has emerged as a critical stromal reaction essential for tumor progression. In the absence of tumor angiogenesis, the tumor enters a state of dormancy characterized by a balance between cell proliferation and apoptosis and its mass stabilizes at a volume of a few cubic millimeters ($\sim 10^5$ - 10^6 cells). The so-called “angiogenetic switch” is often triggered by release of growth factors from hypoxic cells, since neovascularization is required for adequate nutrition of the tumor (Figure II-10). Angiogenesis allows the unhampered growth of the solid tumor and also favors the escape of tumor cells into the blood circulation, which constitutes the initial step of metastatic spreading.^[100]

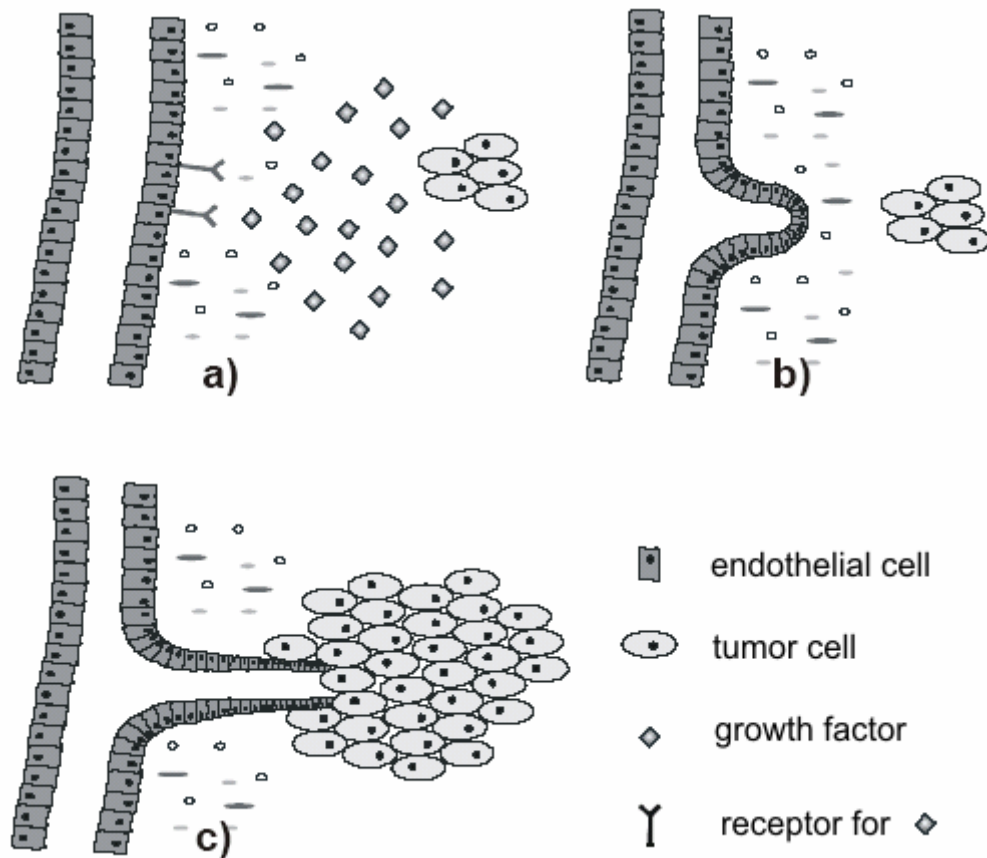


Figure II-10. Schematic view on tumor angiogenesis. a) hypoxic tumor cells release growth factors and stimulate proliferation of endothelial cells. b) Cells increase expression of integrins and activate proteolytic enzymes leading to directed invasion towards the tumor. c) Nutrition of the tumor is maintained, tumor is able to grow and metastasize.

Conventional cancer therapies targeting tumor cells with cytostatic drugs are limited by strong side-effects because all cells exhibiting a generally high proliferation rate are affected. Therapies against angiogenic blood vessels take advantage of the distinct biochemical differences between neovascular vessels and the pre-existing vascular network. This selectivity towards tumor cells is a promising approach of cancer therapy which has been extensively studied in the last decades. The prospect of blocking angiogenesis by blocking ligation of integrins to their native ECM ligands lead to the vast numbers of integrin antagonists which are recorded up to now, comprising monoclonal antibodies, peptide antagonists and small molecules with varying affinities to the respective integrin subtype. ^[101]

One of the first antiangiogenic drugs is the recently approved Ranibizumab (Luzentis[®]), a humanized fragment of an antibody against VEGF-A. It is authorized

for treatment of *age-related macula degeneration*, a disease where extensive angiogenesis destroys the retina, normally resulting in *ablepsia* (blindness).

II.2.8 Role of integrins $\alpha v\beta 3$ and $\alpha 5\beta 1$

Due to their primary expression on activated endothelial cells, the integrins $\alpha v\beta 3$, $\alpha v\beta 5$ and $\alpha 5\beta 1$ represent attractive targets for anti-angiogenetic cancer therapy.^[102] The integrin found to be involved in tumor angiogenesis was $\alpha v\beta 3$. It could be shown, that the blocking of $\alpha v\beta 3$ by a monoclonal antibody^[103] and the peptide cyclo(RGDfV)^[28, 104] was able to suppress cornea vascularization, hypoxia-induced retinal neovascularization and tumor angiogenesis in mouse models.^[105] Furthermore, ligation of $\alpha v\beta 3$ to the ECM was found to activate proliferation and anti-apoptotic pathways such as EFK-activation^[106], NF- κ B activation^[107], increase in the Bcl-2/Bax ratio^[108] and blocking of activator-caspase 8^[109]. Integrin $\alpha v\beta 3$ was also found to be activated by VEGF (*vascular endothelial growth factor*), thus enhancing ligand binding, cell adhesion and migration.^[110] These findings illustrate the role of $\alpha v\beta 3$ as a pro-angiogenic integrin. However, the phenotype of $\beta 3$ or $\beta 5$ knockout mice (viable, fertile, Table 2) displays a rather dispensable role in contrast to $\alpha 5$ (lethal at E5).^[111] Moreover, the $\beta 3$ -negative mice displayed an enhanced postnatal angiogenesis in response to hypoxia and VEGF.^[112, 113] The results are clearly supported by the observation, that αv -deficient mice undergo extensive developmental vasculogenesis and angiogenesis.^[111] The discrepancy between normal or extensive angiogenesis in $\alpha v\beta 3$ deficient mice on the one hand and the suppression of angiogenesis by pharmacological $\alpha v\beta 3$ inhibitors in wild-type mice on the other hand give rise to the question, whether $\alpha v\beta 3$ regulates angiogenesis in a positive or negative way.^[93, 111, 114] Furthermore, the role of those peptides or small molecules has to be re-evaluated in respect of their function as antagonists or agonists. This problem is further complicated by the impact of integrin activation on different integrin types (integrin “cross-talk”).^[96] The binding of $\alpha v\beta 3$ by selective antibodies or a peptide inhibitor inhibit cell migration not only on vitronectin, but also on fibronectin in presence of $\alpha 5\beta 1$.^[115] The same results were obtained with a mutated $\beta 3$ subunit, indicating a modulation of the $\alpha 5\beta 1$ activity by $\alpha v\beta 3$. The role of an integrin ligand as agonist or antagonist may also be a matter of concentration. It

was observed, that small picomolar doses of a cyclic RGD peptide increased binding affinity of $\alpha v\beta 3$ towards vitronectin, fibronectin and fibrinogen, while higher doses up to 10 μM resulted in a dramatic loss of affinity.^[67] Nevertheless, there is a high number of $\alpha v\beta 3$ ligands - antibodies, peptides and small molecules - in different stages of clinical trials.

The results indicating a certain ambivalent effect of $\alpha v\beta 3$ pointed out the importance of integrin $\alpha 5\beta 1$ in anti-angiogenetic therapy. Integrin $\alpha 5\beta 1$ was also found to induce angiogenesis *in vitro*, while anti $\alpha 5$ antibodies suppressed VEGF-induced tumor angiogenesis in both chick embryo and murine models.^[116-118] Engagement of $\alpha 5\beta 1$ to fibronectin promotes proliferation via the NF- κ B-pathway and PKA / caspase 8-suppression. Blocking of $\alpha 5\beta 1$ by antibodies resulted in a caspase 8 induced apoptosis due to sustained PKA activation. Due to the unambiguously pro-angiogenic function of $\alpha 5\beta 1$, it has moved to the focus of drug-targets for anti-angiogenetic tumor therapy. The investigation of the wide range of biological effects which are connected with $\alpha 5\beta 1$ is still hampered by the lack of highly active ligands showing selectivity towards $\alpha v\beta 3$. A rational approach towards selective $\alpha 5\beta 1$ ligands will be presented in this work.

II.3 Biological Relevance of Blood Coagulation Factor VIII

Haemophilia A is one of the most common bleeding disorders affecting between 0.02 and 0.01‰ of the male population.^[119] It is an inherited disease, which can be traced back to a defect gene on chromosome X, which encodes the blood coagulation factor VIII. The disease usually affects males whereas heterozygotic females do not show the phenotype because of their other, intact X-chromosome, but are likely to transmit the disease to their male offspring. Dependent on the FVIII activity loss, several stages of increasing severity of haemophilia are distinguished. The phenotype varies thereby from a mild susceptibility for bleeding after surgery to severe, unprovoked bleeding. Although haemophilia is known since ancient times, the first serious attempts for the treatment came up in the 19th to 20th century with snake venoms to accelerate blood clotting and with blood transfusions. Application of bovine or porcine

plasma proved to be effective, but was accompanied by strong allergic reactions. A major improvement was the discovery of the *cryoprecipitate*, a brownish, FVIII rich precipitate from blood plasma obtained by slow thawing of plasma to 4°C. Novel purification procedures allowed the preparation of FVIII concentrates which facilitated home treatment of patients with haemophilia. A major drawback was the impact of HIV and hepatitis C, which were transmitted via blood transfusions among haemophilia patients and infected a huge number in the 1970s and 80s. The progress in molecular biology in the recent decades allowed the preparation of recombinant FVIII to avoid the use of potentially infective material. Further information about most recent progresses in haemophilia treatments are given on the webpage of the World Federation of Haemophilia (www.wfh.org). Since there is still no cure for haemophilia A, injections of a FVIII concentrate are the only possibilities of treatment. The purification and concentration of FVIII from the plasma (or recombinant cells) is the crucial and most elaborate (and costly) step in the preparation of medical products against haemophilia.

II.3.1 The blood coagulation cascade

Blood clots are the result of a series of zymogen activations.^[120] During the course of the enzymatic cascade, the active form of one enzyme catalyzes the activation of the next downstream factor at a time. Due to the catalytic nature of this process, this leads to a great amplification of the incoming signal, thus providing a fast response on tissue damage. The blood coagulation cascade is sketched in Figure II-11.^[119] A tissue injury exposes the so-called *tissue factor* (TF), which forms a complex together with activated factor VII (VIIa). The activation signal is passed downstream to factor X, which then converts prothrombin into its active form thrombin. Thrombin is the key enzyme of the cascade as it is responsible for the conversion of soluble fibrinogen into insoluble fibrin which forms the clot. The clot is further stabilized by crosslinking, a FXIII dependent process.

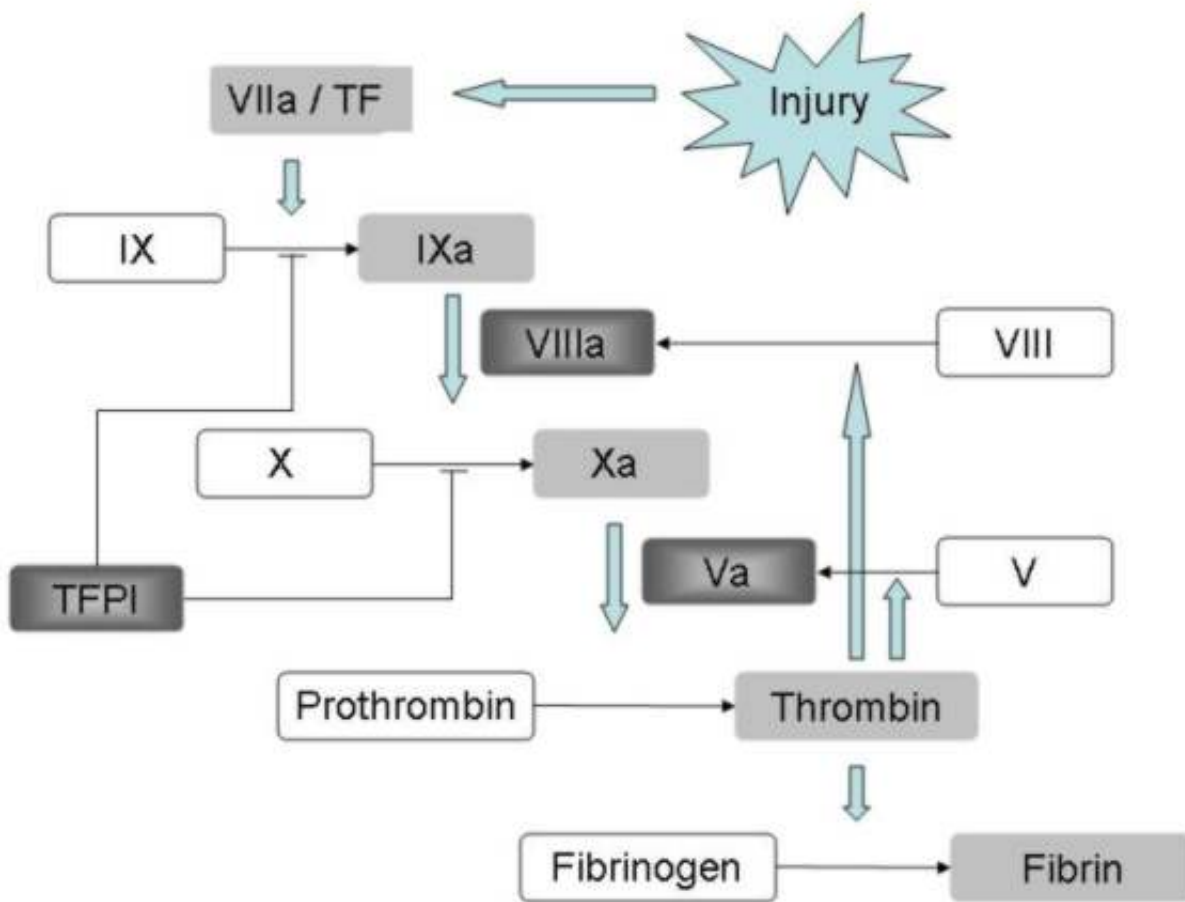


Figure II-11. Schematic model of coagulation *in vivo*.^[119] Activated coagulation factors are shown in light gray, regulatory factors in dark gray.

To avoid extensive clotting, the cascade has to be strictly controlled by negative feedback. In the presence of activated factor X, the tissue-factor pathway inhibitor (TFPI) inhibits further generation of factor Xa. After the inhibition, the amount of FXa is insufficient to maintain coagulation. Further generation of FXa can only be maintained by the FVIII / XI pathway. This pathway begins with the release of the proteins Kininogen and Kallikrein from damaged blood vessels, which activate FXI, which now activates FIX. Activation of the factor X can only be achieved by FIXa in a complex with FVIIIa. This reaction proceeds with the low levels of FVIIIa present in blood plasma and is enhanced by a positive feedback through FVIII activation by the previously generated thrombin. This complex process makes FVIII a key switch in the process of blood clotting.

II.3.2 Structure of Factor VIII

Factor VIII is a large, complex glycoprotein (~290 kD, 2332 aa), which is expressed from a ~180 kb gene on chromosome X, one of the largest genes known. [121] Analysis of the cloned FVIII cDNA revealed the presence of a distinct domain structure: A1-a1-A2-a2-B-a3-A3-C1-C2 (Figure II-12). [122, 123]

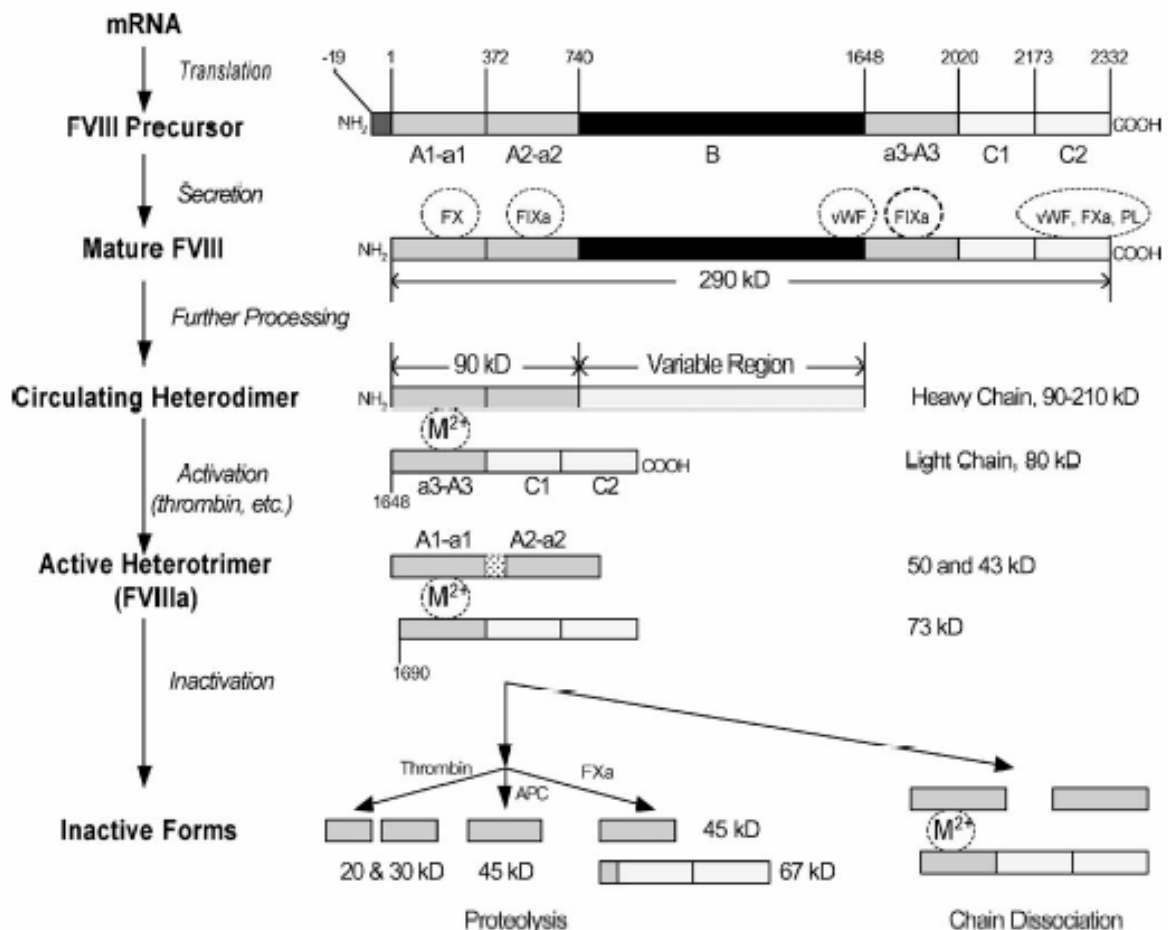


Figure II-12. Structure, function and processing of FVIII. [124] The sites of interaction with other clotting factors, vWF, phospholipids (PL) and metal ions (M²⁺) are illustrated by dotted circles.

The A-domains show approximately 30% homology and are bordered by short spacers (a1-3). The C-domains are structurally related to the C-domains of factor V. The B-domain is unique in that it exhibits no significant homology with any other known protein. The function of this domain is yet unknown as it is not required for anticoagulation activity. [125] The processed FVIII circulating in the plasma is a heterodimer consisting of a heavy chain (A1-a1-A2-a1-B) and a light chain (a3-A3-C1-C2) which are connected by a coordinating, bivalent metal ion (preferably

Ca²⁺ or Mn²⁺). FVIII activation by thrombin gives a heterotrimer (A1-a1, A2, A3-C1-C2) by cleavage at three arginine residues. [121, 122] There are at least three different mechanisms of FVIIIa deactivation resulting in a very limited stability of the protein. *In vivo*, there are also various protein interactions that help to stabilize FVIII and increase its half-life such as vWF [126] or serum albumin. The difficulties connected with factor VIII instability and attempts to overcome this problem are reviewed in the literature. [124]

II.3.3 Purification of Factor VIII

The therapeutically used FVIII concentrates are either plasma derived (cryoprecipitate) or as recombinant factor VIII produced by Chinese hamster ovary cells [127] or baby hamster kidney cells. [128] From the cryoprecipitate, an aluminum hydroxide adsorption step removes vitamin K dependent clotting factors. Further purification can be achieved by ion-exchange chromatography. [129-132] Additional steps include the improvement of immunological and viral safety, which is reviewed in the literature. [133] The immunoaffinity chromatography, employing highly selective monoclonal antibodies could substantially increase the purity of the products. [134, 135] However, the use of antibodies brings along economic disadvantages as well as new health risks. At first, the production of new affinity antibodies follows the same rules as applied to new pharmaceuticals, with equal costs in time and resources. Furthermore, the inevitable leakage of the antibodies into the FVIII concentrates is problematic due to the risk of allergies. Last but not least, monoclonal antibodies are difficult to produce on large scale and – as relatively large proteins – are prone to proteolytic degradation which decreases the lifetime of the affinity columns by far. An approach towards linear peptides as affinity ligands for FVIII purification has been made by the group of *Jungbauer*, who employed combinatorial methods to design a peptide library, which was screened in a binding assay using radioactively labeled FVIII. [136] These findings were taken on in our group with the objection of designing new, selective linear and cyclic affinity ligands with improved binding properties.

II.3.4 Optimization of the lead sequence

The work presented in this chapter was performed by *Sebastian Knör* and is described in his PhD thesis in greater detail. One of the compounds with the highest binding affinities described in the publication of *Jungbauer et al.* was the linear octapeptide EYHSWEYC.^[136] For the binding assay, the peptide had to be immobilized first, which was carried out on epoxy toyopearls. The immobilization should occur by nucleophilic opening of the epoxides by the cysteine thiol function as most nucleophilic moiety. This can be demonstrated by the lack of immobilization of peptides without cysteine. The optimization of the peptide sequence was performed as outlined in chapter II.1.1. The alanine mutation studies revealed the individual importance of each amino acid residue, while a screening with D-amino acids induces various β -turns which arrange the amino acid residues in different three dimensional-orientations (spatial screening).

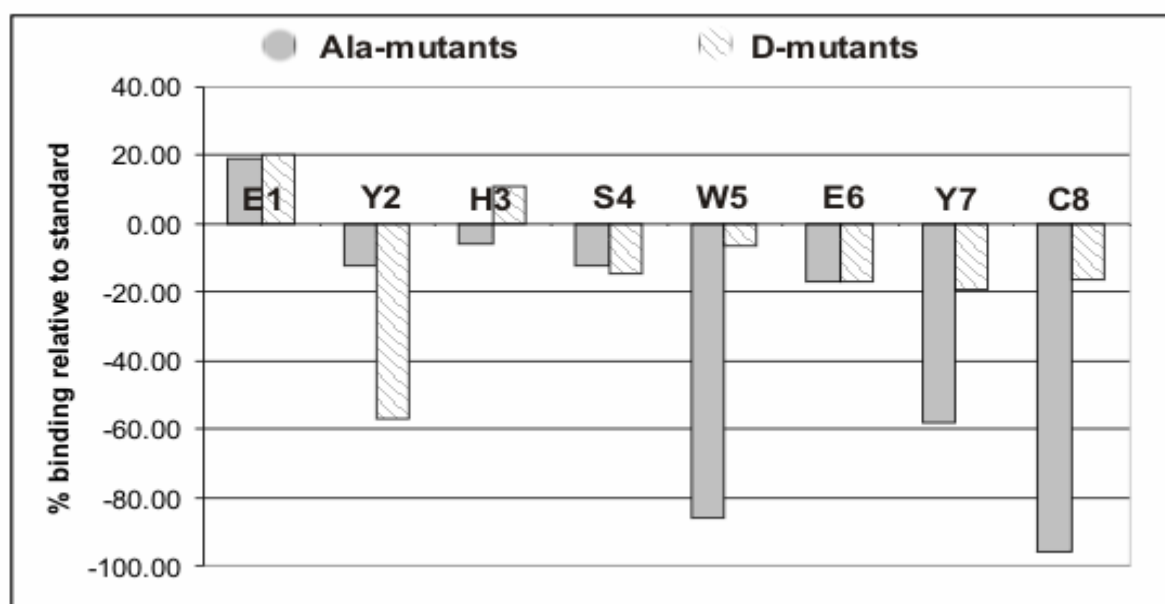


Figure II-13. Results of the Ala and D- scans. Ala-mutants are shown in gray, D-mutants as hatched bars. Binding properties are expressed relative to the lead compound (EYHSWEY).

The results displayed in Figure II-13 stress the relevance of the three residues Trp⁵, Glu⁶ and Tyr⁷ for FVIII affinity. The cysteine – alanine mutation did not show any immobilization and thus displays total loss of affinity. In various examples has been shown that cyclic peptides, especially cyclic hexa- and pentapeptides, display significant advantages in respect of proteolytic stability, enhanced binding activities

due to conformational restrictions and increased bioavailability. The first two issues make cyclic peptides based on a Trp-Glu-Tyr-Cys containing sequence potentially valuable affinity ligands. To check whether the lead sequence can be converted into a cyclic penta- or hexapeptide, the importance of the C- and N-terminus and the impact of sequence truncation were examined. The results showed that the removal of the charges at both termini led to an improvement in binding. Furthermore, the sequence could be broken down to a short binding sequence without big loss of affinity. After previous experiments with cyclized penta- and hexapeptides, two sequences were chosen for further investigations: (FSWEYc) and (FsWEYc). The results are discussed in chapter III.2.

III Results and Discussion

III.1 Rational Design of Selective Integrin Ligands

The role of integrins, especially of the integrins $\alpha 5\beta 1$, $\alpha v\beta 3$ and $\alpha v\beta 5$ in the process of angiogenesis and the resulting potential of integrin antagonists in the antiangiogenic cancer therapy made them attractive targets for pharmaceutical research.^[88, 91] Up to now, a huge number of different peptidic or non-peptidic ligands with various selectivity profiles have been published.^[137] In order to decrease adverse effects caused by inhibition of homologue integrins the design of selective compounds is still a great challenge. Since the function of the αv integrins and $\alpha 5\beta 1$ in angiogenesis had to be reevaluated,^[114, 138] the design of selective $\alpha 5\beta 1$ integrin ligands has become a cutting-edge topic. The X-ray structure of the $\alpha v\beta 3$ -ligand complex^[62] and a published $\alpha 5\beta 1$ -ligand^[85] enabled us to establish the first homology model of $\alpha 5\beta 1$ ^[89], which was used in the structure-based design of new, highly active and selective $\alpha 5\beta 1$ ligands. The extensive SAR data provide deep insights into the active site of the $\alpha 5\beta 1$ receptor point out the pharmacological relevance of our model. The biological testings (ELISA assays) were performed by *Grit Zahn* and *Roland Stragies* at the Jerini AG, Berlin. Compounds were tested for their ability to inhibit the binding of soluble $\alpha 5\beta 1$ / $\alpha v\beta 3$ to their immobilized natural ligands fibronectin and vitronectin. The amount of bound integrin was determined by an antibody against the integrin which is fused to the enzyme HRP (horseradish peroxidase). The activity of the HRP was measured with an appropriate substrate, which is converted into a colored product. The readout was the absorbance at 450 nm, from which the amount of integrin and thus the IC_{50} value could be calculated. In vivo testings were performed by Michael Leiss in the group of Prof. Fässler at the Max-Planck Institute für Biochemie, Martinsried.

III.1.1 Synthesis of integrin ligands based on the tyrosine scaffold

A promising scaffold for the design of new $\alpha 5\beta 1$ ligands is tyrosine, which has been used by MERCK as ligand for integrin $\alpha IIb\beta 3$.^[83] The anti-coagulant Tirofiban[®] is

III. Results and Discussion

based on tyrosine, which provides simple branching points for the introduction of the guanidine mimetic at the phenolic hydroxyl function and an aromatic or aliphatic branch at the amino position.

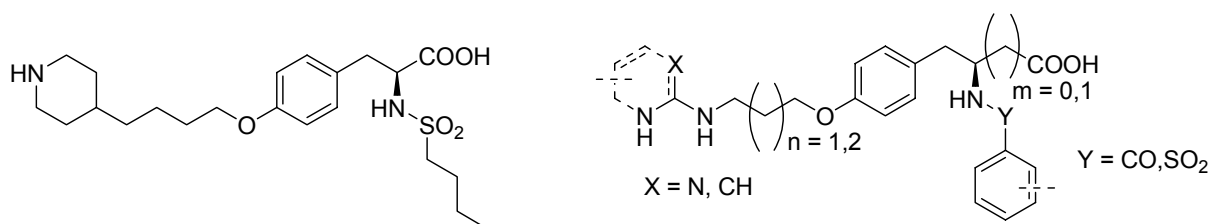
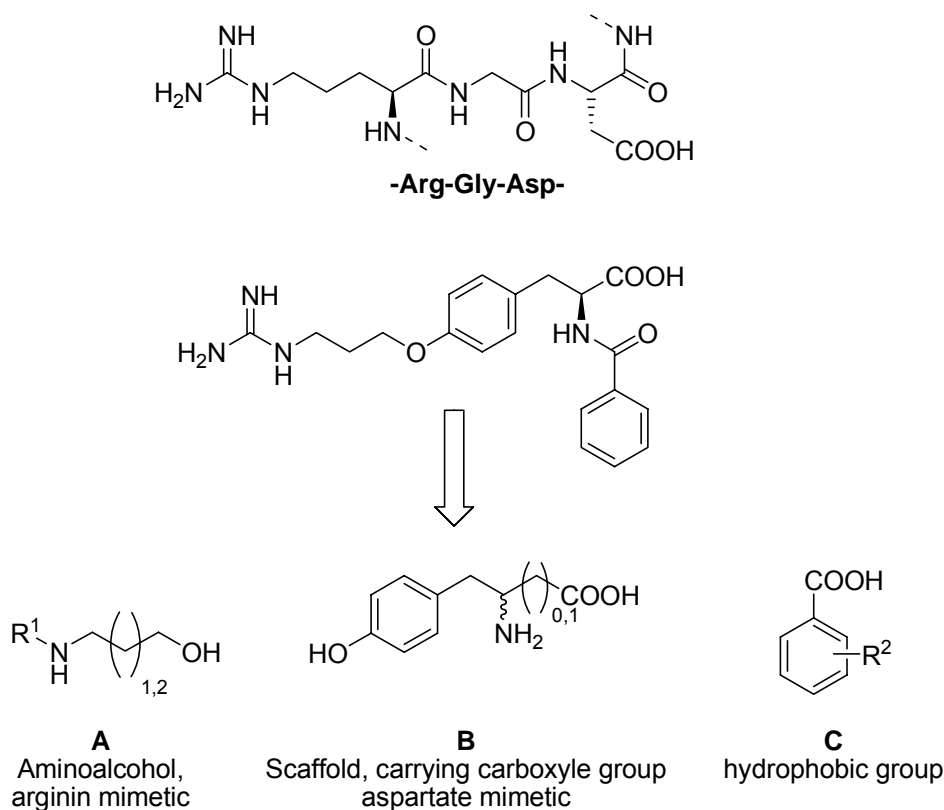


Figure III-1. Tyrosine based ligands. Utilization of the tyrosine scaffold in Tirofiban[®] (left) and possible variations as $\alpha 5\beta 1$ ligands (right).

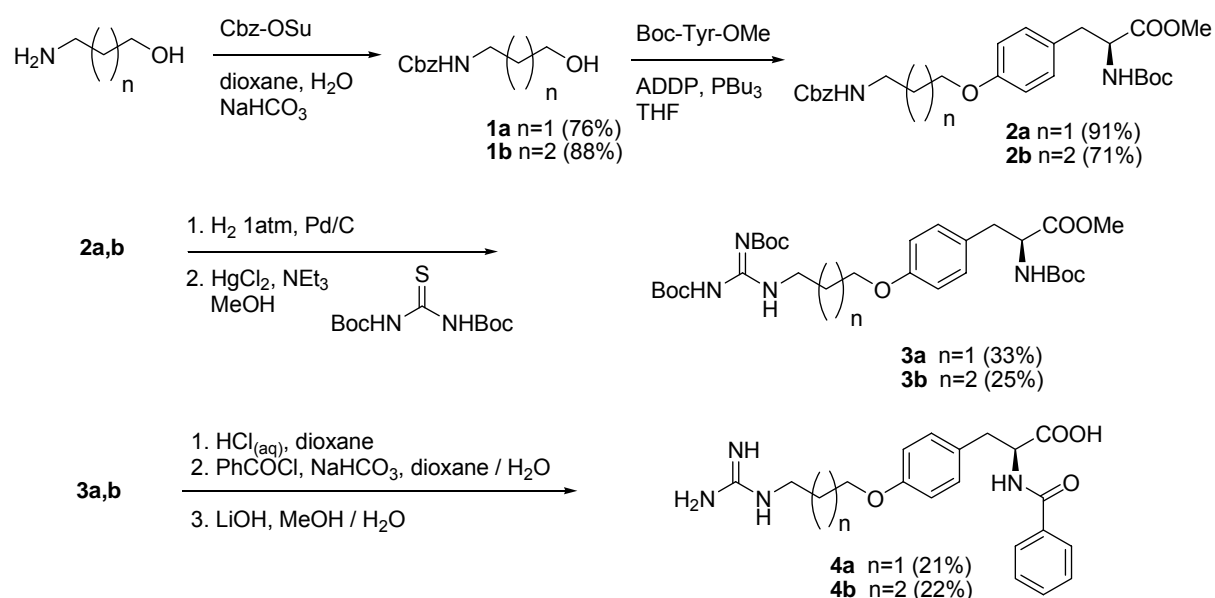
Figure III-1 shows the comparison of the planned series of new compounds and the $\alpha 11\beta 3$ inhibitor Tirofiban[®].



Scheme III-1. Schematic retrosynthetic approach towards tyrosine-based ligands. The molecules consist of three fragments **A-C**, which have to be purchased or synthesized.

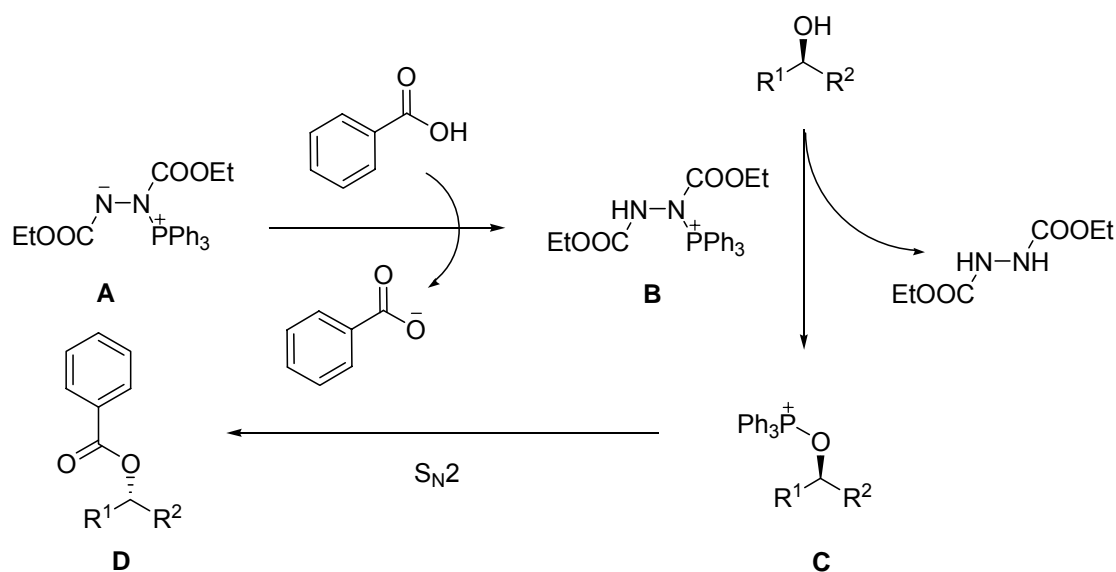
Scheme III-1 represents a retrosynthetic analysis based on a tyrosine ligand class: The arginine mimetic is introduced as an alcohol (fragment **A**) and coupled by a Mitsunobu-type alkylation of the phenolic group of the tyrosine, which serves as scaffold and aspartic acid mimetic. While the amino alcohols **A** could be synthesized

in a large variety, the protected tyrosines were either purchased or synthesized from commercially available starting materials. As for fragment **C**, a hydrophobic carboxylic or sulfonic acid, various substitution patterns were obtained from commercial sources, others could be easily generated by 1-3 step syntheses. The following part of the chapter will concentrate on synthetic pathways towards the tyrosine-based ligands and synthetic problems associated with it. As for the most RGD-like ligand with an aliphatic guanidinium group, the synthesis is described in Scheme III-2. The guanidine group is known to give poor bioavailabilities due to its high basicity and is widely substituted by basic heterocycles in peptidomimetics. Nevertheless, the corresponding guanidine ligands were synthesized to give a reference for comparison with other basic groups screened. ^[139]



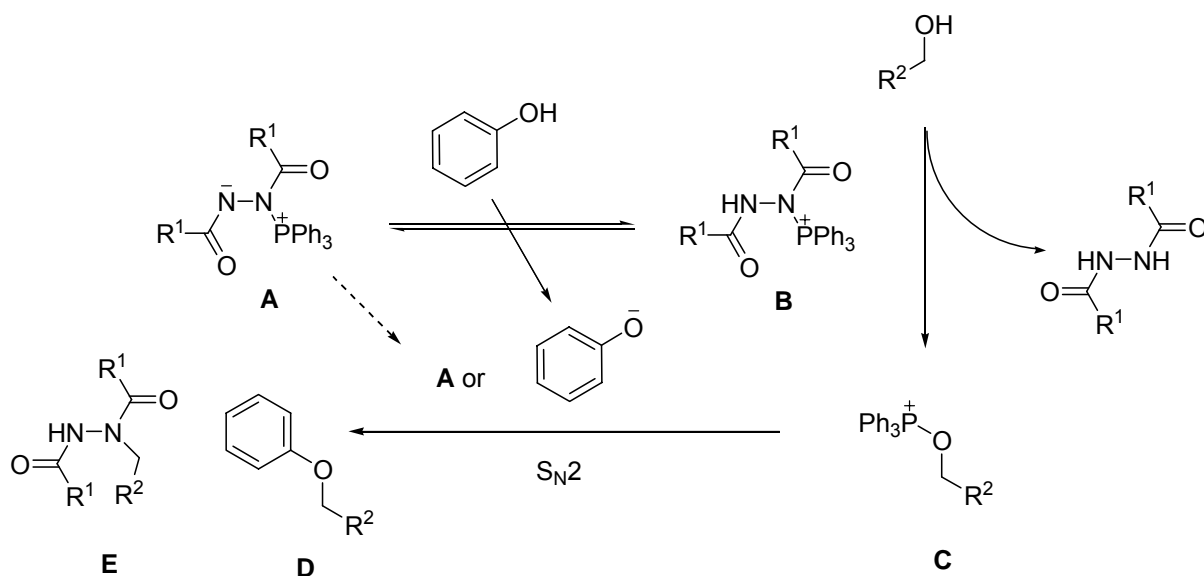
Scheme III-2. Synthesis of ligands **4a,b** containing an aliphatic guanidine function.

The key step of the synthesis of ligands based on the tyrosine scaffold is the coupling of the aliphatic alcohol with the phenolic hydroxyl function. ^[84] The Mitsunobu reaction, originally used for the inversion of chiral alcohols is also used to activate alcohols for substitution with different nucleophiles. ^[140, 141] The mechanism of the reaction is shown in Scheme III-3.



Scheme III-3. Mechanism of the Mitsunobu reaction (inversion of chiral alcohols) using Triphenylphosphine and DEAD as activating agent.

The triphenylphosphine reacts with diethylazodicarboxylate to form the reactive species **A**, which deprotonates the benzoic acid that acts as nucleophile for the final substitution step. The *O*-alkyl triphenylphosphinoxonium species **C** is generated via nucleophilic substitution with diethyl dicarboxylhydrazine as leaving group. **C** is then attacked by the *in situ* formed nucleophile, a reaction driven by the formation of the stable P=O bond. As the S_N2 reaction proceeds under inversion of configuration, the resulting ester **D** gives after saponification the corresponding inverted alcohol. For the alkylation of tyrosines, the phenolic function acts as nucleophile and has to be deprotonated by the species **A**. This may cause problems, as the triphenylphosphine - DEAD adduct only allows deprotonation of protons with a $pK_a < 11$. This is approximately the pK_a of the phenol, resulting in an equilibrium between **A** and **B** (Scheme III-4).



Scheme III-4. Alkylation of phenols under Mitsunobu conditions. Depending on the concentration, **A** competes with the phenolate in the final substitution step to give side-product **E**.

In this case, **A** is not sufficiently protonated and competes with the less nucleophilic phenolate in the final substitution step to give side-product **E** as major product. The problem could partly be overcome by employing azodicarboxylic dipiperidid (ADDP, Scheme III-4, R¹ = piperidine) and PBU₃.^[142] The product of the addition is able to deprotonate protons with a pK_a < 14. Another advantage is the insolubility of the corresponding hydrazine derivative which facilitates the workup. The substitution of triphenylphosphine by tributylphosphine allows an easier chromatographical purification by avoiding the formation of triphenylphosphine oxide. However, the reaction was very sensible to bases, which strongly disfavored product formation while increasing side-product formation. Most of the tyrosine starting material could be reisolated in those cases. The side-product formation turned out to become a serious problem, when differently substituted aminopyridines were employed for ligand synthesis. Beside a reaction temperature of 0°C, the slow addition of a diluted solution of ADDP in order to keep the concentration low at any time seemed to be important for the success of the reaction, but, however, the aminopyridines still gave modest to low yields.

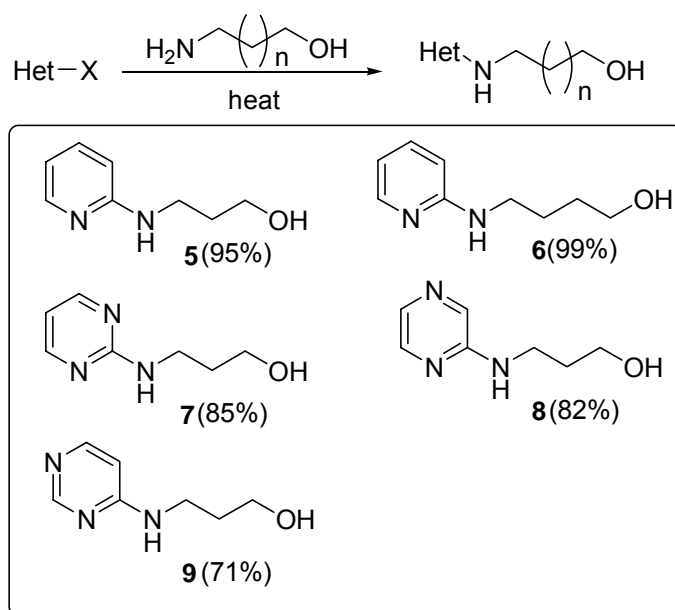
III. Results and Discussion

Table III-1. Correlation of substrate basicity with the yield of the Mitsunobu reaction.

Entry	Alcohol	Product	Yield	Additives
1			75-90%	
2			15-25%	
3			-	1 eq. TEA or 1 eq. DBU
4			-	
5			40-60%	
6			90%	

The experiment, whether the addition of base (TEA or DBU) would support the deprotonation of the phenol only resulted in exclusive formation of the side-product, whereas no desired product could be detected. On the other hand, carbamates (entry 1), aminopyrazines (entry 6) and aminopyrimidines (not shown) give high yields of the alkylated product. In case of the 2-aminopyridines (entries 2, 4), the Boc-protection of the amine could give at least satisfying results (entry 5). As the Boc-protection of the 2-aminopyridines could only be achieved in a three step procedure, the method was only applied in case of extremely poor yields.

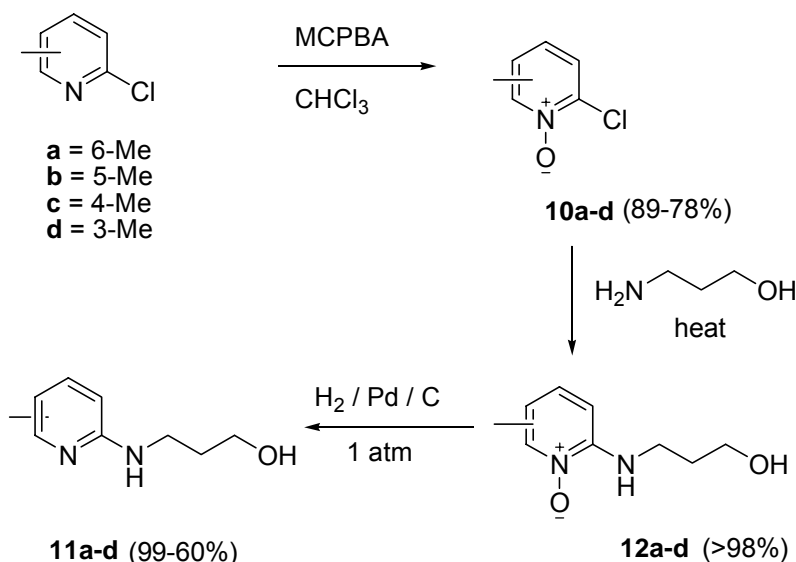
Aminoalcohols containing a heterocycle were synthesized by nucleophilic aromatic substitution of the heteroaryl chlorides or bromides by *neat* aminopropanol or aminobutanol through heating to 140°C for 12 h in excellent yields (Scheme III-5).^[143]



Scheme III-5. Synthesis of heteroaryl aminoalcohols by nucleophilic aromatic substitution.

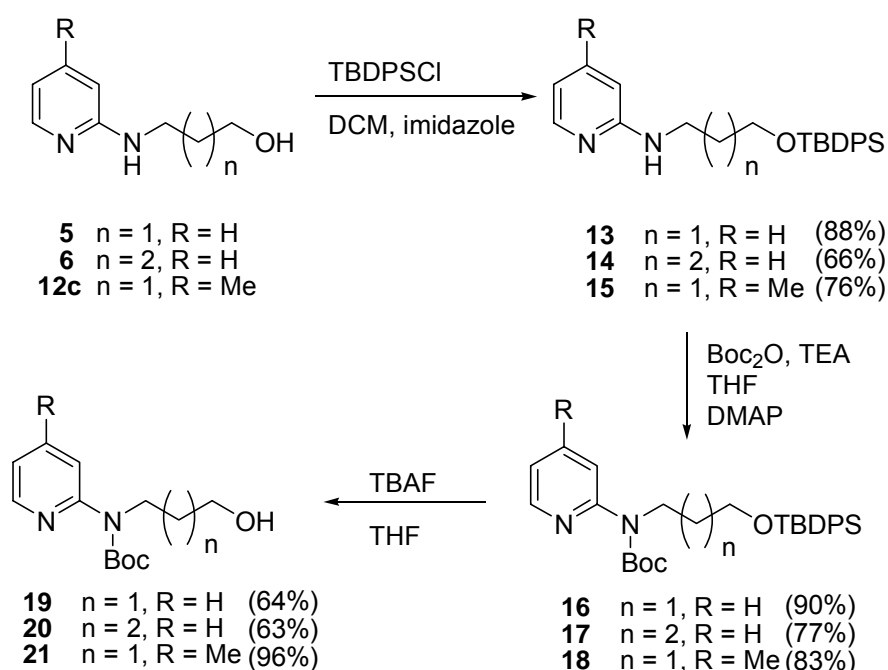
In case of the rather electron-rich, methyl substituted 2-chloropyridines, the direct nucleophilic aromatic substitution proceeded only with low reaction rates. To further increase the electrophilicity of the pyridine, it was firstly activated by oxidation to the corresponding pyridine *N*-oxides^[144] which were further subjected to nucleophilic substitution using the same protocol.^[143] The reduction of the *N*-oxides was performed using a Pd catalyst on carbon and hydrogen at a pressure of 1 atm. The reaction had to be monitored by TLC to avoid further reduction of the pyridine. As already mentioned in Table III-1, the Mitsunobu reaction of **12c** completely failed to yield the desired product. In order to reduce the basicity of the pyridine, the compounds **5**, **6** and **12c** were *N*-Boc protected to increase the yields of the following Mitsunobu reactions.

III. Results and Discussion



Scheme III-6. Activation of methyl-2-chloropyridines by oxidation and preparation of the corresponding aminoalcohols.

Attempts to selectively protect the amino function by reaction with Boc-anhydride and DMAP in various solvents only resulted in formation of the carbonate. Thus, the alcohol function primarily had to be protected by a TBDPS group using TBDPSCI with imidazole as base^[145], before the amine could be Boc-protected. Due to the poor nucleophilicity of the pyridylamine, 0.1 eq. DMAP had to be added to accelerate the slow reaction. Desilylation with TBAF gave the desired Boc-protected aminoalcohols (Scheme III-7).



Scheme III-7. Preparation of *N*-Boc-protected 2-pyridinyl aminoalcohols **19-21**.

The precursors of the guanidine mimetics (**5-9**, **12a-d**, **19-21**) could now be combined with Boc-protected tyrosine (α or β) in a Mitsunobu reaction.^[84] Those scaffold molecules were then deprotected and acylated at the amino group to yield a library of >50 compounds, which were employed in a detailed structure-activity-relationship study on the integrins $\alpha\nu\beta3$ and $\alpha5\beta1$.

III.1.2 Design of $\alpha5\beta1$ selective ligands

Since many experiments give ambiguous results about the role of $\alpha\nu\beta3$ in the process of angiogenesis (see II.2.8, p. 27), $\alpha5\beta1$ is now the only distinctly pro-angiogenic integrin which makes it a promising target for antiangiogenic cancer therapy.^[114] To clearly point out the biological activity of $\alpha5\beta1$ in comparison to $\alpha\nu\beta3$, it is crucial to have selective inhibitors of one integrin for biological testings. The growing interest in $\alpha5\beta1$ leads to a steadily increasing demand in highly active and selective compounds, especially small-molecule inhibitors. Up to now, only a small number of $\alpha5\beta1$ selective ligands have been published, with the small library of *J.M. Smallheer et al.* as most active examples (0.2 nM, 200 fold selectivity towards $\alpha\nu\beta3$).^[85] It can be assumed that most published $\alpha\nu\beta3$ ligands are biselective when tested on $\alpha5\beta1$. This could be verified by testing selected compounds of a previously published library of small-molecule $\alpha\nu\beta3$ antagonists^[80, 81], which showed in most cases a small, almost neglectable preference for $\alpha\nu\beta3$ (unpublished results).

The design of new $\alpha5\beta1$ ligands was primarily focused on the tyrosine scaffold as it already has been found versatile for the design of the $\alpha11\beta3$ inhibitor Tirofiban[®].^[83] The superposition of the $\alpha5\beta1$ homology model^[89] with the X-ray structure of $\alpha\nu\beta3$ ^[62] reveals a hydrophobic cleft in the $\beta1$ subunit, where the ($\beta3$) Arg²¹⁴ has been replaced by ($\beta1$) Gly²¹⁷.

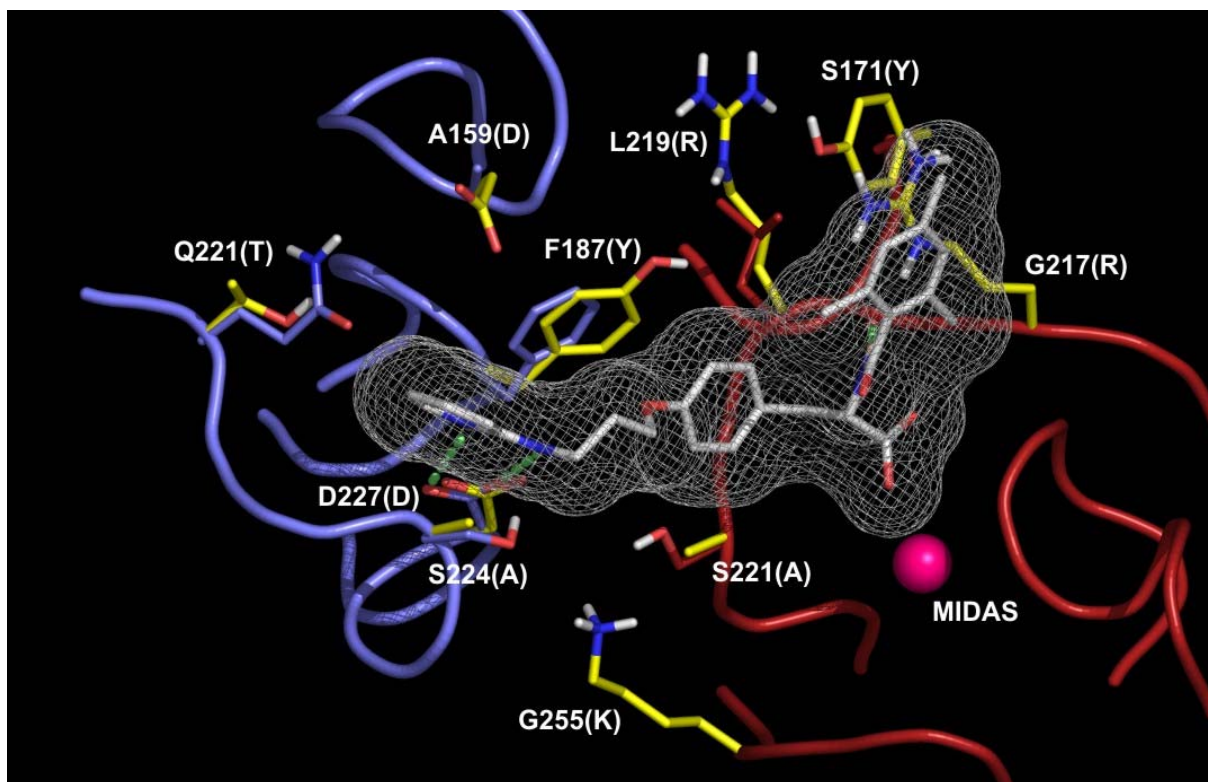
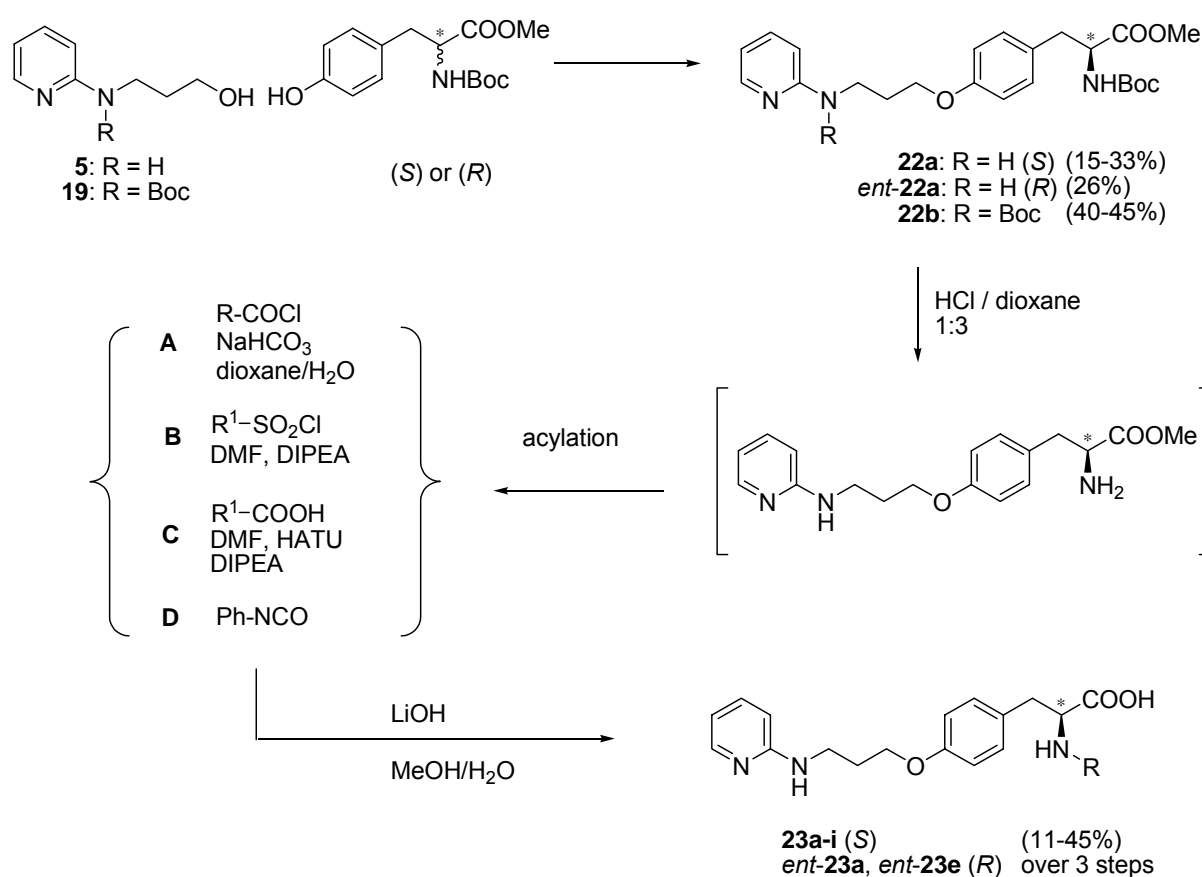


Figure III-2. Ribbon draw of the $\alpha 5\beta 1$ integrin binding pocket ($\alpha 5$ in blue, $\beta 1$ in red) with the predicted binding pose of **23e** (gray). Important receptors side chains are highlighted and corresponding residues of the $\alpha v\beta 3$ integrin are shown in yellow and labeled in parentheses. The MIDAS metal is represented as magenta sphere.

This unoccupied space could be addressed by a sterical demanding, aromatic moiety connected to the α -amino group of the scaffolding tyrosine. A large variety of substituted benzoic acids and sulfonic acids were used to create a sufficiently large compound library. Especially the mesitylenesulfonic acid represented a valuable substituent as the corresponding sulfonamide moiety is already present in the published $\alpha 5\beta 1$ ligand SJ749.^[85] In order to compare the results, the 2-aminopyridine, which has been reported to represent a good guanidine mimetic in many $\alpha v\beta 3$ ligands has been chosen as basic moiety.^[146] The synthesis was performed according to the $\alpha v\beta 3$ selective ligands by coupling of 3-(2-aminopyridyl)propan-1-ol (**5**) to *N*-Boc tyrosine methyl ester to give compound **22a** (Scheme III-8).^[84] The ligand precursor was deprotected and subsequently acylated. Benzoyl groups were introduced with benzoyl chloride in dioxane water using NaHCO_3 as base. The sterical more demanding aromates were coupled to the amine using HATU as coupling reagent. Final step in each synthesis was the saponification of the methyl ester, followed by HPLC purification.

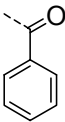
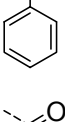
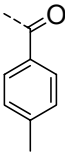
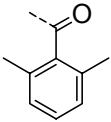
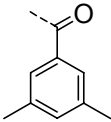
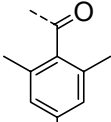
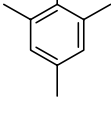
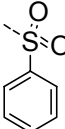
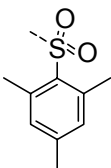
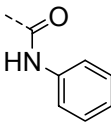
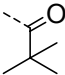


Scheme III-8. Synthesis of ligands bearing different acylated groups at the α -amino group. The different compounds **23** are specified in Table III-2.

The results collected in Table III-2 show that addressing the hydrophobic cavity in $\beta 1$ is the key for the induction of selectivity against $\alpha \nu \beta 3$. This can be easily demonstrated by the substitution of the mesitylenesulfonamide (as present in SJ749), which in this case gives a biselective compound (**23g**) by an amide (**23e**). This can only be explained by the difference in geometry between sulfonamide and carbamide. Compounds **23c** and **23e** highlight the importance of the 2, 6-substitution in contrast to the 4- and 3, 5- substitution. Only the *ortho*-substitution pattern induces a selectivity of 280-520 towards $\alpha 5 \beta 1$. It can be assumed, that the 2, 6-substitution is crucial to turn the aromatic ring out of the plane of the amide bond due to sterical repulsion and to fix the ring in the right position to address the hydrophobic cleft in the $\beta 1$ subunit.

III. Results and Discussion

Table III-2. Affinities of integrin ligands based on the α -tyrosine scaffold bearing various residues in α -position to the tyrosine carboxyl group. The configuration of the α -C of tyrosine is (*S*), the enantiomers with (*R*) configuration are marked with the prefix “*ent-*”, (**23a**, **23e**).

Compound	Procedure	Structure	IC_{50} $\alpha 5\beta 1$ [nM]	IC_{50} $\alpha v\beta 3$ [nM]	S* ($\alpha 5\beta 1$)
23a	A		243	190	0.8
<i>ent</i> - 23a			6700	1030	0.2
23b	C		416	318	0.8
23c	C		3.1	1624	524
23d	C		706	509	0.7
23e	C		2.5	703	281
<i>ent</i> - 23e			150	14700	98
23f	B		284	1.9	0.007
23g	B		46	3.8	0.08
23h	D		1094	37	0.03
23i	A		34	260	7.6

* Selectivity factor for $\alpha 5\beta 1$ calculated as $IC_{50}(\alpha v\beta 3)/IC_{50}(\alpha 5\beta 1)$.

The phenyl urea (**23h**) shows a surprising selectivity for $\alpha\nu\beta3$, which was not further elucidated. The impact of the stereogenic center at the α -carbon could be shown by synthesis of the enantiomeric forms of **23a** and **23e**. Both compounds are 30-60 times less active on $\alpha5\beta1$ and 5-20 times less active on $\alpha\nu\beta3$. In case of the selective compound **23e**, *ent*-**23e** is also less selective, indicating that the proposed binding mode for the (*S*)-enantiomer is not valid for the (*R*)-configuration.

The role of the aromatic residue for selectivity is demonstrated by docking experiments (Figure III-3): The $\alpha5\beta1$ selective ligand **23e** (yellow) and the biselective **23g** (gray) have been docked into both receptors (displayed as Connolly surface, $\alpha5\beta1$ in gray and $\alpha\nu\beta3$ in transparent red). As common feature, both ligands coordinate to the MIDAS-metal ion of the β -subunit and to the Asp residues of the α -subunit. The phenyl ring of the tyrosine is positioned almost the same way for both ligands. The amide bond of **23e** orientates the aromatic residue towards the ($\beta1$)Gly²¹⁷, while the methyl substituents twist the aromatic ring out of the plane of the amide bond. This addresses a hydrophobic cavity, which in $\alpha\nu\beta3$ is blocked completely by the ($\beta3$)Arg²¹⁴ and ($\beta3$)Met¹⁸⁰ side chains. In **23g**, the mesitylene ring is pointing into the open space between the two subunits, directed by the non-planar sulfonamide bond. The lack of selectivity-inducing residue in this region makes **23g** a biselective ligand.

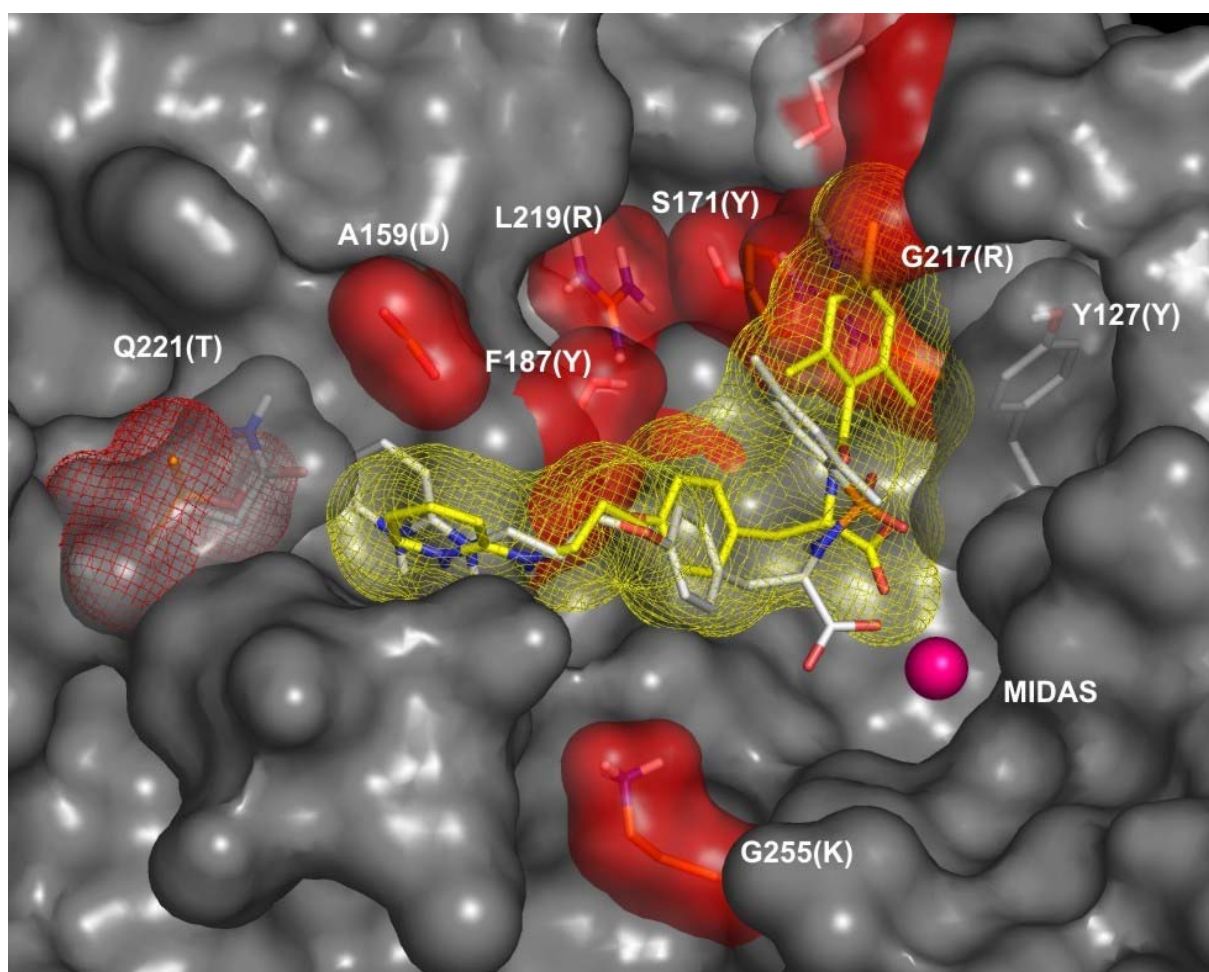
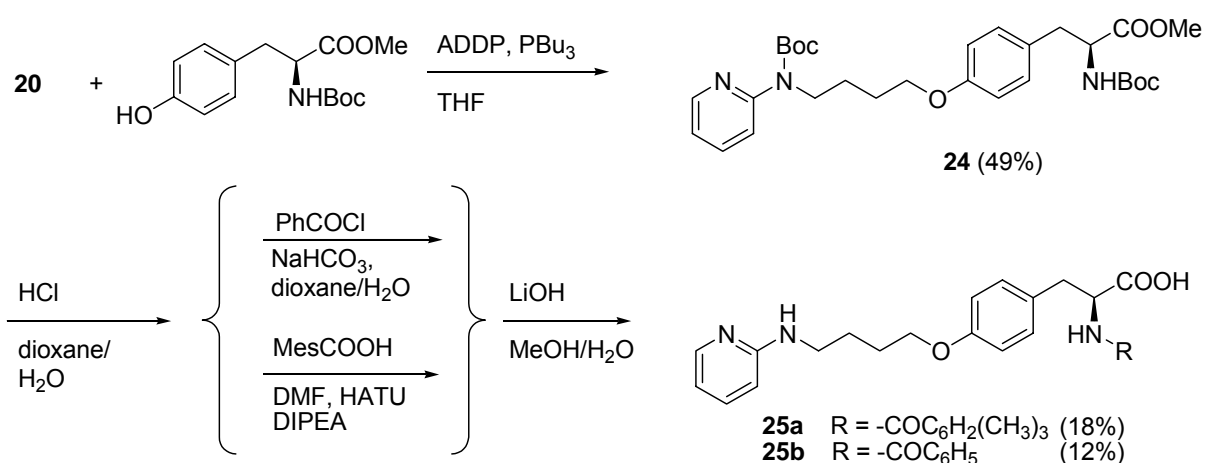


Figure III-3. Superposition of two selected ligands docked into the binding pocket of $\alpha 5\beta 1$ and $\alpha 5\beta 3$. Ligand **23e** (yellow) was found to be $\alpha 5\beta 1$ selective, Ligand **23g** (gray) bisselective. Connolly surface of $\alpha 5\beta 1$ in gray in superposition with $\alpha 5\beta 3$ (transparent red). Bivalent metal ions shown as purple spheres.

It could be argued that there is no need to put the bulky mesitylene group in exactly this position. In fact, docking calculations show alternative binding modes where the aromatic moiety points out of the receptor. However, these binding modes would expose the hydrophobic aromate to the surrounding water, which would result in a decreased affinity. This effect could also be observed to a smaller degree by substitution of the aromatic moiety by a bulky aliphatic substituent (**23i**). Although the receptor affinity and the selectivity is reduced compared to compounds **23c** and **23e**, the reversed selectivity compared to **23a** demonstrates that the aromatic moiety can be substituted by an aliphatic residue suitable to fill the hydrophobic pocket in the $\beta 1$ -subunit. As the results in Table III-2 indicate, the methyl group at position 4 does not contribute to selectivity but points in the direction of the hydroxyl group of the ($\beta 1$)

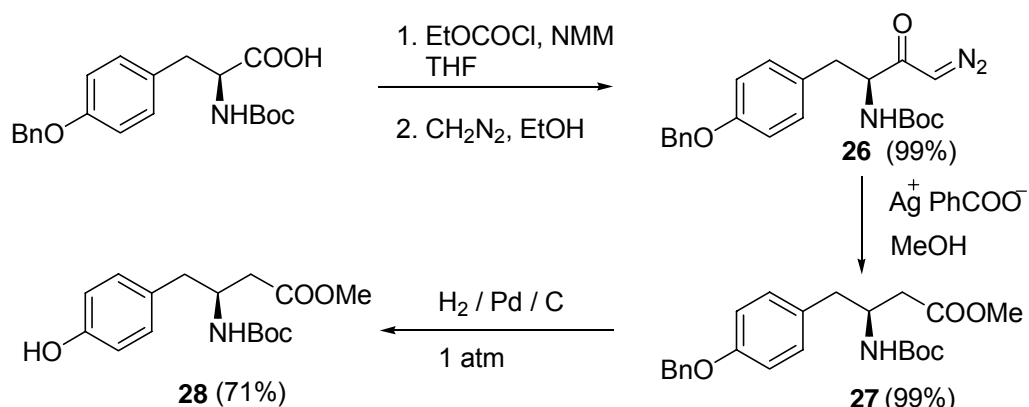
Ser⁵¹⁷ which could be addressed by an H-bond acceptor. Experiments concerning this additional interaction are presented later in this thesis.

The distance between the pyridine C2 and the carboxyl group is 12.65 Å when docked into $\alpha 5\beta 1$. This is a relatively small distance compared to the normally observed distance for $\alpha \nu \beta 3$ ligands (~ 14 Å)^[147] and the molecule SJ749 (13.58 Å docked into $\alpha 5\beta 1$). This difference equals approximately one bond length and is in accordance to other published results.^[148] A novel series of ligands was synthesized to check the effect of ligand length on the binding affinity of the tyrosine based ligands. An elongation of the molecules **23** by one bond could be achieved by either employing β -tyrosine or a 4-(2-aminopyridinyl)butanol in the Mitsunobu coupling. First attempts with unprotected 4-(2-aminopyridinyl)butanol **6** (prepared according to Scheme III-5) didn't afford any product. On activation of the alcohol during the Mitsunobu reaction, the aminoalcohol cyclized under formation of a five-membered ring to give 2-(pyrrolidin-1-yl)pyridine as unique product. This problem could be overcome by *N*-Boc protection following the reaction steps in Scheme III-7.



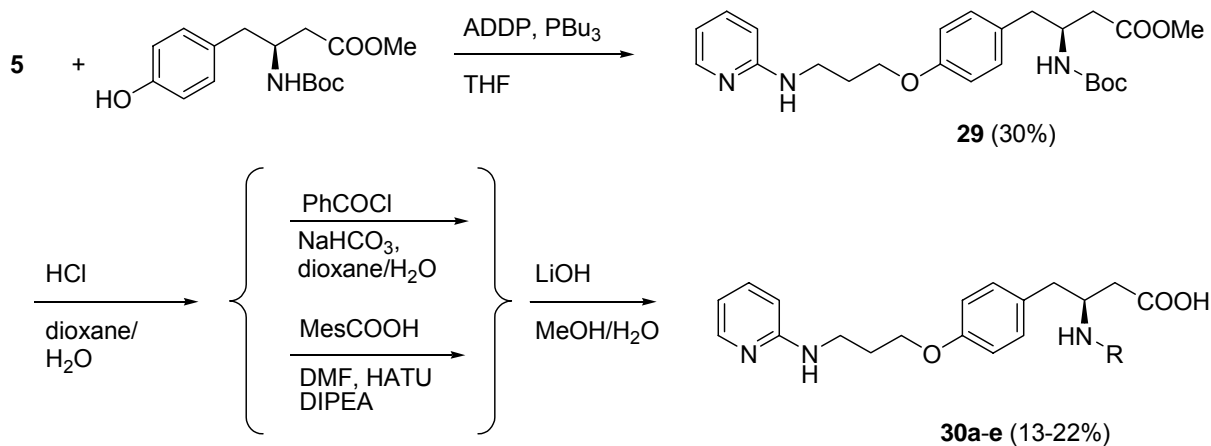
Scheme III-9. Preparation of elongated tyrosine ligands **25a-b**.

The β -tyrosine was synthesized following an Arndt-Eistert protocol starting from the readily available Boc-Tyr(Bn)-OH via generation of a mixed anhydride and reaction with freshly prepared diazomethane.^[149, 150] The diazoketone **26** could be isolated in excellent yields and was subsequently subjected to an Ag⁺ mediated Wolff rearrangement in dry methanol giving the desired methyl ester **27** in moderate yields. After hydrogenolytic cleavage of the benzyl group, the compound **28** could be used as starting material for the Mitsunobu reaction.^[84]



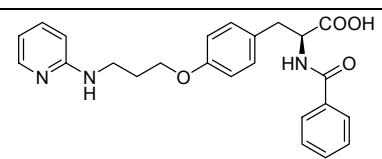
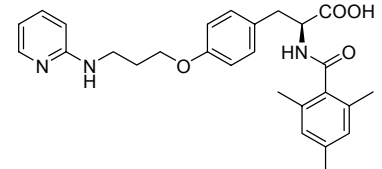
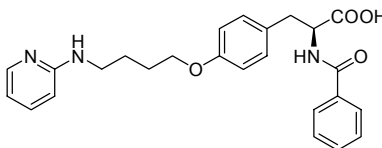
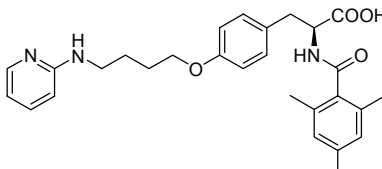
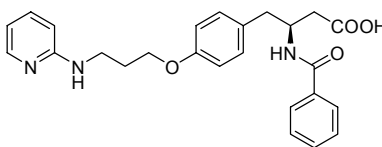
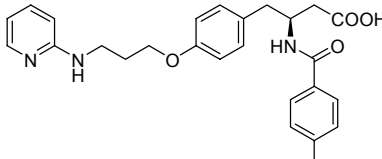
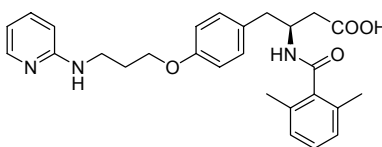
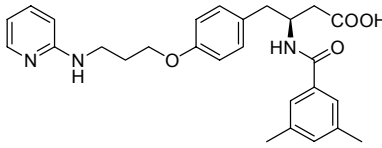
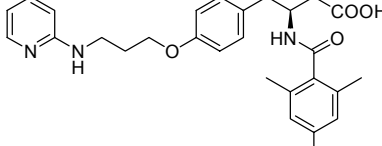
Scheme III-10. Preparation of β -tyrosine via Arndt-Eistert-Homologisation. ^[149, 150]

The elongated ligands synthesized in an analogue manner (Scheme III-11) and provided with a set of differently substituted benzoic acids, which are compared in Table III-3.



Scheme III-11. Preparation of elongated tyrosine ligands based on β -tyrosine. The aromatic residues R are specified in Table III-3.

Table III-3. Comparison of tyrosine ligands with different length.

Compound	Structure	IC_{50} $\alpha 5\beta 1$ [nM]	IC_{50} $\alpha v\beta 3$ [nM]	S^* $\alpha 5\beta 1$
23a		243	190	0.8
23e		2.5	703	280
25a		996	111	0.1
25b		7.2	2685	373
30a		264	1.2	0.005
30b		292	2.2	0.007
30c		142	2.9	0.2
30d		91	5.2	0.06
30e		140	20	0.1

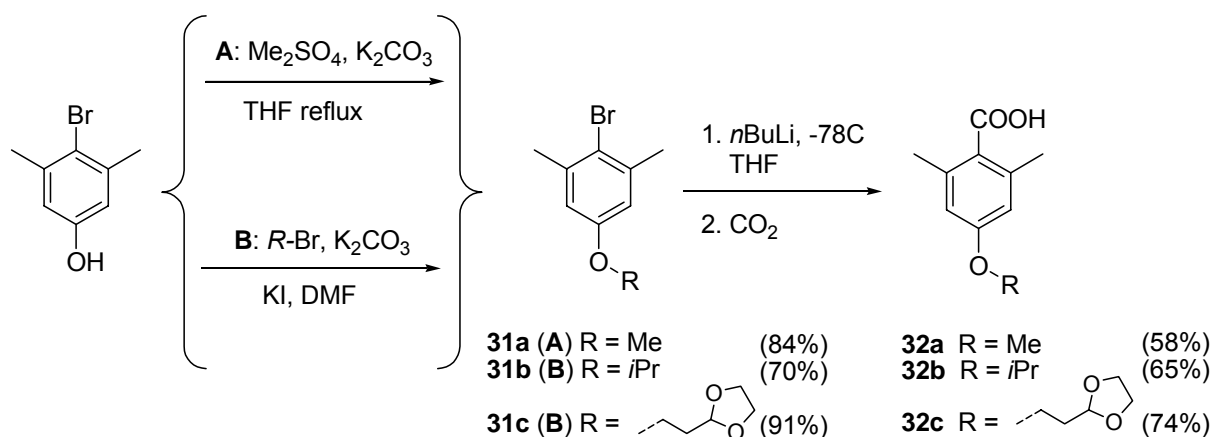
*Selectivity factor for $\alpha 5\beta 1$ calculated as $IC_{50}(\alpha v\beta 3)/IC_{50}(\alpha 5\beta 1)$

Comparing the activities of the “shorter” (**23**) and the “longer” (**25**) α -tyrosine ligands, it is noticeable, that the activities of the elongated compounds drop by the factor 3-4. Simultaneously, the selectivity slightly increases by the factor 1.5. Although both

changes of affinity and selectivity are small considering the absolute value, they are reproducible with differently substituted α -tyrosine ligands. Thus, it can be assumed that the binding pocket of $\alpha 5\beta 1$ is slightly shorter than $\alpha v\beta 3$, favoring ligands of 'reduced' length. Especially striking is the high affinity of the β -tyrosine ligand **30a** towards $\alpha v\beta 3$. It matches the observation, that many previously published $\alpha v\beta 3$ ligands are somehow substituted in β -position.^[81, 84, 137, 151, 152] The β -tyrosine provides higher flexibility and a pullback of the aromate from the selectivity-inducing residues in $\alpha v\beta 3$. Compounds **30b-e** prove that different aromatic substitution pattern have no effect on the selectivity against $\alpha v\beta 3$ when a β -tyrosine scaffold is employed. In contrast to the results with α -tyrosine (Table III-2), the 2, 5-methyl substitution has a visible but almost negligible effect on selectivity. Considering the binding mode shown in Figure III-3, this can be explained by a binding mode for β -tyrosine ligands, where the hydrophobic cavity in $\alpha 5\beta 1$ can not be addressed by the aromatic residue.

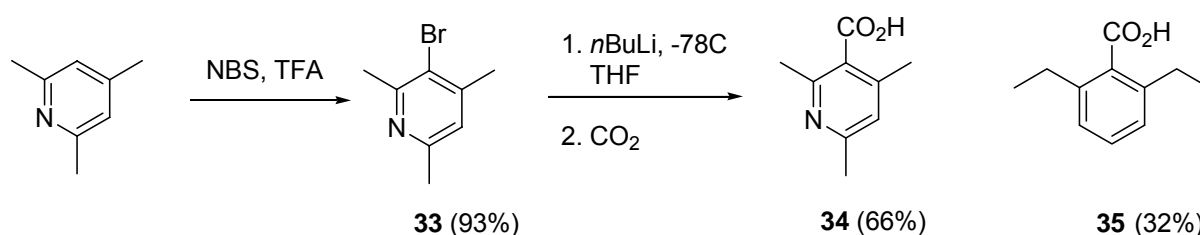
In the knowledge, that the specificity inducing moiety in the discussed ligands is the 2, 6-substituted benzamide, various similarly substituted benzoic acids have been purchased or synthesized to further elucidate the near proximity of the $\beta 1$ binding pocket, which is addressed by the aromatic moiety. Figure III-3 shows the hydroxyl function of ($\beta 1$)Ser⁵¹⁷ in the vicinity of the 4-methyl group of the mesitylene. Substitution of this methyl group by an alkoxy group could both establish an additional hydrogen bond which can only be formed in $\alpha 5\beta 1$ and also serve as connection for a linker – which can be important for labeling and immobilization of the compounds in further studies. The 4-alkoxy benzoic acids **32a-c** were prepared starting from the commercially available 2,6-dimethyl-4-hydroxybromobenzene by alkylation, followed by a bromine-lithium exchange and reaction with solid carbon dioxide. For the alkylation, three different protocols have been used according to the sterical demand of the alkyl group. While methylation proceeded with high yields, the introduction of the isopropyl group demanded higher temperatures, more polar solvents and catalytic amounts of iodide to accelerate the nucleophilic substitution. The acid **32c** contains a protected aldehyde function and was synthesized to enable the introduction of linker systems for immobilization or labeling purposes (Scheme III-12). As predicted by the docked structure (Figure III-3),

substituents in *para*-position of the aromate point out of the receptor and can be used for the attachment of linkers – a fact that has been widely used on $\alpha\text{v}\beta\text{3}$ ligands. [153, 154]



Scheme III-12. Preparation of 2, 6-methyl benzoic acids **32a-c**.

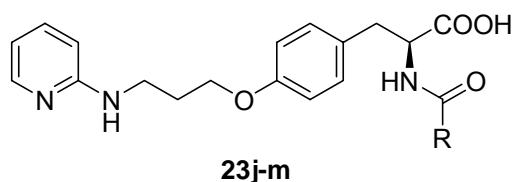
Another 2, 6-dimethyl aromatic acid which could easily be prepared was the 2, 4, 6-trimethyl nicotinic acid. Bromination of collidine using NBS in TFA gave the brominated product in moderate yields which then could be converted to the corresponding acid using the same procedure as in Scheme III-12. The 2, 6-diethyl benzoic acid **35** was prepared from the corresponding bromoarene in an analogue way (Scheme III-13).



Scheme III-13. Preparation of 2, 4, 6-trimethyl nicotinic acid **34** and 2, 6-diethyl benzoic acid **35**.

The synthesized aromatic acids were used to acylate the α -tyrosine ligand precursors **22a,b** with HATU as coupling reagent giving a series of ligands. The resulting ligands and their activity / selectivity profile is shown in Table III-4.

III. Results and Discussion



Scheme III-14. Expanded series of ligands with a 2,6 dimethylarylamide moiety. Residue R is specified in Table III-4.

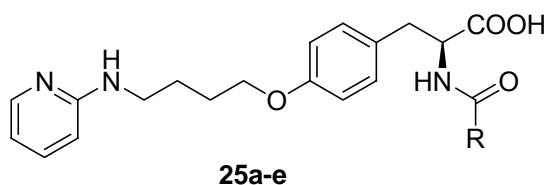
Table III-4: Activity and selectivity profile of ligands bearing 2,6 substituted aryl amides.

Compound	R	IC_{50} $\alpha 5\beta 1$ [nM]	IC_{50} $\alpha v\beta 3$ [nM]	S^* $\alpha 5\beta 1$
23c		3.1	1624	530
23e		2.5	703	281
23j		1.0	188	188
23k		0.7	279	399
23l		2.8	41	15
23m		8.9	188	21

*Selectivity factor for $\alpha 5\beta 1$ calculated as $IC_{50}(\alpha v\beta 3)/IC_{50}(\alpha 5\beta 1)$

The results prove that an additional interaction to the $\beta 1$ -subunit can be established by introduction of a hydrogen bond acceptor in *para*-position. The new compounds

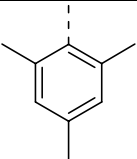
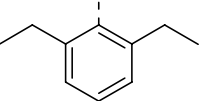
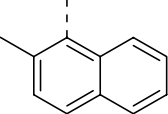
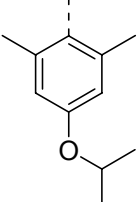
show increased activity, pushing the IC_{50} value into sub-nanomolar range (**23j**, **23k**). The selectivity is not affected and lies still in the area of 200-400 fold. The activity / selectivity profile of compounds **23b**, **c** is approaching the reference compound SJ749 (0.2 nM on $\alpha 5\beta 1$ – 49 nM on $\alpha v\beta 3$), but displays a lower molecular weight and a much easier way of preparation. The tolerance towards bulky alkyl substituents in *para*-position (**23k**) allows - as predicted - the attachment of linker systems for labeling or immobilization purposes. The importance of the 2, 6-substituents, which has been mentioned before was examined by the introduction of different atoms of functional groups in this position which display different sterical demand and different electronic effects. While in comparison to the mesitylene group (**23e**) the corresponding nicotinic acid (entry 8) shows a slight loss of activity on $\alpha 5\beta 1$ (and small gain of $\alpha v\beta 3$ activity), the trichlorophenyl substituent (**23l**) displayed a significant (and surprising) loss of selectivity by revealing a high $\alpha v\beta 3$ activity. Another two ligands with similar, rotationally restricted aromates have been synthesized on the elongated scaffold **25**. Their selectivities benefit for the general increase in selectivity, which was observed on elongated α -tyrosine ligands.



Scheme III-15. Elongated α -tyrosine scaffold **25**. Aryl residues R are defined in Table III-5.

The highly selective compounds in Table III-5 are all more or less highly active (the activity loss and selectivity gain resulting from scaffold elongation has been discussed earlier) and display the highest selectivities of all yet synthesized, tyrosine based compounds (**25c**, **e**). Following the observation that the *para*-methyl group did not contribute to $\alpha 5\beta 1$ binding, the extension of the two *ortho*-substituents has a big impact on selectivity - mostly as a result of decreased $\alpha v\beta 3$ -activity. Due to the sterical profile of the $\beta 3$ -subunit, the aromatic group should point straight out of the $\alpha v\beta 3$ receptor. For α -tyrosine scaffolds, this means that the aromate comes quite near the residues flanking the $\beta 3$ -MIDAS region. It can be assumed that substituents with a higher sterical demand perpendicular to the plane of the aromate disfavor this binding mode and further decrease activity on $\alpha v\beta 3$.

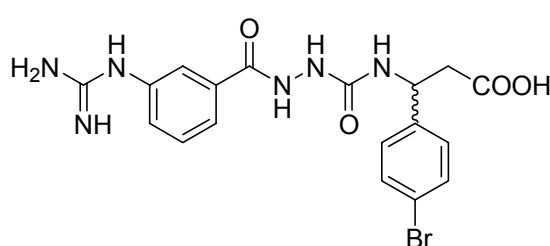
Table III-5. Ligands with 2, 6-disubstituted aryl amides based on the elongated α -tyrosine scaffold **25**.

Compound	R	IC_{50} $\alpha 5\beta 1$ [nM]	IC_{50} $\alpha v\beta 3$ [nM]	S^* $\alpha 5\beta 1$
25b		7.2	2685	373
25c		13.5	16800	1244
25d		6.0	1412	235
25e		2.0	1455	728

III.1.3 Design of $\alpha v\beta 3$ selective ligands

The first $\alpha v\beta 3$ -ligands, which were synthesized for anti-angiogenic cancer therapy, had to face the problem of selectivity against the platelet integrin $\alpha IIb\beta 3$. This problem could be overcome using ligand-based design and gave a huge number of sufficiently $\alpha v\beta 3$ selective compounds. [28, 30, 36, 81, 147] However, due to the lack of reliable testing systems, those ligands were not tested on $\alpha 5\beta 1$. The evaluation of the $\alpha 5\beta 1$ affinity for selected $\alpha v\beta 3$ ligands developed in our group revealed mainly biselective ligands, most of them with a 10-20 fold selectivity towards $\alpha v\beta 3$ (Scheme III-16). In order to study differences in the biological activities of both integrins, it would be necessary to provide not only $\alpha 5\beta 1$ selective ligands but also the inverse selectivity. The previously best $\alpha v\beta 3$ -ligand was the β -tyrosine derived **30a**, with a 220 fold selectivity against $\alpha 5\beta 1$. The selectivity is the sum of the favorable β -substitution (for $\alpha v\beta 3$, see ligands in Scheme III-16) and the unfavorable (for $\alpha 5\beta 1$)

length of the ligand. A close look at the binding pockets (Figure II-5) indicates that the $\alpha 5\beta 1$ binding site is significantly shorter, especially in the α -subunit, which binds the aminopyridine.



cyclo(-RGDfV-)
 $\alpha v\beta 3$ IC_{50} = 3.5 nM
 $\alpha 5\beta 1$ IC_{50} = 62 nM

$\alpha v\beta 3$ IC_{50} = 2.6 nM
 $\alpha 5\beta 1$ IC_{50} = 2.5 nM

cyclo(-RGDfN-MeVal-)
(Cilengitide^(R))
 $\alpha v\beta 3$ IC_{50} = 0.6 nM
 $\alpha 5\beta 1$ IC_{50} = 11 nM

Scheme III-16. Examples of $\alpha 5\beta 1/\alpha v\beta 3$ biselective ligands initially developed for the $\alpha v\beta 3$ integrin. [28, 30, 36, 81]

To elucidate the impact of the shortened $\alpha 5$ -subunit on ligand binding, a new series of β -tyrosine-based compounds was synthesized, each substituted with a methyl group in different positions of the pyridine ring. The methylpyridin-2-ylaminopropanoles were synthesized as described in Scheme III-6 (p. 42). Due to the especially low yield in case of the 4-methyl substitution, the Boc-protection of **12c** was essential (**21**, according to Scheme III-7, p. 42).

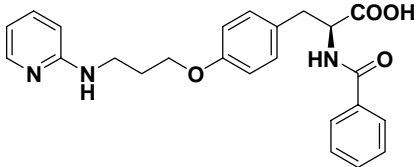
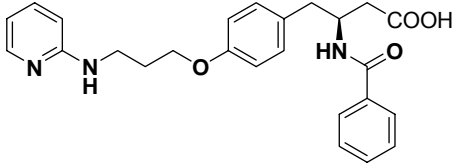
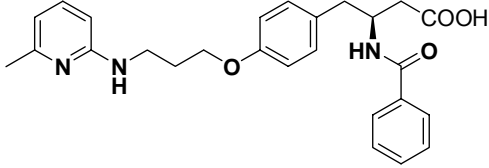
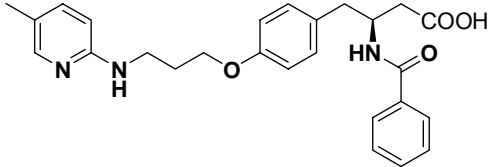
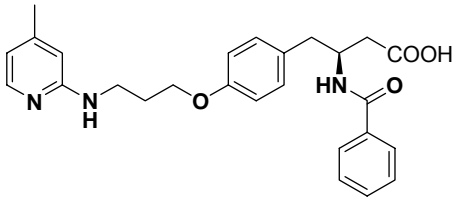
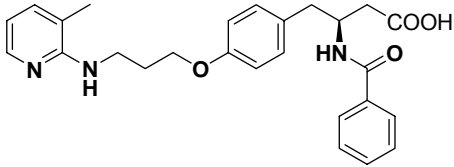


Scheme III-17. Mitsunobu reactions leading to ligand precursors **36a-d**.

The final compounds were prepared from the precursors **36** by first Boc-deprotection with 10% aqueous HCl in dioxane, followed by acylation with benzoyl chloride in aqueous dioxane using NaHCO_3 as base and final saponification of the methyl ester with LiOH in methanol / water. Purification by RP-HPLC afforded the compounds as TFA salts which were tested for $\alpha 5\beta 1$ and $\alpha v\beta 3$.

III. Results and Discussion

Table III-6. Binding affinities of compounds **37a-f**. **37d** shows a good selectivity towards $\alpha\nu\beta3$ against $\alpha5\beta1$. IC_{50} values are from an ELISA assay with immobilized receptor.

Substance	Structure	IC_{50} $\alpha5\beta1$ [nM]	IC_{50} $\alpha\nu\beta3$ [nM]	S* $\alpha\nu\beta3$
23a		243	190	0.8
30a		264	1.2	220
37a		3945	13	303
37b		215	2.2	98
37c		67	0.9	74
37d		6969	490	14

*Selectivity factor for $\alpha\nu\beta3$ calculated as $IC_{50}(\alpha5\beta1)/IC_{50}(\alpha\nu\beta3)$.

The results in Table III-6 are in good agreement with the predictions derived from the homology model. Figure III-4 shows an overlay of the Connolly surfaces of $\alpha\nu\beta3$ (solid gray) and $\alpha5\beta1$ (red mesh). In general, the results show clearly the preference of β -substituted acids in respect of binding affinity towards $\alpha\nu\beta3$ (**23a** vs. **30a**). It can be assumed that the ($\alpha5$)Gln²²¹ (Thr²¹² in $\alpha\nu$) shortens the groove responsible for the binding of the aminopyridine in $\alpha5\beta1$. A methyl substituent at the appropriate position

should result in a sterical clash and a strong decrease of binding affinity, as demonstrated for **37a**. While methyl substitution at position 4 (**37c**) seems to slightly increase affinity towards $\alpha 5\beta 1$, the 3-methyl-2-aminopyridine **37d** surprises with a high loss of receptor affinity. This can be explained by a twist of the aromatic ring around the C2-NH axis in order to avoid sterical repulsion between the methyl group and the alkyl chain at the nitrogen.

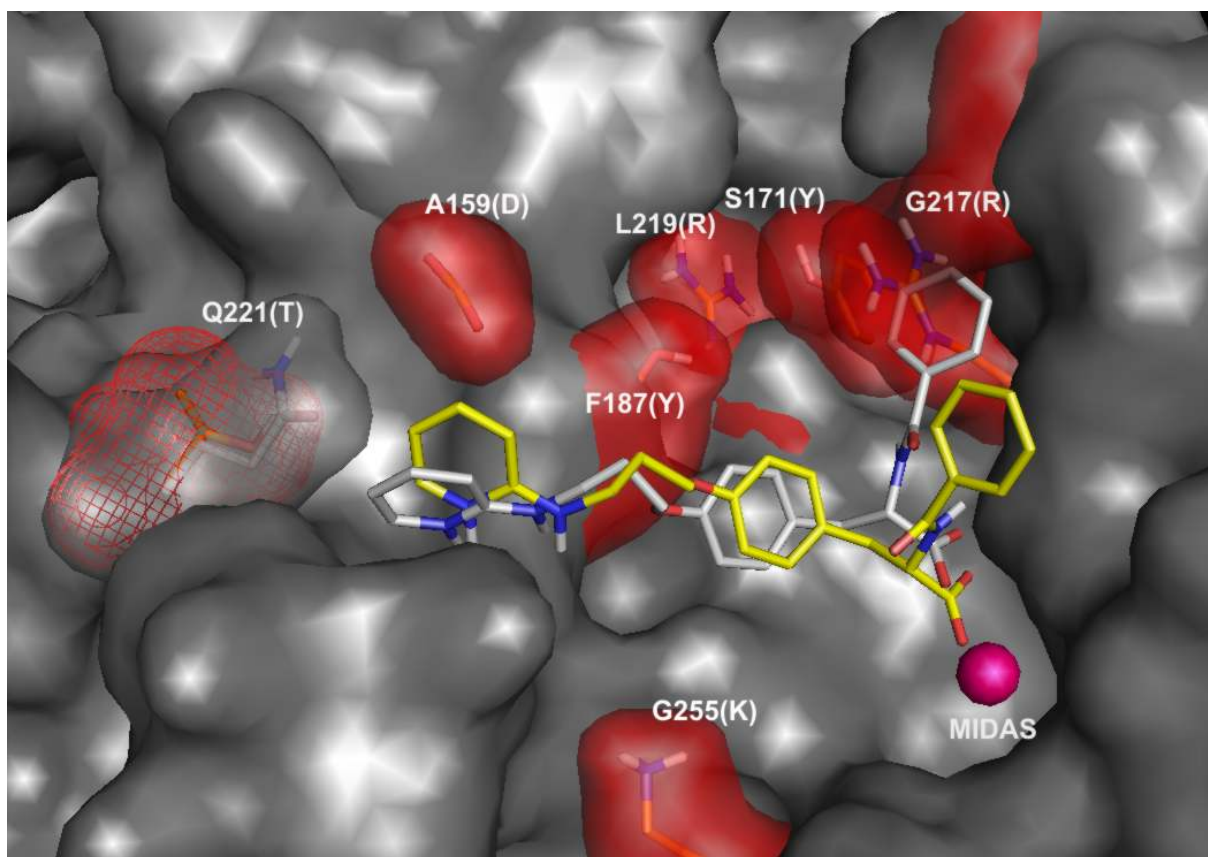


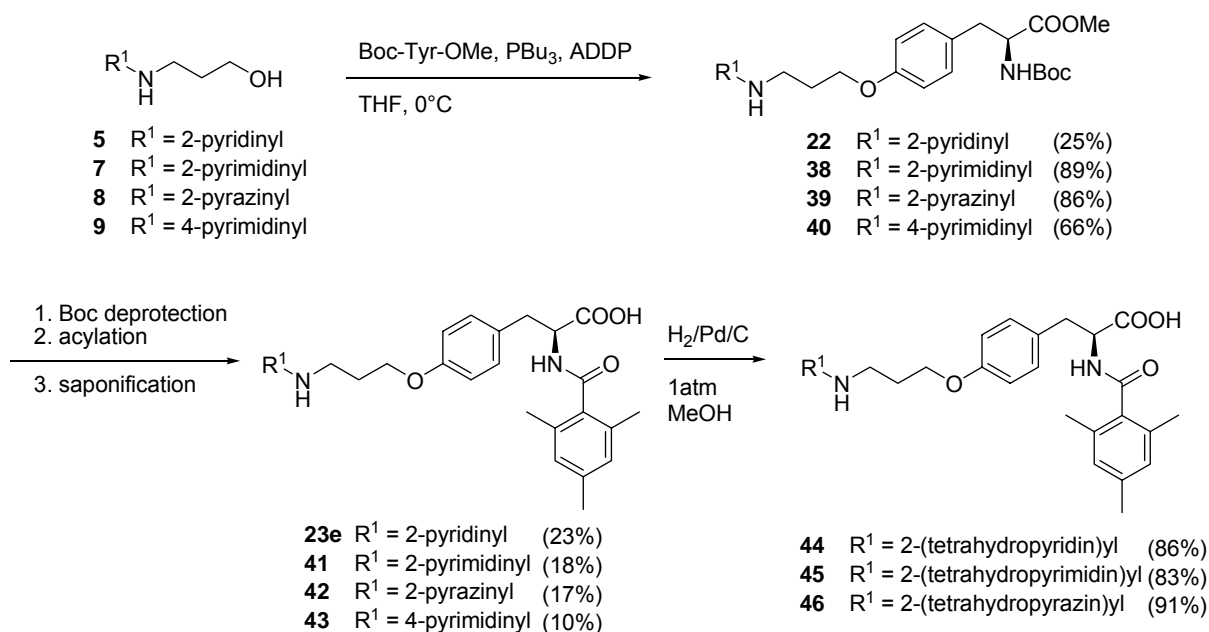
Figure III-4. Overlay of the Connolly-surfaces of $\alpha 5\beta 3$ (red) and $\alpha 5\beta 1$ (gray) with docked structure of compound **23a** (gray in $\alpha 5\beta 1$, yellow in $\alpha 5\beta 3$). The most important residues are labeled for $\alpha 5\beta 1$, residues in $\alpha 5\beta 3$ are given in parentheses. The corresponding β -tyrosine compounds didn't give unambiguous docking results due to their high flexibility.

III.1.4 Impact of different basic moieties on $\alpha 5\beta 1$ / $\alpha 5\beta 3$ affinity

During the course of integrin ligand development in pharmaceutical chemistry, a large variety of different basic moieties have been employed to mimic the arginine in the RGD sequence. The use of the guanidine group is usually hampered by its high basicity and poor bioavailability. Better results have been achieved using e.g.

III. Results and Discussion

aminopyridines, benzamidines and 4,5-dihydroimidazolamines, which exhibit reduced basicity and increased lipophilicity. [30, 137, 155] In an attempt to study the effect of different basic groups on the activity towards $\alpha 5\beta 1$, a series of ligands was prepared with different basic groups and compared to the 'arginine-like' guanidine function in ligands **4a,b**. [139] As predicted in the homology model [89] (chapter II.2.5), the binding pocket of $\alpha 5$ and αv display some major differences: The $\alpha 5$ subunit lacks one of the two Asp residues involved in binding of the ligand's guanidine group and it is slightly shortened by the glutamine side chain ($\alpha 5$)Gln²²¹ (Figure II-7, Figure III-4). This means that the surrounding of the basic function in $\alpha 5$ is more lipophilic and tighter than in αv . The latter issue has already been successfully employed to design $\alpha v\beta 3$ selective ligands (chapter III.1.3). A more lipophilic guanidine mimetic could increase affinity towards $\alpha 5\beta 1$, while at the same time the ($\alpha 5$)Gln²²¹ could be addressed by a hydrogen bond acceptor. This could be achieved by introduction of a second nitrogen atom into the aminopyridine ring.

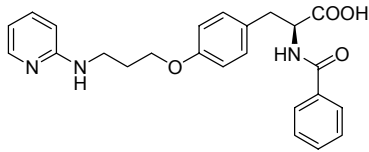
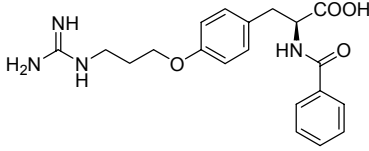
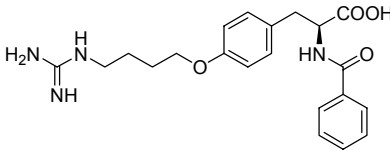
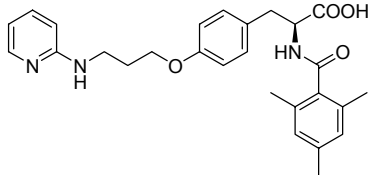
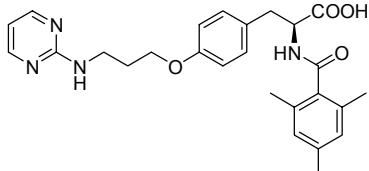


Scheme III-18. Preparation of α -tyrosine based ligands with different heterocyclic basic moieties.

The synthesis of the ligands **41-46** followed the straightforward procedure described at the beginning of this chapter. The heteroaromatic moieties were further reduced by hydrogenation using Pd on carbon as catalyst to give the corresponding cyclic guanidinium groups. As aromatic moiety, the mesitylene group was chosen to be

compared with other $\alpha 5\beta 1$ selective compounds of the previously synthesized aminopyridine series. The results of the affinity testings are resumed in Table III-7. The first two guanidine ligands (**4a**, **b**) exhibit once again the preference of elongated ligands for $\alpha v\beta 3$ and of shortened ligands for $\alpha 5\beta 1$. Compared to the aminopyridine ligand, they show higher affinities on both integrins. Considering that the major interaction between the basic moiety and the ($\alpha 5/\alpha v$)Asp is of pure ionic nature, this is in accordance with the high basicity of the guanidine, which is more extensively protonated* (pKa = ~ 13.0) than the aminopyridine (pKa = ~ 6.7).

Table III-7. Activity / selectivity profile of α -tyrosine based ligands with different basic moieties.

Compound	Structure	IC_{50} $\alpha 5\beta 1$ [nM]	IC_{50} $\alpha v\beta 3$ [nM]	S^* $\alpha 5\beta 1$
23a		243	190	0.8
4a		60	131	2.2
4b		66	39	1.7
23e		2.5	703	280
41		73	n.d.	-

* pKa values were calculated using SPARC v.3.1 [<http://ibmlc2.chem.uga.edu/sparc/>]

III. Results and Discussion

42		99	n.d.	-
43		126	>20000	>160
44		42	5375	128
45		1.8	221	123
46		54	11082	205

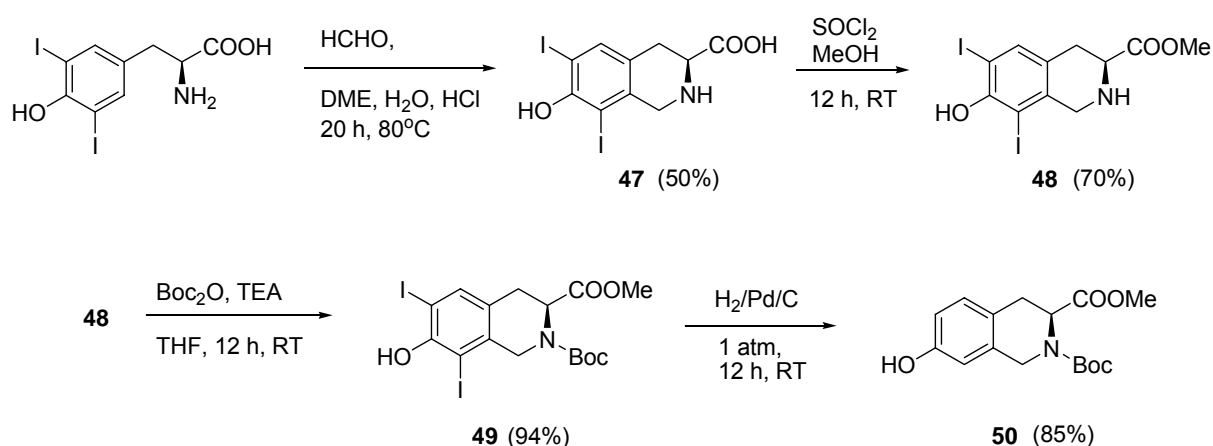
*Selectivity factor for $\alpha 5\beta 1$ calculated as $IC_{50}(\alpha v\beta 3)/IC_{50}(\alpha 5\beta 1)$

n.d. = not determined

The activities of the pyrazine / pyrimidine ligands (**41-43**) also seem to be correlated with the pKa value thus showing reduced affinities for $\alpha 5\beta 1$. The selectivity – as it can be assumed – lies in the same region as the reference ligand **23e**, which pushes the IC_{50} values on $\alpha v\beta 3$ beyond 20 μ M, which was out of the measuring range of the binding assay. Comparison of the reduced tetrahydropyrimidines (**45**) – pyrazines (**46**) displays the same pKa-dependence as stated above. With selectivities of 100-200, which seem to be independent from the basic groups throughout the series, the cyclic guanidine (pKa = ~13.7) is tested 25 fold more active than the tetrahydropyrazine (pKa = ~6.9). An additional hydrogen bond to stabilize the binding in the $\alpha 5$ -subunit could not be observed. It may be argued whether the additional interaction is not present in the ligands **42** and **43**, or whether the effect is simply overruled by the loss of activity due to the decrease in pKa.

III.1.5 Introduction of constraints into tyrosine-based ligands

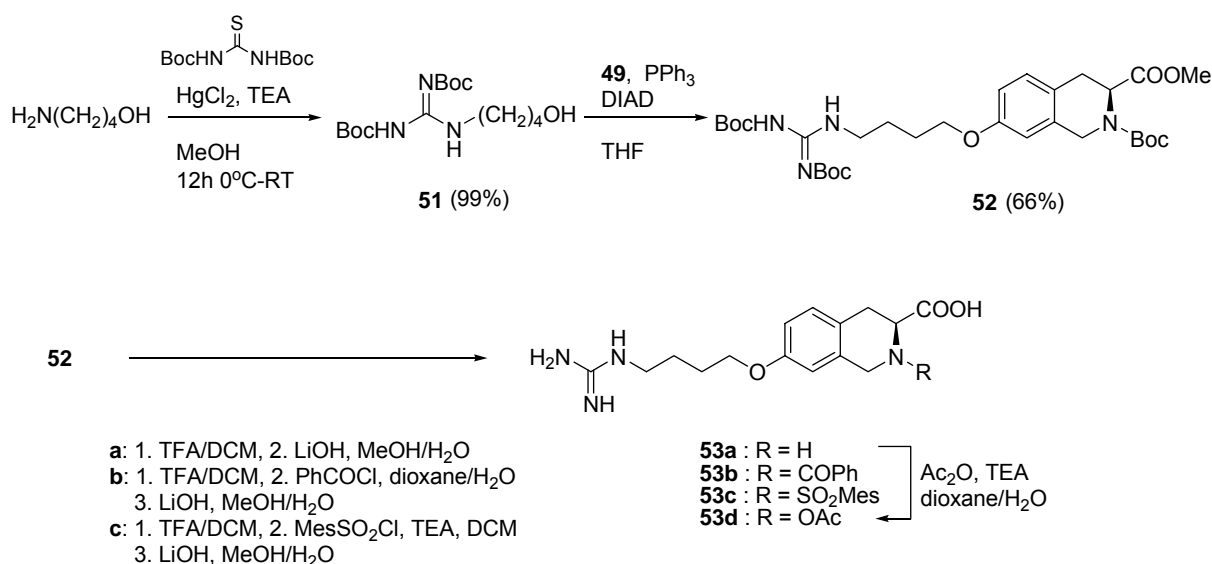
A widely used approach to increase the selectivity of ligands is the introduction of conformational constraints. ^[26] In the case of the tyrosine-based ligands, this could be achieved by ring-closure to the corresponding 7-hydroxy-tetrahydroisochinolines. The fully protected building block **50** was accessible by a four-step synthesis starting from the commercially available 2, 5-diiodotyrosine.



Scheme III-19. Synthesis of fully protected building block **50**.

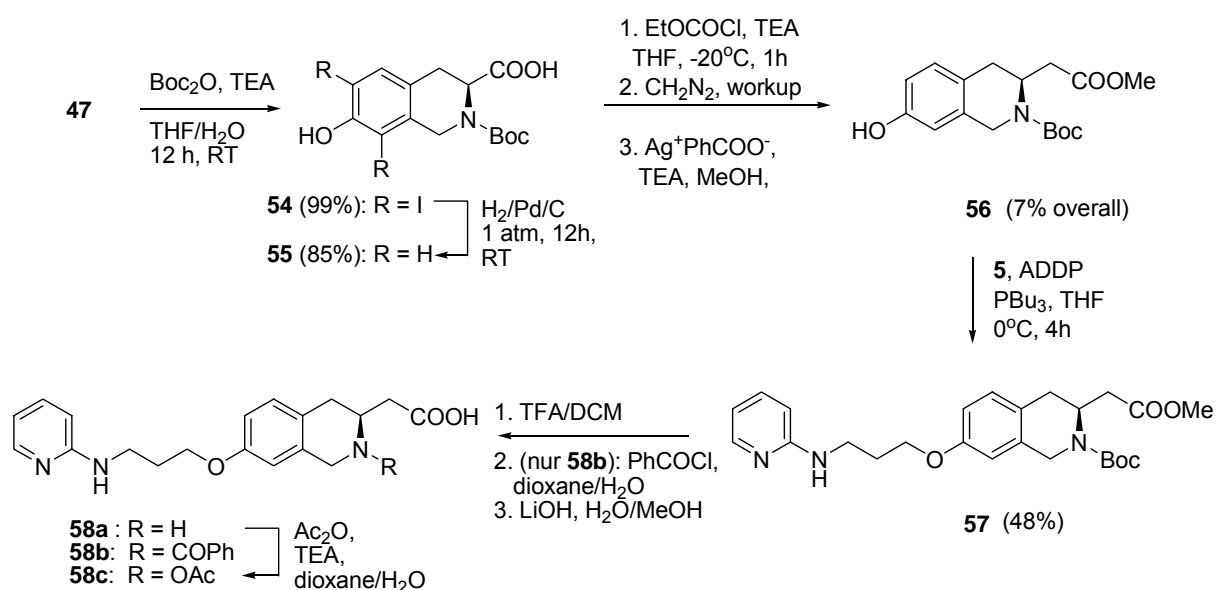
Key step was the Pictet-Spengler cyclization of the 2, 5-diiodotyrosine, which succeeded in moderate yields. ^[156] The iodine serves as protecting group to block the 2 and 5 positions from reacting with formalin, which would result in polymerization. After synthesis of the methyl ester under acidic conditions followed by Boc-protection, the iodine was removed by hydrogenation to give **50** in 28% overall yield. ^[156] The corresponding integrin ligands were synthesized in the usual way according to Scheme III-20.

III. Results and Discussion



Scheme III-20. Synthesis of constrained ligands **53a-d**.

In this series of compounds, the linear aminoalcohol was guanidylated^[139] in the first step and then coupled on the building block **50** by Mitsunobu reaction.^[84] Although the yield was moderate, the results in some cases were not well reproducible and the synthetic strategy was revised in favor of the coupling of Cbz-protected aminoalcohols as described in chapter III.1.2. The strongly constrained tetrahydroisochinolines should be compared with their homologues, derived from the β -amino acid analogue of building block **50**. These compounds should possess higher flexibility as the carboxyl group is not directly attached to the ring system. The synthesis was performed as for the linear compound **27**. Not surprisingly, but in contrast to the literature procedure, the activation of the *O*-unprotected tetrahydroisochinoline via a mixed anhydride gave a high degree of *O*-acylation. As the synthesis was performed only once, the yields are not optimized. Regarding the data, the substitution of the guanidine group by an aminopyridine does not affect the activity very much and should at least allow a qualitative comparison between the compounds **53** and **58**.



Scheme III-21. Synthesis of a series of compounds based on the homologue 7-hydroxy-tetrahydroisochinoline scaffold.

The biological evaluation of the constrained ligands is shown in Table III-8.

Table III-8: Biological evaluation of constrained compounds **53** and **58**.

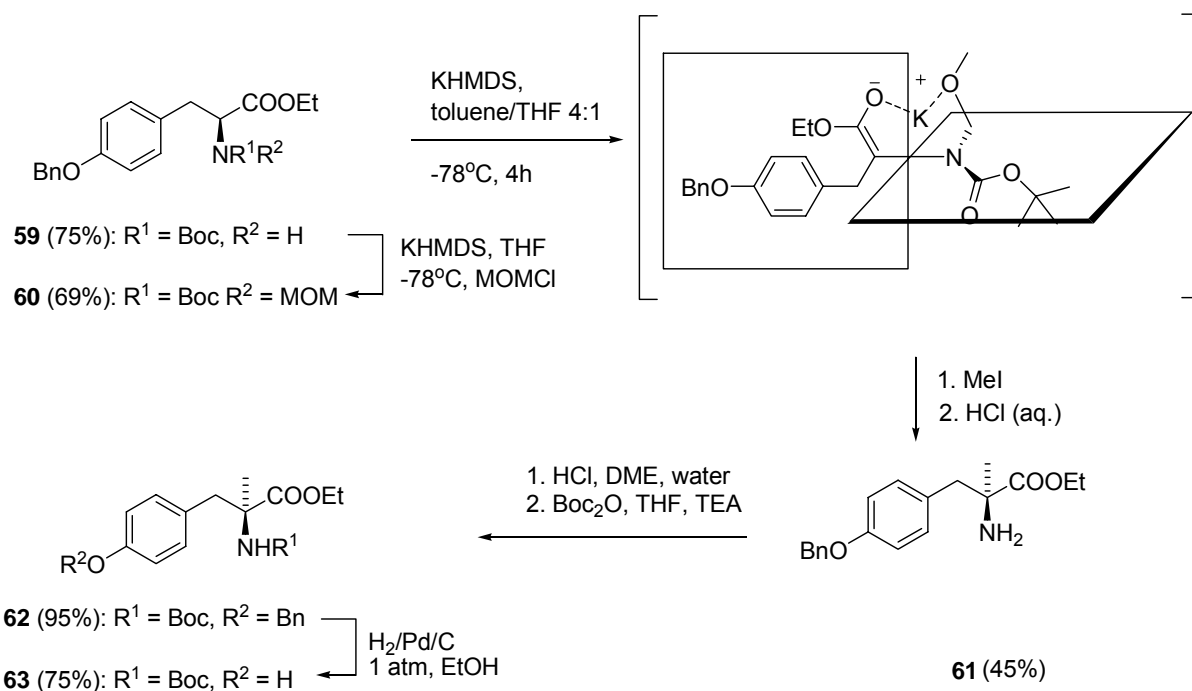
Compound	$IC_{50} \alpha 5\beta 1$ [nM]	$IC_{50} \alpha v\beta 3$ [nM]
53a	>10 μ M	n.d.
53b	>10 μ M	n.d.
53c	15.9 μ M	330
53d	>10 μ M	n.d.
58a	>10 μ M	1411
58b	7669	127
58c	>10 μ M	438

*n.d. = not determined

Unfortunately, the introduction of a six-membered ring spoils any activity towards $\alpha 5\beta 1$. It is obvious that the remaining conformational space of the rigid compound does not include the biologically active conformation. This risk is ubiquitous whenever a constraint is introduced to a biologically active molecule^[26], especially in this case, where the constraint is introduced at such a sensible position as the carboxyl group, where the sterical demanding α -amino-substituent may easily clash with the residues surrounding the MIDAS. As for $\alpha 5\beta 1$, the size of this substituent is regardless. The

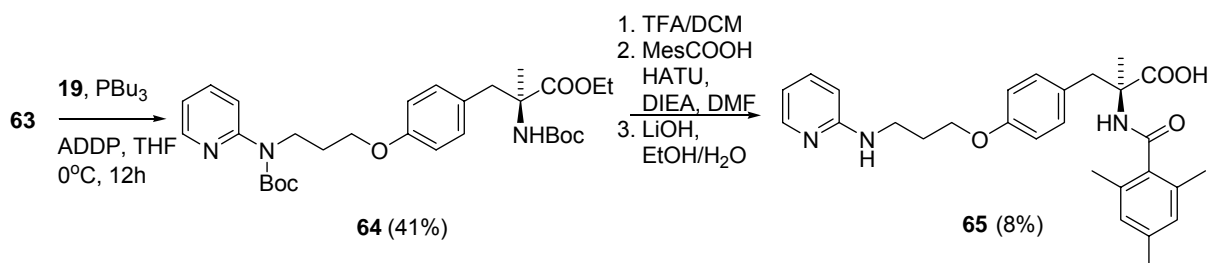
non-substituted **53a** is essentially inactive (in most cases, compounds were not tested beyond 10 μ M), which may be due to a lack of interactions in this region whereas both acetyl and benzoyl substitution were not able to give any activity at all – probably due to sterical clash with the receptor. The series of homologues with a higher flexibility around the carboxylate show only one mentionable compound. The benzoyl-substituted **58b** shows some activity, but still hints at an unfavorable orientation of the phenyl ring. In contrast to $\alpha 5\beta 1$, $\alpha v\beta 3$ tolerates the structural changes to a higher degree. This is firstly demonstrated by the activity of **53c**, the only ligand of the series with an α -cyclic carboxylate showing any activity at all on integrins. The series of homologues (**58**) is active on $\alpha v\beta 3$, highlighting once again the importance of the aromatic substitution (IC_{50} decreases with substituent size **58a**>**58c**>**58b**). Nevertheless, compared to the flexible analogue, **58b** is still 100 fold less active which excludes the tetrahydroisochinoline as a appropriate scaffold for both $\alpha 5\beta 1$ and $\alpha v\beta 3$ integrins.

A possibility to restrain α -tyrosine based ligands without forcing the α -carbon into a ring system is the introduction of an α -methyl group. The potential of α -substituted amino acids in peptide chemistry has already employed to create bioactive compounds. While in the non-methylated compound (**23e**) the α -hydrogen points away from the receptor surface, in the alternative binding modes of **23e** in $\alpha v\beta 3$, were the mesitylene points out of the receptor, the α -hydrogen is turned towards the residues flanking the MIDAS. Substitution of the α -hydrogen with a more sterical demanding methyl group could disfavor especially this binding mode and reduce the activity on $\alpha v\beta 3$. Key step of the synthesis^[157, 158] was the formation of an asymmetric enolate by chelation of potassium by the enolate-oxygen and the MOM-protecting groups at the α -nitrogen (Scheme III-22). Sequential deprotection and protection steps gave building block **63** in 20% yield over 6 steps.



Scheme III-22. Synthesis of α -methyl tyrosine building block **63**.^[157, 158] The displayed intermediate represents a hypothetical chelation complex which is able to conserve chirality.

Compound **63** was used as starting material in the synthesis of **65**. The Boc-protected aminopyridine **19** was used to increase the yields of the Mitsunobu reaction, whereas the following reactions were carried out as described previously. The coupling of the α -methylated compound with 2, 4, 6-trimethylbenzoic acid was hampered by the strong sterical repulsion between the activated acid and the amine. Even though different ways of activation were tried, HATU proved to be the reagent of choice considering the high activity and the selectivity of the acylation of the primary amine against the less nucleophilic secondary pyridinylamine. Still, reaction times exceeded one week of stirring at room temperature.



Scheme III-23. Preparation of α -methylated compound **65**.

Unfortunately, the compound **65** was completely inactive on $\alpha 5\beta 1$ ($IC_{50}(\alpha 5\beta 1) = \sim 13 \mu M$, $IC_{50}(\alpha v\beta 3) = > 20 \mu M$). This may be the result of a sterical clash with the residues around the MIDAS region (which could not be predicted by the model) or the result of an unfavorable arrangement of the mesitylene group due to sterical repulsion between the aromatic methyl groups and the α -methyl group. This strain has already been observed as cause of the extremely poor reaction rate of the acylation step and might hamper the perpendicular arrangement of the plane of the aromatic ring and the plane of the amide bond – which has been proven to be crucial for $\alpha 5\beta 1$ activity.

III.1.6 Introduction of linker-spacer systems to tyrosine based $\alpha 5\beta 1$ ligands

Many biological and medicinal applications of integrin ligands such as implant coating, radiolabels for PET-screening and drug carriers involve the attachment of a prosthetic group (anchor^[159], radiolabel^[154, 160], drug^[161]). To avoid sterical interference of this group with the integrin binding, they are usually separated by a more or less long spacer unit. Much effort has been spent in the past to coat bone grafts with $\alpha v\beta 3$ selective ligands to facilitate tissue growth^[153, 162] or to trace $\alpha v\beta 3$ expressing tumor tissue by *positron emission tomography* with ^{18}F labeled $\alpha v\beta 3$ ligands.^[163] To our knowledge, the most commonly used cyclic peptide *cyclo(-RGDFV-)* has to be considered biselective towards $\alpha 5\beta 1$ (3.5 nM on $\alpha v\beta 3$, 64 nM on $\alpha 5\beta 1$) as well as a variety of peptidomimetics. As to the ongoing reevaluation of the function of both $\alpha 5\beta 1$ and $\alpha v\beta 3$,^[114] the use of our first selective $\alpha 5\beta 1$ integrin ligands in those applications may provide important data about the function of each integrin subtype *in vivo*. Therefore, the focus of the work was concentrated on the synthesis of ligand-linker-systems based on the previously synthesized ligands. Precondition of a useful ligand-linker system should of course be the retention of high affinities and the selectivity towards $\alpha 5\beta 1$. The highly active tyrosine based ligands offer two possibilities of linker attachment (Figure III-5):

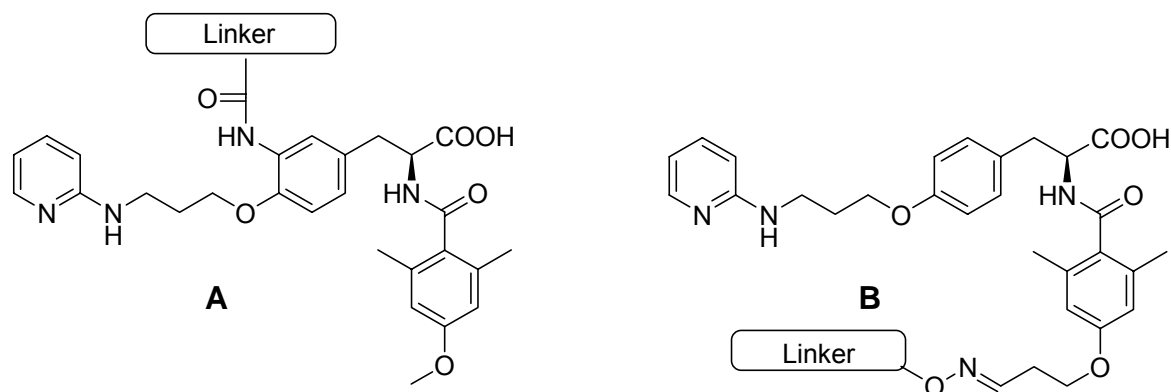
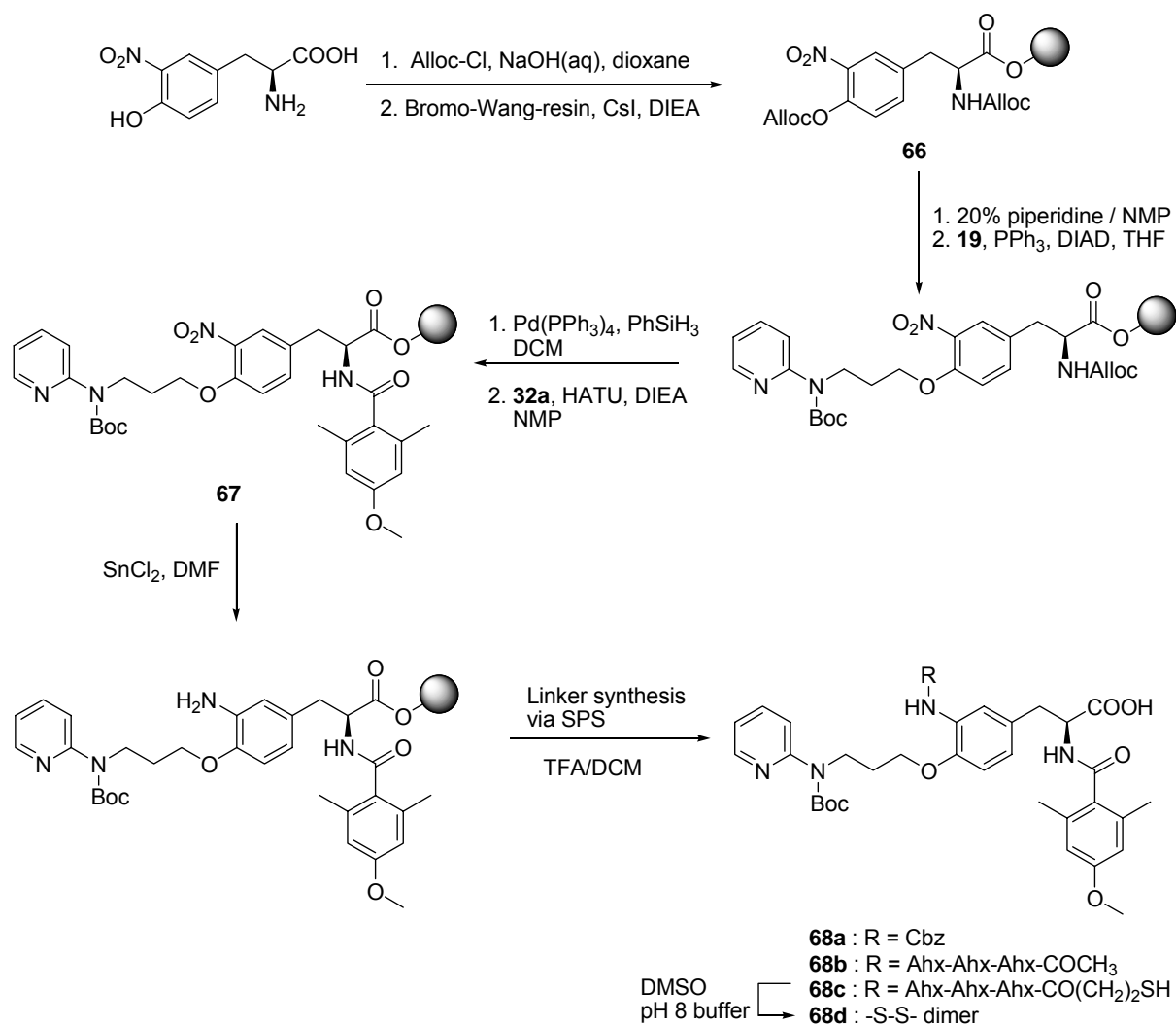


Figure III-5. Two modifications of ligands enabling attachment of prosthetic groups. **A:** Attachment to the scaffold by amide bond formation; **B** Attachment to aromatic substituent by oxime ligation.

The coupling of the linker to an *ortho*-aminotyrosine, outlined in method **A** (Figure III-5) has already been successfully employed by *Biltresse et al.* in order to synthesize α IIb β 3 ligands for immobilization purposes.^[164] The synthesis was modified for solid phase synthesis which should allow the coupling of larger linker systems. This is outlined in Scheme III-24. At first, the commercially available *ortho*-nitrotyrosine was double Alloc-protected.^[165, 166] This protection is simple and allows orthogonal deprotection of the base-labile allyl carbonate while the carbamate remains unaffected. Initially, the synthesis was performed on TCP-resin, which was found to be sensitive towards the conditions of the reduction step (SnCl_2 , DMF), where most of loading was cleaved during the course of the reaction. The bromo-Wang resin^[167] yielded good loadings when the alkylation reaction was accelerated by addition of 0.1 equivalents of cesium iodide.^[168] Once again, the key step was the Mitsunobu reaction. In contrast to the unsubstituted tyrosine, which required the use of ADDP and still gave poor yields, the *ortho*-nitro group lowers the pKa of the aromatic hydroxyl group, giving reasonable yields with DIAD and PPh_3 .^[165] The reaction was carried out with two equivalents of the Boc-protected aminoalcohol **19** and the progress monitored by HPLC. Usually, the reaction had to be repeated once sometimes twice, until a satisfying conversion of the starting material (> 90%) could be observed.

III. Results and Discussion

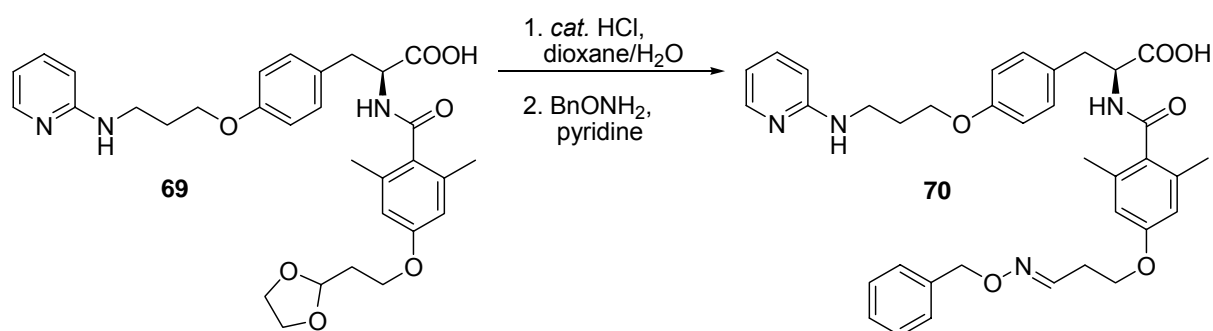


Scheme III-24. Solid phase synthesis of ligand-linker systems (**68a-d**).

Standard Alloc-cleavage using a catalytic amount of Pd⁰ and phenylsilane as reducing agent followed by acylation with the aromatic acid **32a** with HATU / DIEA gave compound **67**, which was successfully reduced with 10 eq. SnCl₂ in DMF over night.^[169] Since the aminopyridine was still Boc-protected, the aromatic amine could be selectively acylated. The Cbz-protected compound **68a** was taken as reference compound for the biological evaluation. As a linker system, three aminohexanoic acid (Ahx) building blocks were coupled to the amine, resulting in a linker long enough for every purpose. While the first two Ahx could be coupled by standard *solid phase peptide synthesis* (SPPS) using HOBt / TBTU, the last one had to be coupled using HATU – a phenomenon that could often be observed in long linker systems and which is probably due to interaction of the flexible linker with the polymer matrix. After introduction of the three spacer units, a small amount of the immobilized ligand was acetylated (**68b**), the rest provided with an anchor unit. As an anchor, trityl-protected

thiopropionic acid was chosen to enable immobilization on gold surfaces as well as dimerization to study a multimeric effect. The dimerization took place after cleavage from the resin, purification of the monomer **68c** and reaction with DMSO and air in a basic, aqueous environment (pH ~8), **68d**. Together with compounds **67** and **68**, the ligands carrying the linker at the aromatic substituent were also evaluated.

Compound **69** was synthesized from the starting material **22** (Scheme III-8) and the aromatic acid **32c** (Scheme III-12) as previously described. Hydrolysis of the acetal with catalytic amounts of HCl in dioxane / water gave the aldehyde which was used without further purification in an oxime ligation reaction with *O*-benzyl hydroxylamine as a substitute for a spacer unit (Scheme III-25). The product **70** was also evaluated for $\alpha 5\beta 1$ affinity.



Scheme III-25. Synthesis of different linker systems by oxime ligation.

Table III-9: Biological evaluation of ligand-linker-systems.

Compound	IC_{50} $\alpha 5\beta 1$ [nM]	IC_{50} $\alpha v\beta 3$ [nM]	S^* ($\alpha 5\beta 1$)
67	8.3	402	48
68a	5.0	198	40
68b	2.3	270	117
68c	5.8	460	79
68d	7.9	130	16
69	0.7	335	479
70	5.2	1600	308

*Selectivity factor for $\alpha 5\beta 1$ calculated as $IC_{50}(\alpha v\beta 3)/IC_{50}(\alpha 5\beta 1)$

The test results display that for the aminotyrosine based ligands (**67**, **68a-d**), the $\alpha v\beta 3$ affinity is very similar compared to the unsubstituted ligand **23j**. However, the affinity towards $\alpha 5\beta 1$ drops down by factor 2-8, regardless of the sterical demand of the group *ortho* to the tyrosine. This results in an overall drop of selectivity even though the ligands are still highly active on $\alpha 5\beta 1$. It seems that substitution in this position is somehow slightly unfavorable for $\alpha 5\beta 1$, which makes the resulting ligands not ideal for the selective targeting of $\alpha 5\beta 1$ integrins. In contrast, the attachment of the spacer units to the aromatic moiety does not affect neither affinity nor selectivity. Even with a sterical demanding group attached by oxime ligation, the activity towards $\alpha 5\beta 1$ is in the low nanomolar range with selectivities >300 . Further experiments are currently ongoing.

III.1.7 Synthesis of $\alpha 5\beta 1$ -ligands based on the *aza*-glycine scaffold

Since the role of integrins $\alpha v\beta 3$ and $\alpha IIb\beta 3$ in pathological processes such as cancer angiogenesis or thrombus formation was discovered, a huge number of peptides and small molecules based on various scaffolds have been used to develop integrin antagonists as drugs.^[137] One approach towards small molecules which was taken in our group for the design of $\alpha v\beta 3$ ligands was the utilization of an *aza*-glycine building block to make peptidomimetic compound libraries.^[80, 81] The discovery that in cyclic peptides the RGD sequence forms a kink around the glycine^[170, 171] allowed the design of *aza*-glycine based mimetics^[172, 173] where the diacylhydrazine-moiety is responsible for the kink-structure. The development from cyclic RGD peptides to *aza*-glycine mimetics is outlined in Figure III-7.^[174] From the discovery of the *aza*-glycine-containing lead structure **B** with a 3-guanidylbenzoic acid as arginine mimetic, it was found that the asparagine could be substituted by an aromatic residue, which could be used to gain some selectivities among the αv integrins (**C**).^[81] In order to improve the pharmacological profile, the guanidine group was substituted by an aminopyridine. Those ligands have already been widely used for immobilization purposes (coating of grafts)^[153, 162] or as radiolabeled compounds for PET-screening.^[154, 163] This posed the question, whether the insights into the $\alpha 5\beta 1$

receptor gained from homology modeling and the extensive SAR-studies with tyrosine-based ligands could be used to modify the *aza*-glycine ligands towards $\alpha 5\beta 1$ selectivity.

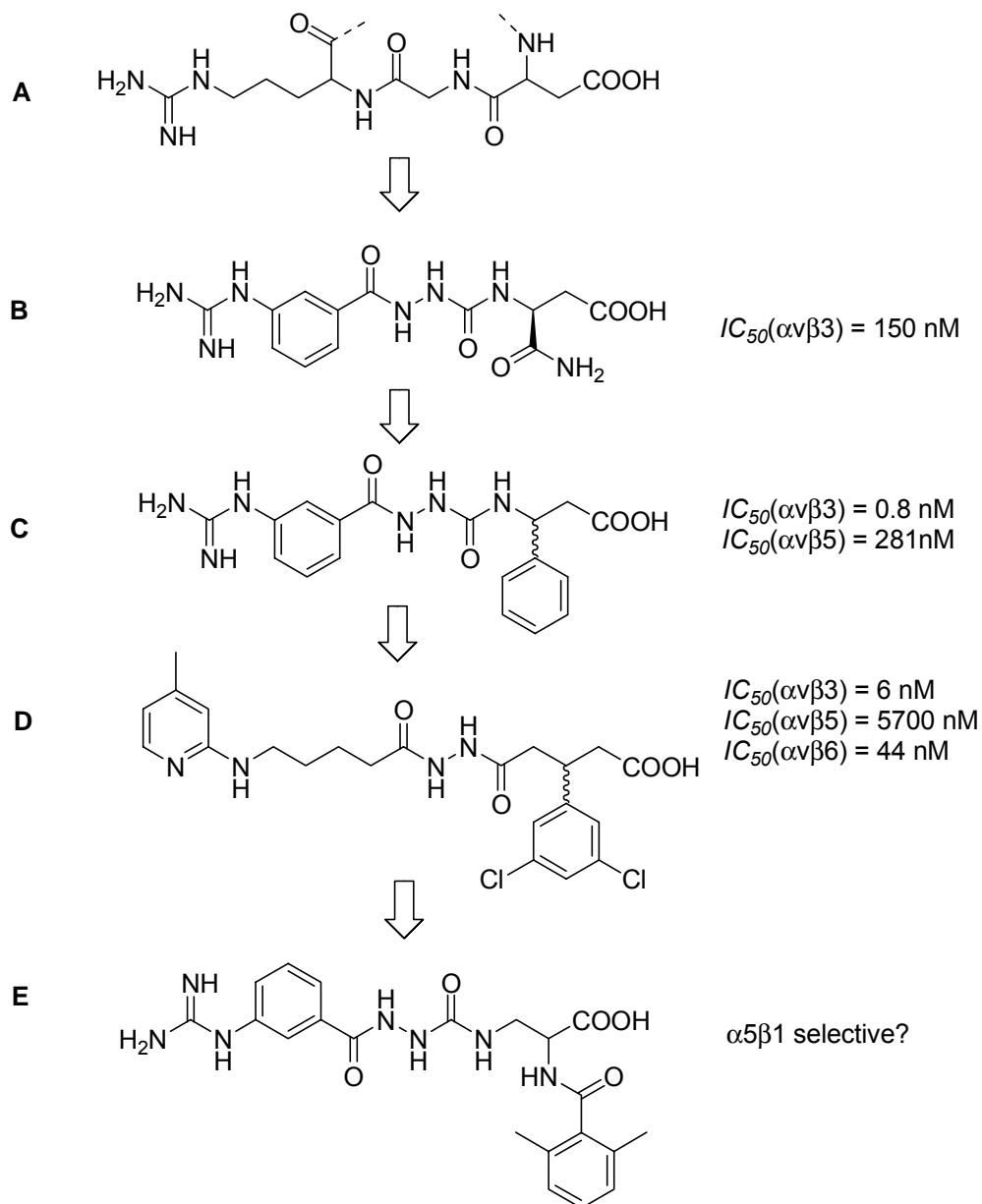
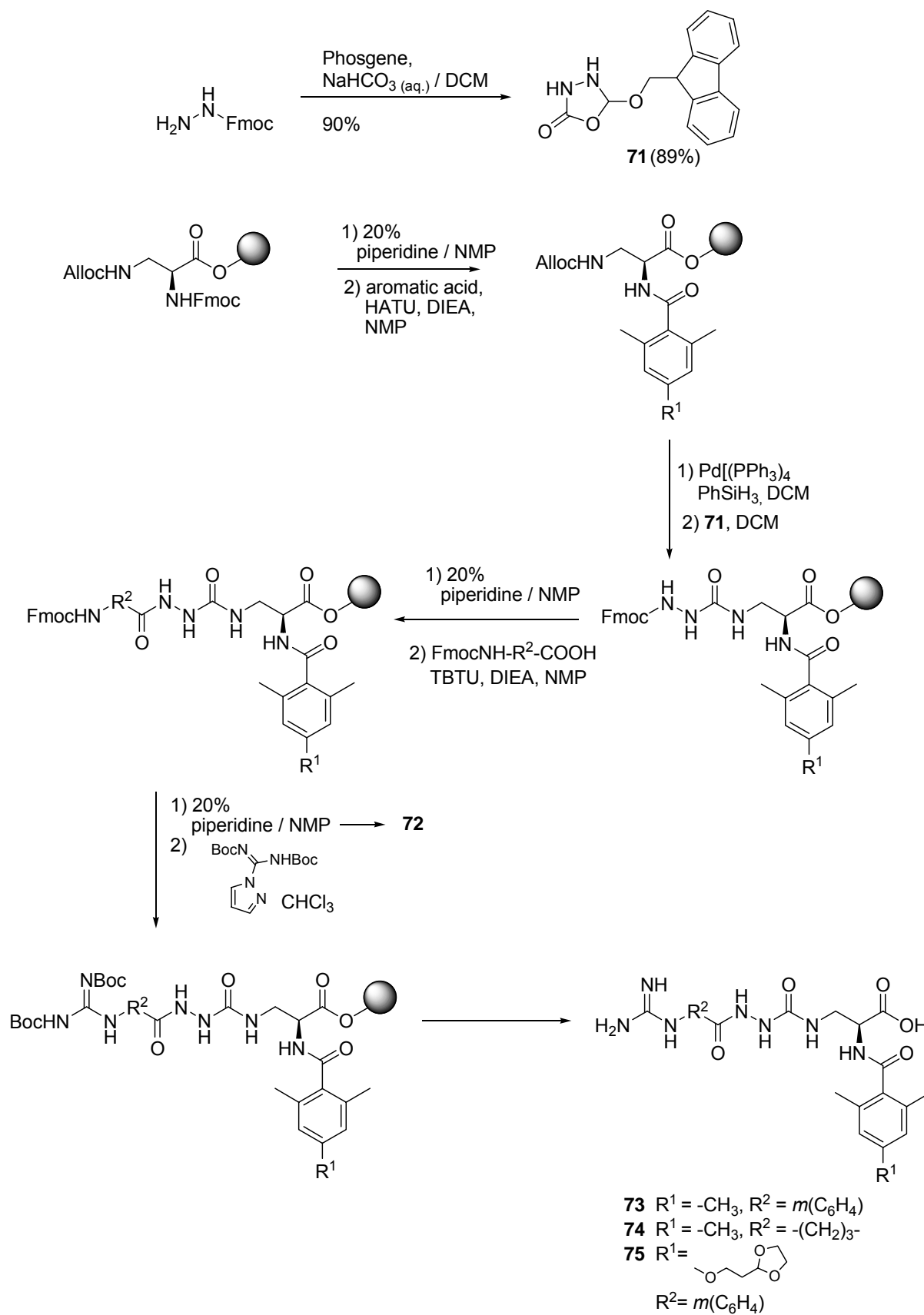
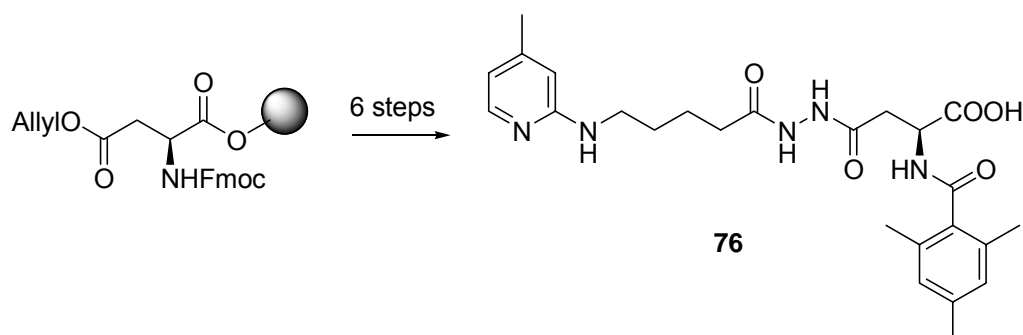


Figure III-6. Development of RGD-mimetics based on the *aza*-glycine scaffold. The ligands were designed to show activities on the αv subfamily.

As common feature, the $\alpha v\beta 3$ ligands **B-D** possess a β -carboxylic acid to bind to the MIDAS region of $\alpha v\beta 3$. This has already been used for the $\alpha v\beta 3$ -selective β -tyrosine ligands. As the selectivity of the $\alpha 5\beta 1$ ligands is mainly owed to sterical interactions concerning the $\beta 1 / \beta 3$ -subunit, the *aza*-glycine ligands should easily be modified by

substituting the aromatic β -carboxylic acid with a 2, 3-diaminopropionic acid and a 2, 6-dimethylbenzoic amide (**E**). The synthesis of the compounds was performed as published before for the α v β 3 ligands – with the difference that an orthogonally protected 2, 3-diaminopropionic acid was used as first amino acid. The *aza*-glycine building block was introduced with 5-(9*H*-fluoren-9-ylmethoxy)-1, 3, 4-oxadiazol-2-(3*H*)-one, which was synthesized freshly before each *aza*-glycine coupling step. Guadinylation was performed using a ten-fold excess of *N, N'*-bis-Boc-guanidinylnpyrazole in dry chloroform for 24 h at 50°C. The excess reagent could be recycled by concentration of the chloroform solution and recrystallization from ethyl acetate / hexane. In case of the aromatic guanidine function, the reaction did not give full conversion after one day. The non-guanidinyln compound (**73**) was separated from the mixture and also sent for biological evaluation. The target compounds **72-75** were cleaved from the resin with 50% TFA to avoid decomposition. Additionally, two compounds with a 4-methyl-2-aminopyridine as basic group were synthesized. Compound **76** was derived from aspartic acid and contains a diacylhydrazine scaffold, whereas **77** – derived from 2, 3-diaminopropanoic acid – have an *aza*-glycine scaffold and were synthesized in an analogue manner.

Scheme III-26. Synthesis of aza-glycine compounds **72-75** as $\alpha 5\beta 1$ ligands.

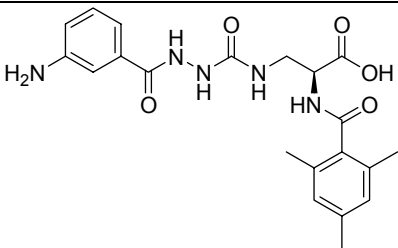
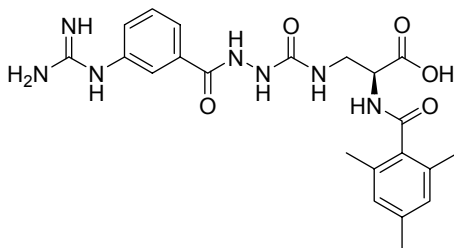
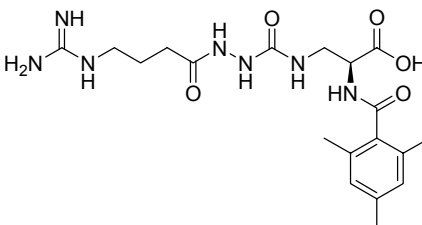
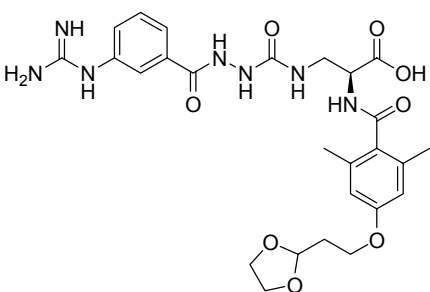
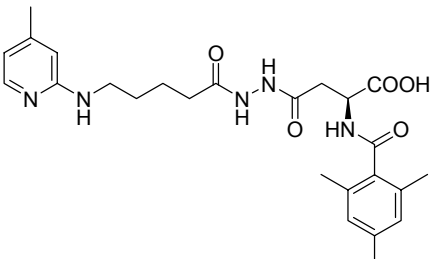


Scheme III-27. Related compound **76** with aminopyridines as arginine mimetics.

The biological testings indeed show a high activity of the *aza*-glycine compounds **73** and **74**, combined with a high selectivity against $\alpha v\beta 3$ (~6000 and beyond). These data make them the most selective $\alpha 5\beta 1$ ligands yet reported. Surprisingly, no activity was observed for the related diacylhydrazin scaffold (**77**).

This class of ligands, especially due to its polarity (calculated $\log P(\mathbf{73}) = 1.24$) which should provide a quick renal clearance from the body, represents promising ligands for PET-screening. The use of both $\alpha v\beta 3$ and $\alpha 5\beta 1$ -selective PET markers may provide valuable information about the specific integrin expression in the tumor tissue and facilitate an adequate treatment.

Table III-10. Biological activities of aza-glycine compounds.

Compound	Structure	IC_{50} $\alpha 5\beta 1$ [nM]	IC_{50} $\alpha v\beta 3$ [nM]	S^* ($\alpha 5\beta 1$)
72		590	>50000	>85
73		1.1	6500	5910
74		6.9	>50000	>7250
75		n.d.	n.d.	n.d.
76		5200	>50000	>10

*Selectivity factor for $\alpha 5\beta 1$ calculated as $IC_{50}(\alpha v\beta 3)/IC_{50}(\alpha 5\beta 1)$

* n.d. = not determined

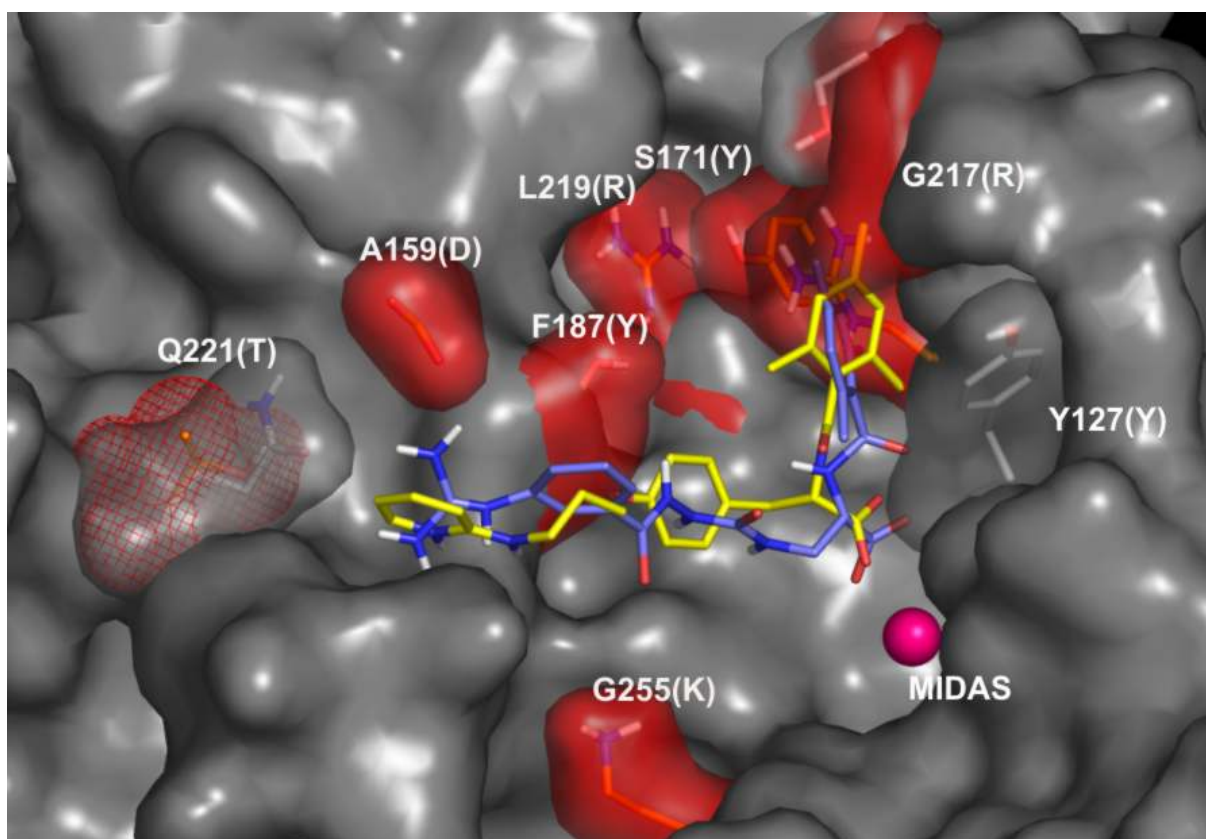


Figure III-7. Comparison of the binding modes of **23e** (yellow) and **75** (blue) docked into the $\alpha 5 \beta 1$ binding pocket. Both ligands show analogue binding modes. The mesitylene group is oriented in a similar way leading to selectivity against $\alpha \nu \beta 3$ as the result of a potential clash with $(\beta 3)$ -Arg²¹⁴.

III.1.8 Hydroxamic acids as aspartic acid substitutes

A comparison of virtually all yet published integrin ligands shows that the most conserved functionality is the carboxylic acid. It is involved in the coordination of the bivalent metal cation at the MIDAS site, which is present in all integrins. Although the nature of the metal is not yet fully determined (Ca^{2+} , Mg^{2+} and Mn^{2+} are under discussion) [62, 66, 67, 175], the importance of the cation-carboxylate interaction is undoubted. As to the nature of the interaction, both ionic attraction and coordinative binding are imaginable. The substitution of the carboxylic group by sulfonic acids (weaker donors, strong negative charge), phosphonic acids (known to coordinate calcium ions) or tetrazoles (a common carboxylic acid substitute in medicinal chemistry) could provide information about the nature of the metal-ligand-interaction

and improve the pharmacological profile of the molecule by alteration of the pKa. However, the successful substitution of a ligand's carboxylic moiety has not yet been reported. Two examples of compounds synthesized in our group are shown in Figure III-8. The sulfonic acid derivative of a $\alpha\text{v}\beta\text{3}$ ligand (RGD-mimetic) ^[176] and the phosphonic acid derivative of a $\alpha\text{4}\beta\text{7}$ ligand (LDT-mimetic) ^[177] gave no satisfying results.

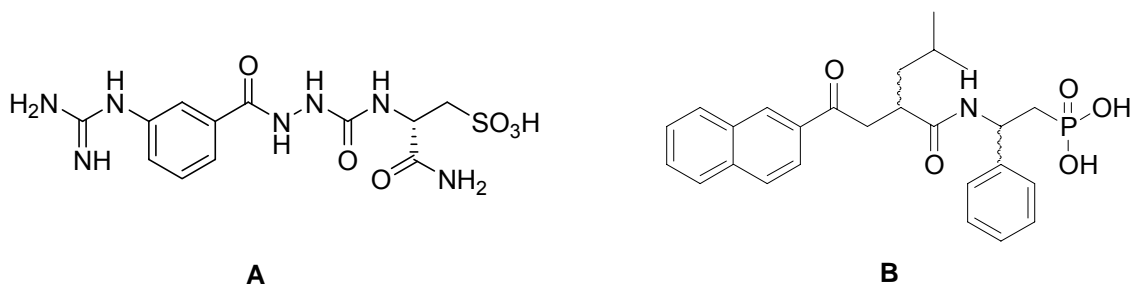
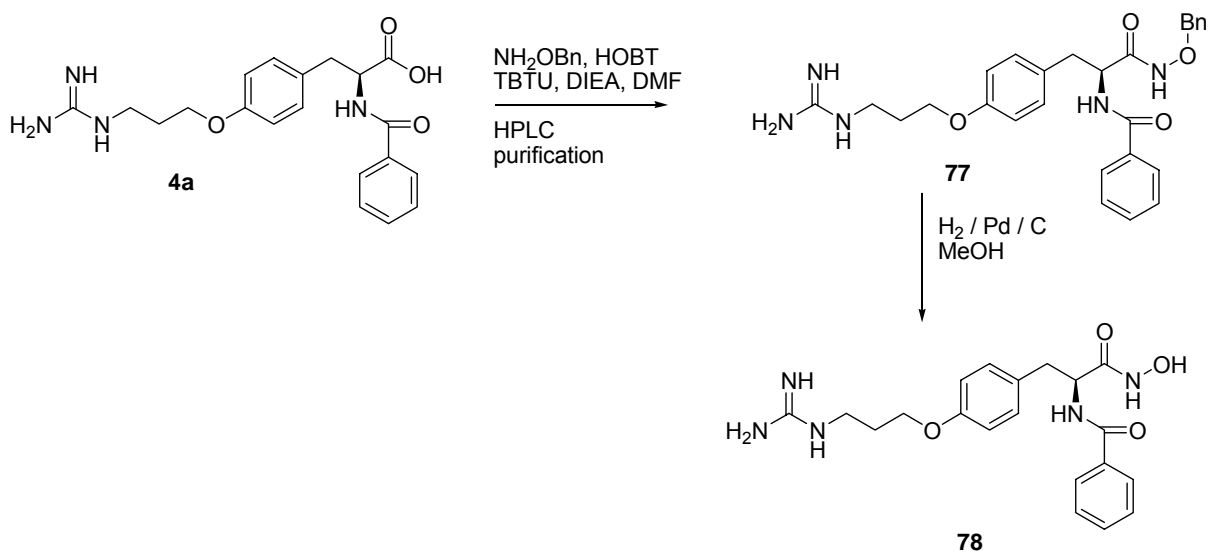


Figure III-8. Derivates of integrin ligands without carboxylic acid. (A = RGD mimetic, B = LDT mimetic). Both compounds showed no activity on their targets.

A new approach for the substitution of carboxylic acids in integrin ligands is the conversion of the carboxylates into hydroxamic acids, which are known to fulfill a variety of roles in biology and medicine. They are used as siderophores for Fe^{III}, ^[178] or selective enzyme inhibitors for peroxidases ^[179], ureases ^[180] and matrix-metalloproteases ^[181]. In all these cases, the mechanism of binding / enzyme inhibition is a result of the coordination of a metal ion (Fe^{III} ^[179], Ni^{II} in ureases ^[180] or Zn^{II} in metalloproteases ^[181]). They are overall less acidic (pKa(*N*-hydroxyacetamide) = 9.40 ^[182], pKa(acetic acid) = 4.76) but have good coordination properties, which could be useful for the binding of a Mn^{II} cation in the MIDAS site. In case of a mainly ionic interaction, a dramatic loss of activity would be expected, while with a mainly coordinative binding, the affinities of carboxyl and hydroxamic acid should be comparable. Two integrin ligands were synthesized in order to evaluate if hydroxamic acid in principle are able to serve as integrin ligands. The hydroxamic acid was prepared from the free carboxylate by coupling of *O*-benzyl hydroxylamine using HOBt / TBTU as standard peptide synthesis reagents. The benzyl group was removed in the next step by catalytic hydrogenation. The first peptidomimetic to be converted ^[182] in its hydroxamic acid analogue was compound **4a**. In contrast to the peptidomimetics carrying a 2-aminopyridine as basic moiety, it was stable towards hydrogenation, it was considerably biselective (as selectivity was not an issue for this

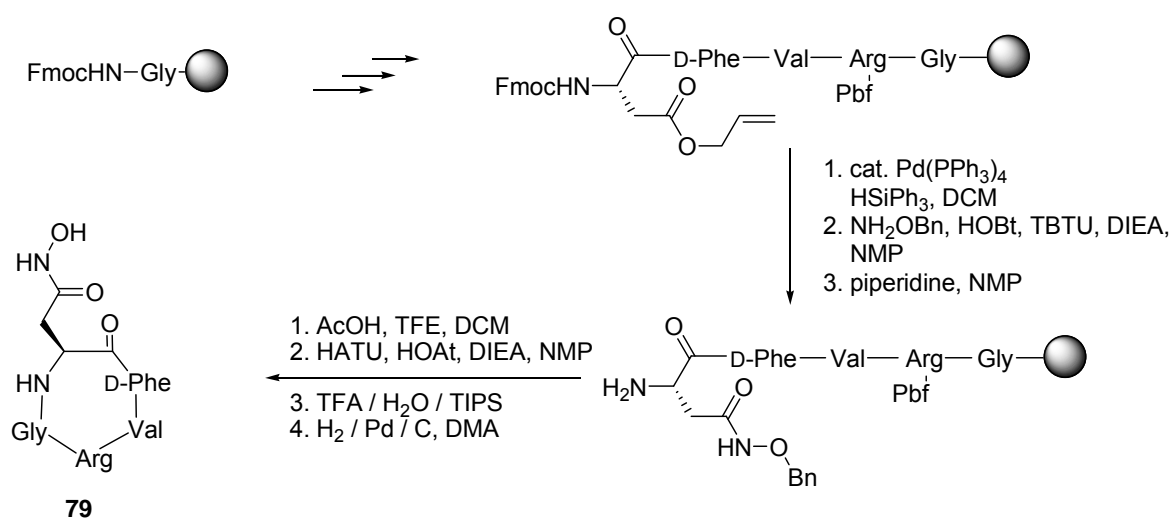
III. Results and Discussion

experiment) and has a “reduced” length – the elongation of the ligand by the N-O bond would not be significant (see **4b**).



Scheme III-28. Preparation of hydroxamic acid RGD mimetic **78**.

As peptidic analogue, the peptide *cyclo*-(RGDFV-) was synthesized on solid phase with an side-chain allyl-protected aspartic acid building block. The allyl ester could be selectively deprotected on solid phase and the free carboxylic acid functionalized as described for **4a**. The hydrogenolytic benzyl deprotection was performed on the cyclized peptide after deprotection of the acid labile Pbf group. Both compounds were tested in an ELISA assay on $\alpha 5\beta 1$ and $\alpha v\beta 3$.



Scheme III-29. Solid phase synthesis of cyclic peptide *cyclo*-(RGD(NHOH)fV-), **79**.

Table III-11. *Biological activities of hydroxamic acid compounds and reference compounds in ELISA and cellular assay.*

Compound	ELISA [nM]		Cellular assay [nM]	
	$\alpha 5\beta 1$	$\alpha v\beta 3$	$\alpha 5\beta 1$	$\alpha v\beta 3$
4a	60	132	n.d.	n.d.
78	6700	53	n.d.	n.d.
cyclo(-RGDfV-)	62	3.5	n.d.	n.d.
79	n.d.	n.d.	n.d.	n.d.

* n.d. = not (yet) determined

The biological testings afforded a surprising selectivity of the hydroxamic acid compound **78** on $\alpha v\beta 3$. Despite the loss of acidity, the compound is approximately twice as potent as its carboxyl derivative. The 100 fold loss of affinity towards $\alpha 5\beta 1$ can not be explained with the structural models. The MIDAS-region is that highly conserved, that a small, non-sterical change should always affect all integrin subtypes. The ELISA tests were all performed in the same buffer solution with the same Mn^{2+} concentration. This should rule out any effects of pH (and therefore of the degree of deprotonation) and of Mn^{2+} preference. Further tests to confirm these surprising results *in vivo* are currently ongoing. Only the determination of the anti-adhesive function of compound **78** and **79** on cells expressing $\alpha 5\beta 1$ or $\alpha v\beta 3$ respectively can unambiguously verify the potency determined in the ELISA. If the results could be confirmed, these ligands were the first integrin antagonists without a negatively charged (or at least less acidic) C-terminus, which might increase their bioavailability.

III.1.9 Biological studies with $\alpha 5\beta 1$ / $\alpha v\beta 3$ selective ligands

The extensive SAR-studies with ligands based on the tyrosine scaffold afforded a large number of integrin ligands with different activity and selectivity profiles for $\alpha 5\beta 1$ and $\alpha v\beta 3$ integrins. The molecules shown in Figure III-9 provide a feasible toolkit for the discrimination of $\alpha 5\beta 1$ and $\alpha v\beta 3$ integrins *in vivo*. This is of special interest since the essential role of $\beta 1$ integrins for the process of embryogenesis^[183], the development of skin^[184], cartilage^[185], the hematopoietic (responsible for blood cell

III. Results and Discussion

formation) system^[186, 187], muscle formation^[188] and – important for drug development - tumor growth and metastasis^[189, 190] is confirmed by a growing number of experiments.^[191] In collaboration with the research group of Prof. R. Fässler at the Max-Planck-Institut für Biochemie, Martinsried, a selection of four ligands was tested in functional assays on mouse fibroblasts. The biological experiments were performed by Michael Leiss and are part of his PhD-Thesis. The studies were aimed at understanding the role of $\alpha 5\beta 1$ integrin in fibronectin assembly. As described in the theoretical section, fibronectin is the exclusive ligand of $\alpha 5\beta 1$ while the more promiscuous $\alpha \nu\beta 3$ integrin binds preferably vitronectin, but also fibronectin and osteopontin. Normally, fibroblasts express soluble fibronectin, which binds to its integrin receptor and is assembled by cross-linking to form insoluble fibers which represent the extracellular matrix (ECM).

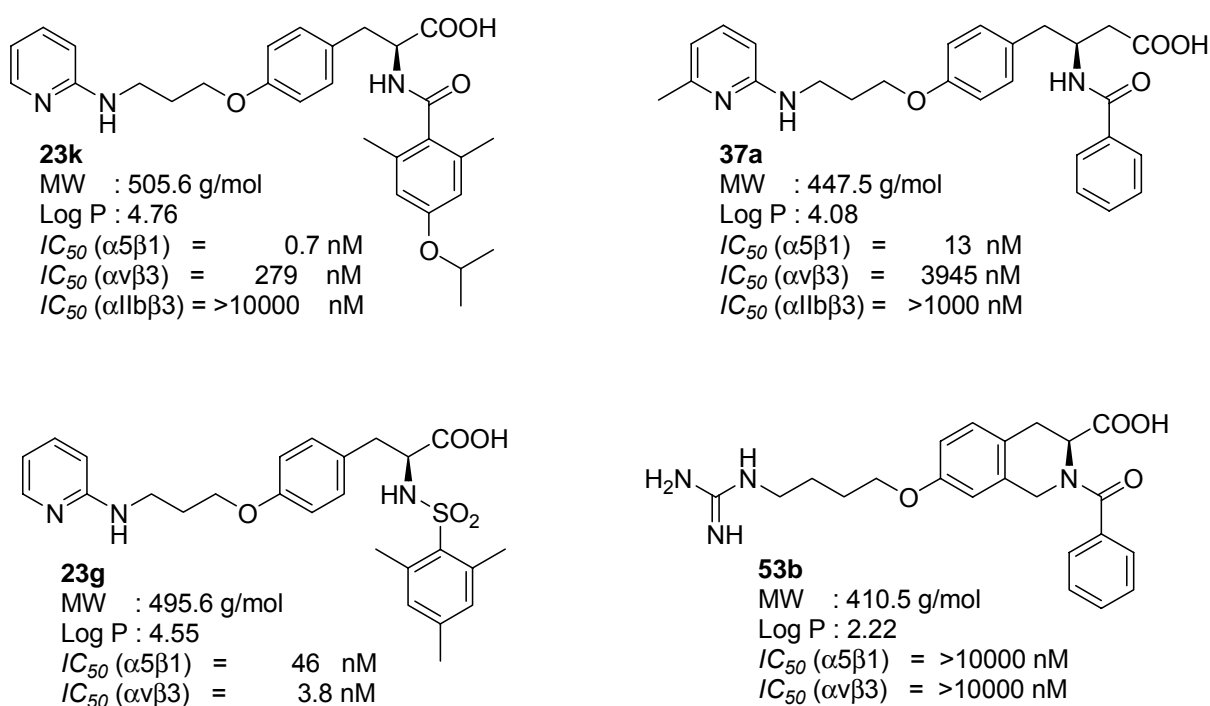


Figure III-9. Biological and physical data of selected compounds used in the functional assays. **23k** is ~400 fold selective against $\alpha \nu\beta 3$, **37a** ~300 fold selective against $\alpha 5\beta 1$. **23g** was considered biselective, **53b** used as nonbinding reference (blank).

Up to now, the function of both fibronectin and $\alpha 5\beta 1$ has mostly been studied by mutual knock-out experiments. Since both ligand and receptor have – apart from cell-adhesion – various different biological functions, it is hard to connect the knock-out phenotype with the loss of the RGD - integrin interaction. To elucidate the impact of

especially this interaction, a mouse line was generated in the laboratory of Prof. Fässler, carrying a Fn knock in allele containing glutamine instead of aspartate in the 10th type III domain (chapter II.2.4.1, p. 15). Fibroblast cell lines derived from mice homozygous for this mutation should be incapable of binding their secreted Fn and hence show no Fn-assembly, since the RGE motif was found to exhibit no affinity towards integrins. Surprisingly Fn-RGE was found to assemble via a novel, RGD independent mechanism, even though the fibrils were shorter and thicker in shape. The selective integrin ligands (Figure III-9) were used to find out whether this phenomenon of a non-RGD mediated fibronectin binding / assembly was caused by $\alpha 5\beta 1$ or $\alpha v\beta 3$ integrins, which are both present on the cells. The mouse fibroblasts (wild type and mutated) were cultivated on laminin in serum-free medium. Cell adhesion on laminin is mediated by $\alpha 6\beta 4$ integrins, which does not bind to Fn. Therefore Fn binding integrins are not required for cell attachment, making them readily available on the cell surface to facilitate (optimal) Fn assembly. The serum-free medium should make sure that only fibronectin expressed by the particular cell line was present outside the cell. Formation of Fn-fibers was observed by immunostaining with fluorescence-labeled antibodies.

The functional assays show for the inactive compound **53b** a regular fibronectin assembly, observable from the red stained fibronectin fibers (Figure III-10, lower right picture). The $\alpha v\beta 3$ selective compound **37a** was found to have no effect on fibronectin assembly as the main receptor for Fn is $\alpha 5\beta 1$ (upper left picture). Inhibition of $\alpha 5\beta 1$ by the selective compound **23k** dramatically reduces the number of formed Fn-fibers (upper right). Due to the relatively high concentrations of the inhibitors (0.5 mg / mL), an inhibition of $\alpha v\beta 3$ might also occur despite the selectivity. The biselective compound **23g** – exhibits a general reduction of Fn-assembly as expected. The cellular assays were hampered by the low solubility of the compounds **23k**, **23g** and **37a**, which is not surprising considering their logP values >4. Although, in this case, solubility could be enhanced by addition of DMSO, the high lipophilicity generally hints at an unfavorable pharmacophoric profile which has to be overcome for the generation of lead structures for e.g. cancer therapy.

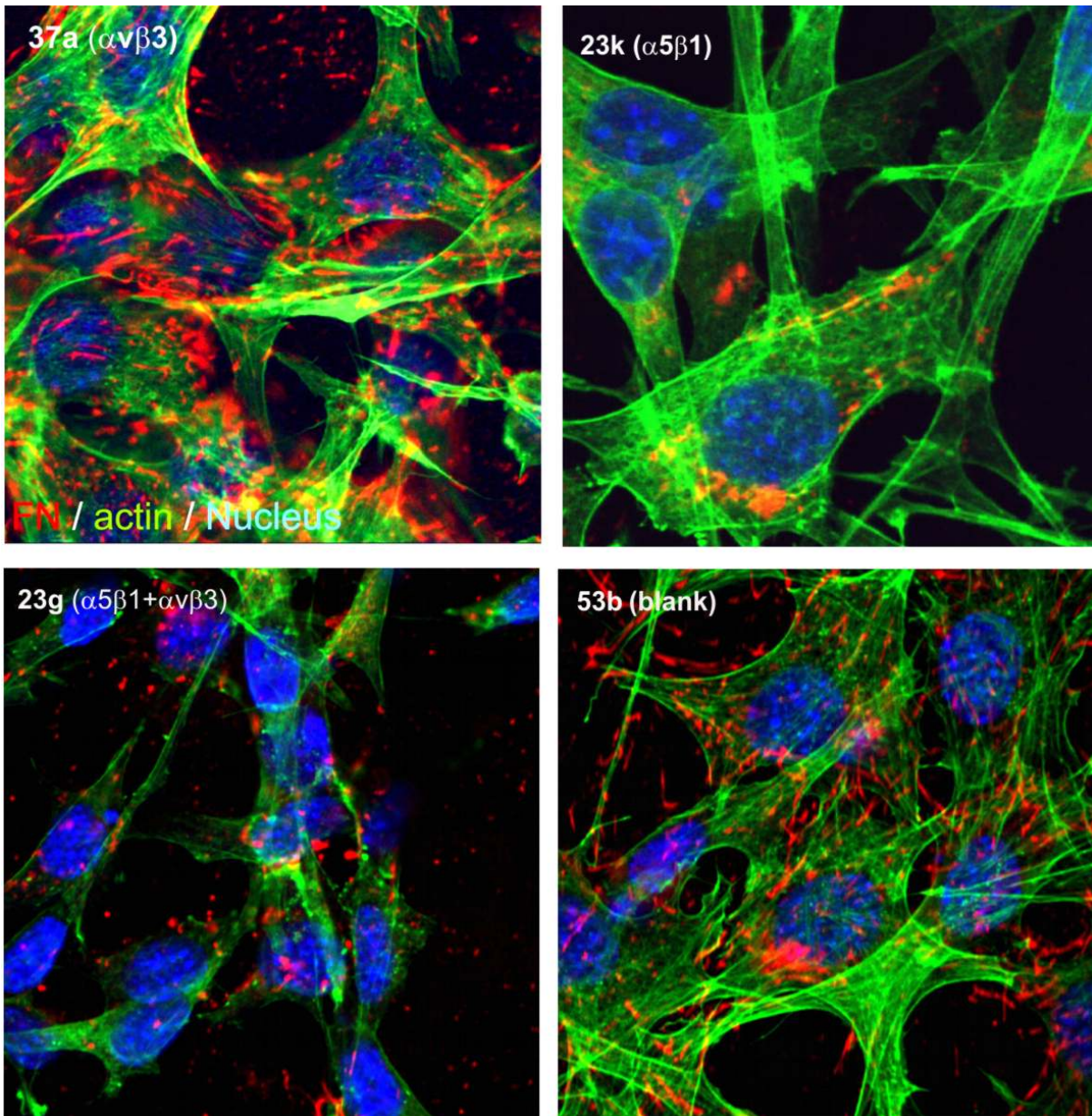


Figure III-10. Confocal fluorescent images of wt-mouse fibroblasts grown in serum-free medium including the integrins ligands. Assembled fibronectin is stained red, the actin filament green and DNA blue.

Mutated mouse fibroblasts, expressing the RGE-sequence in contrast to wild-type Fn, afforded surprising results: While wild-type cells show regular levels of Fn-assembly, the RGE-mutants (D1616E) were also found to show Fn-assembly, even though the regular RGD binding site in Fn (10th type III repeat, see chapter II.2.4.1, p. 15) was replaced by a sequence showing no affinity for neither $\alpha v \beta 3$ or $\alpha 5 \beta 1$ integrins.^[192] Although the phenotype was slightly altered (the shape of the Fn-fibers was found to be shorter and thicker, Figure III-11), the amount of Fn-assembly

was almost the same as in the wild-type cells. To elucidate, which integrin is involved in the binding of the RGE- fibronectin, the selective ligands were used to inhibit the Fn-assembly in mutated fibroblasts. It could be observed, that only the $\alpha\beta3$ -selective compound **26c** was able to block the 'irregular' Fn assembly which suggests, that $\alpha\beta3$ to some extent is able to bind to fibronectin at another binding site (or binding sites) than the 10th type III-RGD sequence.

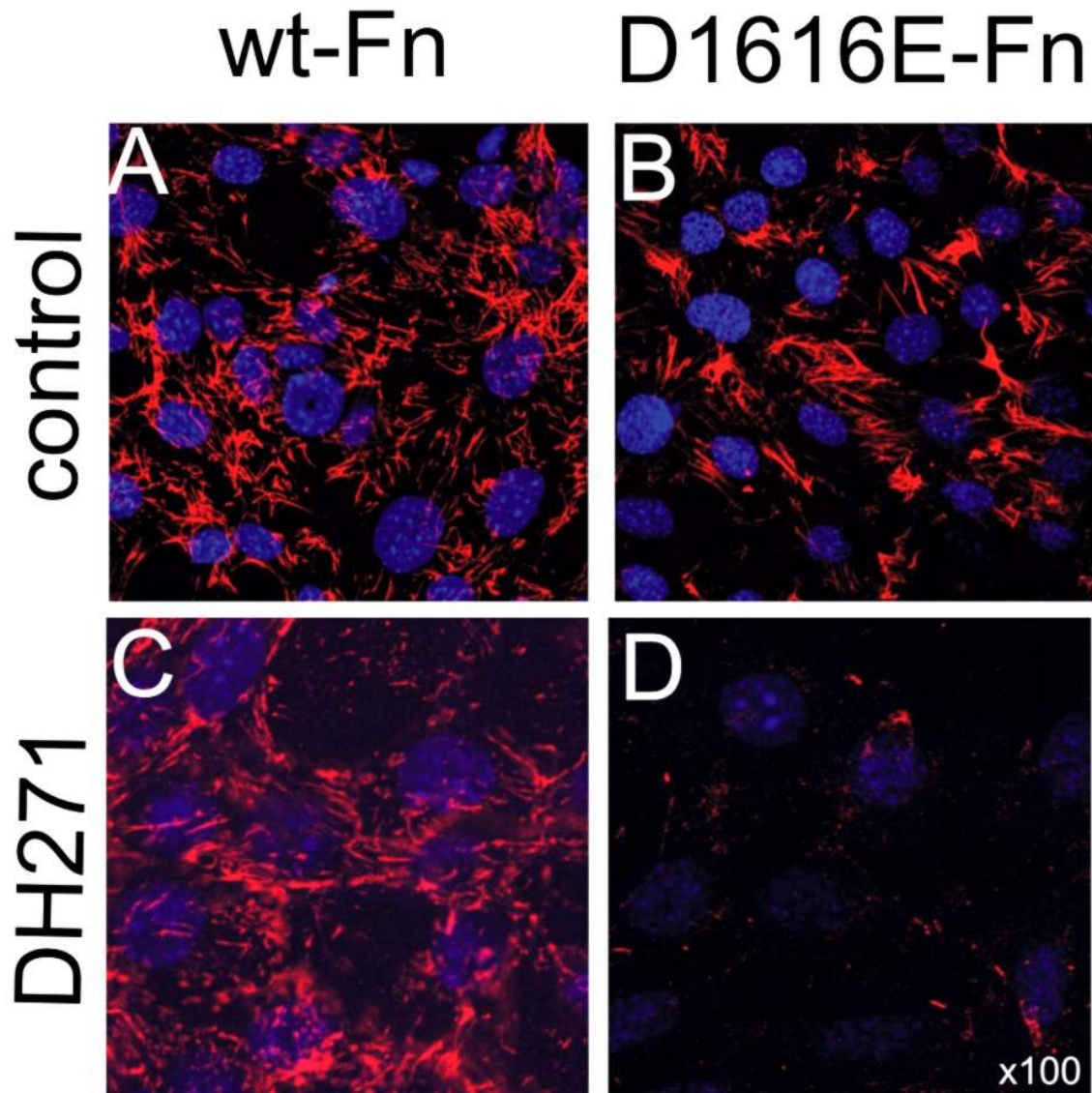
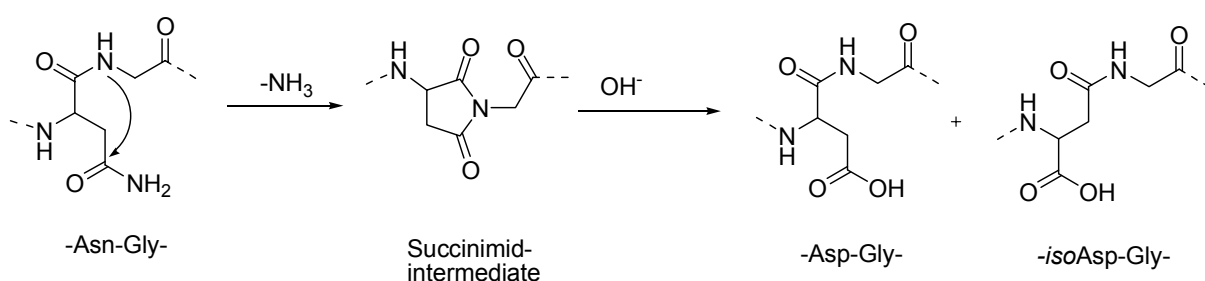


Figure III-11. Confocal fluorescent image of wild-type mouse fibroblasts (A, C) and fibroblasts expressing a mutated RGE-fibronectin (B, D). The RGE-fibronectin assembles despite the deactivation of RGD. Inhibition of $\alpha\beta3$ by **37a** (DH271) gives regular, $\alpha5\beta1$ mediated assembly (C), while it is completely cut off in the mutated cells. Assembled Fn is stained in red, DNA blue.

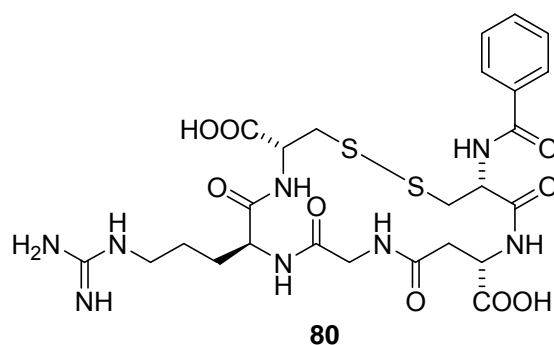
III. Results and Discussion

A hypothetical model for this interaction was proposed by *Curnis et al.*^[193] The NGR (Asn-Gly-Arg) sequence, which is found at four positions in the fibronectin molecule, is able to undergo a rearrangement to *isoDGR* (*isoAsp-Gly-Arg*), which was found to be active on $\alpha v\beta 3$ and – with less potency – on $\alpha 5\beta 1$. The mechanism of Asn-deamination has long been known and was widely understood as a process of degradation acting as a biochemical clock that limits protein lifetimes *in vivo*.^[194-197] The results found by *Curnis et al.* are the first example of the deamination process, which *increases* protein function.^[193, 198] Furthermore, it was observed, that at least one of the NGR sequences in fibronectin rearranges on aging of the protein under physiological conditions (37°C) and thus creates a new binding site on $\alpha v\beta 3$.



Scheme III-30. *Mechanism of Asn-deamination.* Hydrolysis of the reaction intermediate can result in both Asp-Gly and *isoAsp-Gly* formation, which may resemble a new binding site for integrins.

To reproduce the published results in a functional assay, a model peptide of the *isoAsp-Gly-Arg* sequence was synthesized and tested in both Fn-assembly and ELISA-receptor assay. The peptide $\text{PhCO}-(^*\text{Cys-isoAsp-Gly-Arg-Cys}^*)\text{-OH}$ was chosen for synthesis because of its similarity to the published reference peptide. As only difference, an *N*-terminal antigen used to label the peptide^[193] was replaced by a simple benzoyl group, which facilitated preparative HPLC purification by enhancing the UV-absorption of the peptide.



Scheme III-31. Structure of the cyclic peptide **80**, used as a model *isoDGR* peptide in functional cell assays. The synthesis of the linear peptide was performed by standard SPPS using the Fmoc-strategy. Cyclization was achieved by treatment of the linear peptide with 2 eq. H₂O₂ in a pH 9 buffer.

As references to the peptide **80**, the corresponding DGR (**81**), NGR (**82**) and RGD (**83**) peptides were synthesized in an analogue way. The inhibition of Fn-assembly (data not shown) by **80** supported the hypothesis of alternative binding sites. In the functional assay, the NGR peptide gave similar results (inhibition of Fn-assembly) as the *isoDGR*, obviously a result of the deamination / rearrangement during the 16 h of incubation with the cells. A binding affinity of the native NGR sequence can be excluded because the amide function has neither negative charge nor is it a potential coordination ligand for bivalent cations. The data of the receptor assay is presented in Table III-12.

Table III-12. Receptor assays of model peptides **79-82**.

Code	Sequence	IC ₅₀ (α5β1) [nM]	IC ₅₀ (αvβ3) [nM]
80	PhCO(C* <i>iso</i> DGRC*)-OH	4	103
81	PhCO(C*DGRC*)-OH	n.d.	n.d.
82	PhCO(C*NGRC*)-OH	-*	-*
83	PhCO(C*RGDC*)-OH	n.d.	n.d.

*not determined in the receptor assay but gave similar results as **80** in the functional assay.

n.d. = not (yet) determined

The introduction of the *iso*-DGR-sequence into backbone-cyclized peptides and the biological and structural investigations are integral part of the diploma thesis of *Elke Steinhardt* and currently ongoing. The corresponding DGR, RGD and NGR peptides

III. Results and Discussion

were synthesized as reference compounds. The NGR peptide was – as predicted found to undergo a rearrangement as published in the literature. The process was monitored under physiological conditions (0.5 mg / mL in a pH 7.2 PSB buffer at 37°C). Although the reaction proceeded slower than predicted [193, 199], the 10% conversion of the starting material after 16 h was enough to explain the observed activities of the NGR-peptide. The formation of both products of the deamination / rearrangement as a function of time is presented in Figure III-12.

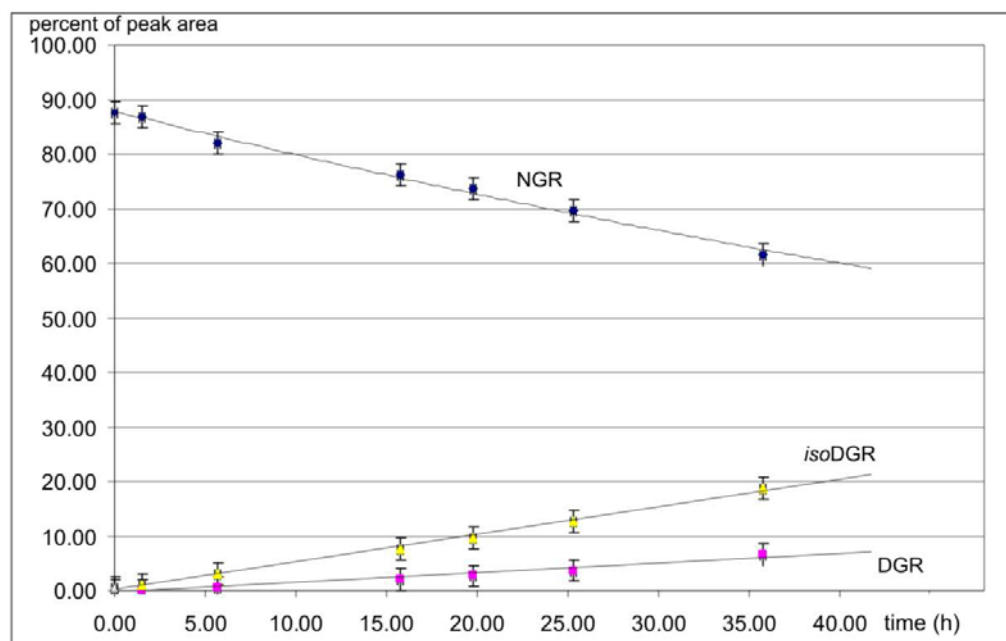


Figure III-12. Kinetics of the transformation of NGR peptide under physiological conditions. Quantification of peptides was performed by HPLC peak integration.

A much discussed issue in the integrin field is the agonist-antagonist nature of integrin ligands. [114] While the anti-adhesive function of soluble integrin ligands suggests an antagonist nature, it is not absolutely clear whether the binding of soluble ligands is able to trigger the *outside-in* signaling pathways of integrins. This is especially important for the antiangiogenic cancer therapy. Even though the antiangiogenic properties of RGD-peptides and peptidomimetics have been demonstrated *in vivo* – and thus point at antagonism – there are still many questions unsolved. [105] Together with the group of Prof. Fässler, we tried to elucidate the agonist-antagonist nature of our integrin ligands on the molecular level. As reporter-protein for integrin activation, we chose the *focal adhesion kinase* (FAK), which is a crucial mediator of many integrin-linked signaling pathways (Figure II-9). On activation of the integrin, the FAK gets activated by autophosphorylation and

promotes downstream-signaling by phosphorylation of its target proteins. The availability of a labeled antibody for activated (phosphorylated) FAK allowed the assay of integrin activation by determination of the levels of activated FAK. The experiments were performed by Michael Leiss and are part of his PhD-thesis. The results of the first experiments are presented in this chapter – however, further tests are still ongoing. In the functional assay, cells were starved in serum-free medium until no phosphorylated FAK could be observed with the antibody in the cell lysate. Then, the starved cells were incubated with the ligands **23k**, **23g**, **37a** and **53b** (0.25 mg/mL) for 30 sec. Additionally, linear and cyclic peptides (lin(RGDfV), lin(RADfV), cy(RGDfV), cy(RADfV), 0.5 mg/mL) were tested. The RAD-peptides and **53b** do not bind to integrins, while the other compounds are known to bind to $\alpha\beta3$ and $\alpha5\beta1$ on nanomolar scale. Soluble fibronectin was employed as positive control, polylysine (PLL) as negative.



Figure III-13: Comparison of the levels of activated FAK (left) and total FAK (right) derived from a Western-Blot. Each lane resembles incubation with a different, soluble integrin ligand.

After lysis of the cells, the cell proteins were analyzed in a western-blot and stained with antibodies for p397-FAK and total FAK. Although the total FAK levels in all lanes are comparable (Figure III-13, right), the only ligand found to induce integrin activation was soluble fibronectin. All ligands, peptidic or non-peptidic gave only lowest levels of activated FAK which are comparable to the negative control. Although experiments to competitively inhibit Fn-FAK activation by soluble ligands still have to be performed, the present data strongly suggests the antagonist nature of the soluble integrin ligands. The synthesis of multivalent integrin ligands and their

evaluation in this assay can afford valuable information about the mechanism of integrin activation. If an integrin clustering is the key to the activation of the signaling cascade, trimeric or tetrameric ligands should act as integrin agonist and induce FAK phosphorylation comparable to fibronectin. The synthesis and biological evaluation of multivalent ligands is subject of present and future efforts in our group.

III.2 Cyclic Peptides as Affinity Ligands for FVIII Purification

The careful analysis of a huge linear peptide library afforded a core sequence Trp-Glu-Tyr which is essential for the binding of factor VIII. The presence of one cysteine residue in the sequence is necessary as a linker to the stationary phase. The testings were performed by Alexey Khrenov in the group of Evgueni Saenko, American Red Cross Laboratories, Maryland, by immobilization of 2.5 mg of the peptide on epoxy-functionalized Toyopearls, incubation with ¹²⁹I-labelled FVIII and, after washing steps, detection of bound FVIII. The analysis of the results of the binding assays was hampered by the transient immobilization, which sometimes varied over a broad range. The different densities on the resin led to results which were sometimes hard to compare. A detailed binding study with the concentration-dependence of the binding affinity could only be performed for selected compounds. The immobilization was measured by the decrease of absorption in the supernatant of the immobilization buffer. Fortunately, the cyclic peptides showed excellent immobilization rates (>90%) which, together with their similar molecular weights, gives a good idea about the relative binding affinities.

III.2.1 Alanine scan of the most active cyclic hexapeptide sequences

A spatial screening of hexapeptides derived from the best linear hexapeptides gave two binders with similar or improved binding affinities. Both cyclic peptides contain one D-amino acid which has been proven to give conformationally stable cycles including β -turns.^[26] The two sequences were primarily examined with an alanine mutation study (Figure III-14). It underlines the importance of each amino acid residue, because the affinity drops down on every alanine substitution. While in the

c(FsWEYC) peptide **P1** ($58\pm 3\%$ FVIII binding) the tripeptide sequence is absolutely crucial for binding ($>70\%$ loss of FVIII binding), in c(FSWEYc) (**P2**, $63\pm 3\%$ FVIII binding) the phenyl alanine plays a more important role than the tyrosine.

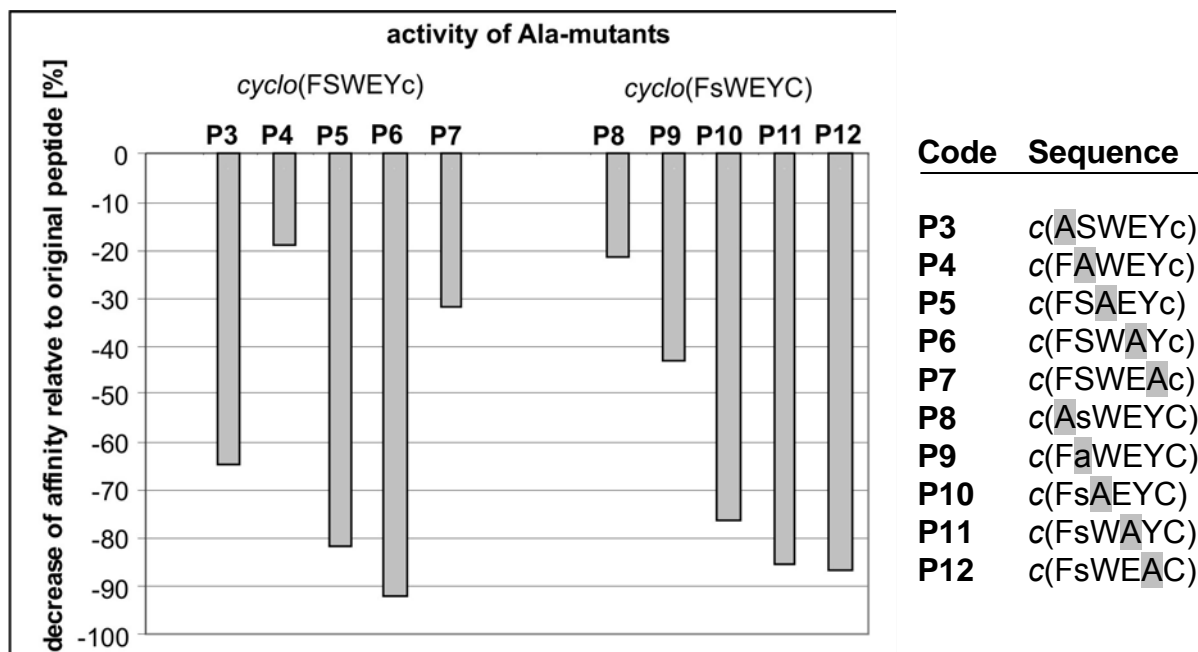


Figure III-14: Alanine scan of two FVIII-binding cyclic peptides. Substitution of cysteine by alanine resulted in a lack of immobilization and thus total loss of binding affinity.

III.2.2 Mutational analysis of P2

After identification of the most important amino acids by the Ala-scan, it was tried to increase the activity of the peptide by mutation studies with natural and unnatural amino acids. In those screenings, only the functionalities on side chains are changed while their orientation remains unchanged. Positive results allow further optimization of the system while negative results give valuable information about crucial interactions of distinct side-chain functionalities with the protein. A collection of different mutants of the original peptide sequence **P2** is given in Figure III-15. The mutation study concentrated on the most important amino acids of the sequence (F, W, E and Y). The phenyl alanine was substituted by a tyrosine, exposing an H-bond donor and polar group at the phenyl ring (**P13**) and the benzoylphenyl alanine (**P14**), representing a bigger, aromatic system. While **P13** gave a similar, slightly reduced affinity, **P14** turned out to be a significantly better binder for FVIII.

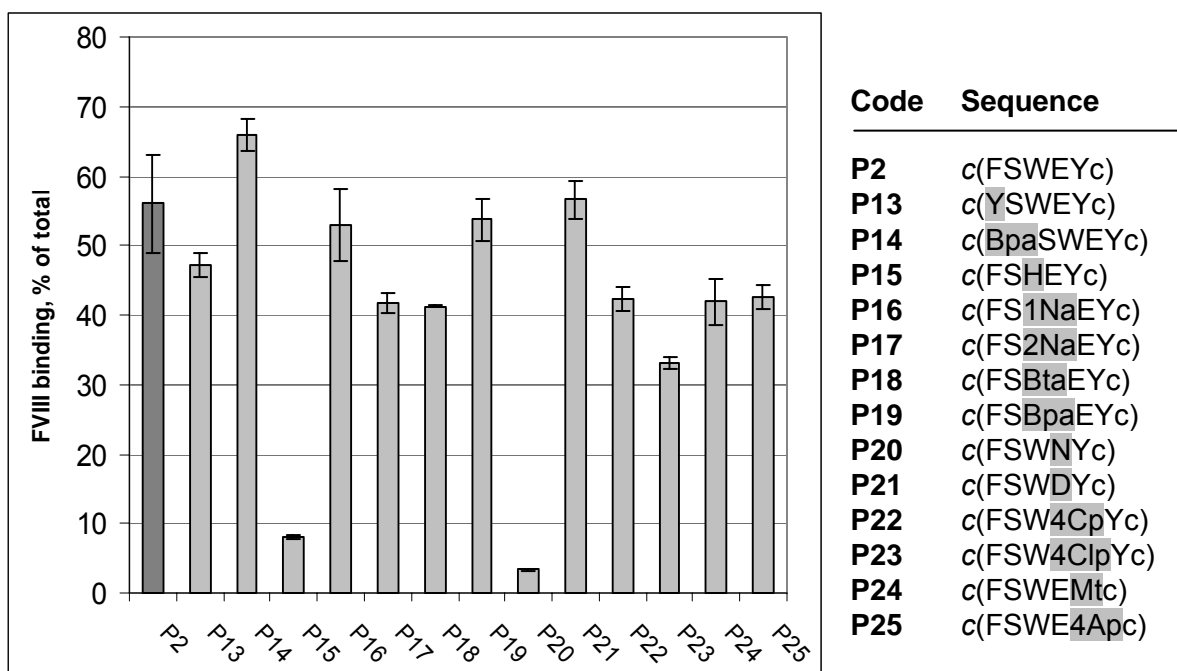


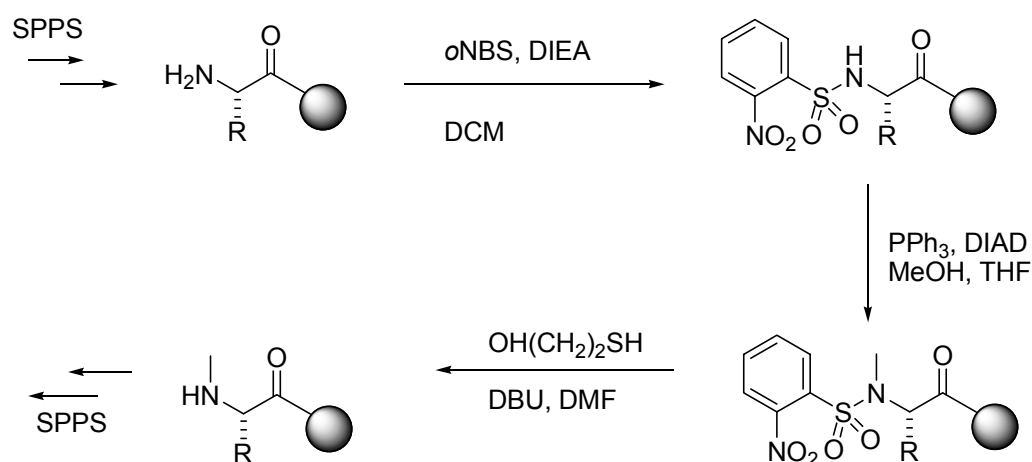
Figure III-15: Results of a mutation study of the peptide **P2** with different natural and unnatural amino acids. Bpa = 4-benzoylphenylalanine, 1Na = 1-naphthylalanine, 2Na = 2-naphthylalanine, Bta = benzo[*b*]thiophenylalanine, 4Cp = 4-carboxyphenylalanine, 4Clp = 4-chlorophenylalanine, Mt = *O*-Methyltyrosine, 4Ap = 4-aminophenylalanine.

This suggests that the phenyl alanine is involved in a hydrophobic, possibly aromatic interaction. The tryptophane was substituted by a variety of aromatic amino acids: The total loss of affinity on substitution by histidine (**P15**) suggests that either a bigger, more unpolar aromatic residue is needed or that a positive charge is extremely unfavorable. The peptides **P16-19** clearly demonstrate that the interaction of FVIII with the tryptophane is an aromatic interaction, since naphthyl alanines are well tolerated with only slight decrease for the similar substituents 2-naphthyl alanine and benzo[*b*]thiophenyl alanine. Surprisingly, the benzoylphenyl alanine was able to retain full affinity despite its different shape. The most important amino acid of the sequence – glutamate, as derived from the Ala-scan - was first substituted with glutamine (**P20**), which resulted in total loss of affinity, similar to the alanine mutant. It can be concluded, that the negative charge is the crucial functionality of this amino acid and builds up an important interaction to FVIII. However, the binding affinity could not be increased by the shorter side chain of asparagine (**P21**), which resulted in total retention of affinity or an aromatic acid (4-carboxyphenyl alanine, **P22**). The tyrosine, which in the linear octapeptide sequence was found to be very important,

was tested less important in the Ala-scan of the cyclic peptides. The substitution by 4-chlorophenyl alanine (more lipophilic, no H-bond donor), 4-methoxyphenyl alanine (no H-bond donor, only acceptor) and 4-aminophenyl alanine (positive charge, H-bond donor) resulted in less active peptides, but to a similar degree as substitution with alanine. This suggests that the hydroxyl group of the tyrosine is somehow involved in FVIII binding, but, for the peptide **P2**, contributes only little to the binding.

III.2.3 *N*-Methyl scan of peptide P2

N-methylation is a useful tool to enhance the biological activity of peptides as well as to improve oral-availability and proteolytic stability of peptides.^[34, 200-202] The *N*-methylation facilitates the formation of *cis*-amide bonds^[203] and thus opens up a new conformational space which may contain a bioactive conformation. A good example of the successful introduction of a methylated amide bond is the antiangiogenic drug candidate Cilengitide, which now undergoes phase III clinical trials.^[36] While highly *N*-methylated cyclic peptides are found to give low yields in the cyclization step due to the sterical strain, a mono-methyl scan is a practical method to screen for better binders. Although several methods for the *N*-methylation of amino acids in solution^[204, 205] as well as on solid phase^[204-206] have been published by now, the method of choice was the Mitsunobu type alkylation of the *o*NBS (*ortho*-nitrophenylsulfonyl) amino acid derivatives described by *Biron et al.*:^[204] The deprotected amino acid is converted into the *o*NBS-sulfonamide, alkylated using DIAD, triphenylphosphine and methanol in dry THF and deprotected with thioethanol / DBU in DMF. The next amino acid is then coupled with HATU. Generally, the *N*-methylation was introduced at the second position of the sequence – but never on the terminal amino acid to enable cyclization with DPPA. The procedure is outlined in Scheme III-32. Although the yields were smaller compared to the unmethylated peptides, satisfying amounts of all six possible mono-*N*-methylated peptides could be obtained.



Scheme III-32. Synthesis of *N*-methyl peptides on solid phase. ^[204]

The improvement of two peptides in respect to the original peptide once more underlines the relevance of peptide *N*-methylation for the optimization of bioactive peptides. While the other peptides display dramatically decreased affinity towards FVIII, a methylation at the glutamine amide increases the activity significantly in respect to **P2**. Although the structure of the **P2E** peptide can not be predicted, there is recent progress in understanding the impact of *N*-methylation on peptide conformation. ^[207]

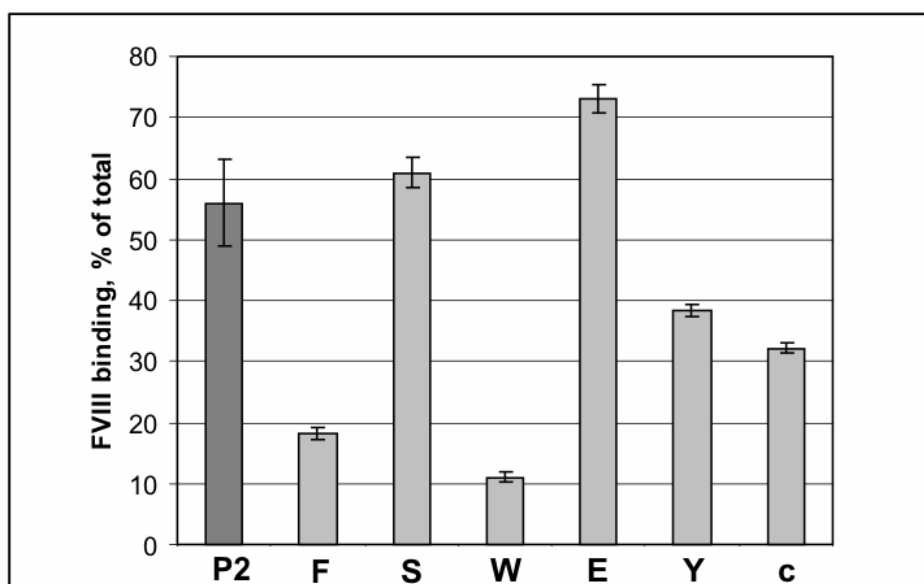


Figure III-16: Effect of *N*-methylation on FVIII binding affinity. The activity of the reference peptide *cyclo*(FSWEYc) **P2** is the mean value of three independent immobilizations and testings.

With more detailed structural data of highly active compounds, it could once be possible to rationally design functional peptides for FVIII purification and – if more structural models of FVIII domains evolve – it could be switched to structure based design. However, against the background of their application as affinity ligands, the peptides have to be accessible in larger quantities which may be not economic for these particular peptides.

III.2.4 Structure determination and binding analysis of P2

As described in the general part of this thesis, the FVIII molecule circulating in blood plasma is a heterodimer of a light and a heavy chain, each exhibiting a strict domain structure. The most potent of the cyclic peptides **P2**, *cyclo*(FSWEYc), has been tested on binding the isolated subunits as well as the available domains (A1, A2, C1; A3 and C2 were not accessible). While the total activity of the tested peptide was slightly smaller than in previous testings, the preference for the FVIII light chain is obvious (Figure III-17). The results of the binding assays with the A1 and A2 domains and the fact that the peptides all bind recombinant (with deleted B-domain) factor VIII is in accordance to the lack of affinity towards the whole heavy chain. The high affinity towards the light chain (A3-C1-C2) leaves only the A3 and C1 domain or the interface between the light chain domains as possible locations of the binding site.

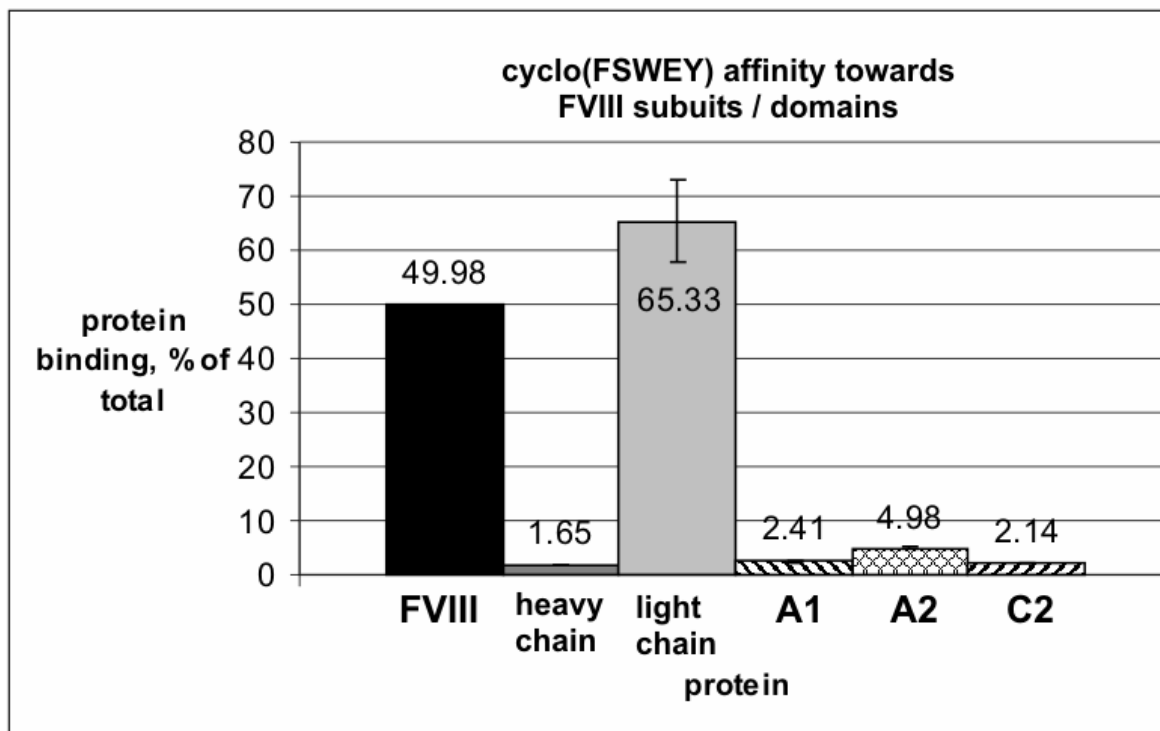


Figure III-17. Binding affinities of peptide *c(FSWEYc)* towards the two subunits of FVIII and three FVIII domains.

In an attempt to identify the epitope on FVIII responsible for ligand binding, the structure of the cyclic peptide **P2** was solved by NMR using the NOE contacts, distance geometry and molecular dynamics calculations. The NOE-contacts were recorded using the ROESY sequence in d^3 -MeOH using the *watergate* suppression of the MeOH proton. The solvent was chosen due to the very low solubility of the peptide in water and to avoid dimerization in DMSO. In addition to the ROESY spectrum, proton spectra were recorded between 295 and 315 K to obtain the temperature coefficients of the amide protons (for details see IV.4.1, p. 209). The structure displays a common turn arrangement which is often found within cyclic peptides with one D-amino acid.^[147] The structure is in good agreement to the predicted structure of cyclic hexapeptides with one D-amino acid. The D-cysteine is found in position $i+1$ of a β II' turn and induces another β II' turn at the far side with Trp in position $i+1$. The MD simulations, performed at the University of Naples by *Luciana Marinelli* indicated a highly stable turn structure for the upper β II'-turn, as expected because of the D-amino acid. The turn at the opposite side was found to be flexible and may also adopt a β I-turn.

The picture presented in Figure III-18 represents the minimum energy conformation which was found in the MD-simulations.

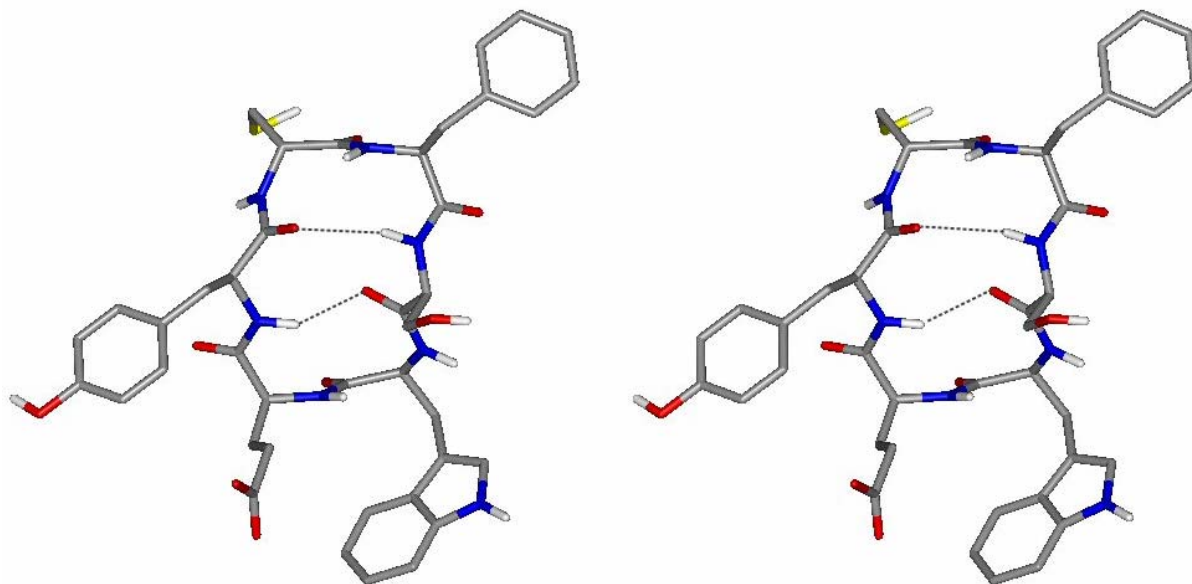


Figure III-18: Stereo view of the calculated structure of **P2** in d_3 -MeOH. Hydrogen bonds are shown as dotted lines.

Table III-13. Φ - und Ψ - angles in ideal β - and γ -turns.

Type	ϕ (i+1) [°]	ψ (i+1) [°]	ϕ (i+2) [°]	ψ (i+2) [°]
β I	-60	-30	-90	0
β I'	60	30	90	0
β II	-60	120	80	0
β II'	60	-120	-80	0
β Via	-60	120	-90	0
β Vib	-120	120	-60	150
γ	70 - 85	-60 - (-70)		
γ i	-70 - (-85)	60 - 70		

The low $N-H$ temperature coefficients display the shielded arrangement of the tyrosine and, particularly, of the Ser-NH (0.2 ppb/K). This is an indicator for little solvent exposure and, maybe, the formation of hydrogen bonds. Another relatively low temperature coefficient was found for the glutamine-NH, while the amide protons of tryptophane and especially Phe and D-Cys are most exposed to the solvents. This additional data matches the approximate model, which possibly can be used look for the binding site in factor VIII by means of molecular docking procedures. This may be part of future works as only few domains of FVIII have been structurally determined yet. The results from the domain binding assays furthermore hint at a binding of either the C1 domain (which was not available for testing) or binding to the interface between two or more domains of the light chain.

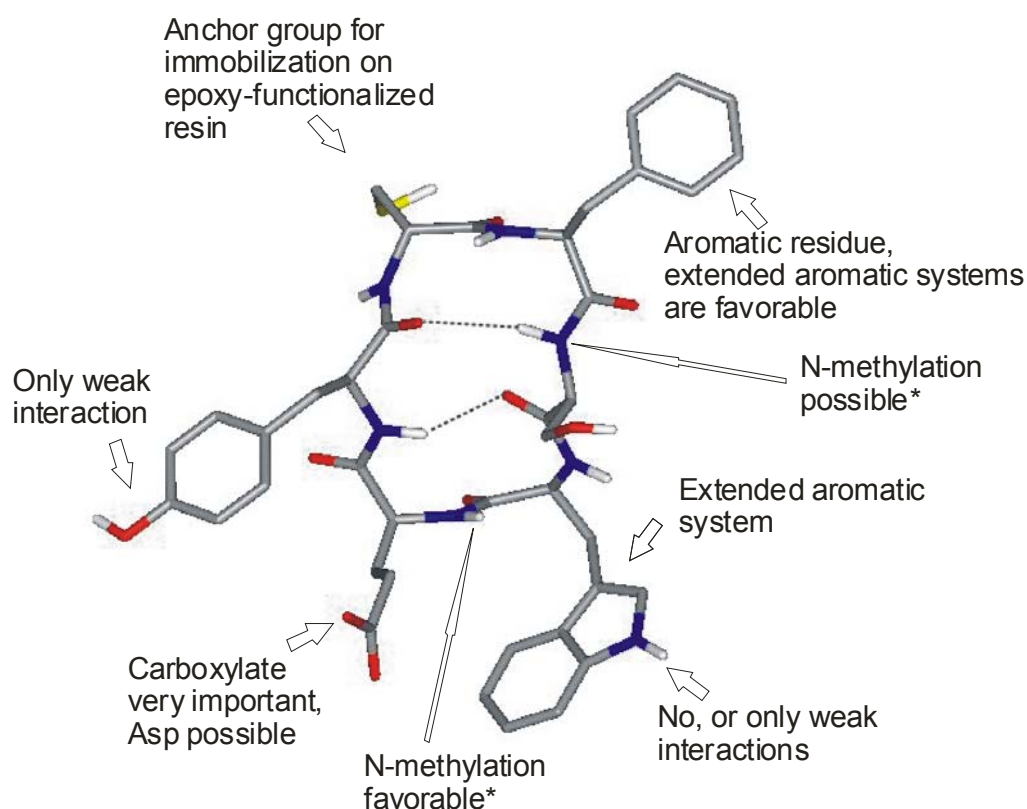


Figure III-19. Summary of pharmacophoric groups and possible modifications for the cyclic peptide **P2**. *It has to be stressed that the position of N -methylations are only denoted. In contrast to side chain modifications, they will completely change the actual conformation.

III.2.5 Outlook

The studies performed in this thesis aim at the ligand-based optimization of a cyclic peptide towards FVIII binding. The data obtained in different spatial screenings and mutagenesis studies allow a refinement of the pharmacophore and an identification of the main interactions crucial for FVIII-binding. Whether the already useful results can be combined in order to further optimize the structure was not determined. Problems arise mainly from contradictory results of modifications at the linear and the cyclic peptide and the testing system, which required rather large quantities of substance – which often was a limiting factor for the peptide synthesis. Even though the most active cyclic peptides synthesized in this thesis are only little less potent than an antibody as reference affinity ligand, the advantages of cyclic peptides over linear ones (stability, higher affinity) have to be carefully weighted against the disadvantages as the rather ineffective synthesis. A common way to overcome those problems is the synthesis of peptidomimetics by subsequent substitution of peptide bonds with isosteric structures. The optimization of the original octapeptide sequence towards the ligand-based design of a peptidomimetic is described in the Ph.D. thesis of *Sebastian Knör*.

The linear peptide sequence could be simplified to yield the pure recognition sequence WEY + the cysteine spacer without losing too much affinity. This short peptide sequence was a promising target for the transformation into a peptidomimetic. Chemical modifications of both the side-chains and peptide bonds finally yielded a small-molecule affinity ligand that shows an affinity profile comparable to the antibody and at the same time combines the advantages of a peptidomimetic concerning proteolytic stability with an easy synthetic accessibility. The availability of larger quantities of the affinity ligand enables the production of FVIII affinity columns at comparably low costs. Initial tests with small columns gave promising results since it was possible to concentrate FVIII directly from blood plasma. Furthermore, the non-peptidic ligands displayed excellent selectivities for FVIII against other plasma proteins and was found to be stable towards the proteolytic enzymes found in the serum.

III. Results and Discussion

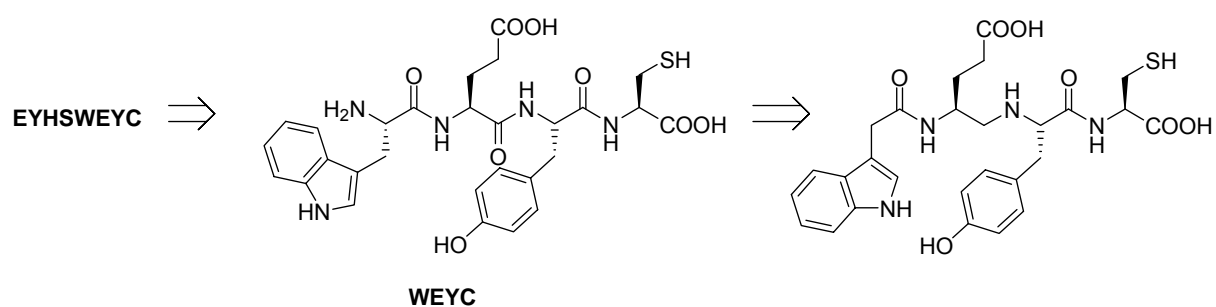


Figure III-20. Downsizing of a linear octapeptide sequence to a tetrapeptide and synthesis of a peptidomimetic with improved FVIII binding properties. The mimetic was able to bind >85% of labeled FVIII (P2: ~55%) and thus exceeds the antibodies used for FVIII purification.

IV Experimental Section

IV.1 Materials and Methods

Mass spectra were obtained by *electrospray ionization* (ESI) *electron impact ionization* (EI). **HPLC-ESI-MS** spectra were recorded on a *Finnigan LCQ* combined with an HPLC system *Hewlett Packard HP1100* (column material Nucleosil 100 5C₁₈). **GC-MS** spectra were recorded on a *Finnigan ThermoElectron Trace DSQ* instrument with direct insertion probe using EI at 70 eV. For sample separation, a fused silica DB-5ms capillary column (15 m x 0.25 mm, coated with 0.25 µm of liquid phase) and helium as carrier gas. Temperature program: 1 min isothermal at 50°C, then 5 K/min up to 300°C. **HPLC-purifications** were performed on following systems:

(A) *Beckman System Gold*, Programmable Solvent Module 125, Programmable Detector Module 166; column material YMC-ODS-A 120 5-C₁₈ (5 µm, 250x20 mm) semipreparative.

(B) *Pharmacia Basic 10 F*, pump unit P-900, Detector UV-900, autosampler A 900, Software: Unicorn, Version 3.00; column material: YMC-ODS-A 120 5-C₁₈ (1 µm, 250 x 4.6 mm), analytical.

(C) *Pharmacia Basic 100 F*, pump unit P-900, Detector UV-900, Software: Unicorn, Version 3.00; column material: (1) YMC-ODS-A 120 10-C₁₈ (10 µm, 250 x 20 mm) semipreparative; (2) YMC-ODS 120 11-C₁₈ (11 µm, 250 x 30 mm), preparative.

(D) *Waters System Breeze*, pump unit 1525, UV-Detector 2487 Dual, Software: Breeze Vers. 3.20; column material: ODS-A C₁₈ (120 Å, 5 µm, 250 mm × 20 mm) semipräparativ.

Different gradients of water and acetonitrile (+0.1% TFA) were used for HPLC separations.

TLC – monitoring was performed on Merck DC silica gel plates (60 F-254 on aluminum foil). Spots were detected by UV-absorption at 254 nm and/or by staining with a 5% solution of ninhydrine in ethanol or Mo-stain (6.25 g phosphormolybdaic acid, 2.5 g cerium-(IV)-sulfate and 15 mL sulfuric acid in 235 mL water) or potassium permanganate (5% in 1N aq. NaOH). All technical solvents were distilled prior to use or purchased as anhydrous solvents. Reagents were purchased *per synthesis* from

E. Merck, Fluka, Sigma, Aldrich, Acros or Lancaster and were used without purifications. Trt-polystyrene resin was purchased from *PepChem* (Tübingen). Wang-resin was obtained from *Novabiochem*. Protected and unprotected amino acids – if not synthesized - HOBt und Fmoc-Cl were purchased from *Alexis, Advanced Chemtech, Bachem, Neosystem, Novabiochem* oder *Iris*. NMP for solid phase synthesis was a kind gift from BASF-AG, Ludwigshafen.

Flash column chromatography was performed using silica gel 60 (63-200 μm) from *Merck* at 1-1.5 atm pressure. **Air / water-sensitive reactions** were performed in flame-dried flasks under an atmosphere of argon (99.996%). **Solid phase peptide synthesis** and other reactions on solid phase with less than 1 g resin were performed in syringes (*Becton-Dickinson*) equipped with a polypropylene frit (*Vetter Labortechnik*). The loaded syringes were stuck into a rubber stopper connected to the rotor of a rotary evaporator and mixed by gentle rotation. $^1\text{H-NMR}$ and $^{13}\text{C-NMR}$ spectra were recorded on Bruker AC250 or DMX500 spectrometers. Chemical shifts (δ) are given in *parts per million* (prussians per munich, ppm) relative to trimethylsilane (TMS). Following solvent peaks were used as internal standards: DMSO- d_5 : 2.50 ppm ($^1\text{H-NMR}$) und 39.46 ppm ($^{13}\text{C-NMR}$); CHCl_3 : 7.26 ppm ($^1\text{H-NMR}$) und 77.0 ppm ($^{13}\text{C-NMR}$). The assignment of protons and carbons was performed using 2D spectra (HMQC-COSY, TOCSY, HMBC). Structural data of peptides were obtained by ROESY experiments, spectra in d^3 -MeOH were recorded using *watergate* pulse programs for MeOH-suppression.

IV.2 General Procedures

IV.2.1 GP1 (Nucleophilic substitution of 2-bromopyridines)

2-Bromopyridine (1 eq.) was dissolved in the particular aminoalcohol (3 eq.) and heated in a sealed glass tube to 140°C over night. After cooling to room temperature, the reaction mixture was directly subjected to column chromatography on silica gel.

IV.2.2 GP2 (Synthesis of tyrosine ethers by Mitsunobu reaction)

In a dried flask, *N*-Boc-tyrosine methyl ester (1 eq.), the aminoalcohol (1.1 eq) and tributylphosphine (1.3 eq.) were dissolved in dry THF (0.05 - 0.1 M) and stirred at 0°C under argon. Azodicarboxylic dipiperidid (ADDP, 1.3 eq.) was dissolved in dry THF (0.2 M) and added dropwise to the reaction mixture in 4 h time. The resulting light

yellow suspension was allowed to warm to room temperature overnight. After addition of silica gel and evaporation of the THF, the product was purified by column chromatography.

IV.2.3 GP3 (Oxidation of 2-chloropyridines with MCPBA)

A solution of the particular 2-chloromethylpyridine (1 eq.) and *m*-chloroperbenzoic acid (70%, 1.2 eq.) in chloroform (~1 M) was stirred at 50°C for 12 h. After cooling to -10°C, most of the acid was removed by filtration and the filtrate concentrated under reduced pressure. The product was purified by column chromatography on silica gel (DCM / MeOH = 95 / 5 + 1% TEA).

IV.2.4 GP4 (Reduction of pyridine-*N*-oxides; reductive cleavage of benzyl protecting groups)

The starting material (1 eq.) was dissolved in methanol. After addition of the catalyst (5 % Pd / C, 15 mg / mmol starting material), the mixture was hydrogenated (1 atm H₂) at ambient temperature. The progress of the reaction was monitored by TLC until all starting material was consumed. The catalyst was removed by filtration over Celite[®], the solvent was removed and the residue purified by flash chromatography on silica gel.

IV.2.5 GP5 (TBDPS protection of pyridin-2-ylamino alcohols)

To an ice-cooled solution of the particular alcohol (1 eq.) in dry DCM (~0.1 - 0.2 M) was added imidazole (2 eq.) followed by TBDPS chloride (1.3 eq.) under argon atmosphere. The resulting suspension was stirred at ambient temperature over night (TLC monitoring). The solvent was removed *in vacuo* and the resulting mixture directly applied onto a silica gel column and purified by flash chromatography.

IV.2.6 GP6a (Boc-protection of 2-pyridinamines)

The particular 2-pyridinamine (1 eq.) was dissolved in dry THF (~0.2 M). Boc-anhydride (1.2 eq.) was added, followed by TEA (2 eq.) and DMAP (0.1 eq.). Stirring was continued until the TLC indicated total consumption of the starting material (usually over night). The solvents were evaporated and the reaction mixture purified directly by flash column chromatography.

GP6b (Boc protection of primary amines)

The corresponding amine was dissolved in THF (0.1 M). Triethylamine was added, followed by a solution of Boc-anhydride (1.1-1.3 eq.) in THF. The reaction was followed by HPLC until the starting material was totally consumed (over night). The reaction mixture was concentrated *in vacuo* and diluted with ethyl acetate. The mixture was washed with 5% citric acid, water and brine, dried over Na₂SO₄, filtered and evaporated. The crude product was purified by column chromatography.

IV.2.7 GP7 (Desilylation of TBDPS-protected alcohols)

The particular TBDPS-protected alcohol was dissolved in THF (~0.2 M). TBAF (1.1 eq.) was added and the reaction stirred for 12 h at ambient temperature. The solvents were evaporated and the alcohol purified directly by flash column chromatography.

IV.2.8 GP8a (Deprotection and acylation of ligand precursors with acid chlorides)

The particular starting material was dissolved in a 3 : 1 mixture of dioxane and concentrated aqueous HCl (~0.1 M). After stirring for 1 h, the solvents were removed under reduced pressure. The deprotected amine was re-dissolved in dioxane – water 1 : 1 (~0.1 M), NaHCO₃ was added and the resulting solution treated with 1.1 eq. of the corresponding acid chloride. After stirring for 30 min, the solvents were removed *in vacuo* and the residue re-dissolved in methanol-water 3 : 1. LiOH (5 eq.) was added under stirring and the course of the reaction followed by analytical HPLC (usually 1 d). The resulting deprotected compound was purified using preparative reverse phase HPLC.

GP8b (Deprotection and acylation of ligand precursors with HATU)

The particular starting material was dissolved in a 3 : 1 mixture of dioxane and concentrated aqueous HCl (~0.1 M). After stirring for 1 h, the solvents were removed under reduced pressure. The deprotected amine was re-dissolved in DMF (~0.2 M) followed by addition of the corresponding aromatic acid (1.3 eq.), HATU (1.3 eq.) and DIEA (5 eq.). The resulting yellow solution was stirred for 24 h at ambient temperature. After evaporation of the DMF, the residue was taken up in methanol-water 3 : 1. LiOH (5 eq.) was added under stirring and the course of the reaction

followed by analytical HPLC (usually 1 d). The resulting deprotected compound was purified using preparative reverse phase HPLC.

GP8c (Deprotection and formation of sulfonamides)

The particular starting material was dissolved in a 3 : 1 mixture of dioxane and concentrated aqueous HCl (~0.1 M). After stirring for 1h, the solvents were removed under reduced pressure. The deprotected amine was taken up in dry DCM (~0.1 M), followed by addition of the corresponding aromatic sulfonic acid chloride and DIEA (5 eq.). After stirring over night at ambient temperature and solvent evaporation, the residue was re-dissolved in methanol – water 3 : 1. LiOH (5 eq.) was added under stirring and the course of the reaction followed by analytical HPLC (usually 1 d). The resulting deprotected compound was purified using preparative reverse phase HPLC.

IV.2.9 GP9 (Guadinylation of a free amine using *N,N'*-bis-Boc-thiourea)

The particular amine (1 eq.) was dissolved in dry methanol (0.05-0.1 M) and cooled to 0°C. After addition of *N,N'*-bis-Boc-thiourea (1.5 eq.) and mercury dichloride (2 eq.), TEA (10 eq.) were added dropwise. A precipitate forms whose color may vary from colorless, yellow, greenish to deep black. The mixture was allowed to warm up to room temperature over night and filtered over a small pad of celite®. The solvent was removed under reduced pressure and the crude mixture purified by flash chromatography on silica gel.

IV.2.10 GP10 (Conversion of aryl bromides to aryl acids)

To a cooled (-78°C) solution of the particular bromide (1 eq.) in dry THF (0.2 M) was added *n*BuLi (1.6 M in hexane, 1.2 eq.) under an argon atmosphere. The resulting white suspension was stirred for 30 min. After addition of crushed dry ice (~10 g), the cooling bath was removed and the reaction mixture allowed to warm to room temperature. The mixture was acidified with 1M HCl and extracted with ethyl acetate. The organic layers were washed with brine, dried over Na₂SO₄, filtered and concentrated. The crude product was recrystallized from DCM/hexane.

IV.2.11 GP11 (Preparation of methyl esters with thionyl chloride)^[208]

The corresponding acid was dissolved in methanol (0.2 M) and cooled in an ice bath. Thionyl chloride (10 eq.) was added dropwise and the resulting mixture was stirred over night. After evaporation of the solvents, the residue was dissolved in ethyl acetate and sat. NaHCO₃ solution, the organic layer was separated, washed with brine, dried over Na₂SO₄, filtered and evaporated. The crude product was purified either by recrystallization or column chromatography.

IV.2.12 GP12 (Loading of TCP-resin)^[209]

Chloro-TCP-resin (theoretical loading 1.04 mmol/g) was filled into a suitable syringe (20 mL for 1 g resin) equipped with a PP-frit and a canula. The amino acid (1.2 mmol, referring to theoretical loading) was dissolved in dry DCM (8 mL / g resin), treated with DIEA (2.5 eq., referring to amino acid) and sucked directly into the syringe with the resin and mixed by gentle rotation for 1 h. The resin was capped by adding 0.2 mL methanol (per gram resin) and 0.2 eq. DIEA to the reaction mixture and shaken for 20 min. The loaded resin was washed with DCM (3x), NMP (3x), NMP / methanol 1 : 1 (1x) and pure methanol (3x). After drying under vacuum, the resin was weighted and the real loading calculated with following equation:

$$c[\text{mol} / \text{g}] = \frac{m_{\text{total}} - m_{\text{resin}}}{(MW - 36.461) \times m_{\text{total}}}$$

Equation IV-1: Calculation of resin loading. m_{total} = mass of loaded resin. m_{resin} = mass of unloaded resin. MW = molecular weight of immobilized amino acid.

In cases, where the loading was not calculated, an average loading of 0.6 mmol / g was assumed.

IV.2.13 GP13 (Loading of Bromo-Wang-resin)

Bromo-Wang resin (theoretical loading 1.40 mmol / g) was filled into a suitable syringe as described in **GP12**. The amino acid (2 eq.), DIEA (3 eq.) and cesium iodide (0.1 eq.) were dissolved in dry DMF (8 mL / g resin), the mixture sucked into the syringe and shaken for 4 h (shaking over night was possible, but didn't affect the real loading). The solution was discarded, the resin washed twice with NMP and capped with a solution of 3 eq. acetic acid and 5 eq. of DIEA in dry DMF (8 mL / g

resin). After thoughtful washing with NMP (5x), the resin was treated with methanol (3x), dried under vacuum and weighted. The particular loading was calculated using a modified equation 1, where the atomic weight of chlorine (36.461) was replaced by bromine (79.90).

IV.2.14 GP14 (Solid phase Fmoc deprotection) ^[210]

The washed and swollen resin was treated twice with a solution of piperidine (20%) in NMP (v/v), 5 min and 15 min, respectively and washed 5 times with NMP.

IV.2.15 GP15 (Solid phase peptide coupling with HOBt / TBTU) ^[211]

The amino acid (2.5 eq. referring to resin loading) was dissolved in a 0.2 M solution of HOBt and TBTU in NMP (2.5 eq.). After addition of DIEA (6.5 eq., 1.3 eq. per acid), the solution was mixed with the resin and shaken for 1.5 h. The mixture was discarded and the resin washed 5 times with NMP.

IV.2.16 GP16 (Solid phase peptide coupling with HOAt / HATU) ^[212]

The amino acid (2 eq. referring to resin loading), HOAt (2 eq.) and HATU (2 eq.) were dissolved in NMP. After addition of DIEA (5.2 eq., 1.3 eq. per acid), the solution was mixed with the resin and shaken for 2 h. The mixture was discarded and the resin washed 5 times with NMP. In case of an over-night coupling, 10 eq. of collidine were used instead of DIEA.

IV.2.17 GP17 (Solid phase coupling of aromatic acids) ^[212]

The aromatic acid (2 eq.) and HATU (2 eq.) were dissolved in NMP, mixed with DIEA (5 eq.) and shaken for 4 h – over night, depending on sterical demand and electronic properties of the aromate. The reaction mixture was discarded and the resin washed 5 times with NMP.

IV.2.18 GP18 (N-methylation of amino acids on solid phase) ^[206]

A solution of *o*-NBS-Cl (4 eq.) and collidine (10 eq.) in NMP was added to the resin-bound free amine peptides and shaken for 15 min at room temperature. The solution was discarded and the resin washed 5 times with NMP followed by dry THF (3x). A solution of triphenylphosphine (5 eq.) and methanol in dry THF was added to the

resin and shaken for 1 min. A solution of DIAD (5 eq.) in dry THF was added in portions to the reaction mixture and shaken for 10 min. The resin was filtered and washed with NMP (5x). For *o*-NBS deprotection, the resin was shaken for 5 min with a solution of mercaptoethanol (10 eq.) and DBU (5 eq.) in NMP. The deprotection procedure was repeated once more and the resin washed 5 times with NMP.

IV.2.19 GP19 (Cleavage of side-chain-protected peptides from TCP-resin)

The resin was swollen in DCM and then treated with a solution of DCM, acetic acid and TFE (6 / 3 / 1, v/v/v). After shaking for 1 h, the procedure was repeated and finally the resin washed once with the cleavage solution. The collected solutions were diluted with toluene and concentrated *in vacuo*. The dilution with toluene and evaporation was repeated twice (no smell of acetic acid). The peptide was obtained as acetate.

IV.2.20 GP20 (Cleavage and full deprotection of peptides from TCP/Wang resin)

The resin was swollen in DCM and then treated with a mixture of TFA, water and triisopropylsilane (95%, 2.5%, 2.5%, v/v/v). The mixture was shaken for 1-2 h at ambient temperature, then the resin was washed with the cleavage mixture and deprotected peptide precipitated from the collected solutions by addition of diethyl ether. The peptide was spun down in a centrifuge, washed twice with ether and dried under vacuum. In case of acid sensible peptides, the amount of TFA was reduced to DCM / TFA / H₂O / TIPS = 47.5 / 47.5 / 2.5 / 2.5 and the course of the deprotection was followed by ESI-MS.

IV.2.21 GP21 (backbone cyclization of peptides) ^[172]

The linear, side-chain protected peptide was diluted with DMF to 10⁻³ - 10⁻⁴ M. After addition of DPPA (3 eq.) and NaHCO₃ (5 eq.), the mixture was stirred until all starting material was consumed (HPLC / LC-MS monitoring), usually 12 h. The solution was concentrated under reduced pressure and the cyclic peptide precipitated by addition of water. In case of an improper precipitation, water was substituted with brine. The

peptide was spun down in a centrifuge, washed twice with water and dried under vacuum.

IV.2.22 GP22 (Peptide cyclization by disulfide formation)

The linear, deprotected peptide was dissolved in water / acetonitrile (10^{-3} M). The pH was adjusted to 8 - 8.5 by addition of NaHCO_3 . After addition of H_2O_2 (30% aqueous solution, 1 eq.) and stirring for 30 min, the reaction was monitored by LC-MS. In case of an improper cyclization, an additional equivalent of H_2O_2 was added, until the reaction was complete. The solvent was evaporated and the resulting peptide purified by *reverse phase* HPLC.

IV.2.23 GP23 (N-Alloc deprotection on solid phase)

The dry resin was swollen with dry DCM for 5 min. The resin was then treated with a solution of *tetrakis*-triphenylphosphinepalladium (0.25 eq.) and phenylsilane (10 eq.) in dry DCM at ambient temperature. Care had to be taken due to gas evolution and the pressure had to be released from the reaction vessel from time to time. After 1.5 h of shaking, the mixture was filtered and the resin washed twice with a 0.5% solution of DDTC (sodium *N,N*-diethyldithiocarbamate) in DMF and a 0.5% solution of DIEA in DMF. The washing procedure was repeated and the resin washed five times with NMP.

IV.2.24 GP24 (Reduction of nitro groups on solid phase)

The swollen resin was treated with a solution of SnCl_2 in DMF (8 mL / g resin) over night. The progress of the reaction was monitored by MS and the procedure repeated for 4 h if necessary. The resin was washed five times with NMP.

IV.2.25 GP25 (coupling of aza-glycine with building block 72) ^[176]

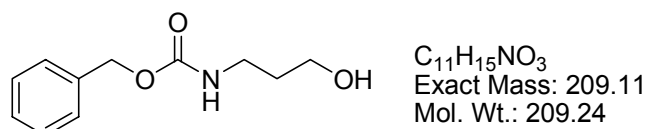
The amino-functionalized, dry resin was swollen with dry DCM for 5 min. The freshly prepared, dry building block **72** was dissolved in dry DCM, mixed with the resin and shaken for 90 minutes. The resin was washed with DCM (5 times).

IV.2.26 GP26 (guanylation on solid phase)

The amino-functionalized resin added to a solution of 10 eq. *N,N'*-bis-Boc-guanidylpyrazole in dry chloroform (10 mL / g resin) in a closed reaction vessel. The mixture was shaken over night at 50°C. The resin was filtered and washed five times with DCM. The unconsumed guanidylpyrazole could be recycled by concentration of the filtrate and recrystallization from hexane / ethyl acetate.

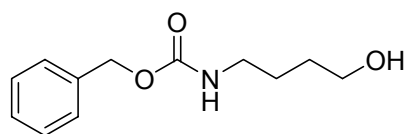
IV.3 Compound Preparation and Analytical Data

IV.3.1 Preparation of 3-(benzyloxycarbonylamino)propan-1-ol, 1a



3-Aminopropanol (1.10 g, 14.65 mmol, 1.1 eq.) and $NaHCO_3$ (1.45 g, 17.32 mmol, 1.3 eq.) were dissolved in water-dioxane 1 : 1 (100 mL) and cooled to 0°C. A solution of benzyloxycarbonyl-*O*-succinimide (3.10 g, 13.32 mmol, 1 eq.) in dioxane (20 mL) was added dropwise and the reaction mixture stirred for 12 h. After partial evaporation of the dioxane, the mixture was acidified with 1 N hydrochloric acid and extracted twice with ethyl acetate. The combined organic layers were washed with brine, dried with Na_2SO_4 and filtered. After evaporation of the solvents, the crude product was purified by flash chromatography on silica gel (hexane : ethyl acetate 1 : 1 - 2 : 3) To give the title compound (2.12 g, 10.12 mmol, 76%) as a colorless solid.

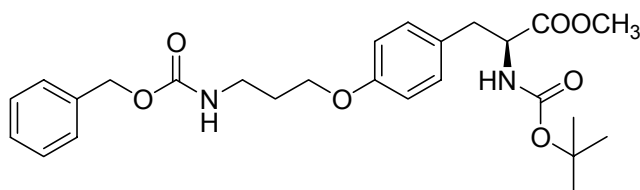
1H -NMR (250 MHz, $CDCl_3$): δ = 7.34 (m, 5H, Ph-*H*), 5.15 (bs, 1H, -*NH*), 5.10 (s, 2H, Ph- CH_2O), 3.66 (t, 3J = 5.8 Hz, 2H, - CH_2OH), 3.33 (dd, 2J = 12.2 Hz, 3J = 6.0 Hz, 2H, - $NHCH_2$ -), 2.73 (bs, 1H, -*OH*), 1.69 (m, 2H, - $CH_2CH_2CH_2$ -). **^{13}C -NMR** (108 MHz, $CDCl_3$): δ = 157.2, 136.4, 128.4, 128.1, 128.0, 66.7, 59.6, 37.8, 32.4. **HPLC** (10-100%, 30 min) t_R = 13.64 min. **MS** (EI): 209.1 [M] $^+$, 108.0 [$BnOH$] $^+$, 91 [Bn] $^+$.

IV.3.2 Preparation of 3-(benzyloxycarbonylamino)butan-1-ol, **1b**

C₁₂H₁₇NO₃
Exact Mass: 223.12
Mol. Wt.: 223.27

3-Aminobutanol (2.94 g, 33.0 mmol, 1.0 eq.) and TEA (5.96 mL, 42.9 mmol, 1.3 eq.) were dissolved in water-dioxane 1 : 1 (100 mL) and cooled to 0°C. A solution of benzyloxycarbonyl-*O*-succinimide (8.22 g, 33.0 mmol, 1 eq.) in dioxane (20 mL) was added dropwise and the reaction mixture stirred for 12 h. After partial evaporation of the dioxane, the mixture was acidified with 1 N hydrochloric acid and extracted twice with ethyl acetate. The combined organic layers were washed with brine, dried with Na₂SO₄ and filtered. After evaporation of the solvents, the crude product was purified by recrystallization from hexane / ethyl acetate to give the title compound (6.45 g, 29.0 mmol, 88%) as a colorless solid.

¹H-NMR (250 MHz, CDCl₃): δ = 7.32 (m, 5H, Ph-*H*), 5.20 (bs, 1H, -*NH*), 5.06 (s, 2H, Ph-*CH*₂O), 3.59 (t, ³*J* = 5.5 Hz, 2H, -*CH*₂OH), 3.17 (m, 2H, -*NHCH*₂-), 2.84 (bs, 1H, -*OH*), 1.54 (m, 4H, -*CH*₂*CH*₂*CH*₂*CH*₂-). **¹³C-NMR** (75 MHz, CDCl₃): δ = 156.5, 136.5, 128.4, 127.9, 127.9, 66.5, 62.0, 40.7, 29.5, 26.3. **HPLC** (10-100%, 30 min) *t*_R = 14.91 min. **MS**: 223.1 [M], 108.0 [BnOH]⁺, 91.0 [Bn]⁺.

IV.3.3 Preparation of methyl 3-[4-(3-benzyloxycarbonylaminopropoxy)phenyl]-2-(*S*)-(tert.butylloxycarbonylamino)propionate, **2a**.

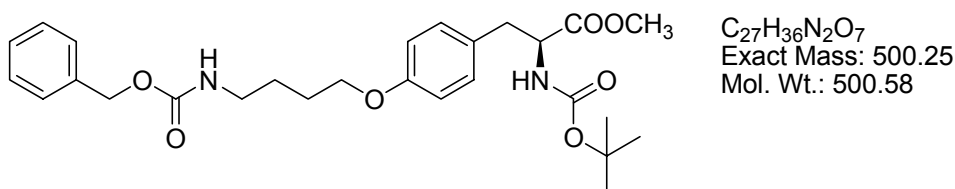
C₂₆H₃₄N₂O₇
Exact Mass: 486.24
Mol. Wt.: 486.56

The title compound was prepared from **1a** (0.63 g, 3.00 mmol), Boc-tyrosine methyl ester (0.89 g, 3.00 mmol), tributylphosphine (0.96 mL, 3.90 mmol) and ADDP (0.98 g, 3.90 mmol) according to **GP2**. Purification by flash chromatography (hexane / ethyl acetate 2 : 1) gave 1.33 g (2.73 mmol, 91%) of a colorless solid.

¹H-NMR (360 MHz, CDCl₃): δ = 7.34 (m, 5H, Ph-*H*), 7.02 (d, 2H, ³*J* = 8.6 Hz, 2H, Tyr-*H*_{3,3'}), 6.78 (d, ³*J* = 8.6 Hz, 2H, Tyr-*H*_{2,2'}), 5.10 (s, 2H, Ph*CH*₂O), 4.53 (m, 1H,

-CHCOOCH₃), 3.99 (t, ³J = 5.9 Hz, 2H, -CH₂OAr), 3.70 (s, 3H, -COOCH₃), 3.40 (q, ³J = 8.0 Hz, 2H, CbzNHCH₂), 3.03 (m, 2H, -CH₂CHCOOCH₃), 1.99 (m, 2H, -CH₂CH₂CH₂-), 1.42 (s, 9H, ^tBu). ¹³C-NMR (108 MHz, CDCl₃): δ = 172.4, 157.8, 156.4, 136.6, 130.3, 128.5, 128.1, 114.6, 79.9, 66.7, 65.8, 54.5, 52.1, 38.7, 37.5, 29.4, 28.3. **HPLC** (10-100%, 30 min) t_R = 24.69 min. **MS** (ESI): m/z = 487.3 [m+H⁺]⁺, 481.3 [m+H⁺-^tBu]⁺, 387.2 [M+H⁺-Boc]⁺.

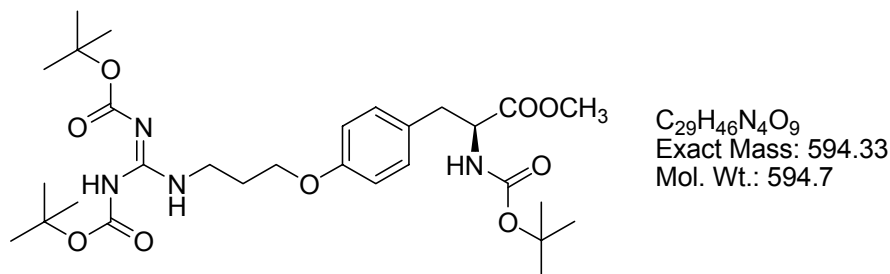
IV.3.4 Preparation of methyl 3-[4-(4-benzyloxycarbonylaminobutoxy)phenyl]-2-(S)-(tert.butylloxycarbonylamino)propionate, **2b**.



The title compound was prepared from **1b** (1.00 g, 4.48 mmol), Boc-tyrosine methyl ester (1.20 g, 4.07 mmol), tributylphosphine (1.3 mL, 5.29 mmol) and ADDP (1.30 g, 5.29 mmol) according to **GP2**. Purification by flash chromatography (hexane / ethyl acetate 2 : 1) gave 1.54 g (3.17 mmol, 71%) of a colorless solid.

¹H-NMR (250 MHz, CDCl₃): δ = 7.35 - 7.04 (m, 5H, Ph-H), 7.01 (d, ³J = 8.4 Hz, 2H, Tyr-H3,3'), 6.79 (d, ³J = 8.2 Hz, 2H, Tyr-H2, 2'), 5.10 (s, 2H, PhCH₂O), 4.98 (d, ³J = 7.7 Hz, 1H, Boc-NH), 4.94 (bs, 1H, Cbz-NH), 4.53 (m, 1H, -CHCOOCH₃), 3.93 (t, ³J = 5.8 Hz, 2H, -CH₂OAr), 3.70 (s, 3H, -COOCH₃), 3.26 (q, ³J = 6.3 Hz, 2H, -CbzNHCH₂-), 3.04 (dd, ²J = 13.7 Hz, ³J = 5.6 Hz, 1H, CHCH(H')CHCOOCH₃), 2.98 (dd, ²J = 13.8 Hz, ³J = 5.7 Hz, 1H, CHCH(H')CHCOOCH₃), 1.80 (m, 2H, -CH₂CH₂O), 1.68 (m, 2H, NHCH₂CH₂-), 1.42 (s, 9H, ^tBu). ¹³C-NMR (75 MHz, CDCl₃): δ = 172.3, 157.9, 156.4, 155.0, 136.6, 130.2, 128.4, 128.0, 114.5, 79.8, 67.3, 66.6, 54.5, 52.1, 40.7, 37.4, 28.3, 26.7, 26.4. **HPLC** (10-100%, 30 min) = 25.25 min. **MS** (ESI): m/z = 1022.9 [2m+Na⁺]⁺, 523.2 [m+Na⁺]⁺, 467.3 [m+Na⁺-^tBu]⁺, 401.4 [m+H⁺-Boc]⁺.

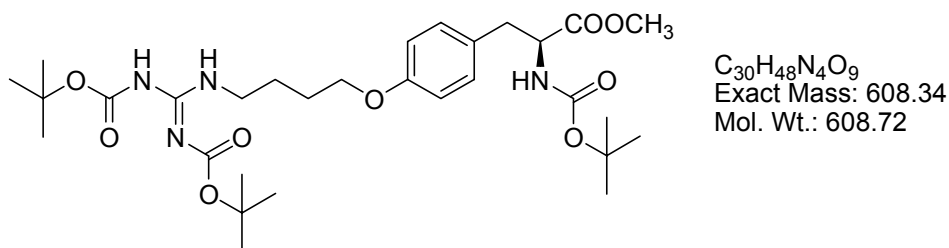
IV.3.5 Preparation of methyl 3-{4-[3-*N,N'*-(bis-*tert*.butyloxycarbonyl)-guanidyl-propoxy]phenyl}-2-(*S*)-(tert.butyloxycarbonylamino)propionate, 3a.



Compound **2a** (0.51 g, 1.05 mmol) was Cbz-deprotected following **GP4**. To avoid catalyst deactivation, 1 drop of 1 N hydrochloric acid was added to the mixture. After filtration, the crude product was guanidylated according to **GP9** [BisBoc-thiourea (0.41 g, 1.5 mmol), HgCl₂ (0.54 g, 2.00 mmol), TEA (1.03 mL, 10 mmol)]. Purification by flash chromatography on silica gel (hexane / ethyl acetate 2 : 1) gave the title compound (206 mg, 0.35 mmol, 33%) as colorless solid.

¹H-NMR (360 MHz, CDCl₃): δ = 11.50 (bs, 1H, BocNHC=N), 8.64 (bs, 1H, N=CNHCH₂), 7.01 (d, ³J = 8.6 Hz, 2H, Tyr-*H*3,3'), 6.87 (d, ³J = 8.7 Hz, 2H, Tyr-*H*3,3'), 4.95 (d, ³J = 7.7 Hz, 1H, -CHNH₂Boc), 4.51 (m, 1H, -CHCOOCH₃), 4.02 (t, ³J = 5.8 Hz, 2H, -CH₂OAr), 3.69 (s, 3H, -COOCH₃), 3.63 (dd, ²J = 11.8 Hz, ³J = 6.3 Hz, 2H, NHCH₂-), 3.01 (m, 2H, -CH₂CHCOOCH₃), 2.05 (m, 2H, -CH₂CH₂CH₂-), 1.50 (s, 9H, ^tBu), 1.49 (s, 9H, ^tBu), 1.41 (s, 9H, ^tBu). **¹³C-NMR** (75 MHz, CDCl₃): δ = 172.4, 163.6, 157.8, 156.1, 153.1, 130.2, 128.1, 114.5, 83.0, 82.5, 79.2, 66.3, 54.5, 52.1, 39.1, 37.5, 28.6, 28.2 (2C), 28.1, 28.0. **HPLC** (10-100%, 30 min) t_R = 23.38 min. **MS**: m/z = 617.26 [m+Na⁺]⁺, 595.19 [m+H⁺]⁺, 495.22 [m+H⁺-Boc]⁺, 395.42 [m+H⁺-2Boc]⁺, 339.42 [m+H⁺-2Boc-^tBu]⁺, 295.51 [m+H⁺-3Boc]⁺.

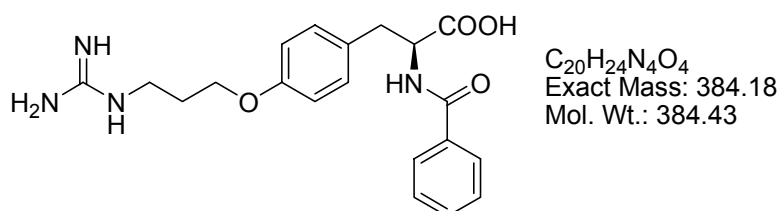
IV.3.6 Preparation of methyl 3-{4-[4-*N,N'*-(bis-*tert*.butyloxycarbonyl)-guanidyl-butoxy]phenyl}-2-(*S*)-(tert.butyloxycarbonylamino)propionate, **3b.**



Compound **2b** (840 mg, 1.68 mmol) was Cbz-deprotected following **GP4**. To avoid catalyst deactivation, 1 drop of 1 N hydrochloric acid was added to the mixture. After filtration, the crude product was guanidylated according to **GP9** [BisBoc-thiourea (696 mg, 2.52 mmol), $HgCl_2$ (910 mg, 3.36 mmol), TEA (2.35 mL, 17 mmol)]. Purification by flash chromatography on silica gel (hexane / ethyl acetate 8 : 2 – 7 : 3) gave the title compound (253 mg, 0.42 mmol, 25%) as colorless solid.

1H -NMR (250 MHz, $CDCl_3$): δ = 11.48 (bs, 1H, BocNHC=N), 8.34 (bs, 1H, N=CHNHCH₂), 6.98 (d, 3J = 8.5 Hz, 2H, Tyr-H3,3'), 6.78 (d, 3J = 8.6 Hz, 2H, Ar-H2,2'), 4.94 (d, 3J = 7.8 Hz, 1H, -NHBoc), 4.49 (m, 1H, -CHNHBoc-), 3.92 (d, 3J = 5.6 Hz, 2H, -CH₂-O-), 3.67 (s, 3H, -COOCH₃), 3.46 (m, 2H, -NHCH₂-), 2.98 (m, 2H, Ar-CH₂-), 1.88 - 1.64 (m, 4H, -CH₂CH₂-), 1.47, 1.46 (2s, 18H, 2 ^tBu), 1.39 (s, 9H, ^tBu). **^{13}C -NMR** (75 MHz, $CDCl_3$): δ = 172.3, 163.5, 157.9, 156.1, 155.0, 153.2, 130.1, 127.8, 114.4, 82.9, 79.7, 77.2, 67.1, 28.2, 28.0, 26.5, 25.7. **HPLC** (10-100%, 30 min): t_R = 24.41 min. **MS** (ESI): m/z = 631.2 [$m+Na$]⁺, 609.1 [$m+H$]⁺, 509.2 [$m+H$ -Boc]⁺, 409.2 [$m+H$ -2Boc]⁺, 353.3 [$m+H$ -2Boc-^tBu]⁺, 309.3 [$m+H$ -3Boc]⁺.

IV.3.7 Preparation of 2-(benzamido)-3-[4-(3-guanidylpropoxy)phenyl]propionic acid, **4a.**

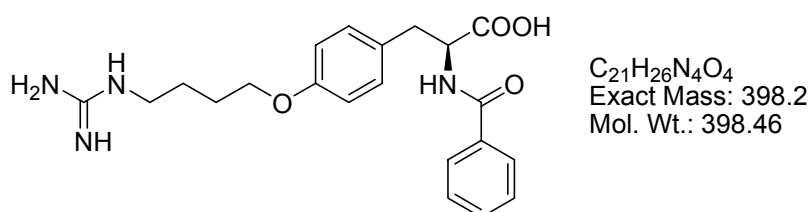


The title compound was synthesized from **3a** (55 mg, 150 μ mol) according to **GP8a** [Benzoyl chloride (20 μ L, 165 μ mol), $NaHCO_3$ (63 mg, 750 μ mol), LiOH (18 mg,

0.75 mmol)]. Purification using preparative HPLC and lyophilization afforded **4a** (12 mg, 31.2 μ mol, 21%) as TFA salt (colorless solid).

$^1\text{H-NMR}$ (500 MHz, DMSO): δ = 12.77 (s, 1H, COOH), 8.66 (d, 3J = 8.0 Hz, 1H, -NHCOPh), 7.80 (d, 3J = 7.3 Hz, 2H, Ph-H2,2'), 7.71 (t, 3J = 5.4 Hz, 1H, -NHCH₂), 7.52 (t, 3J = 7.5 Hz, 1H, Ph-H4), 7.45 (t, 3J = 7.5 Hz, 2H, Ph-H3,3'), 7.23 (d, 3J = 8.8 Hz, 2H, Tyr-H3,3'), 6.83 (d, 3J = 8.4 Hz, 2H, Tyr-H2,2'), 4.57 (m, 1H, -HCOOH), 3.95 (t, 3J = 6.1 Hz, 2H, CH₂OAr), 3.25 (m, 2H, -NHCH₂-), 3.12 (dd, 2J = 13.8 Hz, 3J = 4.2 Hz, 1H, Ar-CH(H')-), 3.00 (dd, 2J = 13.8 Hz, 3J = 10.7 Hz, 1H, Ar-CH(H')-), 1.89 (m, 2H, -CH₂CH₂CH₂-). **$^{13}\text{C-NMR}$** (125 MHz, DMSO): δ = 173.1, 166.2, 156.9, 156.8, 133.8, 131.2, 130.2, 130.0, 128.1, 127.2, 114.1, 64.5, 54.4, 37.8, 35.4, 28.1. **HPLC** (10-50%, 30 min): t_{R} = 12.34 min. **MS** (ESI): m/z = 385.5 [m+H]⁺. **HR-MS** (ESI) (C₂₀H₂₅N₄O₄⁺): Calc.: 385.1870, found: 385.1866.

IV.3.8 Preparation of 2-(benzamido)-3-[4-(4-guanidylbutoxy)phenyl] propionic acid, **4b**.

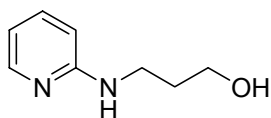


The title compound was synthesized from **3b** (161 mg, 271 μ mol) according to **GP8a** [Benzoyl chloride (50 μ L, 407 μ mol), NaHCO₃ (68 mg, 813 μ mol), LiOH (110 mg, 2.7 mmol)]. Purification using preparative HPLC and lyophilization afforded **4b** (30 mg, 60.2 μ mol, 22%) as TFA salt (colorless solid).

$^1\text{H-NMR}$ (500 MHz, DMSO): δ = 12.76 (bs, 1H, COOH), 8.66 (d, 3J = 8.2 Hz, 1H, -NHCOPh), 7.81 (d, 3J = 7.1 Hz, 2H, Ph-H2,2'), 7.69 (t, 3J = 5.5 Hz, 1H, -NHCH₂), 7.52 (t, 3J = 7.3 Hz, 1H, Ph-H4), 7.45 (t, 3J = 7.5 Hz, 2H, Ph-H3,3'), 7.22 (d, 3J = 8.6 Hz, 2H, Tyr-H3,3'), 6.82 (d, 3J = 8.6 Hz, 2H, Tyr-H2,2'), 4.56 (m, 1H, -CHCOOH), 3.92 (t, 3J = 6.3 Hz, 2H, -CH₂OAr), 3.14 (m, 2H, -NHCH₂-), 3.12 (m, 1H, Ar-CH(H')-), 3.00 (dd, 2J = 13.8 Hz, 3J = 10.7 Hz, Ar-CH(H')-), 1.70 (m, 2H, -CH₂CH₂CH₂OAr), 1.59 (m, 2H, -CH₂CH₂CH₂OAr). **$^{13}\text{C-NMR}$** (125 MHz, DMSO): δ = 173.1, 166.2, 157.0, 156.7, 133.8, 131.2, 129.9, 128.1, 127.2, 114.0, 66.7, 54.4,

40.3, 39.4, 35.3, 25.7, 25.2. **HPLC** (10-50%, 30 min): $t_R = 20.82$ min. **MS** (ESI): $m/z = 399.3$ $[m+H]^+$. **HR-MS** (ESI) ($C_{21}H_{27}N_4O_4$) $^+$: Calc.: 399.2027, Found: 399.2023.

IV.3.9 Preparation of 3-(pyridine-2-ylamino)propan-1-ol, **5**.

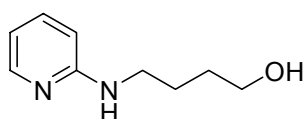


$C_8H_{12}N_2O$
Exact Mass: 152.09
Mol. Wt.: 152.19

The title compound was synthesized from 2-bromopyridine (5.2 g, 33 mmol) and 3-aminopropan-1-ol (6.0 g, 80 mmol) according to **GP1**. Purification by flash chromatography on silica gel (DCM / MeOH 95 : 5) gave **5** (4.8 g, 31.5 mmol, 95%) as a light brown oil.

1H -NMR (250 MHz, $CDCl_3$): $\delta = 7.99$ (dd, $^3J = 5.1$ Hz, $^4J = 1.0$ Hz, 1H, Ar-*H6*); 7.34 (ddd, $^3J = 8.6$ Hz, $^3J = 7.1$ Hz, $^4J = 1.9$ Hz, 1H, Ar-*H5*); 6.51 (ddd, $^3J = 7.0$ Hz, $^3J = 5.2$ Hz, $^4J = 0.8$ Hz, 1H, Ar-*H4*); 6.37 (d, $^3J = 8.4$ Hz, 1H, Ar-*H3*); 4.70 (bs, 1H); 4.60 (bs, 1H); 3.63 (m, 2H, CH_2OH); 3.49 (dd, $^2J = 12.2$ Hz, $^3J = 6.2$ Hz, 2H, - $NHCH_2$ -); 1.73 (m, 2H, - CH_2 -). **^{13}C -NMR** (75 MHz, $CDCl_3$): $\delta = 159.0, 147.4, 136.5, 111.2, 107.8, 58.7, 37.9, 32.4$. **HPLC** (10-50%, 30 min): $t_R = 8.75$ min. **MS** (ESI): $m/z = 153.0$ $[m+H]^+$.

IV.3.10 Preparation of 4-(pyridine-2-ylamino)butan-1-ol, **6**.



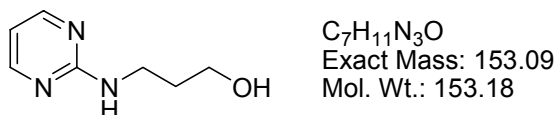
$C_9H_{14}N_2O$
Exact Mass: 166.11
Mol. Wt.: 166.22

The title compound was synthesized from 2-bromopyridine (1.0 g, 6.33 mmol) and 4-aminobutan-1-ol (1.4 g, 15.82 mmol) according to **GP1**. Purification by flash chromatography on silica gel (DCM / MeOH 99 : 1 - 95 : 5 + 1% TEA) gave **6** (1.04 g, 6.26 mmol, 99%) as a light brown oil.

1H -NMR (250 MHz, $CDCl_3$): $\delta = 7.90$ (d, $^3J = 5.2$ Hz, 1H, Py-*H6*), 7.33 (ddd, $^3J = 8.8$ Hz, $^3J = 7.2$ Hz, $^4J = 1.9$ Hz, 1H, Py-*H4*), 6.8 (bs, 1H, Py-NH), 6.46 (ddd, $^3J = 6.9$ Hz, $^3J = 5.2$ Hz, $^4J = 0.8$ Hz, 1H, Py-*H5*), 6.38 (d, $^3J = 8.5$ Hz, 1H, Py-*H3*),

5.27 (bs, 1H, -OH), 3.60 (t, $^3J = 8.5$ Hz, 2H, $-\text{CH}_2\text{-O}-$), 3.23 (m, 2H, N-CH_2-), 1.61 (m, 4H, $-\text{CH}_2\text{CH}_2\text{O}$). $^{13}\text{C-NMR}$ (62.9 MHz, CDCl_3): 158.1, 146.4, 138.0, 112.4, 107.4, 62.1, 41.8, 29.7, 26.0. **HPLC** (5-20%, 30 min): $t_R = 10.13$ min. **MS** (ESI): $m/z = 167.0$ [$m+\text{H}^+$].

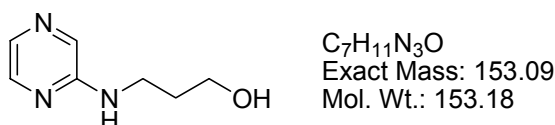
IV.3.11 Preparation of 3-(pyrimidin-2-ylamino)propan-1-ol, 7.



The title compound was synthesized from 2-chloropyrimidine (4.00 g, 34 mmol) and 3-aminopropan-1-ol (8.00 g, 107 mmol) according to **GP1**. Purification by flash chromatography on silica gel (DCM / MeOH 95 : 5) gave **7** (4.54 g, 29.6 mmol, 85%) as a light yellow solid.

$^1\text{H-NMR}$ (250 MHz, CDCl_3): $\delta = 8.24$ (d, $^3J = 4.9$ Hz, 2H, Py- $H_{4,6}$), 6.51 (t, $^3J = 4.8$ Hz, 1H, Py- H_5), 5.68 (bs, 1H, Py-NH-), 3.92 (bs, 1H, -OH), 3.63 (t, $^3J = 5.6$ Hz, 2H, $-\text{CH}_2\text{OH}$), 3.57 (q, $^3J = 6.0$ Hz, 2H, $-\text{NHCH}_2-$), 1.75 (m, 2H, $-\text{CH}_2\text{CH}_2\text{CH}_2-$). $^{13}\text{C-NMR}$ (62.9 MHz, CDCl_3): 162.8, 158.0, 110.4, 99.9, 58.6, 37.5, 33.0. **HPLC** (5-20%, 30 min): $t_R = 11.33$ min. **MS** (ESI): 154.2 [$m+\text{H}^+$] $^+$.

IV.3.12 Preparation of 3-(pyridazin-2-ylamino)propan-1-ol, 8

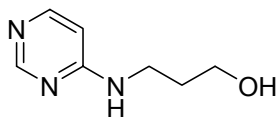


The title compound was synthesized from 2-chloropyridazine (4.00 g, 34 mmol) and 3-aminopropan-1-ol (8 g, 107 mmol) according to **GP1**. Purification by flash chromatography on silica gel (DCM / MeOH 95 : 5) gave **8** (3.71 g, 24.3 mmol, 82%) as a light yellow solid.

$^1\text{H-NMR}$ (250 MHz, CDCl_3): $\delta = 7.90 - 7.85$ (m+s, 2H, Py- $H_{3/5}$), 7.71 (d, $^3J = 2.7$ Hz, 1H, Py- H_5), 5.29 (bs, 1H, -NH), 4.02 (bs, 1H, -OH), 3.66 (t, $^3J = 5.7$ Hz, 2H, $-\text{CH}_2\text{OH}$), 3.50 (dd, $^2J = 11.4$ Hz, $^3J = 5.6$ Hz, 1H, $-\text{NH-CH}_2-$), 1.78 (m, 2H, $-\text{CH}_2\text{CH}_2\text{CH}_2-$).

¹³C-NMR (62.9 MHz, CDCl₃): δ = 154.9, 141.3, 132.9, 132.0, 59.3, 38.1, 32.5. **HPLC** (10-50%, 30 min): t_R = 8.74 min. **MS** (ESI): 154.0 [m+H⁺]⁺, 136.0 [m+H⁺-H₂O]⁺.

IV.3.13 Preparation of 3-(pyrimidin-6-ylamino)propan-1-ol, **9**

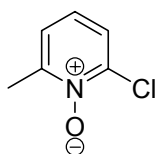


C₇H₁₁N₃O
Exact Mass: 153.09
Mol. Wt.: 153.18

The title compound was synthesized from 6-chloropyrimidine (0.54 g, 4.71 mmol) and 3-aminopropan-1-ol (0.98 g, 26.15 mmol) according to **GP1**. Purification by flash chromatography on silica gel (DCM / MeOH 9 : 1) gave **9** (0.51 g, 3.34 mmol, 71%) as a light yellow solid.

¹H-NMR (360 MHz, CDCl₃): δ = 8.43 (s, Py-H2), 8.00 (dd, ³J = 5.7 Hz, ⁴J = 1.2 Hz, 1H, Py-H4), 6.30 (d, ³J = 6.1 Hz, 1H, Py-H5), 6.07 (s, 1H, -NH), 4.35 (s, 1H, -OH), 3.65 (m, 2H, -CH₂OH), 3.46 (m, 2H, -NHCH₂-), 1.76 (m, 2H, -CH₂CH₂CH₂-). **¹³C-NMR** (62.9 MHz, CDCl₃): δ = 162.2, 158.1, 154.3, 59.4, 38.1, 32.0, 22.8. **HPLC** (5-20%, 30 min): t_R = 8.99 min. **MS** (ESI): 154.0 [m+H⁺]⁺, 136.0 [m+H⁺-H₂O]⁺.

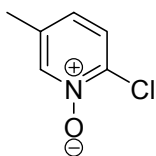
IV.3.14 Preparation of 2-chloro-6-methylpyridin-N-oxid, **10a**



C₆H₆ClNO
Exact Mass: 143.01
Mol. Wt.: 143.57

Prepared from 2-chloro-6-methylpyridine (1.0 g, 7.84 mmol) according to general procedure **GP3**. Purification by flash chromatography on silica gel (DCM / MeOH 95 : 5 + 1 % TEA). Yield: 993 mg (6.94 mmol, 89%) of a yellow solid.

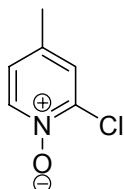
¹H-NMR (250 MHz, CDCl₃): δ = 7.37 (dd, ³J = 8.0 Hz, ⁴J = 1.5 Hz, 1H, Py-H3), 7.19 (dd, ³J = 7.2 Hz, ⁴J = 1.1 Hz, 1H, Py-H5), 7.10 (t, ³J = 8.0 Hz, 1H, Py-H4), 2.53 (s, 3H, -CH₃). **¹³C-NMR** (62 MHz, CDCl₃): δ = 151.1, 142.2, 125.3, 124.6, 124.2, 18.5. **HPLC** (5-20%, 30 min): t_R = 10.75 min. **MS** (ESI): m/z = 144.0 [m+H⁺].

IV.3.15 Preparation of 2-chloro-5-methylpyridin-*N*-oxid, 10b

C₆H₆ClNO
 Exact Mass: 143.01
 Mol. Wt.: 143.57

Prepared from 2-chloro-5-methylpyridine (1.0 g, 7.84 mmol) and MCPBA (1.62 g, 9.36 mmol) according to general procedure **GP3**. Purification by flash chromatography on silica gel (DCM / MeOH 95 : 5 + 1 % TEA). Yield: 915 mg (6.40 mmol, 82%) of a yellow solid.

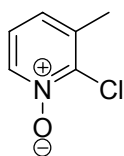
¹H-NMR (500 MHz, CDCl₃): δ = 8.24 (s, 1H, Py-*H*6), 7.38 (d, ³*J* = 8.4 Hz, 1H, Py-*H*3), 7.06 (dd, ³*J* = 8.0 Hz ⁴*J* = 0.4 Hz, 1H, Py-*H*4), 2.31 (s, 3H, -*CH*₃). **¹³C-NMR** (125 MHz, CDCl₃): δ = 140.5, 134.9, 128.0, 126.4, 17.9. **HPLC** (5-20%, 30 min): t_R = 11.10 min. **MS** (ESI): m/z = 144.0 [m+H⁺].

IV.3.16 Preparation of 2-chloro-4-methylpyridin-*N*-oxid, 10c

C₆H₆ClNO
 Exact Mass: 143.01
 Mol. Wt.: 143.57

Prepared from 2-chloro-4-methylpyridine (1 g, 7.84 mmol) and MCPBA (1.62 g, 9.36 mmol) according to general procedure **GP3**. Purification by flash chromatography on silica gel (DCM / MeOH 95 : 5 + 1 % TEA). Yield: 870 mg (6.08 mmol, 78%) of a yellow solid.

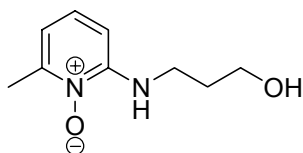
¹H-NMR (500 MHz, CDCl₃): δ = 8.25 (d, ³*J* = 6.8 Hz, 1H, Py-*H*6), 7.29 (d, ⁴*J* = 1.9 Hz, 1H, Py-*H*3), 7.00 (dd, ³*J* = 6.6 Hz, ⁴*J* = 2.2 Hz, 1H, Py-*H*5), 2.32 (s, 3H, -*CH*₃). **¹³C-NMR** (125 MHz, CDCl₃): δ = 139.9, 138.7, 137.3, 127.4, 124.8, 20.0. **HPLC** (5-20%, 30 min): t_R = 11.08 min. **MS** (ESI): m/z = 144.0 [m+H⁺].

IV.3.17 Preparation of 2-chloro-4-methylpyridin-*N*-oxid, 10d

C₆H₆ClNO
Exact Mass: 143.01
Mol. Wt.: 143.57

Prepared from 2-chloro-3-methylpyridine (1 g, 7.84 mmol) and MCPBA (1.62 g, 9.36 mmol) according to general procedure **GP3**. Purification by flash chromatography on silica gel (DCM / MeOH 95 : 5 + 1 % TEA). Yield: 881 mg (6.16 mmol, 79%) of a yellow solid.

¹H-NMR (500 MHz, CDCl₃): δ = 8.22 (d, ³J = 6.1 Hz, 1H, Py-*H*6), 7.12 - 7.06 (m, 2H, Py-*H*4,5), 2.40 (s, 3H, -CH₃). **¹³C-NMR** (125 MHz, CDCl₃): δ = 142.4, 138.1, 136.1, 127.1, 122.4, 20.4. **HPLC** (5-20%, 30 min): t_R = 12.08 min. **MS** (ESI): m/z = 143.9 [m+H⁺].

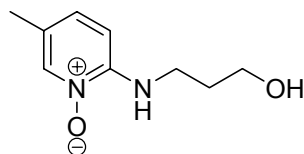
IV.3.18 Preparation of 3-(6-methylpyridin-*N*-oxid-2-ylamino)propan-1-ol, 11a

C₉H₁₄N₂O₂
Exact Mass: 182.11
Mol. Wt.: 182.22

Prepared from **10a** (683 mg, 4.78 mmol) and 3-aminopropan-1-ol (1.05 g, 14.0 mmol) according to general procedure **GP1**. Purification by flash chromatography on silica gel (DCM / MeOH 10 : 1 + 1 % TEA). Yield: 862 mg (4.71 mmol, 99%) of a yellow solid.

¹H-NMR (500 MHz, CDCl₃): δ = 7.97 (d, ³J = 6.2 Hz, 1H, Py-*H*6), 7.14 (bs, 1H, Py-NH), 6.95 (t, ³J = 7.7 Hz, 1H, Py-*H*4), 6.51 (t, ³J = 6.9 Hz, 1H, Py-*H*5), 3.72 (t, ³J = 5.8 Hz, 2H, -CH₂OH), 3.60 (m, 2H, Py-NHCH₂), 2.34 (s, 3H, -CH₃), 1.80 (m, 2H, -CH₂CH₂CH₂-). **¹³C-NMR** (125 MHz, CDCl₃): δ = 151.2, 135.2, 131.6, 120.6, 112.6, 59.3, 41.9, 33.4, 19.1. **HPLC** (5-20%, 30 min): t_R = 13.89 min. **MS** (ESI): m/z = 183.2 [m+H⁺].

IV.3.19 Preparation of 3-(6-methylpyridin-*N*-oxid-2-ylamino)propan-1-ol, **11b**

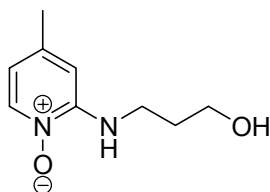


C₉H₁₄N₂O₂
 Exact Mass: 182.11
 Mol. Wt.: 182.22

Prepared from **10b** (670 mg, 4.67 mmol) and 3-aminopropan-1-ol (1.05 g, 14 mmol) according to general procedure **GP1**. Purification by flash chromatography on silica gel (DCM / MeOH 10 : 1 + 1 % TEA). Yield: 840 mg (4.61 mmol, 98%) of a brown solid.

¹H-NMR (250 MHz, CDCl₃): δ = 7.90 (s, 1H, Py-*H*6), 7.06 (m, 1H, Py-NH), 7.03 (d, ³*J* = 8.7 Hz, 1H, Py-*H*3), 6.55 (d, ³*J* = 8.6 Hz, 1H, Py-*H*4), 3.74 (t, ³*J* = 5.6 Hz, 2H, -CH₂OH), 3.45 (q, 2H, ³*J* = 6.2 Hz, Py-NH-CH₂-), 2.17 (s, 3H, Py-CH₃), 1.85 (m, 2H, -CH₂-CH₂-CH₂-). **¹³C-NMR** (62 MHz, CDCl₃): δ = 148.4, 136.9, 130.8, 120.9, 105.8, 59.0, 38.8, 31.3, 17.2. **HPLC** (5-20%, 30 min): t_R = 14.69 min. **MS** (ESI): m/z = 183.0 [m+H⁺], 205.0 [m+Na⁺].

IV.3.20 Preparation of 3-(4-methylpyridin-*N*-oxid-2-ylamino)propan-1-ol, **11c**



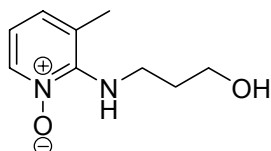
C₉H₁₄N₂O₂
 Exact Mass: 182.11
 Mol. Wt.: 182.22

Prepared from **10c** (633 mg, 4.41 mmol) and 3-aminopropan-1-ol (0.98 g, 13 mmol) according to general procedure **GP1**. Purification by flash chromatography on silica gel (DCM / MeOH 10 : 1 + 1 % TEA). Yield: 802 mg (4.40 mmol, 99%) of a light brown solid.

¹H-NMR (500 MHz, CDCl₃): δ = 7.90 (d, ³*J* = 6.5 Hz, 1H, Py-*H*6), 7.24 (bs, 1H, Py-NH), 6.44 (s, 1H, Py-*H*3), 6.34 (dd, ³*J* = 6.7 Hz, ⁴*J* = 2.1 Hz, 1H, Py-*H*5), 3.74 (t, ³*J* = 5.7 Hz, 2H, -CH₂OH), 3.45 (q, ³*J* = 6.3 Hz, 2H, NHCH₂), 2.28 (s, 3H, -CH₃), 1.86 (m, 2H, -CH₂CH₂CH₂-). **¹³C-NMR** (125 MHz, CDCl₃): δ = 149.6, 141.8, 136.6, 112.4,

106.4, 59.1, 38.9, 31.2, 21.1. **HPLC** (5-20%, 30 min): $t_R = 13.89$ min. **MS** (ESI): $m/z = 183.1$ [$m+H^+$].

IV.3.21 Preparation of 3-(3-methylpyridin-*N*-oxid-2-ylamino)propan-1-ol, **11d**

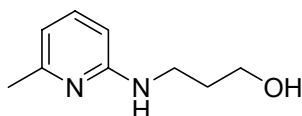


$C_9H_{14}N_2O_2$
Exact Mass: 182.11
Mol. Wt.: 182.22

Prepared from **10d** (683 mg, 4.78 mmol) and 3-aminopropan-1-ol (1.05 g, 14 mmol) according to general procedure **GP1**. Purification by flash chromatography on silica gel (DCM / MeOH 10 : 1 + 1 % TEA). Yield: 862 mg (4.71 mmol, 99%) of a yellow solid.

1H -NMR (500 MHz, $CDCl_3$): $\delta = 7.97$ (d, $^3J = 6.2$ Hz, 1H, Py-*H6*), 7.14 (bs, 1H, Py-NH), 6.95 (t, $^3J = 7.7$ Hz, 1H, Py-*H4*), 6.51 (t, $^3J = 6.9$ Hz, 1H, Py-*H5*), 3.72 (t, $^3J = 5.8$ Hz, 2H, $-CH_2OH$), 3.60 (m, 2H, Py-NH CH_2), 2.34 (s, 3H, $-CH_3$), 1.80 (m, 2H, $-CH_2CH_2CH_2-$). **^{13}C -NMR** (125 MHz, $CDCl_3$): $\delta = 151.2, 135.2, 131.6, 120.6, 112.6, 59.3, 41.9, 33.4, 19.1$. **HPLC** (5-20%, 30 min): $t_R = 13.89$ min. **MS** (ESI): $m/z = 183.2$ [$m+H^+$].

IV.3.22 Preparation of 3-(6-methylpyridin-2-ylamino)propan-1-ol, **12a**



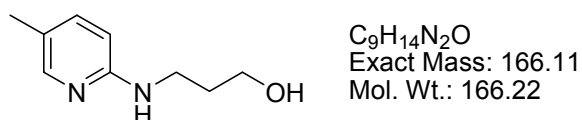
$C_9H_{14}N_2O$
Exact Mass: 166.11
Mol. Wt.: 166.22

Prepared from **11a** (714 mg, 3.92 mmol) according to general procedure **GP4**. Purification by flash chromatography on silica gel (DCM / MeOH / TEA 9 : 1 : 1). Yield: 469 mg (2.82 mmol, 72%) of a light yellow oil.

1H -NMR (250 MHz, $CDCl_3$): $\delta = 7.26$ (t, $^3J = 7.6$ Hz, 1H, Py-*H4*), 6.38 (d, $^3J = 7.2$ Hz, 1H, Py-*H5*), 6.19 (d, $^3J = 8.4$ Hz, 1H, Py-*H3*), 4.79 (bs, 1H, $-NH$), 4.64 (bs, 1H, $-OH$), 3.62 (t, $^3J = 5.6$ Hz, 2H, $-CH_2OH$), 3.51 (dd, $^2J = 12.1$ Hz, $^3J = 6.3$ Hz, 2H, Py-NH- CH_2-), 2.35 (s, 3H, Py- CH_3), 1.72 (m, 2H, $-CH_2-CH_2-CH_2-$). **^{13}C -NMR** (62 MHz,

CDCl_3): $\delta = 158.7, 156.2, 137.8, 111.7, 104.9, 58.4, 37.9, 33.5, 23.8$. **HPLC** (5-20%, 30 min): $t_R = 11.52$ min. **MS** (ESI): $m/z = 167.1$ [$m+H^+$].

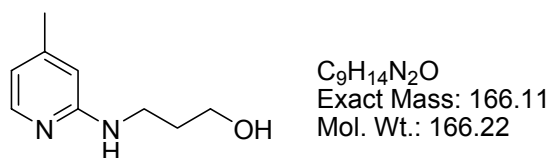
IV.3.23 Preparation of 3-(5-methylpyridin-2-ylamino)propan-1-ol, 12b



Prepared from **11b** (815 mg, 4.47 mmol) according to general procedure **GP4**. Purification by flash chromatography on silica gel (DCM / MeOH / TEA 9 : 1 : 1). Yield: 446 mg (2.68 mmol, 60%) yellow solid.

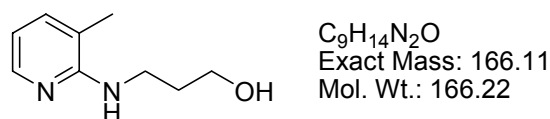
$^1\text{H-NMR}$ (250 MHz, CDCl_3): $\delta = 7.81$ (s, 1H, Py-*H6*), 7.18 (dd, $^3J = 8.5$ Hz, $^4J = 2.2$ Hz, 1H, Py-*H4*), 6.32 (d, $^3J = 8.5$ Hz, 1H, Py-*H3*), 4.99 (bs, 1H, -NH), 4.68 (bs, 1H, -OH), 3.62 (t, $^3J = 5.6$ Hz, 2H, - CH_2OH), 3.51 (m, 2H, Py-NH CH_2 -), 2.12 (s, 3H, Py- CH_3), 1.71 (m, 2H, - $\text{CH}_2\text{-CH}_2\text{-CH}_2$ -). **$^{13}\text{C-NMR}$** (62 MHz, CDCl_3): $\delta = 157.2, 146.4, 138.6, 121.2, 107.9, 58.7, 38.2, 33.3, 17.2$. **HPLC** (5-20%, 30 min): $t_R = 12.65$ min. **MS** (ESI): $m/z = 167.1$ [$m+H^+$].

IV.3.24 Preparation of 3-(4-methylpyridin-2-ylamino)propan-1-ol, 12c



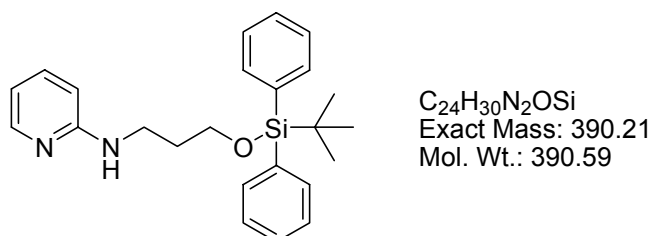
Prepared from **11c** (685 mg, 3.74 mmol) according to general procedure **GP4**. Purification by flash chromatography on silica gel (DCM / MeOH / TEA 9 : 1 : 1). Yield: 404 mg (2.43 mmol, 65%) of a light brown oil.

$^1\text{H-NMR}$ (500 MHz, CDCl_3): $\delta = 7.82$ (d, $^3J = 5.4$ Hz, 1H, Py-*H6*), 6.37 (dd, $^3J = 5.5$ Hz, $^4J = 0.8$ Hz, 1H, Py-*H5*), 6.26 (s, 1H, Py-*H3*), 5.10 (bs, 1H, Py-NH), 3.63 (t, $^3J = 5.7$ Hz, 2H, - CH_2OH), 3.48 (bs, 1H, -OH), 3.08 (q, $^3J = 7.3$ Hz, 2H, Py-NH CH_2 -), 2.20 (s, 3H, - CH_3), 1.74 (m, 2H, - $\text{CH}_2\text{-CH}_2\text{-CH}_2$ -). **$^{13}\text{C-NMR}$** (125 MHz, CDCl_3): $\delta = 149.7, 141.8, 136.6, 112.4, 106.4, 59.1, 38.9, 31.2, 21.1$. **HPLC** (5-20%, 30 min): $t_R = 13.19$ min. **MS** (ESI): $m/z = 167.1$ [$m+H^+$].

IV.3.25 Preparation of 3-(3-methylpyridin-2-ylamino)propan-1-ol, **12d**

Prepared from **11d** (846 mg, 4.61 mmol) according to general procedure **GP4**. Purification by flash chromatography on silica gel (DCM / MeOH / TEA 9 : 1 : 1). Yield: 645 mg (3.88 mmol, 84%) of a light brown oil.

1H -NMR (250 MHz, $CDCl_3$): δ = 7.89 (d, 3J = 4.7 Hz, 1H, Py-*H6*), 7.19 (dt, 3J = 7.1 Hz, 4J = 0.7 Hz, 1H, Py-*H4*), 6.47 (dd, 3J = 7.0 Hz, 3J = 5.2 Hz, 1H, Py-*H5*), 5.45 (bs, 1H, -NH), 4.50 (bs, 1H, -OH), 3.67-3.56 (m, 4H, - CH_2OH , Py-NH CH_2 -), 2.06 (s, 3H, Py- CH_3), 1.73 (m, 2H, - $CH_2CH_2CH_2$ -). **^{13}C -NMR** (62 MHz, $CDCl_3$): δ = 157.4, 144.7, 137.1, 116.2, 112.4, 58.3, 42.5, 33.9, 17.0. **HPLC** (5-20%, 30 min): t_R = 10.93 min. **MS** (ESI): m/z = 167.1 [$m+H^+$].

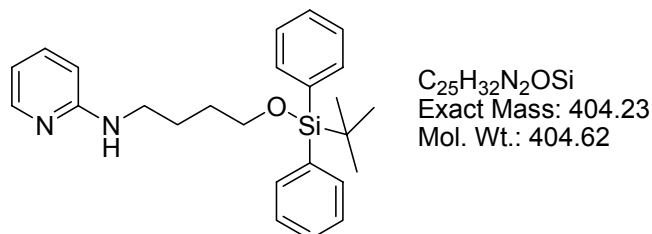
IV.3.26 Preparation of 3-(pyridin-2-ylamino)-1-(*tert*.butyldiphenylsilyloxy)propane, **13**

Prepared from **5** (1.56 g, 10.3 mmol), TBDPS chloride (3.5 mL, 13.4 mmol) and imidazole (1.96 g, 28.8 mmol) according to **GP5**. Purification by flash chromatography (hexane / ethyl acetate 7 : 3 + 1% TEA) gave 3.54 g (9.05 mmol, 88%) of a colorless oil.

1H -NMR (250 MHz, $CDCl_3$): δ = 8.08 (d, 3J = 4.1 Hz, 1H, Py-*H6*), 7.69 (m, 4H, Ph-*H*), 7.70-7.68 (m, 7H, Ph-*H*, Py-*H4*), 6.54 (t, 3J = 6.0 Hz, 1H, Py-*H5*), 6.33 (d, 3J = 8.4 Hz, 1H, Py-*H3*), 3.82 (t, 3J = 5.7 Hz, 2H, - CH_2OSi), 3.44 (q, 3J = 6.2 Hz, 2H, Py-NH CH_2 -), 1.87 (m, 2H, - $CH_2CH_2CH_2$ -), 1.10 (s, 9H, t Bu). **^{13}C -NMR** (63 MHz, $CDCl_3$): δ = 158.7,

147.9, 137.2, 135.5, 133.5, 129.6, 127.7, 112.4, 106.8, 62.1, 39.5, 31.9, 26.9, 19.1.
HPLC (10-100%, 30 min): $t_R = 23.68$ min. **MS** (ESI): $m/z = 391.2$ [$m+H^+$].

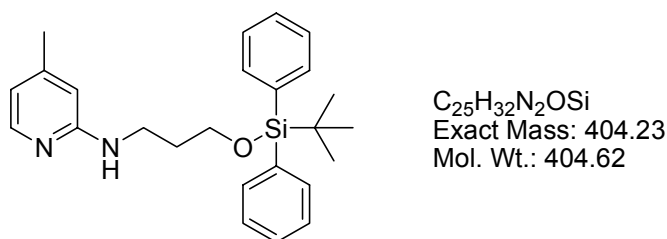
IV.3.27 Preparation of 4-(pyridin-2-ylamino)-1-(*tert*.butyldiphenylsilyloxy)butane, **14**



Prepared from **6** (660 mg, 4.0 mmol), TBDPS chloride (1.35 mL, 5.2 mmol) and imidazole (490 mg, 7.2 mmol) according to **GP5**. Purification by flash chromatography (hexane / ethyl acetate 8 : 2 + 1% TEA) gave 995 mg (2.46 mmol, 66%) of a colorless oil.

1H -NMR (250 MHz, $CDCl_3$): $\delta = 8.08$ (ddd, $^3J = 5.0$ Hz, $^4J = 0.8$ Hz, 1H, Py-*H6*), 7.70 - 7.66 (m, 4H, Ph-*H*), 7.44-7.35 (m, 6H, Ph-*H* + Py-*H4*), 6.55 (ddd, $^3J = 7.1$ Hz, $^3J = 5.0$ Hz, $^4J = 0.9$ Hz, 1H, Py-*H5*), 6.34 (dt, $^3J = 8.4$ Hz, $^4J = 0.8$ Hz, 1H, Py-*H3*), 4.54 (bs, 1H, -NH), 3.73 (t, $^3J = 6.0$ Hz, 2H, - CH_2O), 3.27 (q, $^3J = 6.7$ Hz, 2H, N- CH_2 -), 1.70 (m, 4H, - CH_2CH_2O), 1.07 (s, 9H, *t*Bu). **^{13}C -NMR** (62.9 MHz, $CDCl_3$): $\delta = 158.9, 148.1, 137.3, 135.5, 134.0, 129.5, 127.6, 112.6, 106.4, 63.5, 42.1, 30.0, 26.9, 26.0, 19.2$. **HPLC** (10-100%, 30 min): $t_R = 24.18$ min. **MS** (ESI): $m/z = 405.2$ [$m+H^+$].

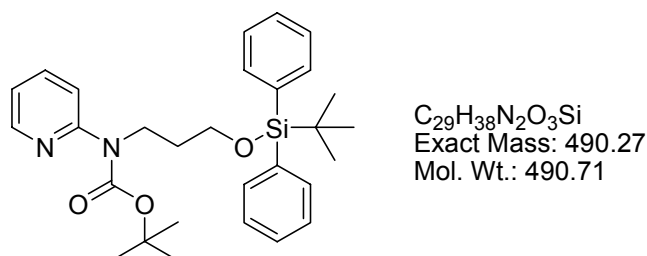
IV.3.28 Preparation of 3-(4-methylpyridin-2-ylamino)-1-(*tert*.butyldiphenylsilyloxy)propane, **15**



Prepared from **12c** (554 mg, 3.33 mmol), TBDPS chloride (1.3 mL, 4.99 mmol) and imidazole (453 mg, 6.66 mmol) according to **GP5**. Purification by flash chromatography (hexane / ethyl acetate 8 : 2 + 1% TEA) gave 1.02 g (2.52 mmol, 76%) of a colorless oil.

¹H-NMR (250 MHz, CDCl₃): δ = 7.95 (d, ³J = 7.3 Hz, 1H, Py-*H*6), 7.70 (m, 4H, Ph-*H*), 7.48-7.35 (m, 6H, Ph-*H*), 6.40 (dd, ³J = 5.2 Hz, ⁴J = 0.8 Hz, 1H, Py-*H*5), 6.15 (s, 1H, Py-*H*3), 4.68 (bt, 1H, Py-NH-), 3.82 (t, ³J = 5.8 Hz, 2H, -CH₂OSi), 3.44 (m, 2H, Py-NHCH₂-), 2.22 (s, 3H, -CH₃), 1.87 (m, 2H, -CH₂-CH₂-CH₂-), 1.11 (s, 9H, Si-*t*Bu). **¹³C-NMR** (62.9 MHz, CDCl₃): δ = 159.1, 148.1, 147.7, 135.5, 133.6, 129.7, 127.7, 114.1, 106.9, 62.1, 32.0, 26.9, 21.1, 19.2. **HPLC** (10-100%, 30 min): t_R = 18.03 min. **MS** (ESI): m/z = 405.3 [m+H⁺].

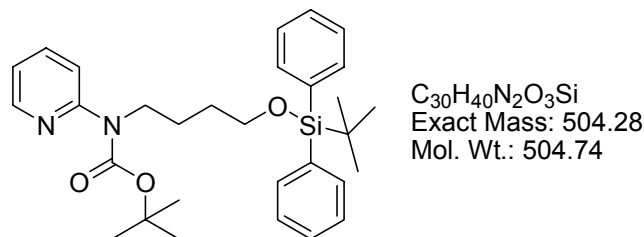
IV.3.29 Preparation of 3-(*N*-*tert*-butyloxycarbonyl-*N*-pyridin-2-ylamino)1-(*tert*-butyldiphenylsilyloxy)propane **16**



Prepared from **13** (616 mg, 1.58 mmol), Boc-anhydride (379 mg, 1.73 mmol), TEA (657 μL, 4.74 mmol) and DMAP (20 mg, 0.16 mmol) according to **GP6a**. Purification by flash chromatography (hexane / ethyl acetate 8 : 2 + 1% TEA) gave **16** (696 mg, 1.42 mmol, 90 %) as colorless oil.

¹H-NMR (250 MHz, CDCl₃): δ = 8.37 (dd, ³J = 5.0 Hz, ⁴J = 1.6 Hz, 1H, Py-*H*6), 7.71 - 7.53 (m, 6H, Ph-*H*, Py-*H*3,4), 7.46-7.33 (m, 6H, Ph-*H*), 7.00 (ddd, ³J = 6.6 Hz, ³J = 4.9 Hz, ⁴J = 1.5 Hz, 1H, Py-*H*5), 4.12 (m, 2H, -CH₂O), 3.72 (t, ³J = 6.3 Hz, 2H, NCH₂), 1.94 (m, 2H, -CH₂CH₂CH₂-), 1.50 (s, 9H, NCOO^{*t*}Bu), 1.05 (s, 9H, Si-*t*Bu). **¹³C-NMR** (62.9 MHz, CDCl₃): δ = 154.7, 154.2, 147.6, 136.8, 135.5, 133.8, 129.5, 127.5, 120.1, 119.4, 80.8, 61.9, 44.3, 32.0, 28.3, 26.8, 19.1. **HPLC** (10-100%, 30 min): t_R = 25.38 min. **MS** (ESI): m/z = 513.2 [m+Na⁺]⁺, 391.4 [m+H⁺-Boc]⁺.

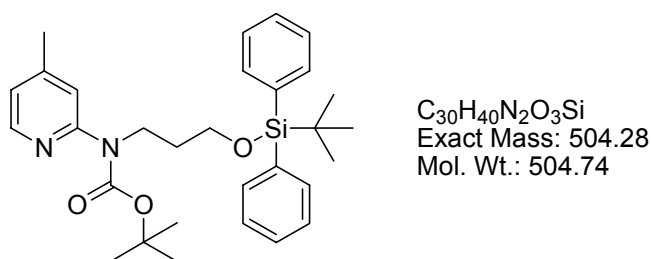
IV.3.30 Preparation of 4-(*N*-*tert*.butyloxycarbonyl-*N*-pyridin-2-ylamino)-1-(*tert*.butyldiphenylsilyloxy)butane, **17**



Prepared from **14** (965 mg, 2.38 mmol), Boc-anhydride (625 mg, 2.86 mmol), TEA (990 μ L, 4.74 mmol) and DMAP (30 mg, 0.24 mmol) according to **GP6a**. Purification by flash chromatography (hexane / ethyl acetate 8 : 2 + 1% TEA) gave **17** (717 mg, 1.84 mmol, 77%) as colorless oil.

1H -NMR (250 MHz, $CDCl_3$): δ = 8.40 (m, 1H, Py-*H*6), 7.74-7.70 (m, 4H, Ph-*H*), 7.64 - 7.36 (m, 8H, Py-*H*3,4, Ph-*H*), 6.99 (ddd, 3J = 6.1 Hz, 3J = 4.9 Hz, 4J = 2.3 Hz, 1H, Py-*H*5), 4.03 (t, 3J = 7.2 Hz, 2H, N-*CH*₂), 3.73 (t, 3J = 6.2 Hz, 2H, -*CH*₂O), 1.77 (m, 2H, -*CH*₂*CH*₂O), 1.65 (m, 2H, N-*CH*₂*CH*₂-), 1.55 (s, 9H, NCOO^{*t*}Bu), 1.09 (s, 9H, Si-^{*t*}Bu). **^{13}C -NMR** (63 MHz, $CDCl_3$): δ = 154.5, 154.1, 147.4, 136.6, 135.4, 133.8, 129.4, 127.4, 119.9, 119.2, 80.6, 63.5, 46.5, 29.9, 28.1, 26.7, 25.3, 19.0. **HPLC** (10-100%, 30 min): t_R = 32.45 min. **MS** (ESI): m/z = 527.1 [$m+Na^+$]⁺, 449.0 [$m+H^+ - ^tBu$]⁺, 405.2 [$m+H^+ - Boc$]⁺.

IV.3.31 Preparation of 3-(*N*-*tert*.butyloxycarbonyl-*N*-(4-methylpyridin-2-ylamino)1-(*tert*.butyldiphenylsilyloxy)propane **18**

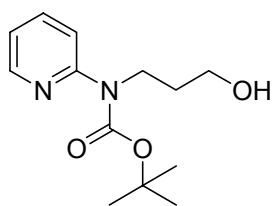


Prepared from **15** (1.02 g, 2.52 mmol), Boc-anhydride (660 mg, 3.02 mmol), TEA (700 μ L, 5.04 mmol) and DMAP (31 mg, 0.25 mmol) according to **GP6a**. Purification

by flash chromatography (hexane / ethyl acetate 8 : 2) gave **18** (1.05 g, 2.08 mmol, 83%) as colorless oil.

¹H-NMR (250 MHz, CDCl₃): δ = 8.26 (d, ³J = 5.2 Hz, 1H, Py-*H*6), 7.70 (m, 4H, Ph-*H*), 7.47-7.35 (m, 6H, Ph-*H*), 6.84 (d, ³J = 4.9 Hz, 1H, Py-*H*5), 4.14 (t, ³J = 7.1 Hz, 2H, CH₂OSi), 3.76 (t, ³J = 6.2 Hz, 2H, Py-NCH₂), 2.34 (s, 3H, -CH₃), 1.97 (m, 2H, -CH₂CH₂CH₂-), 1.52 (s, 9H, NCOO^tBu), 1.08 (s, 9H, Si-^tBu). **¹³C-NMR** (62.9 MHz, CDCl₃): δ = 154.7, 154.2, 147.8, 147.2, 135.4, 133.7, 129.4, 127.5, 120.7, 120.5, 80.5, 61.8, 44.2, 32.0, 28.2, 26.7, 21.0, 19.0. **HPLC** (10-100%, 30 min): t_R = 29.66 min. **MS** (ESI): m/z = 505.3 [m+H⁺], 449.0 [m+H⁺-^tBu], 405.3 [m+H⁺-Boc].

IV.3.32 Preparation of 3-*N*-(pyridin-2-yl)-*N*- (*tert*.butyloxycarbonyl)aminopropan-1-ol, **19**

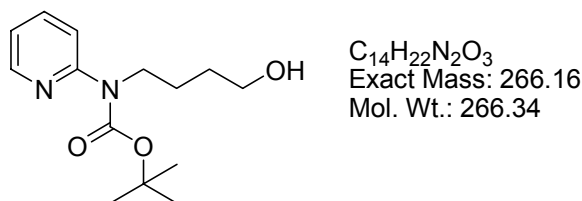


C₁₃H₂₀N₂O₃
Exact Mass: 252.15
Mol. Wt.: 252.31

Prepared from **16** (666 mg, 1.36 mmol) and TBAF (473 mg, 1.50 mmol) according to **GP7**. Purification by flash chromatography (hexane / ethyl acetate 2 : 1) gave **19** (220 mg, 0.87 mmol, 64%) as light brown oil.

¹H-NMR (250 MHz, CDCl₃): δ = 8.16 (dt, ³J = 4.9 Hz, ⁴J = 1.2 Hz, Py-*H*6), 7.49 (m, 2H, Py-*H*3,4), 6.87 (dd, ³J = 8.8 Hz, ³J = 4.5 Hz, 1H, Py-*H*5), 5.24 (t, ³J = 6.8 Hz, 1H, -OH), 3.83 (t, ³J = 6.0 Hz, 2H, -CH₂OH), 3.51 (q, ³J = 6.2 Hz, NCH₂-), 1.78 (m, 2H, -CH₂CH₂CH₂-), 1.38 (s, 9H, ^tBu). **¹³C-NMR** (62.9 MHz, CDCl₃): δ = 155.0, 153.7, 146.6, 137.0, 119.3, 119.1, 81.1, 57.7, 44.0, 31.1, 27.9. **HPLC** (10-100%, 30 min): t_R = 12.52 min. **MS** (ESI): m/z = 253.3 [m+H⁺], 196.2 [m+H⁺-^tBu], 153.2 [m+H⁺-Boc].

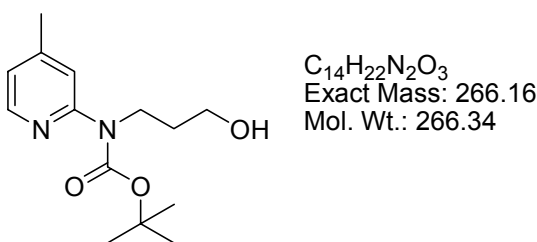
**IV.3.33 Preparation of 4-*N*-(pyridin-2-yl)-*N*-
(*tert*.butyloxycarbonyl)aminobutan-1-ol, **20****



Prepared from **17** (717 mg, 1.84 mmol) and TBAF (637 mg, 2.02 mmol) according to **GP7**. Purification by flash chromatography (hexane / ethyl acetate 2 : 1) gave **20** (292 mg, 1.16 mmol, 63%) as light brown oil.

1H -NMR (250 MHz, $CDCl_3$): δ = 8.24 (m, 1H, Py-*H*6), 7.56-7.44 (m, 2H, Py-*H*3,4), 6.98 (m, 1H, Py-*H*5), 3.82 (t, 3J = 7.3 Hz, 2H, - CH_2OH), 3.52 (t, 3J = 6.2 Hz, 2H, NCH_2 -), 3.37 (bs, - OH), 1.61 (m, 2H, - CH_2CH_2OH), 1.46 (m, 2H, NCH_2CH_2 -), 1.40 (s, 9H, tBu). **^{13}C -NMR** (62.9 MHz, $CDCl_3$): δ = 154.4, 153.9, 147.2, 136.8, 119.9, 119.4, 80.8, 61.7, 46.3, 29.3, 28.0, 24.8. **HPLC** (10-100%, 30 min): t_R = 12.60 min. **MS** (ESI): m/z = 167.0 [$m+H^+$] $^+$.

**IV.3.34 Preparation of 3-*N*-(4-methylpyridin-2-yl)-*N*-
(*tert*.butyloxycarbonyl)aminopropan-1-ol, **21****



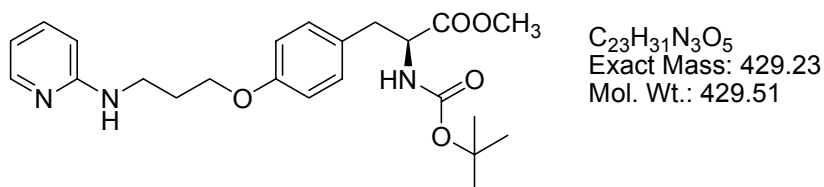
Prepared from **18** (1.05 g, 2.08 mmol) and TBAF (788 mg, 2.49 mmol) according to **GP7**. Purification by flash chromatography (hexane / ethyl acetate 2 : 1) gave **21** (532 mg, 1.99 mmol, 96%) as light brown oil.

1H -NMR (500 MHz, $CDCl_3$): δ = 7.82 (d, 3J = 5.4 Hz, 1H, Py-*H*6), 6.37 (dd, 3J = 5.5 Hz, 4J = 0.8 Hz, 1H, Py-*H*5), 6.26 (s, 1H, Py-*H*3), 5.10 (bs, 1H, Py-NH), 3.63 (t, 3J = 5.7 Hz, 2H, - CH_2OH), 3.48 (bs, 1H, - OH), 3.08 (q, 3J = 7.3 Hz, 2H, Py-NH CH_2 -), 2.20 (s, 3H, - CH_3), 1.74 (m, 2H, - $CH_2-CH_2-CH_2$ -). **^{13}C -NMR** (125 MHz, $CDCl_3$): δ = 149.7, 141.8, 136.6, 112.4, 106.4, 59.1, 38.9, 31.2, 21.1. **HPLC**

IV. Experimental Section

(10-100%, 30 min): $t_R = 12.62$ min. **MS** (ESI): $m/z = 267.2$ [$m+H^+$], 211.1 [$m+H^+-tBu$], 167.1 [$m+H^+-Boc$].

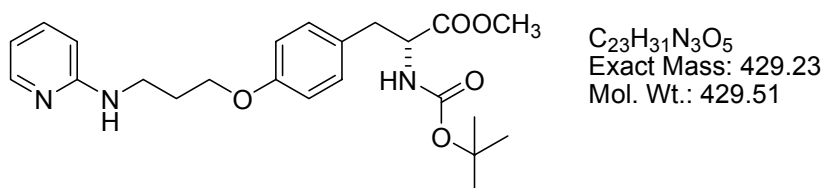
IV.3.35 Preparation of methyl 3-[4-(3-pyridin-2-ylaminopropoxy)-phenyl]-2-(S)-(tert.butyloxycarbonylamino) propionate, **22a**



Prepared from **5** (100 mg, 657 μ mol), Boc-Tyr-OMe (176 mg, 597 μ mol), tributylphosphine (191 μ L, 776 μ mol) and ADDP (196 mg, 776 μ mol) according to **GP2**. Column chromatography on silica gel (DCM / ethyl acetate 2 : 1) gave **22a** (84 mg, 195 μ mol, 33%) as a colorless foam.

1H -NMR (250 MHz, $CDCl_3$): $\delta = 8.05$ (d, $^3J = 4.3$ Hz, 1H, Py-*H6*); 7.37 (m, 1H, Py-*H4*); 7.01 (d, $^3J = 8.6$ Hz, 2H, Ar-*H3,3'*); 6.81 (d, $^3J = 8.6$ Hz, 2H, Ar-*H2,2'*); 6.53 (dd, $^3J = 5.4$ Hz, $^3J = 6.8$ Hz, Py-*H5*); 6.38 (d, $^3J = 8.5$ Hz, 1H, Py-*H3*); 4.99 (bs, 1H, -NH); 4.81 (bs, 1H, -NH); 4.51 (m, 1H, -CHNHoc-); 4.04 (t, $^3J = 5.9$ Hz, 2H, - OCH_2 -); 3.69 (s, 3H, - $COOCH_3$); 3.48 (m, 2H, -NH- CH_2 - CH_2 -); 3.00 (m, 2H, - CH_2 -NHoc-); 2.07 (m, 2H, - $CH_2CH_2CH_2$ -); 1.40 (s, 9H, *t*Bu). **^{13}C -NMR** (63 MHz, $CDCl_3$): $\delta = 172.4, 158.7, 157.9, 155.1, 148.1, 137.4, 130.3, 128.1, 114.5, 112.8, 106.7, 79.8, 65.8, 54.5, 52.1, 39.4, 37.5, 29.2, 28.3$. **HPLC** (10-100%, 30 min): $t_R = 17.01$ min. **MS** (ESI): $m/z = 452.2$ [$m+Na^+$] $^+$, 430.3 [$m+H^+$] $^+$, 374.5 [$m+H^+-tBu$] $^+$, 330.6 [$m+H^+-Boc$] $^+$.

IV.3.36 Preparation of methyl 3-[4-(3-pyridin-2-ylaminopropoxy)-phenyl]-2-(R)-(tert.butyloxycarbonylamino) propionate, *ent*-**22a**

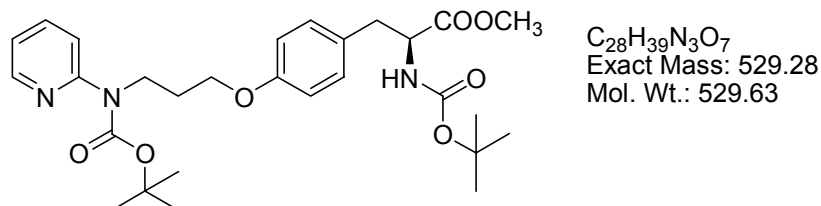


Prepared from **5** (440 mg, 2.46 mmol), Boc-D-Tyr-OMe (660 mg, 2.24 mmol), tributylphosphine (720 μ L, 2.91 mmol) and ADDP (730 mg, 2.91 mmol) according to

GP2. Column chromatography on silica gel (DCM / ethyl acetate 7 : 3) gave *ent-22a* (50 mg, 116 μ mol, 26%) as a colorless foam.

$^1\text{H-NMR}$ (360 MHz, CDCl_3): δ = 8.07 (d, 3J = 5.6 Hz, 1H, Py-*H6*), 7.41 (dd, 3J = 5.6 Hz, 4J = 1.8 Hz, 1H, Py-*H4*), 7.02 (d, 3J = 8.5 Hz, 2H, Ar-*H3,3'*), 6.82 (d, 3J = 8.6 Hz, 2H, Ar-*H2,2'*), 6.57 (m, 1H, Py-*H5*), 6.41 (d, 3J = 8.7 Hz, 1H, Py-*H3*), 4.96 (bs, 1H, -*NH*), 4.81 (bs, 1H, -*NH*), 4.54 (m, 1H, -*CHNH*Boc-), 4.06 (t, 3J = 5.9 Hz, 2H, -*OCH}_2*), 3.71 (s, 3H, -*COOCH}_3*) 3.50 (m, 2H, -*NHCH}_2\text{CH}_2*-), 3.02 (m, 2H, -*CH}_2\text{NH*Boc-), 2.10 (m, 2H, -*CH}_2\text{CH}_2\text{CH}_2*-), 1.42 (s, 9H, *t*Bu). **$^{13}\text{C-NMR}$** (91 MHz, CDCl_3): δ = 172.4, 158.6, 157.9, 155.1, 147.8, 137.6, 130.3, 128.1, 114.6, 112.8, 106.8, 79.8, 65.8, 54.6, 52.2, 39.5, 37.5, 29.2, 28.3. **HPLC** (10-100%, 30 min): t_R = 17.30 min. **MS** (ESI): m/z = 430.2 [$m+\text{H}^+$] $^+$, 374.4 [$m+\text{H}^+$ -*t*Bu] $^+$, 330.5 [$m+\text{H}^+$ -Boc] $^+$.

IV.3.37 Preparation of methyl 4-[4-(3-*N*-pyridin-2-yl-3-*N*-(*tert*.butyloxycarbonylamino)propoxy)phenyl]-3-(*S*)-(*tert*.butyloxycarbonylamino) butanoate, **22b**

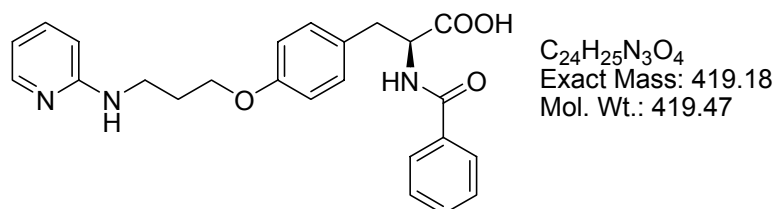


Prepared from **19** (1.2 g, 4.76 mmol), Boc-Tyr-OMe (1.17 g, 3.97 mmol), tributylphosphine (1.3 mL, 5.16 mmol) and ADDP (1.3 g, 5.16 mmol) according to **GP2**. Column chromatography on silica gel (DCM / ethyl acetate 7:3) gave **22b** (418 mg, 790 μ mol, 40%) as a colorless foam.

$^1\text{H-NMR}$ (250 MHz, CDCl_3): δ = 8.31 (dt, 3J = 4.8 Hz, 4J = 1.3 Hz, 1H, Py-*H6*), 7.59 - 7.57 (m, 2H, Py-*H3,4*), 7.00-6.94 (m, 3H, Py-*H5*, Tyr-*H3,3'*), 6.74 (d, 3J = 8.6 Hz, 2H, Tyr-*H2,2'*), 4.96 (d, 3J = 7.8 Hz, 1H, -*NH*Boc), 4.51 (m, 1H, -*CHCOO*Me), 4.12 (t, 3J = 7.0 Hz, 2H, -*CH}_2\text{OAr}*), 3.96 (t, 3J = 6.3 Hz, 2H, -*NCH}_2*-), 3.68 (s, 3H, -*COOCH}_3*), 2.98 (m, 2H, Ar-*CH}_2*-), 2.10 (m, 2H, -*CH}_2\text{CH}_2\text{CH}_2*-), 1.47 (s, 9H, *t*Bu), 1.40 (s, 9H, *t*Bu). **$^{13}\text{C-NMR}$** (62 MHz, CDCl_3): δ = 172.3, 158.0, 155.0, 154.4, 154.1, 147.6, 136.8, 130.1, 127.6, 119.8, 119.4, 114.3, 82.0, 81.0, 79.8, 65.5, 44.0, 37.3, 28.8, 28.2, 28.1. **HPLC** (10-100%, 30 min): t_R = 24.25 min. **MS** (ESI):

$m/z = 552.2 [m+Na^+]^+$, $530.1 [m+H^+]^+$, $474.1 [m+H^+-tBu]^+$, $430.2 [m+H^+-Boc]^+$, $374.3 [m+H^+-Boc-tBu]^+$, $330.6 [m+H^+-2Boc]^+$.

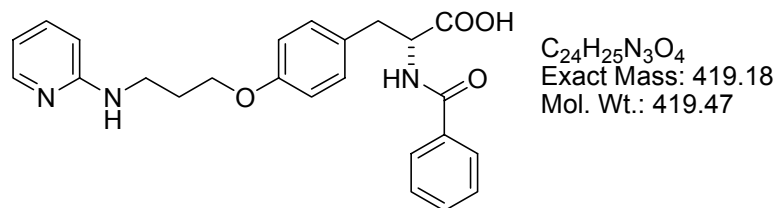
IV.3.38 Preparation of 2-(*S*)-benzamido-3-(4-(3-pyridin-2-ylaminopropoxy)phenyl) propionic acid, **23a**



The title compound was prepared from **22a** (94 mg, 219 μ mol) following **GP8a**. [benzoyl chloride (33 μ L, 285 μ mol), $NaHCO_3$ (92 mg, 1.1 mmol), LiOH (26 mg, 1.1 mmol)] Purification using preparative HPLC and lyophilization afforded **23a** (10 mg, 24.1 μ mol, 11%) as TFA salt (colorless solid).

1H -NMR (500 MHz, DMSO): $\delta = 13.32$ (bs, 1H), 12.77 (bs, 1H), 8.71 (bs, 1H, Py-NH), 8.66 (d, $^3J = 8.2$ Hz, 1H, -NHCOPh), 7.89 (d, $^3J = 6.1$ Hz, 1H, Py-H6), 7.83 (t, $^3J = 7.9$ Hz, 1H, Py-H4), 7.80 (d, $^3J = 7.5$ Hz, 2H, Ph-H2,2'), 7.52 (t, $^3J = 7.3$ Hz, 1H, Ph-H4), 7.45 (t, $^3J = 7.6$ Hz, 2H, Ph-H3,3'), 7.23 (d, $^3J = 8.5$ Hz, 2H, Tyr-H3,3'), 7.00 (d, $^3J = 9.0$ Hz, 1H, Py-H3), 6.83 (d, $^3J = 8.6$ Hz, 2H, Tyr-H2,2'), 6.80 (t, $J = 6.8$ Hz, 1H, Py-H5), 4.57 (m, 1H, -CHCOOH), 4.01 (t, $^3J = 6.0$ Hz, 2H, -CH₂OAr), 3.45 (t, $^3J = 6.2$ Hz, 2H, Py-NHCH₂-), 3.12 (dd, $^2J = 13.8$ Hz, $^3J = 4.3$ Hz, 1H, Ar-CH(H')-), 3.00 (dd, 1H, $^2J = 13.7$ Hz, $^3J = 10.9$ Hz, 1H, Ar-CH(H')-), 2.01 (m, 2H, -CH₂CH₂CH₂-). **^{13}C -NMR** (125 MHz, DMSO): $\delta = 173.1$, 166.2 , 156.8 , 152.9 , 142.4 , 136.5 , 133.8 , 131.2 , 130.1 , 129.9 , 128.1 , 127.2 , 114.0 , 112.7 , 111.7 , 64.6 , 54.3 , 39.4 , 38.5 , 35.4 , 27.6 . **HPLC** (10-50%, 30 min): $t_R = 20.96$ min. **MS** (ESI): $m/z = 420.4 [M+H]^+$.

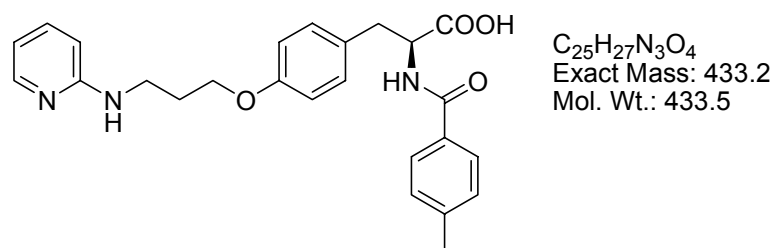
IV.3.39 Preparation of 2-(*R*)-benzamido-3-(4-(3-pyridin-2-ylaminopropoxy)phenyl) propionic acid, *ent*-23a



The title compound was prepared from *ent*-22a (100 mg, 220 μ mol) following **GP8a**. [benzoyl chloride (33 μ L, 285 μ mol), $NaHCO_3$ (92 mg, 1.1 mmol), LiOH (30 mg, 1.25 mmol)] Purification using preparative HPLC and lyophilization afforded *ent*-23a (23 mg, 54.9 μ mol, 25%) as TFA salt (colorless solid).

1H -NMR (500 MHz, DMSO): δ = 8.82 (bs, 1H, Py-NH), 8.66 (d, 3J = 8.2 Hz, 1H, -NHCOPh), 7.89 (d, 3J = 6.2 Hz, 1H, Py-H6), 7.88-7.83 (m, 1H, Py-H4), 7.80 (d, 3J = 7.3 Hz, 2H, Ph-H2,2'), 7.52 (t, 3J = 7.3 Hz, 1H, Ph-H4), 7.45 (t, 3J = 7.5 Hz, 2H, Ph-H3,3'), 7.23 (d, 3J = 8.5 Hz, 2H, Tyr-H3,3'), 7.03 (d, 3J = 9.0 Hz, 1H, Py-H3), 6.83 (d+m, 3J = 8.6 Hz, 2H, Tyr-H2,2'; 1H, Py-H5), 4.57 (m, 1H, -CHCOOH), 4.02 (t, 3J = 6.0 Hz, 2H, -CH₂OAr), 3.46 (t, 3J = 5.9 Hz, 2H, Py-NHCH₂-), 3.12 (dd, 2J = 13.8 Hz, 3J = 4.2 Hz, 1H, Ar-CH(H')-), 3.00 (dd, 1H, 2J = 13.7 Hz, 3J = 10.9 Hz, 1H, Ar-CH(H')-), 2.01 (m, 2H, -CH₂CH₂CH₂-). **^{13}C -NMR** (125 MHz, DMSO): δ = 173.1, 166.2, 156.8, 152.6, 142.7, 135.9, 133.8, 131.2, 130.1, 130.0, 128.1, 127.2, 114.0, 113.3, 111.8, 64.5, 54.3, 38.6, 35.4, 27.5. **HPLC** (10-50%, 30 min): t_R = 20.80 min. **MS** (ESI): m/z = 420.6 [M+H]⁺.

IV.3.40 Preparation of 2-(*S*)-(4-methylbenzamido)-3-[4-(3-pyridin-2-ylaminopropoxy)phenyl]-propionic acid, 23b



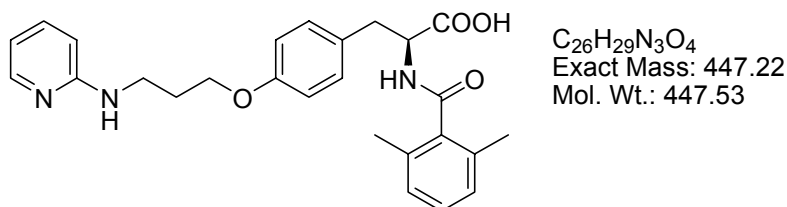
The title compound was prepared from **22a** (100 mg, 233 μ mol) following **GP8b** [4-methylbenzoic acid (33 mg, 280 μ mol), HATU (107 mg, 280 μ mol), DIEA (238 μ L,

IV. Experimental Section

1.4 mmol), LiOH (34 mg, 1.4 mmol]. Purification using preparative HPLC and lyophilization afforded **23b** (28 mg, 65 μ mol, 28%) as TFA salt (colorless solid).

¹H-NMR (500 MHz, DMSO): δ = 14.50 (bs), 8.82 (bs, 1H, Py-NH), 8.54 (d, 3J = 8.2 Hz, 1H, -NHAr), 7.85 (d, 3J = 6.1 Hz, 1H, Py-H6), 7.82 (m, 1H, Py-H4), 7.68 (d, 3J = 7.8 Hz, 2H, Ar-H2), 7.21 (d, 3J = 8.1 Hz, 2H, Tyr-H3/3'), 7.19 (d, 3J = 8.3 Hz, 2H, Ar-H3/3'), 7.00 (d, 3J = 9.0 Hz, 1H, Py-H3), 6.79 (d, 3J = 8.0 Hz, 2H, Tyr-H2/2'), 6.79 (m, 1H, Py-H5), 4.52 (m, 1H, -CHCOOH-), 3.98 (t, 3J = 5.9 Hz, 2H, -CH₂OAr-), 3.42 (m, 1H, Py-NHCH₂-), 3.07 (dd, 2J = 13.8 Hz, 3J = 4.0 Hz, 1H, ArCH(H')-), 2.96 (m, 1H, Ar-CH(H)-), 2.30 (s, 3H, ArCH₃), 1.98 (m, 2H, -CH₂CH₂CH₂-). **¹³C-NMR** (125 MHz, DMSO): δ = 173.2, 166.1, 156.1, 152.7, 142.7, 141.2, 135.9, 131.0, 130.2, 130.0, 128.7, 127.3, 114.0, 113.2, 111.8, 64.5, 54.3, 38.6, 35.4, 27.5, 20.8. **HPLC** (10-50%, 30 min): t_R = 23.21 min. **MS** (ESI): m/z = 434.5 [M+H]⁺. **HRMS** (ESI) (C₂₅H₂₈N₃O₄⁺) Calc.: 434.2074, found: 434.2070.

IV.3.41 Preparation of 2-(S)-(2,6-dimethylbenzamido)-3-[4-(3-pyridin-2-ylaminopropoxy)phenyl]-propionic acid, **23c**

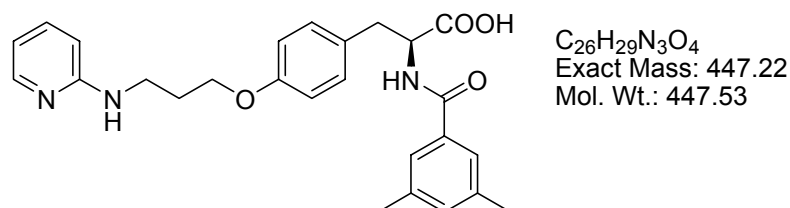


The title compound was prepared from **22a** (75 mg, 175 μ mol) following **GP8b** [2,6-dimethylbenzoic acid (32 mg, 210 μ mol), HATU (80 mg, 210 μ mol), DIEA (149 μ L, 875 μ mol), LiOH (21 mg, 875 mmol)]. Purification using preparative HPLC and lyophilization afforded **23c** (17 mg, 30 μ mol, 17%) as TFA salt (colorless solid).

¹H-NMR (500 MHz, DMSO): δ = 13.56, 12.71 (bs, 1H, COOH), 8.65 (bs, 1H, Py-NH), 8.57 (d, 3J = 8.3 Hz, 1H, -NHCOAr), 7.92 (d, 3J = 6.0 Hz, 1H, Py-H6), 7.85 (t, 3J = 7.7 Hz, 1H, Py-H4), 7.21 (d, J = 8.5 Hz, Tyr-H3,3'), 7.11 (t, 3J = 7.6 Hz, 1H, Ar-H4), 7.01 (d, 3J = 8.9 Hz, 2H, Ar-H3,3'), 6.95 (d, 3J = 7.6 Hz, 1H, Py-H3), 6.86 (d, 3J = 8.5 Hz, 2H, Tyr-H2,2'), 6.82 (t, 3J = 6.6 Hz, 1H, Py-H5), 4.63 (m, 1H, -CHCOOH), 4.05 (t, 3J = 6.0 Hz, 2H, Py-NHCH₂-), 3.47 (m, 2H, -CH₂OAr), 3.11 (dd, 2J = 13.9 Hz, 3J = 4.0 Hz, 1H, Ar-CH(H')-), 2.79 (dd, 2J = 13.7 Hz, 3J = 11.5 Hz, 1H, Ar-CH(H)-), 2.04 (m, 2H, -CH₂CH₂CH₂-), 1.96 (s, 6H, Ar(CH₃)₂). **¹³C-NMR** (125 MHz, DMSO):

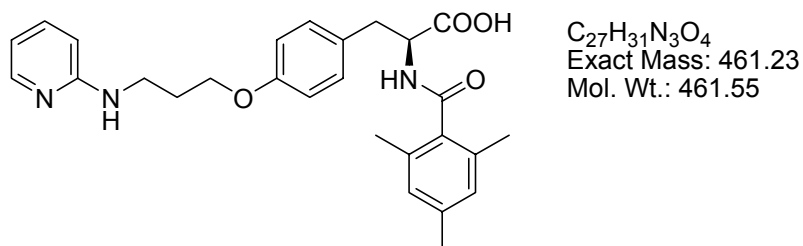
δ = 173.0, 168.9, 156.9, 153.1, 142.2, 137.9, 136.9, 133.7, 130.0, 127.8, 126.7, 114.1, 112.9, 111.7, 64.8, 53.3, 39.4, 38.5, 35.4, 27.6, 18.4. **HPLC** (10-50%, 30 min): t_R = 22.34 min. **MS** (ESI): m/z = 448.4 $[m+H]^+$. **HRMS** ($C_{26}H_{30}N_3O_4^+$): Calc.: 448.2231, found: 448.2227.

IV.3.42 Preparation of 2-(S)-(3,5-dimethylbenzamido)-3-[4-(3-pyridin-2-ylaminopropoxy)phenyl]-propionic acid, **23d**



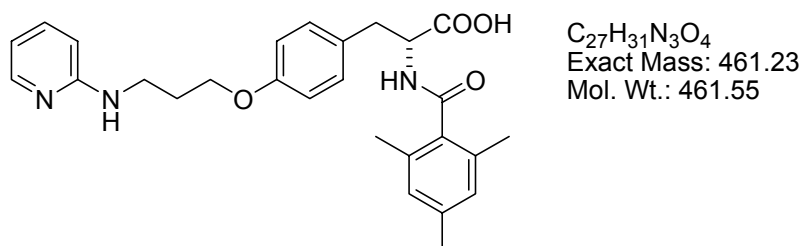
The title compound was prepared from **22a** (75 mg, 175 μ mol) following **GP8b** [3,5-dimethylbenzoic acid (39 mg, 263 μ mol), HATU (107 mg, 263 μ mol), DIEA (149 μ L, 875 μ mol), LiOH (21 mg, 875 mmol)]. Purification using preparative HPLC and lyophilization afforded **23d** (15 mg, 30 μ mol, 15%) as TFA salt (colorless solid).

1H -NMR (500 MHz, DMSO): δ = 13.33 (bs, 1H), 12.47 (bs, 1H), 8.74 (bs, 1H, Py-NH), 8.54 (d, 3J = 8.2 Hz, 1H, -NHCOAr), 7.89 (d, 3J = 6.1 Hz, 1H, Py-H6), 7.84 (t, 3J = 8.0 Hz, Py-H4), 7.42 (s, 2H, Ar-H2,2'), 7.22 (d, 3J = 8.6 Hz, Tyr-H3,3'), 7.15 (s, 1H, Ar-H4), 7.01 (d, 3J = 9.0 Hz, 1H, Py-H3), 6.83 (d, 3J = 8.5 Hz, 2H, Tyr-H2,2'), 6.81 (t, 3J = 6.6 Hz, Py-H5), 4.56 (m, 1H, -CHCOOH), 4.01 (t, 3J = 6.0 Hz, 2H, -CH₂OAr), 3.10 (dd, 2J = 13.9 Hz, 3J = 4.3 Hz, 1H, Ar-CH(H')-), 2.98 (dd, 2J = 13.8 Hz, 3J = 10.7 Hz, 1H, Ar-CH(H')-), 2.30 (s, 6H, Ar(CH₃)₂), 2.02 (m, 2H, -CH₂CH₂CH₂-). **^{13}C -NMR** (125 MHz, DMSO): δ = 173.1, 166.4, 156.8, 152.8, 142.5, 137.2, 136.3, 133.8, 132.5, 130.2, 130.0, 125.0, 114.0, 113.2, 111.8, 64.5, 54.2, 39.4, 38.5, 35.4, 27.5, 20.7. **HPLC** (10-50%, 30 min): t_R = 25.72 min. **MS** (ESI): m/z = 448.4 $[m+H]^+$.

IV.3.43 Preparation of 2-(S)-(2, 4, 6-trimethylbenzamido)-3-[4-(3-pyridin-2-ylaminopropoxy)phenyl]-propionic acid, 23e

The title compound was prepared from **22a** (100 mg, 233 μ mol) following **GP8b** [2,4,6-trimethylbenzoic acid (46 mg, 279 μ mol), HATU (107 mg, 279 μ mol), DIEA (238 μ L, 1.17 mmol), LiOH (28 mg, 1.17 mmol)]. Purification using preparative HPLC and lyophilization afforded **23e** (32 mg, 55 μ mol, 24%) as TFA salt (colorless solid).

¹H-NMR (500 MHz, DMSO): δ = 15-12 (bs, 1H, -COOH), 8.86 (bs, 1H, Py-NH), 8.47 (d, 3J = 7.6 Hz, 1H, NHCOAr), 7.93 (m, 1H, Py-H6), 7.89 (m, 1H, Py-H4), 7.21 (d, 3J = 7.0 Hz, 2H, Tyr-H3,3'), 7.06 (d, 3J = 8.1 Hz, 1H, Py-H3), 6.85 (d, 3J = 6.6 Hz, 3H, Tyr-H2,2' + Py-H5), 6.75 (s, 2H, Ar-H3,3'), 4.62 (m, 1H, -CHCOOH-), 4.05 (m, 2H, -CH₂OAr), 3.48 (m, 2H, PyNHCH₂-), 3.10 (d, 2J = 13.3 Hz, 1H, ArCH(H')-), 2.79 (t, 2J = 12.2 Hz, 1H, Ar-CH(H')-), 2.20 (s, 3H, Ar(CH₃)), 2.05 (m, 2H, -CH₂CH₂CH₂-), 1.93 (s, 6H, Ar(CH₃)₂). **¹³C-NMR** (125 MHz, DMSO): δ = 173.1, 169.1, 156.9, 152.8, 142.7, 136.9, 136.1, 135.3, 133.7, 130.0, 127.3, 114.1, 113.1, 111.8, 64.7, 53.4, 38.6, 35.4, 27.5, 20.5, 18.4. **HPLC** (10-50%, 30 min): t_R = 24.98 min. **MS** (ESI): m/z = 961.4 [2M+K⁺]⁺, 945.4 [2M+Na⁺]⁺, 923.1 [2M+H⁺]⁺, 462.4 [M+H⁺]⁺. **HRMS** (ESI) ($C_{27}H_{32}N_3O_4^+$): Calc.: 462.2387, found: 462.2382.

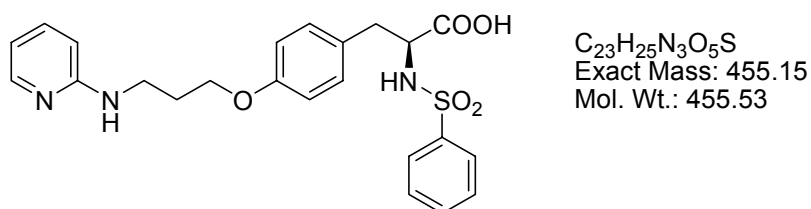
IV.3.44 Preparation of 2-(R)-(2, 4, 6-trimethylbenzamido)-3-[4-(3-pyridin-2-ylaminopropoxy)phenyl]-propionic acid, ent-23e

The title compound was prepared from *ent*-**22a** (125 mg, 291 μ mol) following **GP8b** [2,4,6-trimethylbenzoic acid (57 mg, 347 μ mol), HATU (132 mg, 347 μ mol), DIEA

(247 μL , 1.46 mmol), LiOH (35 mg, 1.46 mmol)]. Purification using preparative HPLC and lyophilization afforded *ent*-**23e** (32 mg, 61 μmol , 21%) as TFA salt (colorless solid).

$^1\text{H-NMR}$ (500 MHz, DMSO): δ = 8.74 (bs, 1H, PyNH), 8.46 (d, 3J = 8.3 Hz, 1H, NHCO-), 7.93 (d, 3J = 6.01 Hz, 1H, Py-H6), 7.88 (t, 3J = 7.92 Hz, 1H, Py-H4), 7.21 (d, 3J = 8.4 Hz, 2H, Tyr-H3,3'), 7.04 (d, 3J = 9.0 Hz, 1H, Py-H3), 6.85 (d + m, 3J = 8.5 Hz, 3H, Tyr-H2,2' + Py-H5), 6.75 (s, 2H, Ar-H3,3'), 4.62 (m, 1H, -CHCOOH-), 4.05 (t, 3J = 7.8 Hz, 2H, -CH₂OAr), 3.47 (m, 2H, PyNHCH₂-), 3.10 (dd, 2J = 13.9 Hz, 3J = 3.8 Hz, 1H, ArCH(H)-), 2.79 (dd, 2J = 13.9 Hz, 3J = 11.7 Hz, 1H, Ar-CH(H)-), 2.20 (s, 3H, Ar(CH₃)), 2.05 (m, 2H, -CH₂CH₂CH₂-), 1.93 (s, 6H, Ar(CH₃)₂). **$^{13}\text{C-NMR}$** (125 MHz, DMSO): δ = 173.1, 169.1, 156.9, 152.8, 142.7, 136.9, 136.1, 135.3, 133.7, 130.0, 127.3, 114.1, 113.2, 111.8, 64.7, 53.4, 38.6, 35.4, 27.5, 20.5, 18.4. **HPLC** (10-50%, 30 min): t_{R} = 15.23 min. **MS** (ESI): m/z = 462.3 [m+H]⁺.

IV.3.45 Preparation of 2-(S)-phenylsulfonamido-3-[4-(3-pyridin-2-ylaminopropoxy)phenyl] propionic acid, **23f**.

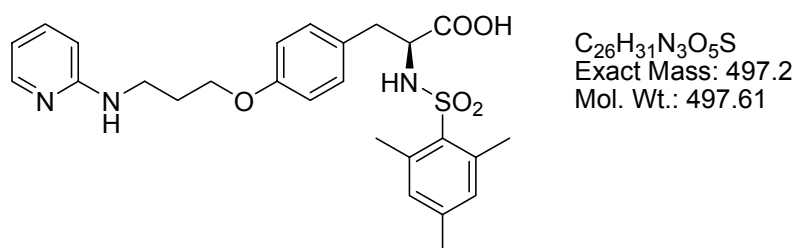


The title compound was prepared from **22a** (60 mg, 140 μmol) following **GP8c** [phenylsulfonic acid chloride (22 μL , 168 μmol), DIEA (143 μL , 840 μmol), LiOH (20 mg, 840 mmol)]. Purification using preparative HPLC and lyophilization afforded **23f** (13 mg, 61 μmol , 16%) as TFA salt (colorless solid).

$^1\text{H-NMR}$ (500 MHz, DMSO): δ = 13.51 (bs, 1H), 12.74 (bs, 1H), 8.70 (bs, 1H, Py-NH), 8.22 (d, 3J = 9.0 Hz, 1H, -NHSO₂Ph), 7.92 (d, 3J = 5.6 Hz, 1H, Py-H6), 7.85 (ddd, 3J = 8.4 Hz, 3J = 7.2 Hz, 4J = 1.4 Hz, 1H, Py-H4), 7.58 (dd, 3J = 8.2 Hz, 4J = 1.0 Hz, 2H, Ph-H2,2'), 7.53 (tt, 3J = 7.4 Hz, 4J = 1.1 Hz, 1H, Ph-H4), 7.43 (t, 3J = 7.7 Hz, 2H, Ph-H3,3'), 7.03 (d, 3J = 8.6 Hz, 3H, Tyr-H3,3' + Py-H3), 6.82 (t, 3J = 6.4 Hz, Py-H5), 6.76 (d, 3J = 8.6 Hz, 2H, Tyr-H2,2'), 4.03 (t, 3J = 6.1 Hz, -CH₂OAr), 3.82 (dt, 3J = 9.0 Hz, 3J = 5.7 Hz, 1H, -CHCOOH), 3.49 (t, 3J = 6.3 Hz, 1H, Py-NHCH₂-), 2.87

(dd, $^2J = 13.8$ Hz, $^3J = 5.6$ Hz, 1H, Ar-CH(H')-), 2.63 (dd, $^2J = 13.8$ Hz, $^3J = 9.0$ Hz, 1H, Ar-CH(H')-), 2.05 (m, 2H, -CH₂CH₂CH₂-). $^{13}\text{C-NMR}$ (125 MHz, DMSO): $\delta = 172.1$, 157.0, 153.1, 142.3, 141.0, 136.7, 131.9, 130.1, 128.6, 126.1, 114.0, 112.8, 111.8, 64.6, 57.5, 39.4, 38.5, 36.9, 27.6. **HPLC** (10-100%, 30 min): $t_R = 14.82$ min. **MS** (ESI): $m/z = 933.0$ [2m+Na⁺]⁺, 911.0 [2m+H⁺]⁺, 456.4 [m+H⁺]⁺.

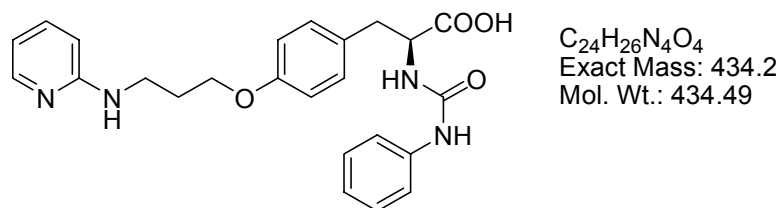
IV.3.46 Preparation of 2-(S)-(2,4,6-trimethylphenylsulfonamido)-3-[4-(3-pyridin-2-ylaminopropoxy)phenyl] propionic acid, **23g**.



The title compound was prepared from **22a** (60 mg, 140 μmol) following **GP8c** [2,4,6-trimethylphenylsulfonic acid chloride (37 mg, 168 μmol), DIEA (143 μL , 840 μmol), LiOH (20 mg, 840 mmol)]. Purification using preparative HPLC and lyophilization afforded **23g** (14 mg, 23 μmol , 15%) as TFA salt (colorless solid).

$^1\text{H-NMR}$ (500 MHz, DMSO): $\delta = 8.86$ (bs, 1H, Py-NH), 8.00 (d, $^3J = 9.5$ Hz, 1H, -NH₂SO₂Ar), 7.93 (d, $^3J = 6.1$ Hz, 1H, Py-H6), 7.88 (t, $^3J = 8.0$ Hz, 1H, Py-H4), 7.06 (d, $^3J = 9.0$ Hz, 1H, Py-H3), 6.96 (d, $^3J = 8.4$ Hz, 2H, Tyr-H3,3'), 6.85 (s, 2H, Ar-H3,3'), 6.85 (m, 1H, Py-H5), 6.65 (d, $^3J = 8.4$ Hz, 2H, Tyr-H2,2'), 4.02 (t, $^3J = 6.1$ Hz, 2H, -CH₂OAr), 3.70 (dt, $^3J = 5.3$ Hz, $^3J = 9.4$ Hz, 1H, -CHCOOH-), 3.49 (t, $^3J = 6.4$ Hz, H, -NHCH₂-), 2.85 (dd, $^2J = 13.8$ Hz, $^3J = 5.2$ Hz, 1H, ArCH(H')-), 2.66 (dd, $^2J = 13.8$ Hz, $^3J = 9.6$ Hz, 1H, ArCH(H')-), 2.41 (s, 6H, Ar(CH₃)₂), 2.21 (s, 3H, Ar(CH₃)), 2.05 (m, 2H, -CH₂CH₂CH₂-). $^{13}\text{C-NMR}$ (125 MHz, DMSO): $\delta = 172.4$, 156.9, 152.8, 142.7, 140.8, 138.0, 136.1, 134.4, 131.2, 129.7, 128.7, 113.8, 113.0, 111.8, 64.5, 57.0, 38.6, 36.7, 27.6, 22.4, 20.2. **HPLC** (10-50%, 30 min): $t_R = 28.24$ min. **MS** (ESI): $m/z = 498.5$ (M+H⁺). **HR-MS** (ESI) (C₂₆H₃₂N₃O₅S⁺): Calc.: 498.2057, found: 498.2049.

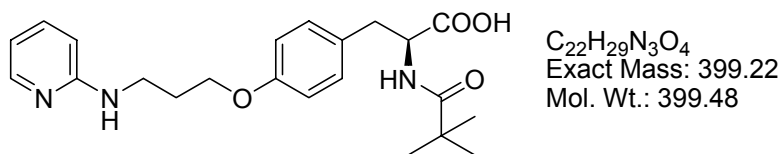
IV.3.47 Preparation of 2-(S)-(3-phenylureido)-3-[4-(3-pyridin-2-ylaminopropoxy)phenyl] propionic acid, 23h



22a (100 mg, 233 μ mol, 1 eq.) dissolved in 3 mL dioxane. After addition of 1 mL concentrated hydrochloric acid, the mixture was stirred at ambient temperature for 30 min. The solvents were evaporated *in vacuo* and the residue taken up in 3 mL of dry DCM. DIEA (210 μ L, 1.76 mmol, 5 eq.) were added, followed by 44 μ L (527 μ mol, 1.5 eq.) of phenyl isocyanate. After 20 min, the reaction was quenched by addition of one drop of water and the solvents were evaporated under reduced pressure. The residue was dissolved in 4 mL of methanol / water (3 : 1). LiOH (42 mg, 1.76 mmol, 5 eq.) was added and the reaction mixture was stirred at ambient temperature for one day (HPLC monitoring). The solvents were removed and the crude product purified by preparative HPLC to give **23h** (53 mg, 97 μ mol, 41 %) as TFA salt (colorless solid).

1 H-NMR (500 MHz, DMSO): δ = 12.85 (bs, 1H, COOH), 8.77 (s, 1H, CONHPh), 8.47 (bs, 1H, Py-NH), 7.92 (t, 3J = 5.9 Hz, 1H, Py-H6), 7.77 (t, 3J = 7.6 Hz, 1H, Py-H4), 7.35 (d, 3J = 7.6 Hz, 2H, Ph-H2,2'), 7.20 (t, 3J = 7.7 Hz, 2H, Ph-H3,3'), 7.13 (d, 3J = 7.7 Hz, 2H, Tyr-H3,3'), 6.94 (d, 3J = 8.9 Hz, Py-H3), 6.89 (m, 1H, Py-H5), 6.86 (d, 3J = 8.3 Hz, 2H, Tyr-H2,2'), 6.76 (t, 3J = 6.5 Hz, 1H, Ph-H4), 6.43 (d, 3J = 8.0 Hz, 1H, CHNHCO), 4.38 (m, 1H, -CHCOOH), 4.04 (t, 3J = 5.9 Hz, 2H, CH₂OAr), 3.45 (m, 2H, PyNHCH₂), 3.01 (dd, 2J = 13.9 Hz, 3J = 4.8 Hz, 1H, Ar-CH(H')), 2.86 (dd, 2J = 13.9 Hz, 3J = 7.8 Hz, 1H, Ar-H(H')-), 2.02 (m, 2H, -CH₂CH₂CH₂-). **13 C-NMR** (125 MHz, DMSO): δ = 173.5, 157.1, 154.6, 153.8, 141.6, 140.2, 138.0, 130.2, 129.2, 128.6, 121.1, 117.4, 114.1, 112.2, 111.7, 64.7, 53.8, 39.4, 36.5, 27.7. **HPLC** (10-50%, 30 min): t_R = 22.53 min. **MS** (ESI): m/z = 869.2 [2M+H]⁺, 435.4 [M+H]⁺. **HR-MS** (ESI) (C₂₄H₂₇N₄O₄)⁺: Calc.: 435.2027, Found: 435.2023.

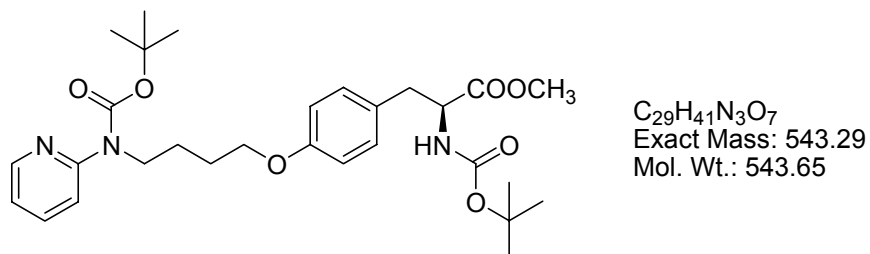
IV.3.48 Preparation of 2-(S)-(tert.butylamido)-3-[4-(3-pyridin-2-ylaminopropoxy)phenyl] propionic acid **23i**



The title compound was prepared from **22a** (300 mg, 577 μ mol) following **GP8a**. [pivalyl chloride (78 μ L, 635 μ mol), NaHCO₃ (145 mg, 1.73 mmol), LiOH (70 mg, 2.89 mmol)] Purification using preparative HPLC and lyophilization afforded **23i** (135 mg, 260 μ mol, 45%) as TFA salt (colorless oil).

¹H-NMR (500 MHz, DMSO): δ = 8.90 (bs, 1H, Py-NH), 7.92 (d, ³J = 6.08 Hz, 1H, Py-H6), 7.88 (t, ³J = 8.25 Hz, Py-H4), 7.45 (d, ³J = 8.3 Hz, 1H, -NHCO-), 7.13 (d, ³J = 8.6 Hz, 2H, Tyr-H3,3'), 7.06 (d, ³J = 9.0 Hz, 1H, Py-H3), 6.84 (m, 1H, Py-H5), 6.82 (d, ³J = 8.6 Hz, 2H, Tyr-H2,2'), 4.36 (ddd, ³J = 9.9 Hz, ³J = 8.4 Hz, ³J = 4.6 Hz, 1H, -CHCOOH), 4.03 (t, ³J = 6.1 Hz, 2H, -CH₂OAr), 3.48 (t, ³J = 6.5 Hz, 2H, NHCH₂-), 3.01 (dd, ²J = 13.8 Hz, ³J = 4.5 Hz, 1H, ArCH(H')-), 2.90 (dd, ²J = 13.7 Hz, ³J = 10.2 Hz, 1H, ArCH(H'')-), 2.03 (m, 2H, -CH₂CH₂CH₂-), 1.01 (s, 9H, ^tBu). **¹³C-NMR** (125 MHz, DMSO): δ = 177.1, 173.2, 156.8, 152.7, 142.8, 136.0, 130.1, 113.9, 113.2, 111.8, 64.6, 53.5, 38.6, 37.8, 35.3, 27.6, 27.1. **HPLC** (10-50%, 30 min): t_R = 28.68 min. **MS** (ESI): m/z = 400.5 [m+H⁺]⁺.

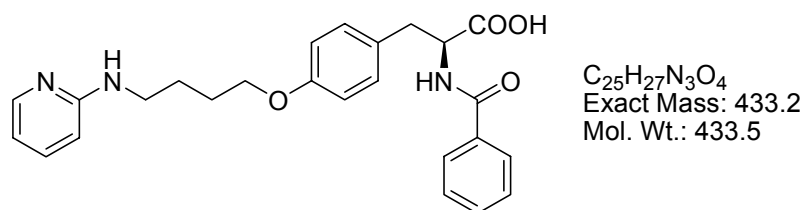
IV.3.49 Preparation of methyl 3-[4-(4-N-tert.butylloxycarbonyl-N-pyridin-2-ylaminopropoxy)phenyl]-2-(S)-(tert.butylloxycarbonylamino) propionate, **24**



Prepared from **20** (641 mg, 2.40 mmol), Boc-Tyr-OMe (647 mg, 2.20 mmol), tributylphosphine (706 μ L, 2.86 mmol) and ADDP (722 mg, 2.86 mmol) according to **GP2**. Purification by flash chromatography (hexane/ethyl acetate 2:1 + 1% TEA) gave the title compound (624 mg, 1.18 mmol, 49%) as colorless foam.

¹H-NMR (250 MHz, CDCl₃): δ = 8.30 (ddd, ³J = 5.0 Hz, ⁴J = 1.2 Hz, ⁵J = 1.2 Hz, 1H, Py-H6), 7.56-7.52 (m, 2H, Py-H3,4), 6.96 (d, ³J = 8.7 Hz, 2H, Tyr-H3,3'), 6.93 (m, 1H, Py-H5), 6.73 (d, 2H, ³J = 8.6 Hz, Tyr-H2,2'), 5.02 (d, ³J = 8.1 Hz, 1H, -NHBoc), 4.46 (m, 1H, -CHCOOMe), 3.96 (t, ³J = 6.7 Hz, 2H, -CH₂-OAr), 3.87 (t, ³J = 5.5 Hz, Py-NCH₂-), 3.64 (s, 3H, -COOCH₃), 2.99 (dd, ²J = 13.7 Hz, ³J = 5.7 Hz, 1H, ArCH(H')-), 2.91 (dd, ²J = 13.9 Hz, ³J = 5.8 Hz, 1H, ArCH(H')), 1.74 (m, 4H, -CH₂CH₂CH₂OAr), 1.45 (s, 9H, ^tBu), 1.36 (s, 9H, ^tBu). **¹³C-NMR** (62.9 MHz, CDCl₃): δ = 172.1, 157.9, 154.3, 153.9, 147.4, 136.6, 130.0, 127.6, 119.8, 119.2, 114.3, 80.6, 79.5, 67.3, 54.4, 51.8, 46.2, 37.2, 28.1, 26.4, 25.3. **HPLC** (10-50%, 30 min): t_R = 25.01 min. **MS** (ESI): m/z = 566.2 [m+Na⁺]⁺, 544.1 [m+H⁺]⁺, 488.1 [m+H⁺-^tBu]⁺, 444.2 [m+H⁺-Boc]⁺, 388.3 [m+H⁺-Boc-^tBu]⁺, 344.4 [m+H⁺-2Boc]⁺.

IV.3.50 Preparation of 2-(S)-benzamido-3-[4-(4-pyridin-2-ylaminobutoxy)phenyl]propionic acid, **25a**

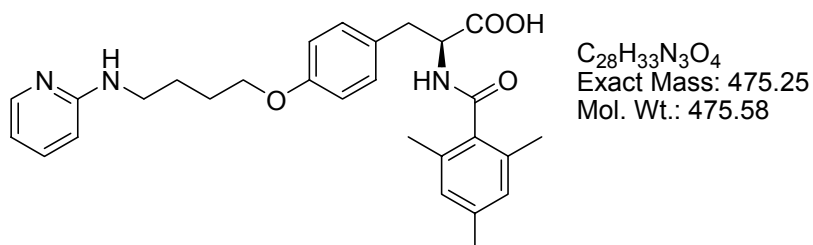


The title compound was prepared from **24** (120 mg, 221 μmol) following **GP8a**. [benzoyl chloride (28 μL, 243 μmol), NaHCO₃ (55 mg, 663 μmol), LiOH (52 mg, 2.21 mmol)] Purification using preparative HPLC and lyophilization afforded **25a** (15 mg, 27 μmol, 12%) as TFA salt (colorless solid).

¹H-NMR (500 MHz, DMSO): δ = 8.65 (d+bs, ³J = 6.5 Hz, 2H, -NHCOPh, Py-NH), 7.89 (d, ³J = 6.2 Hz, 1H, Py-H6), 7.85 (t, ³J = 7.9 Hz, 1H, Py-H4), 7.80 (d, ³J = 7.3 Hz, 2H, Ph-H2,2'), 7.52 (t, ³J = 7.3 Hz, 1H, Ph-H4), 7.45 (t, ³J = 7.5 Hz, 2H, Ph-H3,3'), 7.22 (d, ³J = 8.5 Hz, 2H, Tyr-H3,3'), 7.01 (d, ³J = 9.0 Hz, 1H, Py-H3), 6.86 (d, ³J = 8.5 Hz, 3H, Tyr-H2,2'), 6.85 (m, 1H, Py-H5), 4.56 (m, 1H, -CHCOOH-), 3.95 (t, 1H, ³J = 6.0 Hz, 2H, -CH₂-OAr), 3.11 (dd, ²J = 13.9 Hz, ³J = 4.3 Hz, 1H, -CH(H')COOH), 2.99 (dd, ²J = 13.9 Hz, ³J = 10.8 Hz, -CH(H')COOH), 1.77 (m, 2H, -CH₂CH₂O-), 1.73 (m, 2H, -NHCH₂CH₂-). **¹³C-NMR** (125 MHz, DMSO): δ = 173.0, 166.2, 157.0, 152.7, 142.5, 137.2, 133.8, 131.2, 129.9, 128.1, 127.2, 114.0, 112.2, 111.7, 66.7, 54.3, 41.1,

35.3, 25.9, 24.5. **HPLC** (10-50%, 30 min): $t_R = 22.49$ min. **MS** (ESI): $m/z = 434.5$ $[M+H]^+$. **HR-MS** (ESI) ($C_{25}H_{28}N_3O_4$)⁺: Calc.: 434.2074, Found: 434.2069.

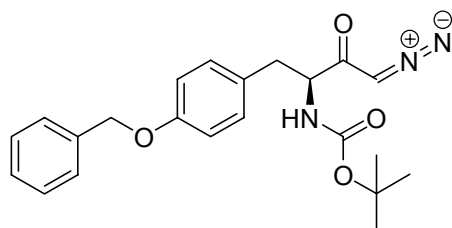
IV.3.51 Preparation of 2-(S)-(2,4,6-trimethylbenzamido-3-[4-(4-pyridin-2-ylaminobutoxy)phenyl]propionic acid, **25b**



The title compound was prepared from **24** (120 mg, 221 μ mol) following **GP8a**. [2,4,6-trimethylbenzoic acid (73 mg, 442 μ mol), HATU (210 mg, 552 μ mol), DIEA (300 μ L, 1.76 mmol), LiOH (52 mg, 2.21 mmol)] Purification using preparative HPLC and lyophilization afforded **25b** (24 mg, 41 μ mol, 18%) as TFA salt (colorless solid).

¹H-NMR (500 MHz, DMSO): 12.68 (bs, 1H, -COOH), 8.74 (bs, 1H, Py-NH), 8.43 (d, $^3J = 8.2$ Hz, 1H, CONH), 7.89 (m, 1H, Py-H6), 7.83 (m, 1H, Py-H4), 7.16 (d, $^3J = 8.1$ Hz, 2H, Tyr-H3,3'), 7.00 (d, $^3J = 8.9$ Hz, 1H, Py-H3), 6.81 (d, $^3J = 8.2$ Hz, 2H, Tyr-H2,2'), 6.72 (s, 2H, Ar-H3,3'), 4.58 (m, 1H, -CHCOOH), 3.94 (m, 2H, -CH₂OAr), 3.33 (m, 2H, -NHCH₂-), 3.06 (d, $^2J = 13.9$ Hz, 1H, ArCH(H)-), 2.75 (dd, $^2J = 14.2$ Hz, $^3J = 11.3$ Hz, 1H, Ar-CH(H)-), 2.15 (s, 3H, Ar-CH₃), 1.89 (s, 6H, Ar(CH₃)₂), 1.76 (m, 2H, -CH₂CH₂OAr), 1.71 (m, 2H, PyNHCH₂CH₂-). **¹³C-NMR** (125 MHz, DMSO): $\delta = 173.1, 169.1, 157.1, 152.8, 142.5, 136.9, 136.2, 135.3, 133.7, 130.0, 129.8, 127.3, 114.1, 113.1, 111.7, 66.9, 53.4, 41.2, 35.4, 25.9, 24.5, 20.5, 18.4$. **HPLC** (10-50%, 30 min): $t_R = 26.31$ min. **MS** (ESI): $m/z = 476.5$ $[M+H]^+$. **HR-MS** (ESI) ($C_{28}H_{34}N_3O_4$)⁺: Calc.: 476.2544, found: 476.2539.

IV.3.52 Preparation of 1-diazo-2-oxo-4-(4-benzyloxyphenyl)-3-(S)-(tert.butylloxycarbonyl)butane, **26**



C₂₂H₂₅N₃O₄
Exact Mass: 395.18
Mol. Wt.: 395.45

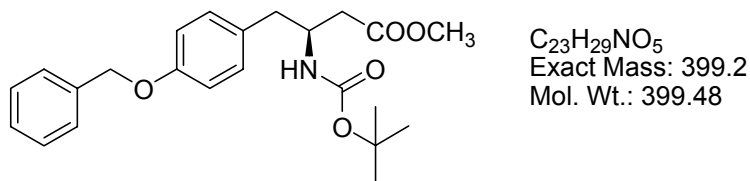
1. Preparation of diazomethane:

A 100 mL Erlenmeyer flask was filled with 35 mL of 40% aqueous KOH solution and 50 mL of diethyl ether and cooled in an ice-salt bath to -5 - 0°C. 5.3 g *N*-methyl nitroso urea was added in portions keeping the temperature below 0°C at any time. After 1.5 h, the mixture was carefully converted into a separating funnel (with a Teflon stopcock), the layer were separated and the organic layer dried for 3 h over KOH.

2. A solution of Boc-Tyr(OBn)-OH (3.71 g, 10.0 mmol, 1 eq.) in 35 mL dry THF under an argon atmosphere was cooled to -15°C. After addition of TEA (2.9 mL, 20 mmol, 2 eq.) and ethyl chloroformate (1.05 mL, 11 mmol, 1.1 eq.), the colorless suspension was stirred for 0.5 h at -5°C. Subsequently, the reaction flask was opened and the freshly prepared diazomethane solution was added carefully via a PP pipette. The yellow suspension was stirred at -15 - -5°C for 1 h. The reaction was quenched by addition of acetic acid (0.5 mL), followed by diethyl ether and saturated NaHCO₃ solution. The layers were separated and the organic layer washed with saturated NH₄Cl solution and brine, dried with Na₂SO₄, filtered and evaporated. The crude diazoketone was purified by column chromatography on silica gel (hexane / ethyl acetate 8 : 2) to give **22** as a yellow solid (3.91 g, 9.89 mmol, 99%).

¹H-NMR (250 MHz, CDCl₃): δ = 7.45-7.30 (m, 5H, Ph-*H*), 7.10 (d, ³J = 8.5 Hz, 2H, Tyr-*H*3,3'), 6.91 (d, ³J = 8.5 Hz, 2H, Tyr-*H*2,2'), 5.19 (bs, 1H, -NHCO-), 5.03 (s, 1H, -CHN₂), 5.04 (m, 2H, PhCH₂O), 4.36 (m, 1H, CHNH-), 2.96 (d, ³J = 6.7 Hz, 2H, ArCH₂-), 1.42 (s, 9H, -NHCOO^tBu). HPLC (10-100%, 30 min): t_R = 25.60 min.

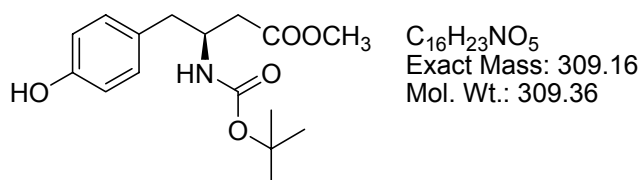
**IV.3.53 Preparation of methyl 4-(4-benzyloxyphenyl)-3-(S)-
(tert.butylloxycarbonylamino) butanoate, 27**



Diazoketon **26** (3.91 g, 9.89 mmol, 1 eq.) was dissolved in 150 mL abs. MeOH and cooled to -25°C. Silver benzoate (228 mg, 1 mmol, 0.1 eq.) was dissolved in triethylamine (5.5 mL, 40 mmol, 4 eq.) and added dropwise to the diazoketon. The mixture was allowed to warm to room temperature over night. After evaporation of the solvent, the residue was taken up in ethyl acetate, washed with sat. NaHCO₃, 5% aqueous citric acid and brine, dried over Na₂SO₄ and filtered. After evaporation, the crude product was purified by column chromatography on silica gel (hexane / ethyl acetate 2 : 1) to give 3.94 g (9.87 mmol, 99%) of a colorless solid.

¹H-NMR (250 MHz, CDCl₃): δ = 7.45 - 7.29 (m, 5H, Ph-H), 7.09 (d, ³J = 8.6 Hz, 2H, Tyr-H_{3,3'}), 6.91 (d, ³J = 8.6 Hz, 2H, Tyr-H_{2,2'}), 5.05 (s, 2H, Ph-CH₂O), 4.11 (m, 1H, -CHCH₂COOMe), 4.94 (bs, 1H, -NHCOO^tBu), 3.68 (s, 3H, -COOCH₃), 2.86 (dd, ²J = 13.6 Hz, ³J = 6.5 Hz, 1H, -CH(H')COOMe), 2.75 (dd, ²J = 13.6 Hz, ³J = 7.6 Hz, 1H, -CH(H')COOMe), 2.52 (dd, ²J = 15.7 Hz, ³J = 5.6 Hz, 1H, Ar-CH(H')-), 2.43 (dd, ²J = 15.7 Hz, ³J = 5.7 Hz, 1H, ArCH(H')-), 1.42 (s, 9H, NHCOO^tBu). ¹³C-NMR (125 MHz, DMSO): δ = 172.0, 157.6, 155.1, 137.1, 130.3, 130.0, 128.5, 127.8, 127.3, 114.9, 79.3, 70.0, 51.5, 49.0, 39.5, 37.6, 28.3. HPLC (10-100%, 30 min): t_R = 26.41 min. MS (ESI): m/z = 422.2 [m+Na⁺]⁺, 366.4 [m+Na⁺-^tBu]⁺, 300.4 [m+H⁺-Boc]⁺. MS (EI): m/z = 399.1 [M]⁺, 282.0, 202.0 [BocNHCHCH₂COOCH₃], 146.0 [OOCNHCHCH₂COOCH₃], 102.0 [NHCHCH₂COOCH₃], 91.0 [Bn], 57.1 [^tBu].

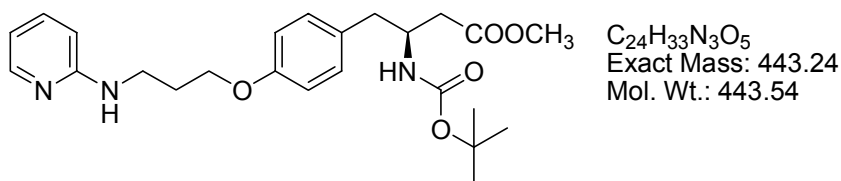
**IV.3.54 Preparation of methyl 4-(4-hydroxyphenyl)-3-(S)-
(tert.butylloxycarbonylamino) butanoate, (Boc-β-Tyr-OMe), 28**



Benzyl ether **27** (3.94 g, 9.87 mmol) was hydrogenated according to **GP4** (400 mg 5% Pd/C). After filtration over Celite[®] and evaporation of the solvents, the product was purified by flash chromatography on silica gel (hexane / ethyl acetate 2 : 1) to give **28** (2.21 g, 7.14 mmol, 71%) as colorless solid.

¹H-NMR (250 MHz, CDCl₃): δ = 7.15 (bs, 1H, -OH), 6.97 (d, ³J = 8.3 Hz, 2H, Tyr-H3,3'), 6.75 (d, ³J = 8.4 Hz, 2H, Tyr-H2,2'), 5.16 (d, ³J = 7.6 Hz, 1H, -NH₂Boc), 4.10 (m, 1H, -CHNH₂Boc), 2.81 (dd, ²J = 12.9 Hz, ³J = 5.0 Hz, 1H, -CH(H')COOMe ArCH(H')-), 2.68 (dd, ²J = 13.3 Hz, ³J = 7.7 Hz, 1H, -CH(H')COOMe), 2.49 (dd, ²J = 15.9 Hz, ³J = 5.5 Hz, 1H, ArCH(H')-), 2.39 (dd, ²J = 15.8 Hz, ³J = 6.1 Hz, 1H, ArCH(H')-), 1.40 (s, 9H, ^tBu). **¹³C-NMR** (125 MHz, DMSO): δ = 172.3, 155.5, 155.1, 130.3, 128.7, 115.4, 79.8, 51.7, 49.1, 39.6, 37.5, 28.3. **HPLC** (10-100%, 30 min): t_R = 18.54 min. **MS** (ESI): m/z = 310.2 [m+H⁺].

IV.3.55 Preparation of methyl 4-[4-(3-pyridin-2-ylaminopropoxy)-phenyl]-3-(S)-(tert.butylloxycarbonylamino) butanoate, **29**

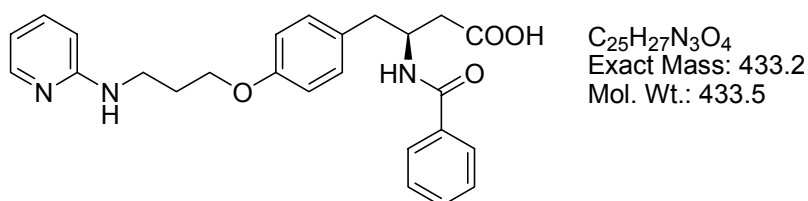


Prepared from **5** (152 mg, 1.0 mmol), Boc-β-Tyr-OMe (**28**) (261 mg, 825 μmol), tributylphosphine (264 μL, 1.07 mmol) and ADDP (269 mg, 1.07 mmol) according to **GP2**. Column chromatography on silica gel (DCM / ethyl acetate 2 : 1) gave **29** (106 mg, 244 μmol, 30%) as a colorless foam.

¹H-NMR (250 MHz, CDCl₃): δ = 8.03 (d, ³J = 7.6 Hz, 1H, Py-H6); 7.36 (m, 1H, Py-H5); 7.06 (d, ³J = 8.4 Hz, 2H, Tyr-H3,3'); 6.80 (d, ³J = 8.4 Hz, 2H, Tyr-H2,2'); 6.52 (dd, ³J = 5.2 Hz, ³J = 6.9 Hz, 1H, Py-H4); 6.37 (d, ³J = 8.4 Hz, 1H, Py-H3); 5.05 (bs, 1H, -NH), 4.95 (bs, 1H, -NH); 4.08 (m, 1H, -CHNH₂Boc-); 4.05 (t, ³J = 5.9 Hz, 2H, ArOCH₂-); 3.65 (s, 3H, -COOCH₃); 3.46 (m, 2H, -NH-CH₂-CH₂-); 2.84 (m, 2H, -CH(H')COOMe); 2.71 (dd, ²J = 13.6 Hz, ³J = 7.7 Hz, 1H, -CH(H')COOMe), 2.44 (m, 2H, Ar-CH₂CHNH₂Boc-); 2.07 (m, 2H, -CH₂-CH₂-); 1.39 (s, 9H, ^tBu).

$^{13}\text{C-NMR}$ (63 MHz, CDCl_3): $\delta = 178.0, 158.6, 157.5, 155.0, 147.8, 137.4, 130.2, 129.8, 114.4, 112.6, 106.6, 79.2, 65.7, 51.6, 48.9, 39.4, 39.3, 37.3, 29.0, 28.3$. **HPLC** (10-100%, 30 min): $t_{\text{R}} = 17.19$ min. **MS** (ESI): $m/z = 466.2$ $[\text{m}+\text{Na}]^+$, 444.2 $[\text{m}+\text{H}]^+$, 388.2 $[\text{m}+\text{H}-t\text{Bu}]^+$, 344.3 $[\text{m}+\text{H}-\text{Boc}]^+$.

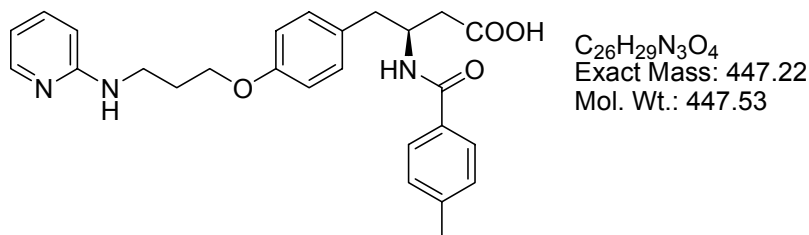
IV.3.56 Preparation of 3-(S)-benzamido-4-(4-(3-pyridin-2-ylaminopropoxy)phenyl) butanoic acid, **30a**



The title compound was prepared from **29** (50 mg, 112 μmol) following **GP8a**. [benzoyl chloride (17 μL , 145 μmol), NaHCO_3 (34 mg, 404 μmol), LiOH (13 mg, 560 μmol)] Purification using preparative HPLC and lyophilization afforded **30a** (11 mg, 20 μmol , 18%) as TFA salt (colorless solid).

$^1\text{H-NMR}$ (500 MHz, DMSO): $\delta = 13.51$ (bs, 1H), 12.26 (bs, 1H), 8.82 (bs, 1H, Py-NH), 8.32 (d, 1H, $^3J = 8.4$ Hz, 1H, -CONHPh), 7.91 (d, $^3J = 6.1$ Hz, 1H, Py-H6), 7.85 (t, $^3J = 7.9$ Hz, 1H, Py-H4), 7.76 (d, $^3J = 7.2$ Hz, 2H, Ph-H2,2'), 7.50 (t, $^3J = 7.3$ Hz, 1H, Ph-H4), 7.44 (t, $^3J = 7.5$ Hz, 2H, Ph-H3,3'), 7.14 (d, $^3J = 8.5$ Hz, 2H, Tyr-H3,3'), 7.03 (d, $^3J = 9.0$ Hz, Py-H3), 6.83 (d, $^3J = 8.5$ Hz, 2H, Tyr-H2,2'), 6.81 (t, $^3J = 6.5$ Hz, 1H, Py-H5), 4.44 (m, 1H, -CHCH₂COOH), 4.02 (t, $^3J = 6.0$ Hz, 2H, -CH₂OAr), 3.47 (t, $^3J = 6.5$ Hz, 2H, PyNHCH₂-), 2.82 (dd, $^2J = 13.6$ Hz, $^3J = 8.0$ Hz, 1H, -CH(H')COOH), 2.76 (dd, $^2J = 13.6$ Hz, $^3J = 5.9$ Hz, 1H, -CH(H')COOH), 2.53 (dd, $^2J = 15.5$ Hz, $^3J = 7.7$ Hz, 1H, ArCH(H')-), 2.44 (dd, $^2J = 15.4$ Hz, $^3J = 6.2$ Hz, 1H, Ar-CH(H')-), 2.02 (m, 2H, -CH₂CH₂CH₂-). $^{13}\text{C-NMR}$ (125 MHz, DMSO): $\delta = 172.3, 165.5, 156.7, 152.9, 142.6, 136.3, 134.6, 130.9, 130.8, 130.0, 128.0, 127.0, 114.1, 112.9, 111.7, 64.6, 48.3, 38.8, 38.7, 38.5, 27.6$. **HPLC** (10-50%, 30 min): $t_{\text{R}} = 21.68$ min. **MS** (ESI): $m/z = 434.3$ $[\text{m}+\text{H}]^+$. **HRMS** (ESI) ($\text{C}_{25}\text{H}_{28}\text{N}_3\text{O}_4^+$): Calc.: 434.2074, found: 434.2076.

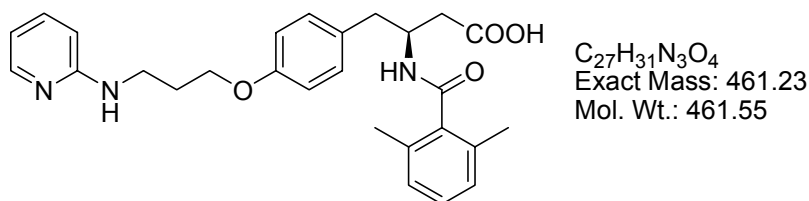
IV.3.57 Preparation of 3-(S)-(4-methylbenzamido)-4-[4-(3-pyridin-2-ylaminopropoxy)phenyl]butanoic acid, **30b**



The title compound was prepared from **29** (71 mg, 161 μ mol) following **GP8b**. [4-methylbenzoic acid (44 mg, 320 μ mol), HATU (122 mg, 320 μ mol), DIEA (220 μ L, 1.28 mmol), LiOH (20 mg, 0.8 mmol)] Purification using preparative HPLC and lyophilization afforded **30b** (12 mg, 21 μ mol, 13%) as TFA salt (colorless solid).

1 H-NMR (500 MHz, DMSO): δ = 13.46 (bs, 1H), 12.20 (bs, 1H), 8.22 (d, 3J = 8.0 Hz, 1H, -NHCOAr), 7.90 (d, 3J = 6.2 Hz, 1H, Py-H6), 7.78 (t, 3J = 7.8 Hz, 1H, Py-H4), 7.67 (d, 3J = 8.1 Hz, 2H, Ph-H2,2'), 7.23 (d, 3J = 8.1 Hz, 2H, Tyr-H3,3'), 7.12 (d, 3J = 8.5 Hz, 2H, Ph-H3,3'), 6.95 (d, 3J = 9.2 Hz, 1H, Py-H3), 6.82 (d, 3J = 8.8 Hz, 2H, Tyr-H2,2'), 6.76 (t, 3J = 6.5 Hz, 1H, Py-H5), 4.42 (m, 1H, -CHCH₂COOH), 4.01 (t, 3J = 6.0 Hz, 2H, -CH₂OAr), 3.44 (m, 2H, Py-NHCH₂-), 2.80 (dd, 2J = 13.8 Hz, 3J = 7.6 Hz, 1H, -CH(H')COOH), 2.74 (dd, 2J = 13.4 Hz, 3J = 5.7 Hz, 1H, -CH(H')COOH), 2.50 (dd, 2J = 14.9 Hz, 3J = 7.7 Hz, ArCH(H')-), 2.42 (dd, 2J = 15.5 Hz, 3J = 6.3 Hz, 1H, Ar-CH(H')-), 2.33 (s, 3H, -CH₃), 2.00 (m, 2H, -CH₂CH₂CH₂-). **13 C-NMR** (125 MHz, DMSO): δ = 172.4, 165.4, 156.7, 153.6, 141.8, 140.7, 137.6, 131.8, 130.7, 130.0, 128.6, 127.1, 114.1, 112.4, 111.7, 64.6, 48.2, 38.8, 38.7, 38.4, 27.7, 20.8. **HPLC** (10-50%, 30 min): t_R = 23.61 min. **MS** (ESI): m/z = 448.3 [$m+H^+$]⁺. **HR-MS** (ESI) ($C_{26}H_{30}N_3O_4$)⁺: Calc.: 448.2231, Found: 448.2226.

IV.3.58 Preparation of 3-(S)-(2,6-dimethylbenzamido)-4-[4-(3-pyridin-2-ylaminopropoxy)phenyl]butanoic acid, **30c**

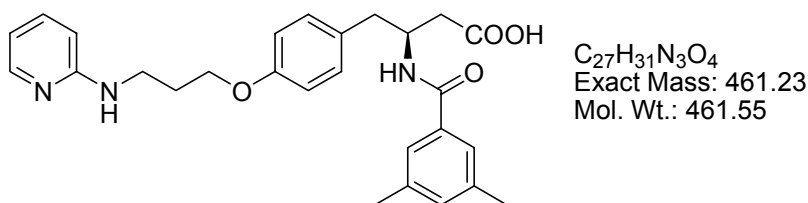


IV. Experimental Section

The title compound was prepared from **25b** (71 mg, 161 μ mol) following **GP8b**. [2,6-dimethylbenzoic acid (48 mg, 320 μ mol), HATU (122 mg, 320 μ mol), DIEA (220 μ L, 1.28 mmol), LiOH (20 mg, 0.8 mmol)] Purification using preparative HPLC and lyophilization afforded **30b** (10 mg, 17 μ mol, 11%) as TFA salt (colorless solid).

¹H-NMR (500 MHz, DMSO): δ = 13.52 (bs, 1H), 12.23 (bs, 1H), 8.80 (bs, 1H, Py-NH), 8.25 (d, 3J = 8.4 Hz, 1H, -NHCOAr), 7.93 (d, 3J = 5.8 Hz, 1H, Py-H6), 7.87 (t, 3J = 7.7 Hz, 1H, Py-H4), 7.16 (d, 3J = 8.4 Hz, 2H, Tyr-H3,3'), 7.11 (t, 3J = 7.5 Hz, 1H, Ar-H4), 7.04 (d, 3J = 8.8 Hz, 1H, Py-H3), 6.95 (d, 3J = 7.7 Hz, 2H, Ar-H3,3'), 6.87 (d, 3J = 8.4 Hz, 2H, Tyr-H2,2'), 6.83 (t, 3J = 6.7 Hz, 1H, Py-H5), 4.49 (m, 1H, Ar-CH₂CH-), 4.05 (t, 3J = 5.9 Hz, 2H, -CH₂OAr), 3.49 (m, 2H, PyNHCH₂-), 2.73 (m, 2H, -CH₂COOH), 2.47 (dd, 2J = 15.6 Hz, 3J = 9.6 Hz, 1H, Ar-CH(H')), 2.38 (dd, 2J = 15.6 Hz, 3J = 5.9 Hz, 1H, Ar-CH(H')), 2.05 (m, 2H, -CH₂CH₂CH₂-), 2.02 (s, 6H, Ar-(CH₃)₂). **¹³C-NMR** (125 MHz, DMSO): δ = 172.3, 168.1, 156.8, 153.0, 142.5, 138.5, 136.5, 133.5, 130.7, 130.0, 127.7, 126.8, 114.2, 112.9, 111.8, 64.7, 47.6, 38.9, 38.7, 38.5, 27.6, 18.5. **HPLC** (10-50%, 30 min): t_R = 22.58 min **MS** (ESI): m/z = 462.1 [m+H]⁺. **HR-MS** (ESI) (C₂₇H₃₂N₃O₄)⁺: Calc.: 462.2387, Found: 462.2385.

IV.3.59 Preparation of 3-(S)-(3,5-dimethylbenzamido)-4-[4-(3-pyridin-2-ylaminopropoxy)phenyl]butanoic acid **30c**

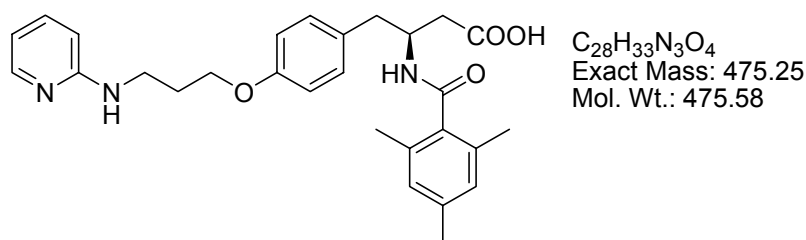


The title compound was prepared from **29** (71 mg, 161 μ mol) following **GP8b**. [3,5-dimethylbenzoic acid (48 mg, 320 μ mol), HATU (122 mg, 320 μ mol), DIEA (220 μ L, 1.28 mmol), LiOH (20 mg, 0.8 mmol)] Purification using preparative HPLC and lyophilization afforded **30c** (15 mg, 26 μ mol, 16%) as TFA salt (colorless solid).

¹H-NMR (500 MHz, DMSO): δ = 13.50 (bs, 1H), 12.27 (bs, 1H), 8.87 (bs, 1H, Py-NH), 8.22 (d, 3J = 8.4 Hz, 1H, NHCOAr), 7.91 (d, 3J = 6.1 Hz, 1H, Py-H6), 7.86 (t, 3J = 7.8 Hz, 1H, Py-H4), 7.47 (s, 2H, Ar-H2,2'), 7.13 (d, 3J = 8.5 Hz, 2H, Tyr-H3,3'), 7.12 (s, 1H, Ar-H4), 7.04 (d, 3J = 8.8 Hz, 1H, Py-H3), 6.84 (d, 3J = 8.7 Hz, 2H,

Tyr-*H*2,2'), 6.81 (t, $^3J = 6.9$ Hz 1H, Pyr-*H*5), 4.43 (m, 1H, CHCH_2COOH), 4.02 (t, $^3J = 5.9$ Hz, 2H, $-\text{CH}_2\text{OAr}$), 3.47 (t, $^3J = 6.3$ Hz, 2H, Py-NH CH_2 -), 2.81 (dd, $^2J = 13.6$ Hz, $^3J = 7.9$ Hz, 1H, $-\text{CH}(\text{H}')\text{COOH}$), 2.73 (dd, $^2J = 13.8$ Hz, $^3J = 6.1$ Hz, 1H, $-\text{CH}(\text{H}')\text{COOH}$), 2.51 (dd, $^2J = 15.5$ Hz, $^3J = 7.8$ Hz, 1H, Ar- $\text{CH}(\text{H}')$ -), 2.42 (dd, $^2J = 15.3$ Hz, $^3J = 6.2$ Hz, 1H, Ar- $\text{CH}(\text{H}')$ -), 2.29 (s, 6H, Ar- $(\text{CH}_3)_2$), 2.03 (m, 2H, $-\text{CH}_2\text{CH}_2\text{CH}_2$ -). $^{13}\text{C-NMR}$ (125 MHz, DMSO): $\delta = 172.4, 165.8, 156.7, 152.9, 142.7, 137.1, 136.2, 134.6, 132.1, 130.8, 130.0, 124.8, 114.1, 113.0, 111.7, 64.6, 48.2, 38.8, 38.6, 38.6, 27.6, 20.7$. **HPLC** (10-50%, 30 min): $t_R = 25.97$ min. **MS** (ESI): $m/z = 462.2$ $[\text{m}+\text{H}]^+$. **HR-MS** ($\text{C}_{27}\text{H}_{32}\text{N}_3\text{O}_4$) $^+$: Calc.: 462.2387, Found: 462.2382.

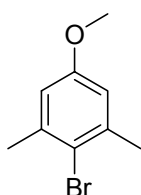
IV.3.60 Preparation of 3-(*S*)-(3,5-dimethylbenzamido)-4-[4-(3-pyridin-2-ylaminopropoxy)phenyl]butanoic acid **30d**



The title compound was prepared from **29** (71 mg, 161 μmol) following **GP8b**. [2,4,6-trimethylbenzoic acid (50 mg, 320 μmol), HATU (122 mg, 320 μmol), DIEA (220 μL , 1.28 mmol), LiOH (20 mg, 0.8 mmol)] Purification using preparative HPLC and lyophilization afforded **30d** (21 mg, 36 μmol , 22%) as TFA salt (colorless solid).

$^1\text{H-NMR}$ (500 MHz, DMSO): $\delta = 8.88$ (bs, 1H, Py-NH), 8.16 (d, $^3J = 8.8$ Hz, 1H, $-\text{NHCOAr}$), 7.93 (d, $^3J = 6.1$ Hz, 1H, Py-*H*6), 7.87 (t, $^3J = 7.9$ Hz, 1H, Py-*H*4), 7.15 (d, $^3J = 8.5$ Hz, 2H, Tyr-*H*3,3'), 7.06 (d, $^3J = 8.8$ Hz, 1H, Py-*H*3), 6.86 (d, $^3J = 8.8$ Hz, 2H, Tyr-*H*2,2'), 6.83 (t, $^3J = 6.5$ Hz, 1H, Py-*H*5), 6.76 (s, 2H, Ar-*H*3,3'), 4.47 (m, 1H, $-\text{CHCH}_2\text{COOH}$), 4.05 (t, $^3J = 5.9$ Hz, $-\text{CH}_2\text{OAr}$), 3.49 (t, $^3J = 6.5$ Hz, 2H, Py-NH CH_2 -), 2.73 (m, 2H, $-\text{CH}_2\text{COOH}$), 2.46 (dd, $^2J = 15.7$ Hz, $^3J = 7.7$ Hz, 1H, Ar- $\text{CH}(\text{H}')$ -), 2.37 (dd, $^2J = 15.3$ Hz, $^3J = 6.2$ Hz, 1H, Ar- $\text{CH}(\text{H}')$ -), 2.19 (s, 3H, Ar- (CH_3)), 2.04 (m, 2H, $-\text{CH}_2\text{CH}_2\text{CH}_2$ -), 1.97 (s, 6H, Ar- $(\text{CH}_3)_2$). $^{13}\text{C-NMR}$ (125 MHz, DMSO): $\delta = 172.3, 168.3, 156.8, 152.9, 142.7, 136.8, 136.3, 135.8, 133.5, 130.7, 130.0, 127.4, 114.2, 113.0, 111.8, 64.7, 47.6, 38.9, 38.7, 38.6, 27.6, 20.5, 18.5$. **HPLC** (10-50%, 30 min): $t_R = 26.03$ min. **MS** (ESI): $m/z = 476.4$ $[\text{m}+\text{H}]^+$.

IV.3.61 Preparation of 1-bromo-2,6-dimethyl-4-methoxybenzene, 31a

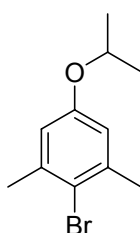


C₉H₁₁BrO
Exact Mass: 214
Mol. Wt.: 215.09

4-bromo-3,5-dimethylphenol (3.0 g, 15.0 mmol, 1 eq.) was dissolved in 150 mL dry THF. After addition of K₂CO₃ (4.2 g, 30.0 mmol, 2 eq.) and dimethyl sulfate (1.1 mL, 11.3 mmol, 0.75 eq.), the mixture was refluxed for 8 h. After cooling to room temperature, the reaction was quenched with saturated NH₄Cl solution, the mixture extracted with ethyl acetate (2x 50 mL). The organic layers were washed with brine, dried over Na₂SO₄, filtered and concentrated *in vacuo*. The crude product was purified by flash chromatography on silica gel (hexane / ethyl acetate 8 : 2) to give the title compound (2.7 g, 12.6 mmol, 84%) as colorless oil.

¹H-NMR (250 MHz, CDCl₃): δ = 6.68 (s, 2H, Ar-H_{3,3'}), 3.79 (s, 3H, Ar-OCH₃), 2.43 (s, 6H, Ar-(CH₃)₂). ¹³C-NMR (62.9 MHz, CDCl₃): δ = 158.0, 138.9, 118.0, 113.7, 55.1, 23.9. HPLC (10-100%): t_R = 27.59 min. GC-MS (EI): t_R = 13.76 min, m/z = 214.1 [M]⁺(1Br), 199.1 [M-CH₃]⁺(1Br), 171.1 [M-CH₃-CO]⁺(1Br), 135.2 [M-Br]⁺.

IV.3.62 Preparation of 1-bromo-2,6-dimethyl-4-isopropoxybenzene, 31b



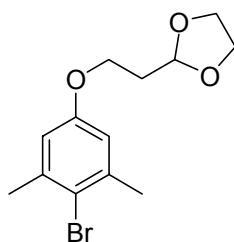
C₁₁H₁₅BrO
Exact Mass: 242.03
Mol. Wt.: 243.14

4-bromo-3,5-dimethylphenol (1.0 g, 5.0 mmol, 1 eq.) was dissolved in 60 mL dry DMF. After addition of K₂CO₃ (4.2 g, 15.0 mmol, 3 eq.), 2-bromopropane (3.1 g, 25.0 mmol, 5 eq.) and potassium iodide (2.5 g, 15.0 mmol, 3 eq.), the mixture was heated to 120 °C for 8 h. After cooling to room temperature, the DMF was removed under reduced pressure, the residue taken up in ethyl acetate, washed with water

and brine, dried over Na_2SO_4 , filtered and concentrated *in vacuo*. The crude product was purified by flash chromatography on silica gel (hexane / ethyl acetate 8 : 2) to give the title compound (0.86 g, 3.5 mmol, 70%) as colorless oil.

$^1\text{H-NMR}$ (250 MHz, CDCl_3): δ = 6.69 (s, 2H, Ar- $H_{3,3'}$), 4.53 (sept, 3J = 6.1 Hz, 1H, $-\text{CH}(\text{CH}_3)_2$), 2.42 (s, 6H, Ar- $(\text{CH}_3)_2$), 1.36 (d, 3J = 6.1 Hz, 6H, $-\text{CH}(\text{CH}_3)_2$). **$^{13}\text{C-NMR}$** (63 MHz, DMSO): δ = 156.3, 138.9, 117.9, 115.8, 69.9, 23.9, 22.0. **HPLC** (10-100%): t_R = 30.67 min. **GC-MS** (EI): t_R = 16.05 min; m/z = 242.2 $[\text{M}]^+(1\text{Br})$, 200.1 $[\text{M}-\text{C}_3\text{H}_7]^+(1\text{Br})$, 121.2 $[\text{M}-\text{C}_3\text{H}_7-\text{Br}]^+$.

IV.3.63 Preparation of 2-(2-(4-bromo-3,5-dimethylphenoxy)ethyl)-1,3-dioxolane, 31c

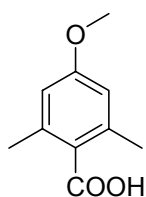


$\text{C}_{13}\text{H}_{17}\text{BrO}_3$
Exact Mass: 300.04
Mol. Wt.: 301.18

4-bromo-3,5-dimethylphenol (2.47 g, 12.3 mmol, 1 eq.) was dissolved in 20 mL dry DMF. After addition of K_2CO_3 (3.4 g, 24.6 mmol, 2 eq.) and 2-bromoethyl-1,3-dioxolane (4.5 mL, 24.6 mmol, 2 eq.), the mixture was heated to 80°C for 12 h. After cooling to room temperature, the DMF was removed under reduced pressure, the residue taken up in ethyl acetate, washed with water and brine, dried over Na_2SO_4 , filtered and concentrated *in vacuo*. The crude product was purified by flash chromatography on silica gel (hexane / ethyl acetate 8 : 2 + 1% TEA) to give the title compound (3.39 g, 11.2 mmol, 91%) as colorless oil.

$^1\text{H-NMR}$ (500 MHz, DMSO): δ = 6.65 (s, 1H, Ar- $H_{2,2'}$), 5.07 (t, 3J = 4.8 Hz, 1H, $-\text{CH}(\text{OCH}_2)_2$), 4.07 (t, 3J = 6.6 Hz, 2H, $-\text{CH}_2\text{OAr}$), 4.03-3.83 (m, 4H, $-\text{OCH}_2\text{CH}_2\text{O}-$), 2.37 (s, 6H, Ar- $(\text{CH}_3)_2$), 2.14 (dt, 3J = 6.6 Hz, 3J = 4.9 Hz, 2H, $-\text{CH}_2\text{CH}_2\text{OAr}$). **$^{13}\text{C-NMR}$** (125 MHz, DMSO): δ = 157.2, 138.8, 118.1, 114.3, 101.9, 64.8, 63.5, 33.7, 23.9. **HPLC** (10-100%): t_R = 30.10 min. **GC-MS** (EI): t_R = 27.92 min; m/z = 300.2 $[\text{M}]^+(1\text{Br})$, 200.2 $[\text{M}-\text{C}_5\text{H}_9\text{O}_2]^+$.

IV.3.64 Preparation of 2,6-dimethyl-4-methoxybenzoic acid, 32a

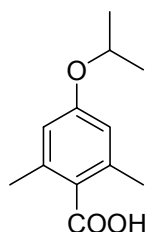


C₁₀H₁₂O₃
Exact Mass: 180.08
Mol. Wt.: 180.2

The title compound was prepared from **31a** (2.7 g, 12.55 mmol, 1 eq.) and *n*BuLi (1.6 M in hexane, 9.4 mL, 15.06 mmol, 1.2 eq.) according to **GP10**. Recrystallization from DCM / hexane gave 1.30 g (7.23 mmol, 58 %) of colorless crystals.

¹H-NMR (250 MHz, DMSO): δ = 12.8 (bs, 1H, -COOH), 6.64 (s, 2H, Ar-H_{2,2'}), 3.74 (s, 3H, -OCH₃), 2.26 (s, 6H, Ar-(CH₃)₂). **¹³C-NMR** (62.9 MHz, DMSO): δ = 170.4, 159.1, 136.0, 127.6, 112.7, 54.9, 19.8. **HPLC** (10-100%): t_R = 15.83 min. **MS** (EI): m/z = 180.1 [M], 163.0 [M-OH]⁺, 135.1 [M-COOH]⁺.

IV.3.65 Preparation of 2,6-dimethyl-4-isopropoxybenzoic acid, 32b

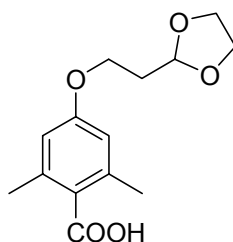


C₁₂H₁₆O₃
Exact Mass: 208.11
Mol. Wt.: 208.25

The title compound was prepared from **31b** (0.86 g, 3.5 mmol, 1 eq.) and *n*BuLi (1.6 M in THF, 2.6 mL, 4.2 mmol, 1.2 eq.) according to **GP10**. Recrystallization from DCM / hexane gave 0.47 g (2.28 mmol, 65 %) of colorless crystals.

¹H-NMR (250 MHz, DMSO): δ = 12.78 (bs, 1H, -COOH), 6.61 (s, 2H, Ar-H_{2,2'}), 4.60 (sept, ³*J* = 6.0 Hz, 1H, -CH(CH₃)₂), 2.25 (s, 6H, Ar-(CH₃)₂), 1.24 (d, ³*J* = 6.0 Hz, 6H, -CH(CH₃)₂). **¹³C-NMR** (62.9 MHz, DMSO): δ = 170.4, 157.3, 136.1, 127.3, 114.3, 68.8, 21.7, 19.8. **HPLC** (10-100%): t_R = 19.42 min. **MS** (EI): m/z = 208.1 [M]⁺, 166.0 [M-C₃H₇]⁺, 148.0 [M-C₃H₇-H₂O].

IV.3.66 Preparation of 4-(2-(1,3-dioxolan-2-yl)ethoxy)-2,6-dimethylbenzoic acid, **32c**

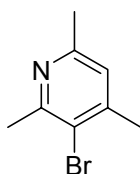


C₁₄H₁₈O₅
Exact Mass: 266.12
Mol. Wt.: 266.29

The title compound was prepared from **31b** (3.15 g, 10.5 mmol, 1 eq.) and *n*BuLi (1.6 M in THF, 7.8 mL, 12.5 mmol, 1.2 eq.) according to **GP10**. Recrystallization from DCM / hexane gave 2.07 g (7.76 mmol, 74 %) of colorless crystals.

¹H-NMR (500 MHz, DMSO): δ = 12.84 (s, 1H, -COOH), 6.64 (s, 2H, Ar-H), 4.97 (t, ³J = 4.9 Hz, 1H, -CH(OCH₂)₂), 4.05 (t, ³J = 6.6 Hz, 2H, -CH₂OAr), 3.94-3.75 (m, 4H, -OCH₂CH₂O-), 2.25 (s, 6H, Ar(CH₃)₂), 2.01 (dd, ²J = 11.6 Hz, ³J = 6.6 Hz, 2H, -CH₂CH₂OAr). **¹³C-NMR** (125 MHz, DMSO): δ = 170.4, 158.2, 136.1, 127.6, 113.2, 101.1, 64.2, 33.2, 32.5, 19.8. **HPLC** (10-100%): *t*_R = 19.97 min. **MS** (EI): *m/z* = 266.1 [M]⁺, 166.0 [M-C₅H₈O₂]⁺, 100.0 [C₅H₈O₂]⁺, 73.0 [C₃H₅O₂]⁺.

IV.3.67 Preparation of 3-bromo-2,4,6-trimethylpyridine, **33**

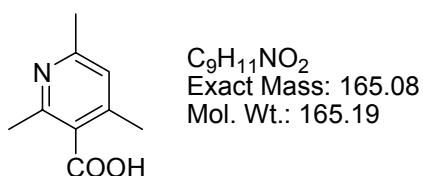


C₈H₁₀BrN
Exact Mass: 199
Mol. Wt.: 200.08

2,4,6-Trimethylpyridine (18.3 g, 154 mmol, 1 eq.) was dissolved in 30 ml trifluoroacetic acid cooled by a water bath. After addition of 40 mL of concentrated sulfuric acid, NBS (30.2 g, 169.4 mmol, 1.1 eq.) was added in small portions. The resulting red solution was stirred at ambient temperature for 24 h. The reaction mixture was poured on ice, alkalized with sodium hydroxide and extracted with ethyl acetate (3 x 100 mL). The combined organic layers were dried over Na₂SO₄, filtered and concentrated on a rotary evaporator. The resulting oil was purified by fractionized distillation under vacuum (6.5 mbar, *bp*_(collidine) = ~50°C, *bp*_(product) = 75-77°C). Yield was 28.74 g (144 mmol, 93%) of a colorless liquid, which turned brown on standing.

¹H-NMR (360 MHz, CDCl₃): δ = 6.68 (s, 1H, Py-*H5*), 2.50 (s, 3H, -CH₃), 2.29 (s, 3H, -CH₃), 2.19 (s, 3H, -CH₃). **¹³C-NMR** (125 MHz, DMSO): δ = 156.1, 155.2, 146.9, 122.8, 120.8, 25.3, 23.3, 22.8. **HPLC** (10-100%): t_R = 18.08 min. **MS** (ESI): m/z = 200.3 [m+H⁺]⁺(1Br).

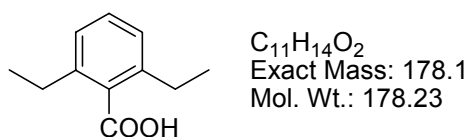
IV.3.68 Preparation of 2,4,6-trimethylnicotinic acid, **34**



To a cooled (-78°C) solution of the **33** (2.00 g, 10 mmol, 1 eq.) in dry THF (40 mL) was added *n*BuLi (1.6 M in hexane, 6.25 mL, 10 mmol, 1 eq.) under an argon atmosphere. The resulting reaction mixture was stirred for 30 min. After addition of crushed dry ice (~10 g), the cooling bath was removed and the reaction mixture allowed to warm to room temperature. The THF was evaporated and the residue dissolved in 2N NaOH / diethyl ether. The aqueous phase was separated and acidified to pH 6. The mixture was concentrated, triturated with ethanol and filtered. The filtrate was evaporated and the product recrystallized from methanol / ethyl acetate. Yield: 1.49 g (7.4 mmol, 74%) of a tan solid (as hydrochloride salt).

¹H-NMR (500 MHz, DMSO): δ = 7.57 (s, 1H, Ar-*H*), 6.89 (bs, 1H, PyNH⁺), 2.67 (s, 3H, Ar-*CH*₃), 2.66 (s, 3H, Ar-*CH*₃), 2.42 (s, 3H, Ar-*CH*₃). **¹³C-NMR** (125 MHz, DMSO): δ = 166.6, 153.5, 152.1, 150.0, 130.7, 125.7, 19.9, 19.5, 18.4. **HPLC** (5-20%): t_R = 22.03 min. **MS** (ESI): m/z = 166.3.

IV.3.69 Preparation of 2,6-diethylbenzoic acid **35**

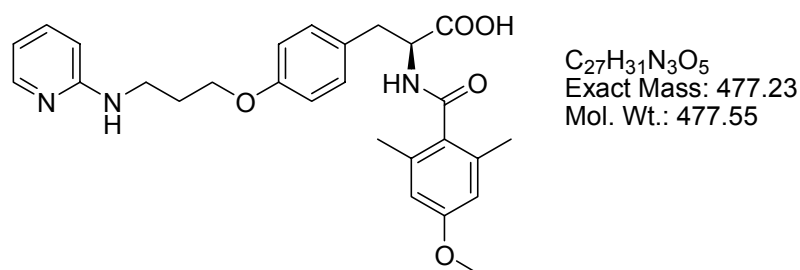


The title compound was prepared from 2,6-diethylbenzoic acid (1 g, 4.69 mmol, 1 eq.) and *n*BuLi (1.6 M in THF, 3.81 mL, 6.10 mmol, 1.3 eq.) according to **GP10**.

Recrystallization from DCM / hexane gave 0.27 g (1.5 mmol, 32%) as colorless crystals.

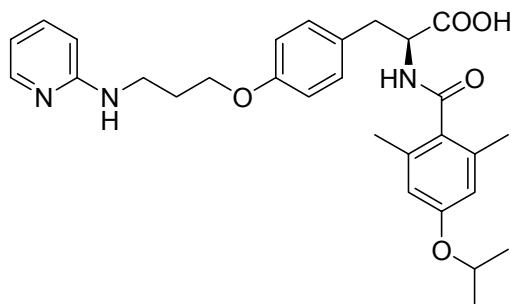
¹H-NMR (500 MHz, DMSO): δ = 7.28 (t, 3J = 7.6 Hz, 1H, Ph-*H*₄), 7.11 (d, 3J = 7.6 Hz, 2H, Ph-*H*_{3,3'}), 2.58 (q, 3J = 7.5 Hz, 2H, -CH₂CH₃), 1.16 (t, 3J = 7.5 Hz, 3H, -CH₂CH₃). **¹³C-NMR** (125 MHz, DMSO): δ = 170.8, 139.3, 134.6, 128.8, 125.8, 26.1, 15.6. **HPLC** (10-100%, 30 min): t_R = 20.16 min. **MS** (EI): m/z = 178.1 [M], 160.0 [M-H₂O]⁺.

IV.3.70 Preparation of 2-(*S*)-(2,6-dimethyl-4-methoxybenzamido)-3-[4-(3-pyridin-2-yl-aminopropoxy)phenyl]propionic acid, **23j**



The title compound was prepared from **22a** (66 mg, 155 μ mol) following **GP8b** [**32a** (34 mg, 186 μ mol), HATU (71 mg, 186 μ mol), DIEA (131 μ L, 775 μ mol), LiOH (19 mg, 775 μ mol)]. Purification using preparative HPLC and lyophilization afforded **23j** (25 mg, 42 μ mol, 27%) as TFA salt (colorless solid).

¹H-NMR (500 MHz, DMSO): δ = 13.32 (bs, 1H), 12.67 (bs), 8.62 (s, 1H, Py-NH), 8.43 (d, 3J = 8.3 Hz, 1H, -NHCOAr), 7.92 (d, 3J = 6.0 Hz, 1H, Py-*H*₆), 7.84 (t, 3J = 7.7 Hz, 1H, Py-*H*₄), 7.20 (d, 3J = 8.6 Hz, 2H, Tyr-*H*_{3,3'}), 7.01 (d, 3J = 9.0 Hz, 1H, Py-*H*₃), 6.85 (d, 3J = 8.6 Hz, Tyr-*H*_{2,2'}), 6.82 (t, 3J = 6.6 Hz, 1H, Py-*H*₅), 6.52 (s, 2H, Ar-*H*_{3,3'}), 4.61 (m, 1H, -CHCOOH), 4.05 (t, 3J = 6.1 Hz, 2H, -CH₂OAr), 3.69 (s, 3H, Ar-OCH₃), 3.47 (m, 2H, PyNHCH₂-), 3.09 (dd, 2J = 14.0 Hz, 3J = 4.1 Hz, 1H, Ar-CH(*H'*)-), 2.79 (dd, 2J = 13.9 Hz, 3J = 11.4 Hz, Ar-CH(*H'*)-), 2.04 (m, 2H, -CH₂CH₂CH₂-), 1.95 (s, 6H, Ar(CH₃)₂). **¹³C-NMR** (125 MHz, DMSO): δ = 173.1, 169.0, 158.5, 156.9, 152.7, 142.7, 136.0, 135.5, 130.9, 130.1, 130.0, 114.1, 113.3, 113.2, 111.8, 64.7, 54.9, 53.5, 39.4, 38.6, 35.4, 27.5, 18.7. **HPLC** (10-50%, 30 min): t_R = 22.73 min. **HPLC** (10-100%, 30 min): t_R = 14.20 min. **MS** (ESI): m/z = 478.6 [m+H]⁺, 163.2 [COC₆H₂(CH₃)₂OCH₃]⁺. **HR-MS** (ESI) (C₂₇H₃₂N₃O₅⁺): Calc.: 478.2336, found: 478.2332.

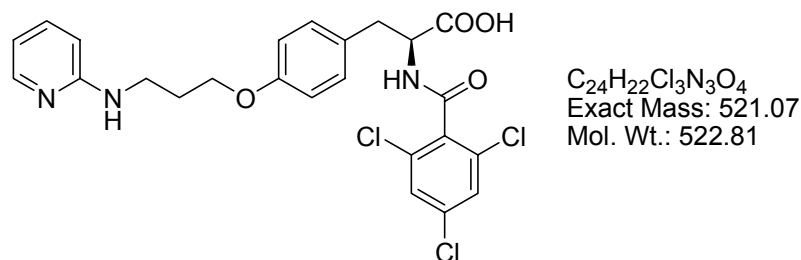
IV.3.71 Preparation of 2-(S)-(2,6-dimethyl-4-isopropoxybenzamido)-3-[4-(3-pyridin-2-yl-aminopropoxy)phenyl]propionic acid, 23k

C₂₉H₃₅N₃O₅
Exact Mass: 505.26
Mol. Wt.: 505.61

The title compound was prepared from **22a** (66 mg, 155 μ mol) following **GP8b** [**32b** (39 mg, 186 μ mol), HATU (71 mg, 186 μ mol), DIEA (131 μ L, 775 μ mol), LiOH (19 mg, 775 μ mol)]. Purification using preparative HPLC and lyophilization afforded **23k** (27 mg, 44 μ mol, 28%) as TFA salt (colorless solid).

¹H-NMR (500 MHz, DMSO): δ = 13.40, 12.70 (bs, 1H, -COOH), 8.74 (bs, 1H, Py-NH), 8.45 (d, 3J = 8.3 Hz, 1H, -CONHAr), 7.92 (d, 3J = 5.8 Hz, 1H, Py-H6), 7.86 (t, 3J = 7.7 Hz, 1H, Py-H4), 7.20 (d, 3J = 8.3 Hz, 2H, Tyr-H3,3'), 7.03 (d, 3J = 8.9 Hz, 1H, Py-H3), 6.85 (d, 3J = 8.3 Hz, 2H, Tyr-H2,2'), 6.83 (t, 3J = 6.7 Hz, 1H, Py-H5), 6.50 (s, 2H, Ar-H2,2'), 4.60 (m, 1H, Ar-OCH(CH₃)₂), 4.55 (m, 1H, -CHCOOH), 4.05 (t, 3J = 5.1 Hz, 2H, -CH₂OAr), 3.47 (m, 2H, PyNHCH₂-), 3.09 (dd, 2J = 13.8 Hz, 3J = 3.5 Hz, 1H, ArCH(H')-), 2.79 (dd, 2J = 13.4 Hz, 3J = 11.7 Hz, 1H, ArCH(H')-), 2.04 (m, 2H, -CH₂CH₂CH₂-), 1.94 (s, 6H, -CH(CH₃)₂). **¹³C-NMR** (125 MHz, DMSO): δ = 173.1, 169.0, 156.9, 156.7, 152.9, 142.5, 136.6, 135.5, 130.7, 130.0, 130.0, 114.1, 113.8, 113.1, 111.8, 68.7, 64.7, 53.4, 39.4, 38.5, 27.5, 21.7, 18.7. **HPLC** (10-100%, 30 min): t_R = 16.18 min. **MS** (ESI): m/z = 506.5 [m+H]⁺, 191.2 [COC₆H₂(CH₃)₂OCH(CH₃)₂]⁺, 149.2 [C₆H₂(CH₃)₂OCH(CH₃)₂]⁺, **HRMS** (ESI) (C₂₇H₃₂N₃O₅⁺): Calc.: 506.2649, found: 506.2645.

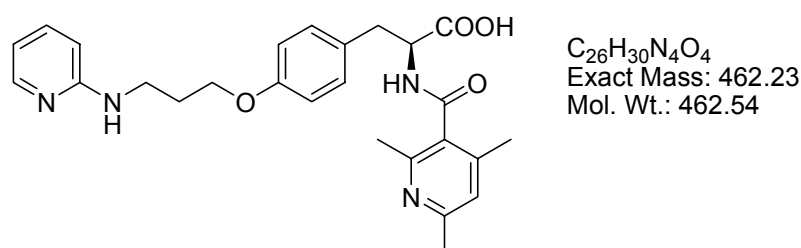
IV.3.72 Preparation of 2-(S)-(2,4,6-trichlorobenzamido)-3-[4-(3-pyridin-2-yl-aminopropoxy)phenyl]propionic acid, **23l**



The title compound was prepared from **22a** (60 mg, 140 μ mol) following **GP8a** [2,4,6-trichlorobenzoic acid chloride (41 mg, 168 μ mol), $NaHCO_3$ (36 mg, 420 μ mol), $LiOH$ (17 mg, 700 μ mol)]. Purification using preparative HPLC and lyophilization afforded **23l** (56 mg, 88 μ mol, 63%) as TFA salt (colorless solid).

1H -NMR (500 MHz, DMSO): δ = 12.81 (bs, 1H, -COOH), 9.08 (d, 3J = 8.2 Hz, 1H, -NHCOAr), 8.77 (bs, 1H, PyNH-), 7.92 (d, 3J = 5.8 Hz, 1H, Py-H6), 7.87 (t, 3J = 7.7 Hz, 1H, Py-H4), 7.66 (s, 2H, Ar-H2,2'), 7.19 (d, 3J = 8.3 Hz, 2H, Tyr-H3,3'), 7.04 (d, 3J = 8.8 Hz, 1H, Py-H3), 6.84 (d, 3J = 8.2 Hz, 2H, Tyr-H2,2'), 6.83 (m, 1H, Py-H5), 4.61 (m, 1H, -CHCOOH), 4.04 (t, 3J = 5.7 Hz, 2H, -CH₂OAr), 3.47 (m, 2H, -NHCH₂-), 3.06 (dd, 2J = 14.0 Hz, 3J = 4.8 Hz, 1H, Ar-CH(H')-), 2.84 (dd, 2J = 13.9 Hz, 3J = 9.8 Hz, 1H, Ar-CH(H')-), 2.04 (m, 2H, -CH₂CH₂CH₂-). **^{13}C -NMR** (125 MHz, DMSO): δ = 172.1, 162.6, 157.0, 152.8, 142.6, 136.3, 135.2, 134.1, 132.1, 130.1, 129.2, 127.6, 114.1, 113.1, 111.8, 64.7, 53.6, 38.5, 35.9, 27.5. **HPLC** (10-50%, 30 min): t_R = 26.93 min. **HPLC** (10-100%, 30 min): t_R = 16.35 min. **MS** (ESI): m/z = 1042.9 [$2m+H$]⁺ (6Cl), 522.6 [$m+H$]⁺ (3Cl). **HR-MS** (ESI) ($C_{24}H_{23}Cl_3N_3O_4$)⁺: Calc.: 522.0749, Found: 522.0744.

IV.3.73 Preparation of 2-(S)-(2,4,6-trimethylpyridincarboxamido)-3-[4-(3-pyridin-2-yl-aminopropoxy)phenyl]propionic acid, **23m**

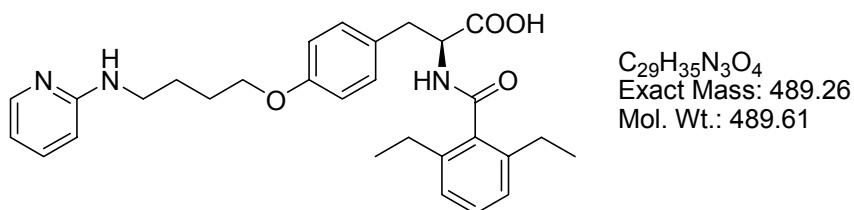


IV. Experimental Section

The title compound was prepared from **22a** (66 mg, 155 μ mol) following **GP8b** [**34** (31 mg, 155 μ mol), HATU (59 mg, 155 μ mol), DIEA (131 μ L, 775 μ mol), LiOH (19 mg, 775 μ mol)]. Purification using preparative HPLC and lyophilization afforded **23m** (18 mg, 31 μ mol, 20%) as TFA salt (colorless solid).

¹H-NMR (500 MHz, DMSO): δ = 13.14 (bs, 1H), 9.01 (d, 3J = 8.4 Hz, 1H, -CONHAr), 8.92 (bs, 1H, Py-NH), 7.95 (d, 3J = 6.2 Hz, 1H, Py-H6), 7.88 (t, 3J = 8.0 Hz, 1H, Py-H4), 7.42 (s, 1H, Ar-H5), 7.20 (d, 3J = 8.5 Hz, 2H, Tyr-H3,3'), 7.06 (d, 3J = 9.0 Hz, 1H, Py-H3), 6.87 (d, 3J = 8.5 Hz, 2H, Tyr-H2,2'), 6.84 (t, 3J = 6.7 Hz, 1H, Py-H5), 4.69 (m, 1H, -CHCOOH), 4.05 (m, 2H, -CH₂OAr), 3.49 (t, 3J = 6.4 Hz, 2H, PyNHCH₂-), 3.18 (dd, 2J = 14.0 Hz, 3J = 4.0 Hz, 1H, Ar-CH(H')-), 2.79 (dd, 2J = 13.9 Hz, 3J = 11.4 Hz, 1H, Ar-H(H')-), 2.56 (s, 3H, Ar-CH₃), 2.31 (s, 3H, Ar-CH₃), 2.10 (s, 3H, Ar-CH₃), 2.04 (m, 2H, -CH₂CH₂CH₂-). **¹³C-NMR** (125 MHz, DMSO): δ = 172.5, 164.8, 157.1, 153.2, 152.9, 151.8, 149.9, 142.7, 136.3, 132.6, 130.0, 129.5, 124.6, 114.2, 113.0, 111.8, 64.8, 53.4, 39.4, 38.6, 35.4, 27.6, 19.9, 18.6, 18.0. **HPLC** (10-50%, 30 min): t_R = 14.39 min. **MS** (ESI): m/z = 463.3 [m+H]⁺, 232.3 [M+2H]²⁺.

IV.3.74 Preparation of 2-(S)-(2,4-diethylbenzamido)-3-[4-(4-pyridin-2-ylaminobutoxy)phenyl]propionic acid, **25c**



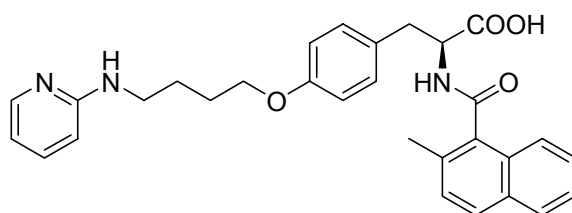
The title compound was prepared from **24** (120 mg, 220 μ mol) following **GP8b** [**35** (47 mg, 265 μ mol), HATU (100 mg, 265 μ mol), DIEA (187 μ L, 1.10 mmol), LiOH (26 mg, 1.10 mmol)]. Purification using preparative HPLC and lyophilization afforded **25c** (34 mg, 69 μ mol, 32%) as TFA salt (colorless solid).

¹H-NMR (500 MHz, DMSO): δ = 8.75 (bs, 1H, Py-NH), 8.53 (d, 3J = 8.3 Hz, 1H, -NHCOAr), 7.93 (d, 3J = 6.1 Hz, 1H, Py-H6), 7.89 (t, 3J = 7.9 Hz, 1H, Py-H4), 7.20 (d, 3J = 8.1 Hz, 2H, Tyr-H3,3'), 7.18 (t, 3J = 7.3 Hz, 1H, Ar-H4), 7.03 (d, 3J = 9.0 Hz, 1H, Py-H3), 6.99 (d, 3J = 7.2 Hz, 2H, Ar-H3,3'), 6.85 (d, 3J = 8.5 Hz, 2H, Tyr-H2,2'), 6.82 (t, 3J = 6.7 Hz, 1H, Py-H5), 4.70 (m, 1H, -CHCOOH), 3.99 (t, 3J = 6.0 Hz, 2H,

-CH₂OAr), 3.38 (m, 2H, PyNHCH₂-), 3.12 (dd, ⁴J = 14.0 Hz, ³J = 3.9 Hz, 1H, ArCH(H')CHCOOH), 2.79 (dd, ⁴J = 13.7 Hz, ³J = 11.7 Hz, 1H, ArCH(H'')CHCOOH), 2.80-1.80 (bs, 2H, Ar-(CH₂CH₃)₂)*, 1.80 (m, 2H, -CH₂CH₂OAr), 1.75 (m, 2H, PyNHCH₂CH₂-), 0.97 (bs, 3H, Ar(CH₂CH₃)₂)*. ¹³C-NMR (125 MHz, DMSO): δ = 172.3, 168.4, 156.9, 141.3, 139.6, 137.7, 137.6, 136.8, 129.5, 127.7, 124.7, 114.0, 111.7, 111.3, 66.9, 53.0, 40.8, 35.3, 25.7, 24.8, 24.5, 14.8. **HPLC** (10-100%, 30 min): t_R = 16.40 min. **MS** (ESI): m/z = 979.0 [2m+H⁺]⁺, 490.3 [m+H⁺]⁺, 161.0 [C₆H₂(C₂H₅)₂CO]⁺.

* rotation around the -CH₂-CH₃- bond is restricted and lies on NMR-timescale. Spectra at lower temperature show line-sharpening, but still no *J*-coupling.

IV.3.75 Preparation of (S)-2-(2-methylnaphthalene-1-carboxamido)-3-[4-(4-(pyridin-2-ylamino)butoxy)phenyl]propanoic acid, **25d**



C₃₀H₃₁N₃O₄
Exact Mass: 497.23
Mol. Wt.: 497.58

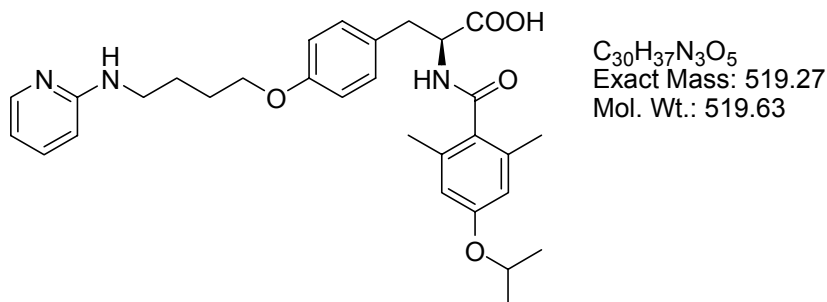
The title compound was prepared from **24** (120 mg, 220 μmol) following **GP8b** [2-methylnaphthalene-1-carboxylic acid (49 mg, 265 μmol), HATU (100 mg, 265 μmol), DIEA (187 μL, 1.10 mmol), LiOH (26 mg, 1.10 mmol)]. Purification using preparative HPLC and lyophilization afforded **25d** (60 mg, 98 μmol, 45%) as TFA salt (colorless solid).

¹H-NMR (500 MHz, DMSO): δ = 8.83 (d, ³J = 8.3 Hz, 1H, CONH-), 8.82 (bs, 1H, Py-NH), 7.93 (d, ³J = 6.9 Hz, 1H, Py-H6), 7.89-7.80 (m, 3H, Py-H4, Naph-H), 7.42 (t, ³J = 6.9 Hz, 1H, Naph-H6), 7.32 (d, ³J = 8.3 Hz, 2H, Naph-H), 7.23 (d, ³J = 8.3 Hz, 2H, Tyr-H3,3'+Naph-H), 7.05 (d, ³J = 8.9 Hz, 1H, Py-H3), 6.89 (d, ³J = 8.4 Hz, 2H, Tyr-H2,2'), 6.83 (t, ³J = 6.5 Hz, 1H, Py-H5), 4.82 (m, 1H, -CHCOOH), 4.03 (t, ³J = 5.2 Hz, 2H, CH₂OAr), 3.39 (m, 2H, PyNHCH₂-), 3.19 (dd, ²J = 11.6 Hz, ³J = 3.1 Hz, 1H, ArCH(H')), 2.81 (dd, ²J = 12.6 Hz, ³J = 6.3 Hz, 1H, ArCH(H'')), 2.19 (bs, 3H, Naph-CH₃), 1.84 (m, 2H, -CH₂CH₂OAr), 1.79 (m, 2H, PyNHCH₂CH₂-). ¹³C-NMR (125 MHz, DMSO): δ = 173.0, 168.4, 157.2, 152.8, 142.5, 136.3, 134.4, 131.3, 131.0, 130.1, 129.9, 129.6, 128.2, 127.8, 127.4, 125.9, 125.0, 114.1, 113.1,

IV. Experimental Section

111.7, 66.9, 53.6, 41.2, 35.4, 26.0, 24.6, 18.7. **HPLC** (10-50%, 30 min): $t_R = 26.22$ min. **MS** (ESI): $m/z = 1169.3 [2m+H^+]^+$, $512.6 [m+H^+]^+$.

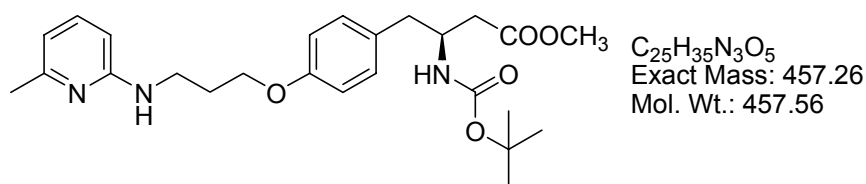
IV.3.76 Preparation of (S)-2-(2,6 dimethyl-4-isopropoxy)-3-[4-(4-(pyridin-2-ylamino)butoxy)phenyl]propanoic acid, **25e**



The title compound was prepared from **24** (120 mg, 220 μ mol) following **GP8b** [**32b** (48 mg, 265 μ mol), HATU (100 mg, 265 μ mol), DIEA (187 μ L, 1.10 mmol), LiOH (26 mg, 1.10 mmol)]. Purification using preparative HPLC and lyophilization afforded **25e** (47 mg, 74 μ mol, 34%) as TFA salt (colorless solid).

1H -NMR (500 MHz, DMSO): $\delta = 13.40$ (bs, 1H), 12.70 (bs, 1H), 8.74 (bs, 1H, Py-NH), 8.44 (d, $^3J = 8.3$ Hz, 1H, -CONHAr), 7.92 (d, $^3J = 6.1$ Hz, 1H, Py-H6), 7.87 (t, $^3J = 7.5$ Hz, 1H, Py-H4), 7.19 (d, $^3J = 8.5$ Hz, 2H, Tyr-H3,3'), 7.04 (d, $^3J = 9.0$ Hz, 1H, Py-H3), 6.84 (d, $^3J = 8.3$ Hz, 2H, Tyr-H2,2'), 6.83 (m, 1H, Py-H5), 6.50 (s, 2H, Ar-H2,2'), 4.60 (m, 1H, Ar-OCH(CH₃)₂), 4.55 (m, 1H, -CHCOOH), 3.98 (t, $^3J = 5.9$ Hz, 2H, -CH₂OAr), 3.37 (m, 2H, PyNHCH₂-), 3.09 (dd, $^2J = 14.0$ Hz, $^3J = 4.0$ Hz, 1H, Ar-CH(H')-), 2.79 (dd, $^2J = 13.8$ Hz, $^3J = 11.4$ Hz, 1H, Ar-CH(H')-), 1.94 (s, 6H, -CH(CH₃)₂), 1.80 (m, 2H, -CH₂CH₂OAr), 1.74 (m, 2H, Py-NHCH₂CH₂-). **^{13}C -NMR** (125 MHz, DMSO): $\delta = 173.1, 169.0, 157.1, 156.7, 152.8, 142.5, 136.3, 135.5, 130.7, 130.0, 129.8, 114.1, 113.8, 113.1, 111.7, 68.7, 66.9, 53.4, 41.2, 35.3, 25.9, 24.5, 21.7, 18.7$. **HPLC** (10-50%, 30 min): $t_R = 16.45$ min; (10-100%, 30 min): $t_R = 28.17$ min. **MS** (ESI): $m/z = 534.7 [m+H^+]^+$.

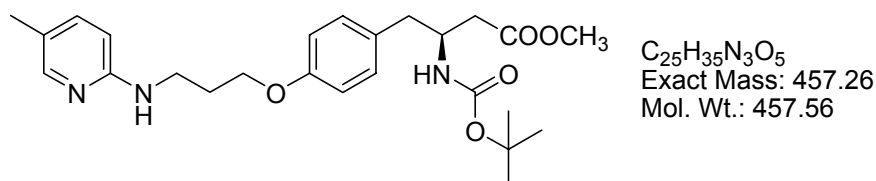
IV.3.77 Preparation of methyl 4-[4-(3-(6-methylpyridin-2-yl)aminopropoxy)phenyl]-3-(S)-(tert.butylloxycarbonylamino)butanoate, 36a



Prepared from **12a** (130 mg, 782 μ mol), Boc- β -Tyr-OMe (**27**) (160 mg, 517 μ mol), tributyl phosphine (190 μ L, 782 μ mol) and ADDP (196 mg, 782 μ mol) according to **GP2**. Column chromatography on silica gel (DCM / ethyl acetate 7 : 3) gave **36a** (160 mg, 350 μ mol, 68%) as a colorless foam.

1 H-NMR (250 MHz, $CDCl_3$): δ = 7.29 (t, 3J = 7.5 Hz, 1H, Py-*H4*), 7.05 (d, 3J = 8.2 Hz, 2H, Tyr-*H3/3'*), 6.79 (d, 3J = 8.2 Hz, 2H, Tyr-*H2/2'*), 6.40 (d, 3J = 7.2 Hz, 1H, Py-*H5*), 6.20 (d, 3J = 8.3 Hz, 1H, Py-*H3*), 5.01 (bs, 1H, NH-Boc), 4.77 (bs, 1H, Py-NH-), 4.08 (m, 1H, -CHNH₂Boc-), 4.01 (t, 3J = 5.9 Hz, 2H, -CH₂OAr-), 3.64 (s, 3H, -COOCH₃), 3.41 (q, 3J = 5.9 Hz, 2H, -NHCH₂-), 2.83 (dd, 2J = 13.4 Hz, 3J = 6.7 Hz, 1H, -CH(*H'*)COOMe), 2.71 (dd, 2J = 13.9 Hz, 3J = 7.3 Hz, 1H, -CH(*H''*)COOMe), 2.43 (m, 2H, Ar-CH₂-), 2.33 (s, 3H, Py-CH₃), 2.07 (m, 2H, -CH₂CH₂CH₂-), 1.39 (s, 9H, *t*Bu).
 13 C-NMR (125 MHz, $CDCl_3$): δ = 171.9, 158.8, 157.7, 156.6, 155.1, 138.0, 130.2, 129.8, 115.4, 114.5, 102.7, 79.2, 65.7, 51.5, 49.0, 39.5, 39.4, 37.5, 29.2, 28.2, 23.9.
HPLC (10-100%, 30 min): t_R = 17.83 min. **MS** (ESI): m/z = 458.3 [$m+H$]⁺, 402.2 [$m+H-t$ Bu]⁺, 358.2 [$m+H$ -Boc]⁺.

IV.3.78 Preparation of methyl 4-[4-(3-(5-methylpyridin-2-yl)aminopropoxy)phenyl]-3-(S)-(tert.butylloxycarbonylamino)butanoate, 36b

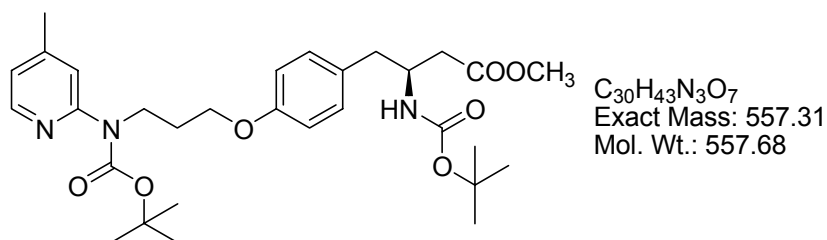


Prepared from **12b** (258 mg, 970 μ mol), Boc- β -Tyr-OMe (**27**) (150 mg, 485 μ mol), tributyl phosphine (239 μ L, 970 μ mol) and ADDP (245 mg, 970 μ mol) according to

GP2. Column chromatography on silica gel (DCM / ethyl acetate 7 : 3) gave **36b** (60 mg, 131 μ mol, 27%) as a colorless foam.

¹H-NMR (500 MHz, CDCl₃): δ = 7.88 (m, 1H, Py-*H*6), 7.24 (m, 1H, Py-*H*4), 7.07 (d, ³*J* = 8.5 Hz, 2H, Tyr-*H*3,3'), 6.82 (d, ³*J* = 8.5 Hz, 2H, Tyr-*H*2,2'), 6.34 (d, ³*J* = 8.4 Hz, 1H, Py-*H*3); 4.98 (bs, 1H, -*NH*), 4.69 (bs, 1H, -*NH*), 4.10 (m, 1H, -*CHNH*Boc-), 4.04 (t, ³*J* = 5.92 Hz, 2H, -*CH*₂OAr), 3.67 (s, 3H, -COOCH₃), 3.46 (q, ³*J* = 6.4 Hz, 2H, -*NHCH*₂-), 2.85 (dd, ²*J* = 13.8 Hz, ³*J* = 6.8 Hz, 1H, -*CH*(*H'*)COOMe), 2.72 (dd, ²*J* = 13.8 Hz, ³*J* = 7.6 Hz, 1H, -*CH*(*H'*)COOMe), 2.45 (m, 2H, ArCH₂-), 2.15 (s, 3H, Py-CH₃), 2.07 (m, 2H, -CH₂CH₂CH₂-); 1.41 (s, 9H, *t*Bu). **¹³C-NMR** (125 MHz, CDCl₃): δ = 172.1, 157.5, 156.5, 155.1, 146.2, 139.0, 130.2, 129.8, 121.4, 114.5, 106.6, 79.2, 65.6, 51.6, 48.9, 39.5, 39.4, 37.4, 29.1, 28.3, 17.2. **HPLC** (10-100%, 30 min): *t*_R = 17.78 min, **MS** (ESI): *m/z* = 458.2 [m+H]⁺, 402.3 [m+H-*t*Bu]⁺, 358.3 [m+H-Boc]⁺.

**IV.3.79 Preparation of methyl 4-[4-(3-*N*-(4-methylpyridin-2-yl)-3-*N*-
(*tert*.butyloxycarbonylamino)propoxy)phenyl]-3-(*S*-
(*tert*.butyloxycarbonylamino) butanoate, **36c****

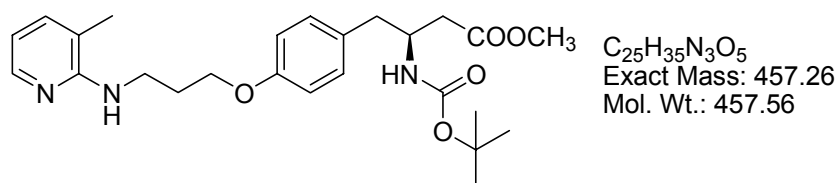


Prepared from **21** (223 mg, 838 μ mol), Boc- β -Tyr-OMe (**27**) (216 mg, 698 μ mol), tributylphosphine (224 μ L, 907 μ mol) and ADDP (229 mg, 970 μ mol) according to **GP2**. Column chromatography on silica gel (hexane / ethyl acetate 2 : 1) gave **36c** (90 mg, 161 μ mol, 23%) as a colorless foam.

¹H-NMR (500 MHz, CDCl₃): δ = 8.17 (d, ³*J* = 4.9 Hz, 1H, Py-*H*6), 7.40 (s, 1H, Py-*H*3), 7.03 (d, ³*J* = 8.1 Hz, 2H, Tyr-*H*3,3'), 6.79 (d, ³*J* = 4.4 Hz, 1H, Py-*H*5), 6.74 (d, ³*J* = 8.2 Hz, 2H, Tyr-*H*2,2'), 5.01 (d, ³*J* = 5.7 Hz, 1H, -*NH*Boc), 4.10 (t, ³*J* = 6.8 Hz, 2H, -*CH*₂O-), 4.08 (m, 1H, -*CHCH*₂COOMe), 3.95 (t, 2H, ³*J* = 6.1 Hz, PyNBoc-*CH*₂-), 3.65 (s, 3H, -COOCH₃), 2.83 (m, 1H, -*CH*(*H'*)COOMe), 2.70 (dd, ²*J* = 13.3 Hz, ³*J* = 7.9 Hz, 1H, -*CH*(*H'*)COOMe), 2.28 (s, 3H, Py-CH₃), 2.46 (dd, ²*J* = 15.6 Hz,

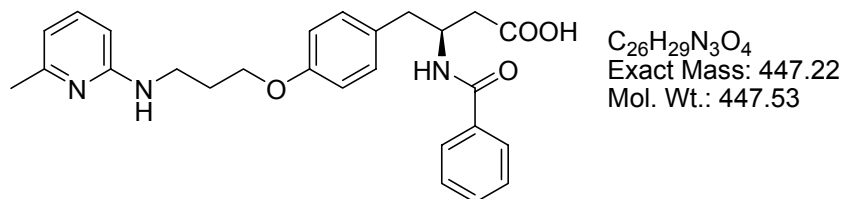
$^3J = 5.2$ Hz, 1H, Ar-CH(H')-), 2.39 (dd, $^2J = 15.7$ Hz, $^3J = 5.5$ Hz, 1H, Ar-CH(H')-), 2.07 (m, 2H, -CH₂CH₂CH₂-), 1.47 (s, 9H, t Bu), 1.37 (s, 9H, t Bu). $^{13}\text{C-NMR}$ (125 MHz, CDCl₃): $\delta = 172.0, 157.7, 155.0, 154.5, 154.1, 148.0, 147.2, 130.0, 129.4, 120.7, 120.4, 114.4, 80.8, 79.2, 65.6, 51.5, 48.8, 40.0, 39.3, 37.3, 28.8, 28.3, 28.2, 21.0$. **HPLC** (10-100%, 30 min): $t_R = 22.17$ min. **MS** (ESI): $m/z = 580.2$ [$m+\text{Na}$]⁺, 558.1 [$m+\text{H}$]⁺, 502.1 [$m+\text{H}-t\text{Bu}$]⁺, 458.3 [$m+\text{H}-\text{Boc}$]⁺, 402.4 [$m+\text{H}-\text{Boc}-t\text{Bu}$]⁺, 358.6 [$m+\text{H}-2\text{Boc}$]⁺.

IV.3.80 Preparation of methyl 4-[4-(3-(3-methylpyridin-2-yl)aminopropoxy)phenyl]-3-(S)-(tert.butylloxycarbonylamino)butanoate, 36d



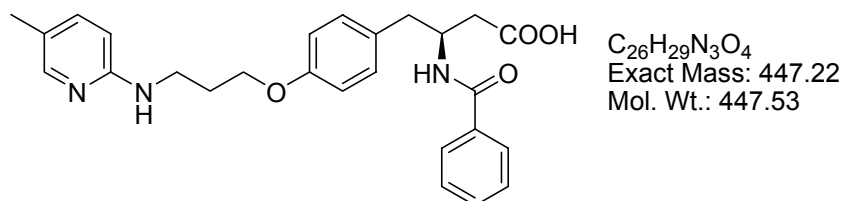
Prepared from **12d** (117 mg, 702 μmol), Boc- β -Tyr-OMe (**27**) (181 mg, 585 μmol), tributyl phosphine (188 μL , 761 μmol) and ADDP (195 mg, 761 μmol) according to **GP2**. Column chromatography on silica gel (DCM / ethyl acetate 7 : 3) gave **36d** (55 mg, 120 μmol , 21%) as a colorless foam.

$^1\text{H-NMR}$ (250 MHz, CDCl₃): $\delta = 7.99$ (d, $J = 5.0$ Hz, 1H, Py- $H6$), 7.19 (d, $J = 7.1$ Hz, 1H, Py- $H4$), 7.08 (d, $J = 8.5$ Hz, 2H, Tyr- $H3/3'$), 6.82 (d, $J = 8.6$ Hz, 2H, Tyr- $H2/2'$), 6.49 (dd, $J = 5.2$ Hz, $J = 7.0$ Hz, 1H, Py- $H5$), 5.04, 5.02 (2 bs, 2H, Py-NH-, -NH Boc), 4.66 (m, 1H, -CHNH Boc -), 4.08 (t, $J = 5.7$ Hz, 2H, ArOCH₂-), 3.67 (s+m, 5H, -COOCH₃ + -NHCH₂-CH₂-), 2.85 (dd, $J = 13.5$ Hz, $J = 6.3$ Hz, 1H, -CH(H')COOMe), 2.72 (dd, $J = 13.6$ Hz, $J = 7.7$ Hz, 1H, -CH(H')COOMe), 2.45 (m, 2H, Ar-CH₂CHNH Boc -), 2.14 (m, 2H, -CH₂CH₂CH₂-), 2.07 (s, 3H, Py-CH₃), 1.40 (s, 9H, t Bu). $^{13}\text{C-NMR}$ (62 MHz, CDCl₃): $\delta = 172.1, 157.5, 156.7, 155.8, 146.1, 136.7, 130.3, 129.9, 116.7, 114.4, 112.9, 79.4, 67.0, 51.7, 39.9, 39.4, 37.5, 29.0, 28.3, 17.0$. **HPLC** (10-100%, 30 min): $t_R = 17.52$ min. **MS** (ESI): $m/z = 480.2$ [$m+\text{Na}$]⁺, 458.2 [$m+\text{H}$]⁺, 402.4 [$m+\text{H}-t\text{Bu}$]⁺, 358.4 [$m+\text{H}-\text{Boc}$]⁺.

IV.3.81 Preparation of 3-(S)-benzamido-4-(4-(3-(6-methylpyridin)-2-ylaminopropoxy)phenyl) butanoic acid, 37a

The title compound was prepared from **36a** (150 mg, 328 μ mol) following **GP8a**. [benzoyl chloride (58 μ L, 495 μ mol), $NaHCO_3$ (124 mg, 1.47 mmol), LiOH (39 mg, 1.64 mmol)] Purification using preparative HPLC and lyophilization afforded **37a** (49 mg, 87 μ mol, 27%) as TFA salt (colorless solid).

1H -NMR (500 MHz, DMSO): δ = 8.73 (bs, 1H, Py-NH), 8.34 (d, 3J = 8.4 Hz, 1H, -CONH-), 7.76 (d+m, 3J = 7.2 Hz, 2+1H, Ph-H2/2'+ Py-H4), 7.50 (t, 1H, 3J = 7.3 Hz, Ph-H4), 7.44 (t, 3J = 7.4 Hz, 2H, Ph-H3/3'), 7.14 (d, 3J = 8.6 Hz, 2H, Tyr-H3/3'), 6.88 (d, 3J = 9.0 Hz, 1H, Py-H3), 6.83 (d, 3J = 8.6 Hz, 2H, Tyr-H2/2'), 6.65 (d, 1H, 3J = 7.2 Hz, Py-H5), 4.44 (m, 1H, -CHNHBOc-), 4.01 (t, 3J = 6.0 Hz, 2H, -CH₂OAr), 3.49 (t, 3J = 6.0 Hz, 2H, Py-NHCH₂-), 2.81 (dd, 3J = 13.6 Hz, 3J = 8.0 Hz, 1H, Ar-CH(H')-), 2.75 (dd, 2J = 13.6 Hz, 3J = 5.9 Hz, 1H, Ar-CH(H')-), 2.52 (dd, 2J = 15.5 Hz, 3J = 7.7 Hz, 1H, -CH(H')COOH), 2.44 (dd, 2J = 15.5 Hz, 3J = 6.2 Hz, 1H, -CH(H')COOH), 2.40 (s, 3H, Py-CH₃), 2.01 (m, 2H, -CH₂CH₂CH₂-). **^{13}C -NMR** (125 MHz, DMSO): δ = 172.4, 165.6, 156.7, 153.3, 147.4, 143.5, 134.6, 130.9, 130.8, 130.0, 128.1, 127.1, 114.1, 111.4, 108.8, 64.6, 48.4, 38.8, 38.7, 28.7, 18.7. **HPLC** (10-50%, 30 min): t_R = 23.04 min. **MS** (ESI): m/z = 448.4 [$m+H$]⁺. **HRMS** (ESI) ($C_{26}H_{30}N_3O_4^+$): Calc.: 448.2231, found: 448.2232.

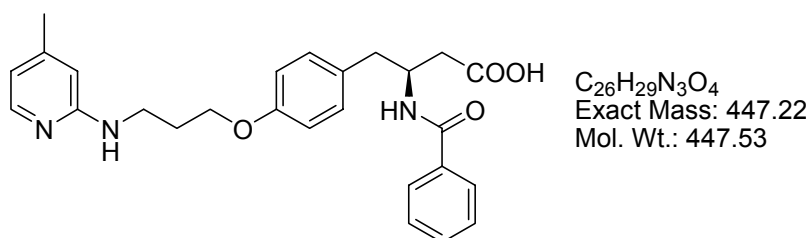
IV.3.82 Preparation of 3-(S)-benzamido-4-(4-(3-(5-methylpyridin)-2-ylaminopropoxy)phenyl) butanoic acid, 37b

The title compound was prepared from **36b** (59 mg, 131 μ mol) following **GP8a**. [benzoyl chloride (23 μ L, 197 μ mol), $NaHCO_3$ (55 mg, 655 μ mol), LiOH (16 mg,

655 mmol)] Purification using preparative HPLC and lyophilization afforded **37b** (35 mg, 62 μ mol, 48%) as TFA salt (colorless solid).

$^1\text{H-NMR}$ (500 MHz, DMSO): δ = 8.67 (bs, 1H, Py-NH), 8.33 (d, 3J = 8.4 Hz, 1H, -NHCOPh), 7.77-7.72 (s, 1H, Py-H6 + d, 2H, Ph-H2,2' + d, 1H, Py-H4), 7.51 (t, 3J = 7.3 Hz, 1H, Ph-H4), 7.44 (t, 3J = 7.4 Hz, 2H, Ph-H3,3'), 7.14 (d, 3J = 8.5 Hz, 2H, Tyr-H3,3'), 6.98 (d, 3J = 9.1 Hz, 1H, Py-H3), 6.84 (d, 3J = 8.5 Hz, 1H, Tyr-H2,2'), 4.43 (m, 1H, -CH(NHCOPh)), 4.02 (t, 3J = 6.0 Hz, 2H, -CH₂OAr), 3.44 (t, 3J = 6.3 Hz, Py-NH-CH₂-), 2.81 (dd, 2J = 13.6 Hz, 3J = 8.0 Hz, 1H, Ar-CH(H')-), 2.75 (dd, 2J = 13.6 Hz, 3J = 5.9 Hz, 1H, Ar-CH(H')-), 2.52 (dd, 2J = 15.7 Hz, 3J = 7.7 Hz, 1H, -CH(H')COOH), 2.44 (dd, 2J = 15.4 Hz, 3J = 6.2 Hz, -CH(H')COOH), 2.16 (s, 3H, Py-CH₃), 2.01 (m, 2H, -CH₂CH₂CH₂-). **$^{13}\text{C-NMR}$** (125 MHz, DMSO): δ = 172.4, 165.6, 156.7, 151.2, 144.8, 134.6, 133.3, 131.0, 130.8, 128.1, 127.1, 121.2, 114.1, 113.0, 65.5, 49.3, 39.8, 39.7, 39.6, 28.6, 17.2. **HPLC** (10-50%, 30 min): t_R = 23.08 min. **MS** (ESI): m/z = 448.4 [m+H]⁺. **HRMS** (ESI) (C₂₆H₃₀N₃O₄⁺): Calc.: 448.2231, found: 448.2228.

IV.3.83 Preparation of 3-(S)-benzamido-4-(4-(3-(4-methylpyridin)-2-ylaminopropoxy)phenyl) butanoic acid, **37c**

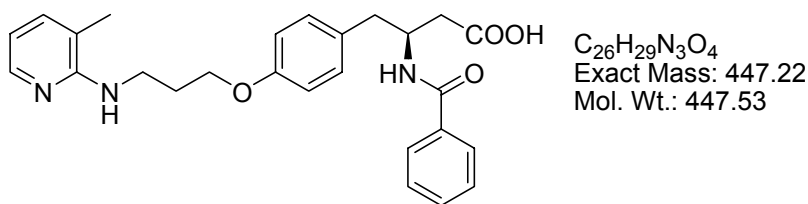


The title compound was prepared from **36c** (90 mg, 161 μ mol) following **GP8a**. [benzoyl chloride (19 μ L, 161 μ mol), NaHCO₃ (68 mg, 805 μ mol), LiOH (20 mg, 805 mmol)] Purification using preparative HPLC and lyophilization afforded **37c** (17 mg, 30 μ mol, 19%) as TFA salt (colorless solid).

$^1\text{H-NMR}$ (500 MHz, DMSO): δ = 13.44 (bs, 1H), 12.22 (bs, 1H), 8.71 (bs, 1H, Py-NH), 8.34 (d, 3J = 8.4 Hz, -NHCOPh), 7.82 (d, 3J = 6.5 Hz, 1H, Py-H6), 7.77 (d, 3J = 7.4 Hz, 2H, Ph-H2,2'), 7.51 (t, 3J = 7.3 Hz, 1H, Ph-H4), 7.44 (t, 3J = 7.5 Hz, 2H,

Ph-*H*3,3'), 7.15 (d, $^3J = 8.5$ Hz, 2H, Tyr-*H*3,3'), 6.85 (s, 1H, Py-*H*3), 6.84 (d, $^3J = 8.4$ Hz, 2H, Tyr-*H*2,2'), 6.69 (d, $^3J = 6.8$ Hz, 1H, Py-*H*5), 4.44 (m, 1H, -CHCH₂COOH), 4.01 (t, $^3J = 5.9$ Hz, 2H, -CH₂OAr), 3.45 (m, 2H, PyNHCH₂-), 2.82 (dd, $^2J = 13.6$ Hz, $^3J = 8.1$ Hz, 1H, -CH(*H'*)COOH), 2.76 (dd, $^2J = 13.6$ Hz, $^3J = 5.8$ Hz, 1H, -CH(*H'*)COOH), 2.53 (dd, $^2J = 15.8$ Hz, $^3J = 8.0$ Hz, 1H, ArCH(*H'*)-,), 2.44 (dd, $^2J = 15.4$ Hz, $^3J = 6.1$ Hz, 1H, ArCH(*H'*)-,), 2.30 (s, 3H, Py-CH₃), 2.01 (m, 2H, -CH₂CH₂CH₂-). **¹³C-NMR** (125 MHz, DMSO): $\delta = 172.4, 165.5, 156.7, 155.1, 152.4, 135.3, 134.6, 130.9, 130.8, 130.0, 128.0, 127.1, 114.1, 113.8, 111.2, 64.5, 48.3, 38.8, 38.7, 38.4, 27.7, 21.3$. **HPLC** (10-50%, 30 min): $t_R = 23.36$ min. **MS** (ESI): $m/z = 448.6$ [m+H]⁺. HR-ESI (C₂₆H₃₀N₃O₄⁺): Calc.: 448.2231, found: 448.2230.

IV.3.84 Preparation of 3-(*S*)-benzamido-4-(4-(3-(3-methylpyridin)-2-ylaminopropoxy)phenyl) butanoic acid, 37d

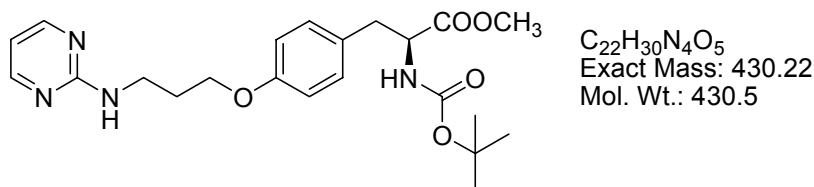


The title compound was prepared from **36d** (55 mg, 120 μ mol) following **GP8a**. [benzoyl chloride (17 μ L, 144 μ mol), NaHCO₃ (36 mg, 432 μ mol), LiOH (17 mg, 432 mmol)] Purification using preparative HPLC and lyophilization afforded **37d** (24 mg, 42 μ mol, 36%) as TFA salt (colorless solid).

¹H-NMR (500 MHz, DMSO): $\delta = 13.32$ (bs, 1H), 12.25 (bs, 1H), 8.32 (d, $^3J = 8.3$ Hz, 1H, -NHCOPh), 8.03 (bs, 1H, Py-NH), 7.80 (d, $^3J = 6.2$ Hz, 1H, Py-*H*6), 7.76 (d, $^3J = 7.4$ Hz, 2H, Ph-*H*2,2'), 7.74 (d, $^3J = 7.2$ Hz, 1H, Py-*H*4), 7.50 (t, $^3J = 7.2$ Hz, 1H, Ph-*H*4), 7.44 (t, $^3J = 7.5$ Hz, 2H, Ph-*H*3,3'), 7.14 (d, $^3J = 8.3$ Hz, 2H, Tyr-*H*3,3'), 6.81 (d, $^3J = 8.7$ Hz, 2H, Tyr-*H*2,2'), 6.80 (m, 1H, Py-*H*5), 4.43 (m, 1H, -CHCH₂COOH), 4.03 (t, $^3J = 5.8$ Hz, 2H, -CH₂OAr), 3.56 (m, 2H, Py-NHCH₂-), 2.81 (dd, $^2J = 13.5$ Hz, $^3J = 8.1$ Hz, 1H, -CH(*H'*)COOH), 2.75 (dd, $^2J = 13.6$ Hz, $^3J = 5.8$ Hz, 1H, -CH(*H'*)COOH), 2.52 (dd, $^2J = 15.8$ Hz, $^3J = 7.7$ Hz, 1H, Ar-CH(*H'*)-,), 2.43 (dd, $^2J = 15.4$ Hz, $^3J = 6.1$ Hz, 1H, Ar-CH(*H'*)-,), 2.17 (s, 3H, Py-(CH₃)), 2.05 (m, 1H, -CH₂CH₂CH₂-). **¹³C-NMR** (125 MHz, DMSO): $\delta = 172.4, 165.5, 156.7, 151.6, 141.1, 134.6, 133.5, 130.9, 130.7, 130.0, 128.1, 127.0, 122.6, 114.0, 111.8, 64.8, 48.3, 38.9,$

38.8, 38.7, 27.5, 16.6. **HPLC** (10-100%, 30 min): $t_R = 22.26$ min. **MS** (ESI): $m/z = 448.4$ $[m+H]^+$. **HRMS** (ESI) ($C_{26}H_{30}N_3O_4^+$): Calc.: 448.2231, found: 448.2227.

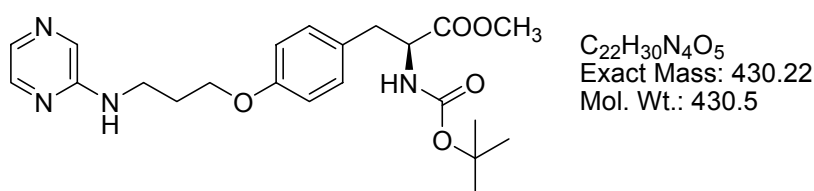
IV.3.85 Preparation of methyl (S)-2-(tert.butylloxycarbonyl)-3-[4-(3-(pyrimidin-2-ylamino)propoxy)phenyl]propanoate, **38**



Prepared from **7** (611 mg, 3.99 mmol, 1.1 eq.), Boc-Tyr-OMe (1.07 g, 3.63 mmol, 1 eq.), tributylphosphine (1.17 mL, 4.72 mmol, 1.3 eq.) and ADDP (1.19 g, 4.72 mmol, 1.3 eq.) according to **GP2**. Purification by flash chromatography on silica gel (DCM / ethyl acetate 2 : 1) afforded **38** (1.39 g, 3.23 mmol, 89%) as colorless solid.

1H -NMR (250 MHz, $CDCl_3$): $\delta = 8.24$ (d, $^3J = 4.8$ Hz, 2H, Py-*H4,6*), 7.00 (d, $^3J = 8.6$ Hz, 2H, Tyr-*H3,3'*), 6.80 (d, $^3J = 8.6$ Hz, 2H, Tyr-*H2,2'*), 6.49 (t, $^3J = 4.8$ Hz, 1H, Py-*H3*), 5.59 (t, $^3J = 5.1$ Hz, 1H, Py-NH), 5.04 (d, $^3J = 8.1$ Hz, 1H, -NH_{Boc}), 4.52 (m, 1H, -CHNH_{Boc}), 4.03 (t, $^3J = 6.0$ Hz, 2H, -CH₂-OAr), 3.69 (s, 3H, -COOCH₃), 3.60 (q, $^3J = 6.5$ Hz, 2H, -NHCH₂-CH₂-), 2.08 (m, 2H, -CH₂CH₂CH₂-), 1.40 (s, 9H, -^tBu). **^{13}C -NMR** (125 MHz, $CDCl_3$): $\delta = 172.4, 162.4, 157.9, 155.1, 130.0, 128.0, 114.5, 140.4, 79.8, 65.8, 54.5, 52.1, 38.7, 37.4, 29.1, 28.3$. **HPLC** (10-100%, 30 min): $t_R = 17.20$ min. **MS** (ESI): $m/z = 453.3$ $[m+Na]^+$, 431.2 $[m+H]^+$, 375.4 $[m+H^+{}^tBu]^+$, 331.6 $[m+H^+{}Boc]^+$.

IV.3.86 Preparation of methyl (S)-2-(tert.butylloxycarbonyl)-3-[4-(3-(pyridazin-2-ylamino)propoxy)phenyl]propanoate, **39**

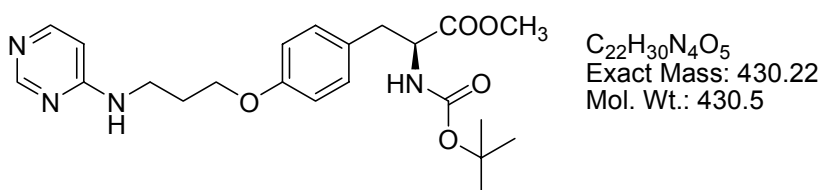


Prepared from **8** (611 mg, 3.99 mmol, 1.1 eq.), Boc-Tyr-OMe (1.07 g, 3.63 mmol, 1 eq.), tributylphosphine (1.17 mL, 4.72 mmol, 1.3 eq.) and ADDP (1.19 g,

4.72 mmol, 1.3 eq.) according to **GP2**. Purification by flash chromatography on silica gel (DCM / ethyl acetate 2:1) afforded **39** (1.34 g, 3.21 mmol, 86%) as colorless solid.

¹H-NMR (500 MHz, CDCl₃): δ = 7.96 (m, 1H, Py-*H*6), 7.89 (s, 1H, Py-*H*3), 7.78 (d, ³*J* = 3.1 Hz, 1H, Py-*H*5), 7.03 (d, ³*J* = 8.4 Hz, 2H, Tyr-*H*3,3'), 6.82 (d, ³*J* = 8.4 Hz, 2H, Tyr-*H*2,2'), 4.97-4.95 (m, 2H, PyNH-, -NH*Boc*), 4.53 (m, 1H, -CHCOOMe), 4.07 (t, ³*J* = 5.7 Hz, 2H, -CH₂OAr), 3.71 (s, 3H, -COOCH₃), 3.56 (m, 2H, -Py-NHCH₂-), 3.04 (dd, ²*J* = 13.8 Hz, ³*J* = 5.0 Hz, 1H, Ar-CH(*H'*)-), 3.00 (dd, ²*J* = 13.4 Hz, ³*J* = 5.4 Hz, 1H, Ar-CH(*H''*)-), 2.11 (m, 2H, -CH₂CH₂CH₂-), 1.41 (s, 9H, NHCOO^tBu). **¹³C-NMR** (125 MHz, CDCl₃): δ = 172.3, 157.6, 155.0, 154.6, 141.7, 132.3, 132.1, 130.2, 128.1, 114.4, 79.7, 65.7, 54.5, 52.0, 38.7, 37.3, 28.7, 28.1. **HPLC** (10-100%, 30 min): *t*_R = 17.71 min. **MS** (ESI): 453.3 [m+Na⁺]⁺, 431.2 [m+H⁺]⁺, 375.3 [m+H⁺-^tBu]⁺, 331.5 [m+H⁺-Boc]⁺.

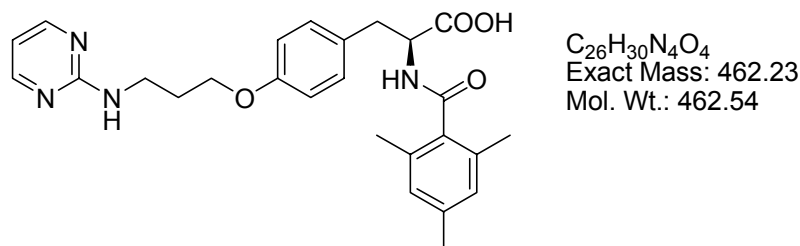
IV.3.87 Preparation of methyl (*S*)-2-(tert.butyloxycarbonyl)-3-[4-(3-(pyrimidin-6-ylamino)propoxy)phenyl]propanoate, **40**



Prepared from **9** (0.39 g, 2.35 mmol, 1.0 eq.), Boc-Tyr-OMe (0.69 g, 2.35 mmol, 1 eq.), tributyl phosphine (0.22 mL, 3.06 mmol, 1.3 eq.) and ADDP (0.22 g, 3.06 mmol, 1.3 eq.) according to **GP2**. Purification by flash chromatography on silica gel (DCM / methanol 95 : 5) afforded **40** (0.66 g, 1.55 mmol, 66%) as colorless solid.

¹H-NMR (360 MHz, CDCl₃): δ = 9.40 (s, 1H, Py-*H*2), 8.74 (m, 1H, Py-*H*4), 8.20 (m, 1H, Py-*H*3), 7.32 (d, 1H, ³*J* = 8.0 Hz, Tyr-*H*3,3'), 7.32 (d, ³*J* = 8.4 Hz, 2H, Tyr-*H*2,2'), 6.82 (bs, 1H, Py-NH), 4.18 (m, 1H, -CHCOOMe), 4.10 (t, ³*J* = 6.1 Hz, -CH₂OAr), 3.68 (s, 3H, -COOCH₃), 2.59 (m, 2H, Ar-CH₂), 2.19 (m, 2H, -CH₂CH₂CH₂-). **¹³C-NMR** (90.6 MHz, CDCl₃): δ = 162.9, 161.2, 155.2, 151.4, 140.9, 130.3, 114.5, 106.7, 106.7, 80.0, 67.1, 65.4, 52.2, 37.5, 29.7, 28.3. **HPLC** (10-50%, 30 min): *t*_R = 16.37 min. **MS** (ESI): *m/z* = 431.3 [m+H⁺]⁺. **HR-MS** (ESI) (C₂₆H₃₁N₄O₄)⁺: Calc.: 463.2340, Found: 463.2336.

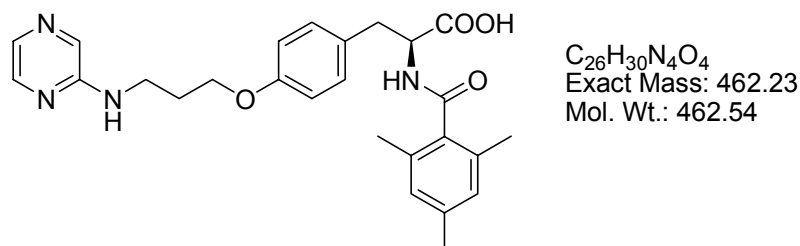
IV.3.88 Preparation of (S)-2-(2,4,6-trimethylbenzamido)-3-[4-(3-(pyrimidin-2-ylamino)propoxy)phenyl]propanoic acid, 41.



The title compound was prepared from **38** (260 mg, 604 μ mol) following **GP8b** [2,4,6-trimethylbenzoic acid (118 mg, 725 μ mol), HATU (276 mg, 725 μ mol), DIEA (514 μ L, 3.02 mmol), LiOH (73 mg, 3.02 mmol)]. Purification using preparative HPLC and lyophilization afforded **41** (62 mg, 108 μ mol, 18%) as TFA salt (colorless solid).

1 H-NMR (500 MHz, DMSO): δ = 8.47 (d, 3J = 8.4 Hz, 1H, -NHCOAr), 8.40 (d, 3J = 4.2 Hz, 2H, Py-H4,6), 7.89 (bs, 1H, Py-NH), 7.19 (d, 3J = 8.4 Hz, 2H, Tyr-H3,3'), 6.84 (d, 3J = 8.4 Hz, 2H, Tyr-H2,2'), 6.74 (s, 2H, Ar-H3,3'), 6.71 (t, 3J = 4.9 Hz, 1H, Py-H5), 4.62 (m, 1H, -CHCOOH), 4.01 (t, 3J = 6.3 Hz, 2H, -CH₂OAr), 3.47 (t, 3J = 6.9 Hz, 2H, PyNHCH₂-), 3.10 (dd, 2J = 14.0 Hz, 3J = 4.0 Hz, 1H, ArCH(H')-), 2.79 (dd, 2J = 13.8 Hz, 3J = 11.5 Hz, 1H, ArCH(H')-), 2.19 (s, 3H, Ar(CH₃)), 1.99 (m, 2H, -CH₂CH₂CH₂-), 1.94 (s, 6H, Ar(CH₃)₂). **13 C-NMR** (125 MHz, DMSO): δ = 173.1, 169.2, 159.4, 157.5, 157.1, 136.9, 135.3, 133.7, 130.0, 129.8, 127.4, 114.2, 109.7, 65.3, 53.4, 37.9, 35.4, 28.3, 20.5, 18.4. **HPLC** (10-100%, 30 min): t_R = 15.48 min. **MS** (ESI): m/z = 1399.4 [3m+H]⁺, 933.4 [2m+H]⁺, 467.6 [m+H]⁺. **HR-MS** (ESI) ($C_{26}H_{31}N_4O_4^+$) Calc.: 463.2340, found: 467.2335.

IV.3.89 Preparation of (S)-2-(2,4,6-trimethylbenzamido)-3-[4-(3-(pyrimidin-2-ylamino)propoxy)phenyl]propanoic acid, 42



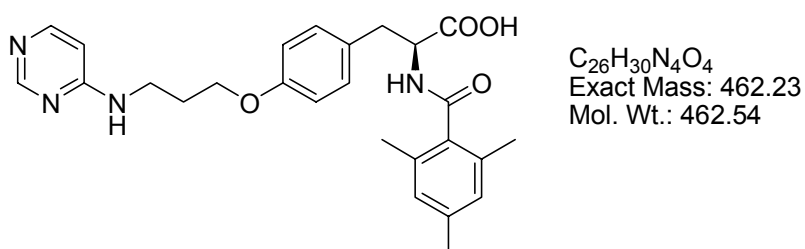
The title compound was prepared from **39** (256 mg, 594 μ mol) following **GP8b** [2,4,6-trimethylbenzoic acid (117 mg, 714 μ mol), HATU (271 mg, 714 μ mol), DIEA

IV. Experimental Section

(506 μL , 2.98 mmol), LiOH (72 mg, 2.98 mmol)]. Purification using preparative HPLC and lyophilization afforded **42** (59 mg, 102 μmol , 17%) as TFA salt (yellow solid).

$^1\text{H-NMR}$ (500 MHz, DMSO): δ = 8.46 (d, 3J = 8.3 Hz, 1H, -NHCOAr), 8.00 (s, 1H, Py-H3), 7.95 (d, 3J = 1.6 Hz, 1H, Py-H6), 7.67 (d, 3J = 2.8 Hz, 1H, Py-H5), 7.20 (d, 3J = 8.4 Hz, 1H, Tyr-H3,3'), 6.85 (d, 3J = 8.5 Hz, 1H, Tyr-H2,2'), 6.75 (s, 2H, Ar-H3,3'), 4.63 (m, 1H, -CHCOOH), 4.03 (t, 3J = 6.2 Hz, 1H, -CH₂OAr), 3.42 (t, 3J = 6.8 Hz, 1H, -NHCH₂-), 3.10 (dd, 2J = 13.9 Hz, 3J = 4.0 Hz, 1H, ArCH(H')-), 2.80 (dd, 2J = 13.8, 3J = 11.4 Hz, 1H, ArCH(H')), 2.19 (s, 3H, Ar-CH₃), 1.99 (m, 2H, -CH₂CH₂CH₂-), 1.94 (s, 6H, Ar-(CH₃)₂). **$^{13}\text{C-NMR}$** (125 MHz, DMSO): δ = 173.1, 169.2, 157.1, 154.3, 140.4, 136.9, 135.3, 133.7, 133.5, 130.0, 129.8, 127.4, 114.2, 65.2, 53.4, 37.2, 35.4, 28.2, 20.5, 18.4. **HPLC** (10-50%, 30 min): t_{R} = 20.08 min. **MS** (ESI): m/z = 1399.4 [3m+H⁺]⁺, 933.4 [2m+H⁺]⁺, 467.6 [m+H⁺]⁺. **HR-MS** (ESI) (C₂₆H₃₁N₄O₄⁺).

IV.3.90 Preparation of (S)-2-(2,4,6-trimethylbenzamido)-3-[4-(3-(pyrimidin-6-ylamino)propoxy)phenyl]propionic acid, **43**

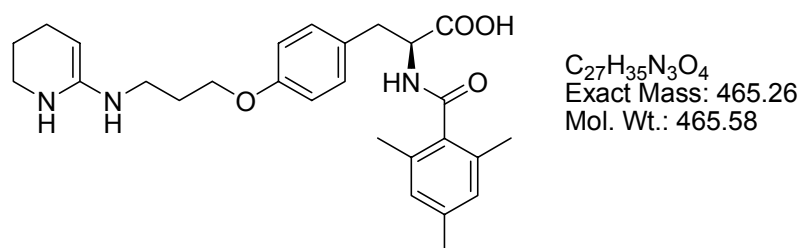


The title compound was prepared from **40** (150 mg, 348 μmol) following **GP8b** [2,4,6-trimethylbenzoic acid (180 mg, 1.08 μmol), HATU (410 mg, 1.08 μmol), DIEA (830 μL , 4.90 mmol), LiOH (115 mg, 4.8 mmol)]. Purification using preparative HPLC and lyophilization afforded **43** (21 mg, 36 μmol , 10%) as TFA salt (colorless solid).

$^1\text{H-NMR}$ (500 MHz, DMSO): δ = 12.70 (bs, 1H), 9.43 (bs, 1H, Py-NH), 8.78 (s, 1H, Py-H6), 8.47 (d, 3J = 8.2 Hz, 1H, -NHCOAr), 7.20 (d, 3J = 8.2 Hz, 2H, Tyr-H3,3'), 6.84 (d, 3J = 8.2 Hz, 2H, Tyr-H2,2'), 6.76 (m, 3H, Ar-H3,3', Py-H3), 4.62 (m, 1H, -CHCOOH), 4.02 (t, 3J = 5.5 Hz, 2H, -CH₂OAr), 3.62 (m, 2H, PyNH-CH₂-), 3.09 (dd, 2J = 13.9 Hz, 3J = 3.5 Hz, 1H, Ar-CH(H')-), 2.79 (dd, 2J = 13.3 Hz, 3J = 11.9 Hz, 1H, Ar-CH(H')-), 2.19 (s, 3H, Ar(CH₃)), 2.01 (m, 2H, -CH₂CH₂CH₂-), 1.93 (s, 6H,

Ar(CH₃)₂). ¹³C-NMR (125 MHz, DMSO): δ = 173.1, 169.1, 162.2, 156.9, 152.6, 142.3, 136.9, 135.3, 133.7, 130.0, 127.3, 114.1, 106.0, 64.9, 53.4, 39.4, 37.8, 35.4, 27.8, 20.5, 18.4. **HPLC** (10-50%, 30 min): t_R = 24.42 min. **MS** (ESI): m/z = 463.3 [M+H]⁺, 147.1 [COC₆H₂(CH₃)₃]⁺. **HR-MS** (ESI) (C₂₆H₃₁N₄O₄⁺) Calc.: 463.2340, found: 463.2336.

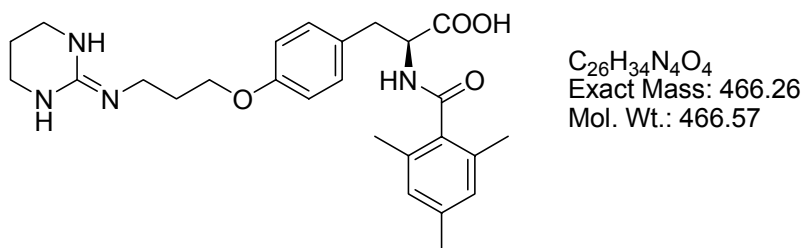
IV.3.91 Preparation of (S)-2-(2,4,6-trimethylbenzamido)-3-(4-(3-(1,4,5,6-tetrahydropyridin-2-ylamino)propoxy)phenyl)propanoic acid **44**



Compound **23e** (TFA salt, 31 mg, 54 μmol) was dissolved in 4 mL of methanol. After addition of 0.1 mL of acetic acid and 10 mg Pd on carbon, the resulting mixture was hydrogenated in an autoclave at 30 bar for 1 h. The mixture was filtered, concentrated and purified by preparative HPLC to give **43** (27 mg, 62 μmol, 86 %) as TFA salt (colorless solid).

¹H-NMR (500 MHz, DMSO): δ = 9.16 (bs, 1H, -NH), 9.13 (bs, 1H, -NH), 8.47 (d, ³J = 8.3 Hz, -NHCO-), 7.21 (d, ³J = 8.6 Hz, 2H, Tyr-H3,3'), 6.85 (d, ³J = 8.6 Hz, 2H, Tyr-H2,2'), 6.77 (s, 2H, Ar-H3,3'), 4.61 (m, 1H, -CHCOOH), 4.01 (m, 2H, -CH₂OAr), 3.03 (m, 3H, -CH₂CH₂CH₂O, NC=CH), 3.10 (dd, ²J = 13.9 Hz, ³J = 4.1 Hz, 1H, Ar-CH(H')), 2.80 (dd, ²J = 13.9 Hz, ³J = 11.3 Hz, 1H, Ar-H(H')), 2.54 (t, ³J = 5.8 Hz, 2H, ^{cy}CH₂N), 2.20 (s, 3H, Ar-CH₃), 1.98 (m, 2H, -CH₂CH₂CH₂O), 1.95 (s, 6H, Ar-(CH₃)₂), 1.71 (m, 4H, N-C=CHCH₂CH₂-). ¹³C-NMR (125 MHz, DMSO): δ = 173.1, 169.1, 162.7, 156.8, 136.9, 135.7, 133.7, 130.1, 130.0, 127.3, 114.1, 64.6, 53.4, 41.0, 38.1, 35.4, 26.9, 25.8, 20.5, 20.4, 18.4, 17.6. **HPLC** (10-100%, 30 min): t_R = 15.22 min. **MS** (ESI): m/z = 1419.2 [3m+Na]⁺, 1396.1 [3m+H]⁺, 953.2 [2m+Na]⁺, 931.1 [2m+H]⁺, 466.3 [m+H]⁺.

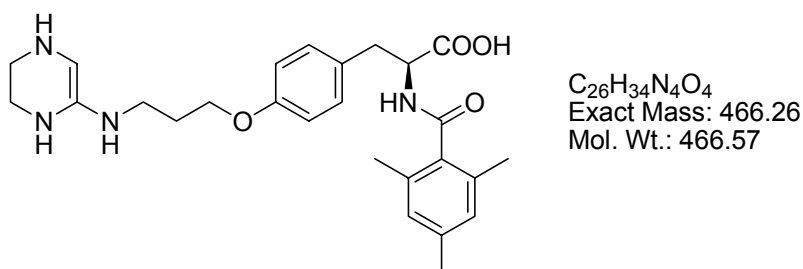
IV.3.92 Preparation of (S)-2-(2,4,6-trimethylbenzamido)-3-(4-(3-(tetrahydropyrimidin-2(1H)-ylideneamino)propoxy)phenyl)propanoic acid, 45



Compound **41** (TFA salt, 43 mg, 75 μ mol) was dissolved in 4 mL of methanol. After addition of 0.1 mL of acetic acid and 10 mg Pd on carbon, the resulting mixture was hydrogenated in an autoclave at 30 bar for 1 h. The mixture was filtered, concentrated and purified by preparative HPLC to give **45** (36 mg, 62 μ mol, 83 %) as TFA salt (colorless solid).

1H -NMR (500 MHz, DMSO): δ = 12.68 (bs, 1H), 8.48 (d, 3J = 8.8 Hz, 1H, -NHCOAr), 7.71 (bs, 2H, N=C-NH-), 7.21 (d, 3J = 8.4 Hz, 2H, Tyr-H3,3'), 6.85 (d, 3J = 8.1 Hz, 2H, Tyr-H2,2'), 6.77 (s, 2H, Ar-H3,3'), 4.61 (m, 1H, -CHCOOH), 3.97 (m, 2H, -CH₂OAr), 3.24 (m, 4H, CH₂(CH₂N-)₂), 3.23 (m, 2H, =N-CH₂-), 3.09 (dd, 2J = 13.8 Hz, 3J = 3.1 Hz, 1H, Ar-CH(H')-), 2.79 (dd, 2J = 13.8 Hz, 3J = 11.5 Hz), 2.20 (s, 3H, Ar-CH₃), 1.94 (s, 6H, Ar-(CH₃)₂), 1.91 (m, 2H, -CH₂CH₂CH₂OAr), 1.79 (m, 2H, -NHCH₂CH₂CH₂NH-). **^{13}C -NMR** (125 MHz, DMSO): δ = 173.1, 169.1, 156.9, 152.6, 136.9, 135.3, 133.7, 130.0, 127.3, 114.1, 64.7, 53.4, 38.0, 37.4, 35.4, 28.1, 20.5, 19.6, 18.4. **HPLC** (10-100%, 30 min): t_R = 16.18 min. HPLC (10-50%, 30 min): t_R = 24.72 min. **MS** (ESI): m/z = 467.6 [M+H]⁺. **HR-MS** (ESI) (C₂₆H₃₅N₄O₄⁺) Calc.: 467.2653, found: 467.2649.

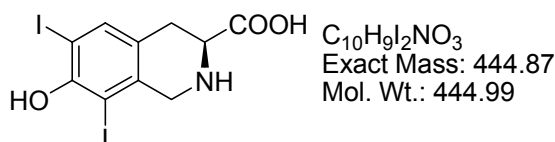
IV.3.93 Preparation of (S)-2-(2,4,6-trimethylbenzamido)-3-(4-(3-(1,4,5,6-tetrahydropyrazin-2-ylamino)propoxy)phenyl)propanoic acid 46



Compound **42** (TFA salt, 40 mg, 70 μmol) was dissolved in 4 mL of methanol. After addition of 0.1 mL of acetic acid and 10 mg Pd on carbon, the resulting mixture was hydrogenated in an autoclave at 30 bar for 1 h. The mixture was filtered, concentrated and purified by preparative HPLC to give **46** (37 mg, 64 μmol , 91 %) as TFA salt (colorless solid).

$^1\text{H-NMR}$ (500 MHz, DMSO): δ = 9.92 (bs, 1H, =C-NH), 9.83 (bs, 1H, =C-NH), 9.74 (bs, 1H, =C-NH), 8.49 (d, 3J = 8.2 Hz, 1H, -NHCOMes), 7.22 (d, 3J = 8.3 Hz, 2H, Tyr-H3,3'), 6.86 (d, 3J = 8.3 Hz, 2H, Tyr-H2,2'), 6.77 (s, 2H, Ar-H3,3'), 4.61 (m, 1H, NHCH-COOH), 4.09 (m, 2H), 4.01 (m, 2H, -CH₂OAr), 3.51 (m, 2H), 3.38 (m, 2H), 3.33 (m, 2H), 3.09 (dd, 2J = 13.9 Hz, 3J = 3.5 Hz, 1H, Ar-CH(H')-), 2.80 (dd, 2J = 13.4 Hz, 3J = 11.7 Hz, 1H, Ar-CH(H'')-), 2.20 (s, 3H, Ar-CH₃), 2.00 (m, 2H, -CH₂CH₂CH₂-), 1.95 (s, 6H, Ar-(CH₃)₂). **$^{13}\text{C-NMR}$** (125 MHz, DMSO): δ = 173.1, 169.1, 157.6, 156.8, 136.9, 135.3, 133.7, 130.1, 130.0, 127.4, 114.1, 64.4, 53.4, 41.2, 38.5, 38.0, 35.4, 26.8, 20.5, 18.4. **HPLC** (10-50%, 30 min): t_R = 20.08 min. **MS** (ESI): m/z = 1399.4 [3m+H]⁺, 933.4 [2m+H]⁺, 467.6 [m+H]⁺. **HR-MS** (C₂₆H₃₅N₄O₄⁺) Calc.: 467.2653, found: 467.2649.

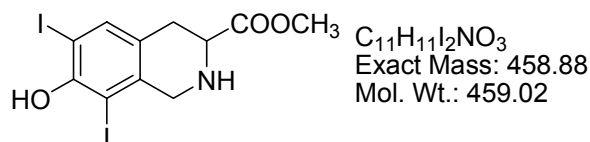
IV.3.94 Preparation of (S)-1,2,3,4-tetrahydro-7-hydroxy-6,8-diiodoisoquinoline-3-carboxylic acid, **47**



Ortho-diiodotyrosine (20 g, 42.6 mmol, 1 eq.) was dissolved in a mixture of conc. hydrochloric acid (200 mL) and DME (13 mL). 15 mL of a 35% aqueous solution of formalin was added and the resulting suspension was stirred at 75°C for 30 min. After an additional 100 mL of hydrochloric acid, 8 mL of DME and 8 mL of formalin, heating and stirring was continued for additional 18 h. The mixture was cooled down with an ice bath and filtered. The residue was washed twice with cold DME and dried under reduced pressure. The yield was 10.3 g (21.4 mmol, 50%) of **47** as hydrochloride (light brown solid).

¹H-NMR (500 MHz, DMSO): δ = 14.08 (bs, 1H, -COOH), 10.23 (bs, 2H, -NH), 9.66 (s, 1H, -OH), 7.71 (s, 1H, Ar-H5), 4.31 (dd, 3J = 11.1 Hz, 3J = 4.9 Hz, 1H, -CHCOOH), 4.10 (d, 2J = 16.1 Hz, 1H, Ar-CH(H')N-), 4.01 (d, 2J = 16.4 Hz, 1H, Ar-CH(H')N-), 3.21 (dd, 2J = 16.8 Hz, 3J = 4.6 Hz, 1H, Ar-CH(H')CH), 3.09 (dd, 2J = 16.8 Hz, 3J = 11.1 Hz, 1H, Ar-CH(H')CH). **¹³C-NMR** (125 MHz, DMSO): δ = 169.4, 154.3, 138.7, 132.0, 127.0, 90.8, 86.1, 52.4, 50.0, 27.0. **HPLC** (10-100%, 30 min): t_R = 10.97 min. **MS** (ESI): m/z = 890.4 [$2m+H^+$]⁺, 445.9 [$m+H^+$]⁺, 400.0 [$m+H^+-COOH$].

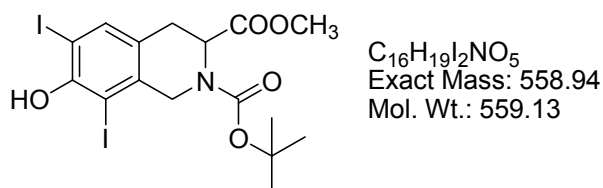
IV.3.95 Preparation of methyl (S)-1,2,3,4-tetrahydro-7-hydroxy-6,8-diiodoisoquinoline-3-carboxylate, 48



The title compound was synthesized from **47** (10.0 g, 22.5 mmol, 1 eq.) according to **GP11**. Yield was 7.1 g (15.3 mmol, 69%) of an orange solid.

¹H-NMR (500 MHz, DMSO): δ = 7.55 (s, 1H, Ar-H5), 3.83 (d, 2J = 16.8 Hz, 1H, Ar-CH(H')N), 3.72 (dd, 3J = 9.3 Hz, 3J = 4.6 Hz, 1H, CHCOOMe), 3.68 (s, 3H, -COOCH₃), 3.68-3.64 (m, 1H, Ar-CH(H')N), 2.89 (dd, 2J = 16.0 Hz, 3J = 4.5 Hz, 1H, Ar-CH(H')CH), 2.78 (dd, 2J = 15.9 Hz, 3J = 9.5 Hz, 1H, Ar-CH(H')CH). **¹³C-NMR** (125 MHz, DMSO): δ = 172.2, 153.2, 138.6, 137.7, 129.2, 91.4, 84.2, 53.5, 53.0, 51.8, 29.3. **HPLC** (10-100%, 30 min): t_R = 11.89 min. **MS** (ESI): m/z = 459.9 [$m+H^+$]⁺, 400.0 [$m+H^+-COOCH_3$]⁺.

IV.3.96 Preparation of methyl 1-(tert.butylloxycarbonyl)-2-(S)-1,2,3,4-tetrahydro-7-hydroxy-6,8-diiodoisoquinoline-3-carboxylate, 49



The title compound was synthesized from **48** (6.0 g, 13.07 mmol, 1 eq.), Boc-anhydride (3.1 g, 14.38 mmol, 1.1 eq.) and triethylamine (2.36 mL, 16.99 mmol,

1.3 eq.) according to **GP6b**. Purification by column chromatography on silica gel (hexane / ethyl acetate 2 : 1) gave 6.9 g (12.3 mmol, 94%) of a yellow foam.

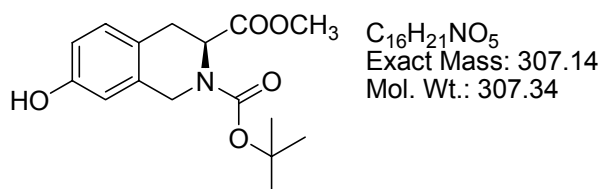
¹H-NMR (250 MHz, CDCl₃): δ = 7.49 (s, 1H, TIC-*H5*), 5.83 (bs, 1H, Ar-*OH*), 5.13 (m, 1H**, CHCOOCH₃), 4.89 (m, 1H*, CHCOOCH₃), 4.62 (d, ²J = 18.0 Hz, 1H, -CH(*H'*)N), 4.24 (d, ²J = 18.0 Hz, 1H, CH(*H'*)N), 3.65 (s, 3H*, -COOCH₃), 3.64 (s, 3H**, -COOCH₃), 3.12-3.09 (m, 2H, ArCH₂CH), 1.54 (s, 9H**, ^tBu), 1.48 (s, 9H*, ^tBu). **¹³C-NMR** (125 MHz, DMSO): δ = (171.4, 171.3), (155.1, 154.5), (152.3, 152.2), (138.6, 138.3), (137.2, 136.6), (127.6, 127.4), 113.0, (86.9, 86.4), 81.149, (79.7, 79.5), 53.3, 52.5, 51.7, 51.0, 50.2, 30.3, 29.9, 29.7, 28.3. **HPLC** (10-100%, 30 min): t_R = 26.71 min. **MS** (EI): m/z = 501.9 [M-^tBu]⁺, 457.9 [M-Boc]⁺, 400.0 [M-Boc-COOMe]⁺.

*represents the minor rotamer of the Boc group.

** represents the major rotamer of the Boc group.

¹³C shifts that could be assigned to one carbon are given in parentheses.

IV.3.97 Preparation of methyl 1-(*tert*.butyloxycarbonyl)-2-(*S*)-1,2,3,4-tetrahydro-7-hydroxy-isoquinoline-3-carboxylate, **50**



Compound **49** (6.9 g, 12.3 mmol, 1 eq.) was dissolved in methanol (200 mL). 3.75 mL triethylamine (27.1 mmol, 2.2 eq.) and catalyst (5 % Pd/C, 500 mg) were added and the resulting mixture hydrogenated at 1 atm H₂ under rapid stirring for 12 h. After the TLC indicated total conversion, the catalyst was removed by filtration over Celite[®], the filtrate was evaporated and the crude product subjected to flash chromatography on silica gel (hexane / ethyl acetate 1 : 1) to yield 3.21 g (10.4 mmol, 85 %) of a light yellow foam.

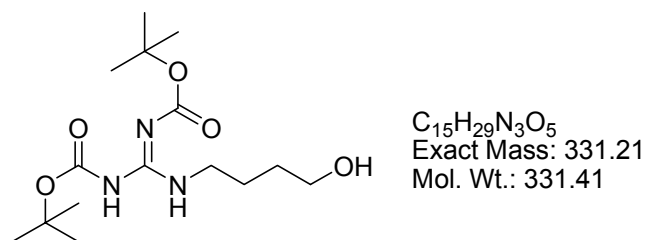
¹H-NMR (250 MHz, CDCl₃): δ = 7.36 (bs, 1H, -*OH*)**, 7.16 (bs, 1H, -*OH*)*, 7.00-6.92 (m, 1H, Ar-*H5*), 6.70-6.60 (m, 2H, Ar-*H6,2*), 5.08 (dd, ²J = 5.5 Hz, ²J = 3.2 Hz, 1H, CHCOOMe)*, 4.74 (t, ³J = 5.5 Hz, 1H, CHCOOMe)**, 4.63 (d, ²J = 15.9 Hz, 1H, Ar-CH(*H'*)N)**, 4.60 (d, ²J = 16.7 Hz, 1H, Ar-CH(*H'*)N)*, 4.46 (d, ²J = 16.6 Hz, 1H,

Ar-CH(*H'*)N)*, 4.42 (d, $^2J = 16.1$ Hz, 1H, Ar-CH(*H'*)N)**, 3.64 (s, 3H, -COOCH₃), 3.57 (s, 3H, -COOCH₃), 3.20-3.00 (m, 2H, Ar-CH₂CH), 1.51 (s, 9H, ^tBu)*, 1.45 (s, 9H, ^tBu)**. **¹³C-NMR** (62.9 MHz, CDCl₃): $\delta = 172.7^{**}$, 172.5*, 155.7*, 155.6**, 155.2, 134.5**, 133.8*, 129.4*, 128.8**, 123.1**, 122.9*, 114.4, 112.9**, 112.8*, 81.2**, 81.0*, 54.8, 53.0*, 52.3**, 44.8*, 44.3**, 30.8**, 30.5*, 28.4*, 28.3**. **HPLC** (10-100%, 30 min): $t_R = 21.77$ min. **MS** (ESI): $m/z = 308.3$ [m+H⁺]⁺, 208.2 [m+H⁺-Boc]⁺. **MS** (EI): $m/z = 307.1$ [M]⁺, 250.0 [M-^tBu], 206.0 [M-Boc]⁺, 192.0 [M-Boc-CH₃]⁺, 148.1 [M-Boc-COOCH₃], 57.1 [^tBu]⁺.

*represents the minor rotamer of the Boc-group

**represents the major rotamer of the Boc-group

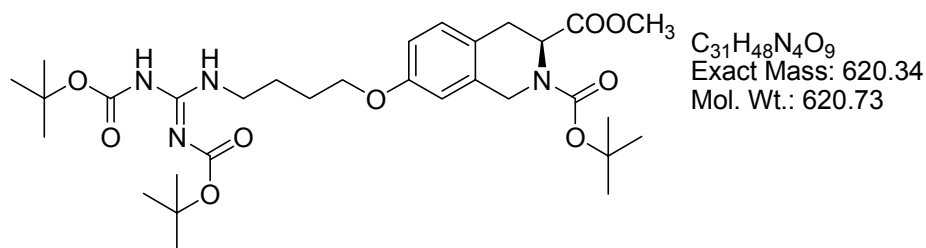
IV.3.98 Preparation of 4-(*N,N'*-bis-*tert*.butyloxycarbonyl)guanidinylobutan-1-ol, **51**



4-Aminobutan-1-ol (168 μ mol, 1.81 mmol) was guanidylated using *N,N'*-bis-Boc-thiourea (750 μ mol, 2.72 mmol), HgCl₂ (983 mg, 3.62 mmol) and triethylamine (2.5 mL, 18.1 mmol) according to **GP9**. Purification by flash chromatography on silica gel (hexane / ethyl acetate 1 : 1) yielded **51** (599 mg, 1.81 mmol, 99%) as colorless solid.

¹H-NMR (250 MHz, CDCl₃): $\delta = 8.36$ (bs, 1H, NH), 3.67 (t, $^3J = 5.9$ Hz, 2H, -CH₂OH), 3.43 (pq, $J = 6.7$ Hz, 2H, NHCH₂-), 2.21 (bs, 1H, -OH), 1.76-1.57 (m, 4H, -CH₂CH₂CH₂-), 1.47 (s, 18H, 2^tBu). **¹³C-NMR** (62.9 MHz, CDCl₃): $\delta = 163.4$, 156.2, 153.2, 83.1, 79.2, 28.3, 28.2, 28.1, 27.9. **HPLC** (10-100%, 30 min): $t_R = 16.83$ min. **MS** (EI): $m/z = 331.2$ [M]⁺, 275.1 [M-^tBu]⁺, 219.0 [M-2^tBu]⁺, 202.0 [M-2^tBu-H₂O], 188.1 [M-2^tBu-CH₂OH], 57.1 [^tBu].

IV.3.99 Preparation of methyl 1-(*tert*.butyloxycarbonyl)-7-[4-(*N,N'*-(bis-*tert*.butyloxycarbonyl)guanidinyloxy)-1,2,3,4-tetrahydroisochinolin-2-(*S*)-carboxylate, **52**



The title compound was prepared from **51** (300 mg, 905 μ mol), **50** (252 mg, 823 μ mol), triphenyl phosphine (717 mg, 1.15 mmol) and DIAD (194 μ L, 988 μ mol) according to **GP2**. The reaction mixture was evaporated with silica gel and purified by flash chromatography (hexane / ethyl acetate 8 : 2) to give **52** (372 mg, 600 μ mol, 66%) as colorless solid.

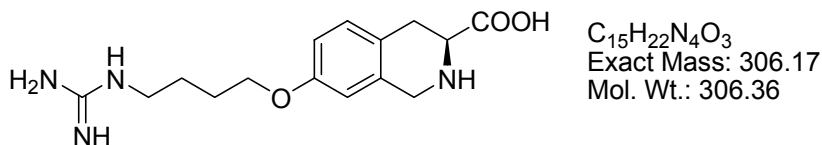
¹H-NMR (500 MHz, CDCl₃): δ = 11.50 (s, 1H, -NH), 8.37 (s, 1H, -NH), 7.02 (d, ³J = 8.2 Hz, 1H, TIC-H5), 6.74-6.60 (m, 2H, TIC-H6,2), 5.11 (dd, ³J = 6.1 Hz, ³J = 3.4 Hz, 1H^o, -CHCOOMe), 4.74 (m, 1H^{**}, -CHCOOMe), 4.70 (d, ²J = 6.0 Hz, 1H^{*}, Ar-CH(H')N), 4.64 (d, ²J = 6.0 Hz, 1H^{**}, Ar-CH(H')N), 4.48 (d, ²J = 12.1 Hz, 1H^{**}, Ar-CH(H')N), 4.41 (d, ²J = 11.7 Hz, 1H^{*}, Ar-CH(H')N), 3.94 (t, J = 5.8 Hz, 1H, -CH₂OAr), 3.63 (s, 3H^{*}, -COOCH₃), 3.61 (s, 3H^{**}, -COOCH₃), 3.48 (pq, J = 6.6 Hz, 2H, -NHCH₂CH₂-), 3.22-3.01 (m, 2H, Ar-CH₂CH), 1.91-1.68 (m, 4H, -CH₂CH₂CH₂CH₂-), 1.51 (s, 9H^{**}, NCOO^tBu), 1.50 (s, 9H, ^{Guanidine}NCOO^tBu), 1.49 (s, 9H, ^{Guanidine}NCOO^tBu), 1.45 (s, 9H^{*}, NCOO^tBu). **¹³C-NMR** (125 MHz, CDCl₃): δ = (172.5, 172.0), 163.6, (157.9, 157.7), 156.2, (155.4, 154.8), 153.3, (135.0, 133.9), (129.4, 128.7), (124.1, 123.8), 113.4, (112.0, 111.6), 83.1, 80.5, 79.2, 67.3, (54.6, 52.7), 52.1, (44.7, 44.2), 40.5, (30.8, 30.4), (28.4, 28.2), 28.3, 28.1, 26.6, 25.8. **HPLC** (10-100%, 30 min): t_R = 25.72 min. **MS** (ESI): m/z = 1240.8 [2m+H⁺]⁺, 621.5 [m+H⁺]⁺, 521.4 [m+H⁺-Boc]⁺, 421.6 [m+H⁺-2Boc]⁺.

*represents the minor rotamer of the Boc-group

**represents the major rotamer of the Boc-group

¹³C signals with different chemical shifts in both rotamers are given in parentheses.

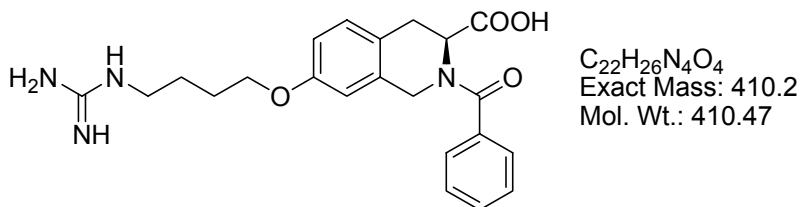
IV.3.100 Preparation of 2-(S)-carboxy-7-(4-guanidylbutoxy)-1,2,3,4-tetrahydroisochinolin, **53a**



The title compound was synthesized from **52** (100 mg, 161 μ mol) by Boc-deprotection (dioxane / *conc.* hydrochloric acid 3:1) and evaporation followed by saponification of the methyl ester with LiOH (38 mg, 1.6 mmol, 10 eq.) in methanol / water 3 : 1. Purification via preparative HPLC afforded **53a** (56 mg, 105 μ mol, 65 %) as colorless solid (double TFA salt).

1H -NMR (500 MHz, DMSO): δ = 9.66 (bs, 1H, NH), 7.86 (s, 1H, NH), 7.50-7.00 (bs, 2H, NH₂), 7.17 (d, 3J = 8.5 Hz, 1H, TIC-*H5*), 6.87-6.83 (m, 2H, TIC-*H6,2*), 4.34 (dd, 3J = 11.3 Hz, 3J = 6.7 Hz, 1H, CHCOOH), 4.29 (m, 2H, Ar-CH₂NH), 3.95 (t, 3J = 6.4 Hz, 2H, -CH₂OAr), 3.22 (dd, 2J = 16.8 Hz, 3J = 4.9 Hz, 2H, Ar-CH(H')CH), 3.16 (dd, 2J = 12.9 Hz, 3J = 6.7 Hz, 1H, NHCH(H')-), 3.01 (dd, 2J = 16.7, 3J = 11.5 Hz, 1H, Ar-CH(H')CH), 1.72 (m, 2H, CH₂CH₂OAr), 1.60 (m, 2H, NHCH₂CH₂-). **^{13}C -NMR** (125 MHz, DMSO): δ = 170.0, 157.3, 156.8, 129.8, 129.3, 122.5, 114.5, 111.6, 67.1, 53.5, 43.9, 40.3, 27.4, 25.7, 25.2. **HPLC** (10-50%, 30 min): t_R = 12.00 min. **MS** (ESI): m/z = 321.2 [$m+H^+$]⁺.

IV.3.101 Preparation of 1-Benzoyl-2-(S)-carboxy-7-(4-guanidylbutoxy)-1,2,3,4-tetrahydroisochinolin, **53b**



The title compound was synthesized from **52** (250 mg, 403 μ mol), benzoyl chloride (46 μ L, 403 μ mol), NaHCO₃ (68 mg, 806 μ mol) and LiOH (96 mg, 4.30 mmol) according to **GP8a**. Purification via preparative HPLC gave **53b** (25 mg, 48 μ mol, 12%) as colorless solid (TFA salt).

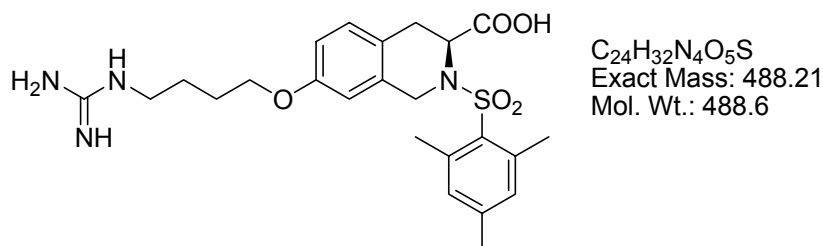
¹H-NMR (500 MHz, DMSO): δ = 7.51-7.39 (m, 5H, Ph-*H*), 7.08 (m, 1H, TIC-*H*5), 6.82 (s, 1H*, TIC-*H*2), 6.72 (m, 1H, TIC-*H*6), 6.61 (s, 1H**, TIC-*H*2), 5.14 (t, J = 4.7 Hz, 1H**, -CHCOOH), 4.93 (d, 17.8 Hz, 1H*, -CHCOOH), 4.60-4.39 (m, 2H, Ar-CH(*H'*)N), 3.93 (t, J = 5.9 Hz, 2H**, -CH₂OAr), 3.85 (t, J = 5.9 Hz, 2H*, -CH₂OAr), 3.18-3.01 (m, 4H, NHCH₂, Ar-CH(*H'*)CH), 1.72-1.49 (m, 4H, -CH₂CH₂CH₂OAr). **¹³C-NMR** (125 MHz, DMSO): δ = (172.0, 171.8), (170.9, 170.8), 157.2, 156.6, 138.3, (136.0, 135.9), 133.0, (129.8, 129.6), (129.4, 129.1), (128.6, 128.5), (126.7, 126.2), (124.5, 123.6), (113.8, 113.3), (111.7, 111.1), 66.9, (56.2, 51.9), (47.5, 43.1), (40.4, 40.3), (30.0, 29.3), (25.7, 25.7), (25.2, 25.2). **HPLC** (10-50%, 30 min): t_R = 21.88 min **MS** (ESI): m/z = 411.4 [$m+H^+$]⁺, 821.3 [$2m+H^+$]⁺, 1231.4 [$3m+H^+$]⁺.

*represents the minor rotamer of the benzoyl-group

**represents the major rotamer of the benzoyl-group

¹³C signals with different chemical shifts in both rotamers are given in parentheses.

IV.3.102 Preparation of 1-(2,4,6-trimethylphenylsulfonyl)-2-(*S*)-carboxy-7-(4-guanidylbutoxy)-1,2,3,4-tetrahydroisochinolin, **53c**

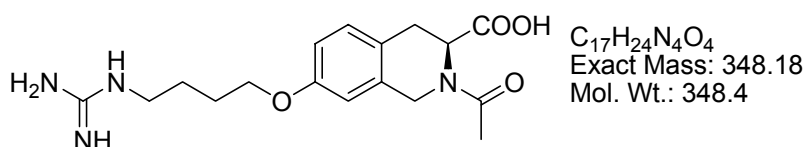


The title compound was synthesized from **52** (295 mg, 476 μ mol), 2,4,6-trimethylphenylsulfonyl chloride (208 mg, 952 μ mol), DIEA (404 μ L, 2.38 mmol) and LiOH (57 mg, 2.38 mmol) according to **GP8c**. Purification via preparative HPLC gave **53c** (63 mg, 105 μ mol, 22%) as colorless solid (TFA salt).

¹H-NMR (500 MHz, DMSO): δ = 7.71 (t, 3J = 5.2 Hz, 1H, ^{Guanidine}NH), 7.50-6.90 (bs, 2H, ^{Guanidine}NH), 7.07 (s, 2H, Ar-*H*3,3'), 7.05 (d, 3J = 8.5 Hz, 1H, TIC-*H*5), 6.76 (d, 4J = 2.0 Hz, 1H, TIC-*H*8), 6.73 (dd, 3J = 8.4 Hz, 4J = 2.3 Hz, 1H, TIC-*H*6), 4.64 (dd, 3J = 6.1 Hz, 3J = 1.0 Hz, -CHCOOH), 4.50 (d, 2J = 16.3 Hz, 1H, ArCH(*H'*)N), 4.33 (d, 2J = 16.3 Hz, 1H, ArCH(*H'*)N), 3.92 (t, 3J = 6.3 Hz, 1H, -CH₂OAr), 3.14 (m, 2H, NHCH₂CH₂), 3.10 (d, 2J = 17.0 Hz, 1H, ArCH(*H'*)CH), 2.99 (dd, 2J = 16.1, 3J = 6.6 Hz, 1H), 2.55 (s, 6H, Ar(CH₃)₂), 2.27 (s, 3H, ArCH₃), 1.79-1.65 (m, 2H, -CH₂CH₂OAr),

1.62-1.56 (m, 2H, NHCH₂CH₂-). ¹³C-NMR (125 MHz, DMSO): δ = 171.5, 157.0, 156.7, 156.7, 142.3, 139.5, 132.5, 131.8, 129.7, 122.8, 113.6, 111.1, 66.8, 52.6, 43.0, 40.3, 29.8, 25.7, 25.1, 22.2, 20.3. **HPLC** (10-100%, 30 min): t_R = 19.70 min. **MS** (ESI): m/z = 489.7 [m+H⁺]⁺.

IV.3.103 Preparation of 1-acetyl-2-(S)-carboxy-7-(4-guanidylbutoxy)-1,2,3,4-tetrahydroisochinolin, 53d



Compound **53a** (20 mg, 37 μmol, 1 eq.) was dissolved in 0.5 mL dioxane / water 1 : 1. NaHCO₃ (16 mg, 187 μmol, 5 eq.) and acetic acid anhydride (4 μL, 41 μmol, 1.1 eq.) were added and the mixture stirred for 0.5 h. Evaporation followed by preparative HPLC purification gave **53d** (15 mg, 32 μL, 88%) as colorless solid (TFA salt).

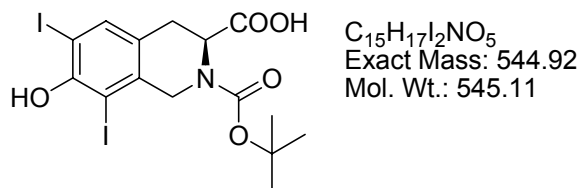
¹H-NMR (500 MHz, DMSO): δ = 12.76 (bs, 1H, COOH), 7.69 (m, 1H, ^{Guandidine}NH), 7.70-7.60 (bs, ^{Guandidine}NH), 7.10 (d, ³J = 8.4 Hz, 1H, TIC-H5), 6.80-6.72 (m, 2H, TIC-H6,2), 5.13 (dd, ³J = 6.0 Hz, ³J = 5.1 Hz, 1H**, -CHCOOH), 4.91 (d, ³J = 3.3 Hz, 1H*, -CHCOOH), 4.70 (d, ²J = 18.9 Hz, 1H*, Ar-CH(H')N), 4.70 (d, ²J = 15.5 Hz, 1H**, Ar-CH(H')N), 4.58 (d, ²J = 15.9 Hz, 1H**, Ar-CH(H')N), 4.27 (d, ²J = 17.6 Hz, 1H*, Ar-CH(H')N), 3.94 (m, 2H, -CH₂OAr), 3.15 (m, 2H, NHCH₂-), 3.15-3.01 (m, 1H+1H*, ArCH(H')CH), 2.94 (dd, ²J = 15.6 Hz, ³J = 6.2 Hz, 1H**, Ar-CH(H')CH), 2.14 (s, 3H**, NCOCH₃), 2.05 (s, 3H*, NCOCH₃), 1.71 (m, 2H, -CH₂CH₂OAr), 1.60 (m, 2H, NHCH₂CH₂-). ¹³C-NMR (125 MHz, DMSO): δ = (172.4*, 172.3**), (170.0*, 169.7**), 157.1, 156.7, (134.0**, 133.8*), 129.0, (124.2**, 124.0*), (113.3**, 113.1*), (111.7*, 111.5**), (66.9**, 66.8*), (55.0*, 50.8**), (45.6**, 42.8*), 40.3, (30.4*, 29.7**), 25.7, 25.2, (21.7**, 21.6*). **HPLC** (10-50%, 30 min): t_R = 16.37 min. **MS** (ESI): m/z = 349.4 [m+H⁺]⁺. **HR-MS** (ESI)(C₁₇H₂₅N₄O₄)⁺: Calc. 349.1870, Found: 349.1868.

*represents the minor rotamer of the acetyl-group

**represents the major rotamer.of the acetyl-group

¹³C signals with different chemical shifts in both rotamers are given in parentheses.

IV.3.104 Preparation of 2-(S)-carboxy-6,8-diiodo-7-hydroxy-1-(tert.butylloxycarbonyl)-1,2,3,4-tetrahydroisochinolin, 54.



The title compound was synthesized from **47** (9.1 g, 18.9 mmol, 1 eq.), Boc-anhydride (4.32 g, 19.9 mmol, 1.1 eq.) and triethyl amine (6 mL, 43.5 mmol, 2.3 eq.) according to **GP6b**. Yield was 10.2 g, 18.7 mmol, 99%) of an orange foam.

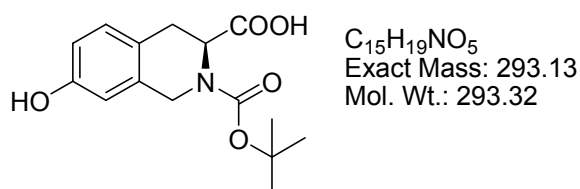
1H -NMR (500 MHz, DMSO): δ = 12.60 (bs, 1H, -COOH), 9.46 (bs, 1H, TIC-OH), 7.63 (s, 1H, TIC-H5), 4.82 (dd, 3J = 5.5 Hz, 3J = 3.1 Hz, 1H*, -CHCOOH), 4.68 (m, 1H**, -CHCOOH), 4.47 (d, 2J = 17.3 Hz, 1H*, Ar-CH(H')N), 4.41 (d, 2J = 17.2 Hz, 1H**, Ar-CH(H')N), 4.19 (d, 2J = 17.2 Hz, 1H*+1H**, Ar-CH(H')N), 3.09-3.01 (m, 2H, ArCH₂), 1.46 (s, 9H*, ^tBu), 1.40 (s, 9H**, ^tBu). **^{13}C -NMR** (125 MHz, DMSO): δ = (173.4, 173.1), (155.3, 155.1), 154.8, (139.2, 138.9), (137.9, 137.3), (129.1, 129.0), 92.4, 85.7, (80.8, 80.7), (54.0, 52.5), (52.1, 51.3), (30.7, 30.4), (28.9, 28.8). **HPLC** (10-100%, 30 min): t_R = 23.10. **MS** (ESI): m/z = 567.8 [$m+Na^+$]⁺, 446.0 [$m+H^+$ -Boc]⁺.

*represents one rotamer of the Boc-group

**represents the other rotamer of the Boc-group

¹³C signals with different chemical shifts in both rotamers are given in parentheses, present in ~ 1:1 ratio.

IV.3.105 Preparation of 2-(S)-carboxy-7-hydroxy-1-(tert.butylloxycarbonyl)-1,2,3,4-tetrahydroisochinolin, 55.



Compound **53** (2.0 g, 3.67 mmol, 1 eq.) was dissolved in methanol (70 mL). 1.02 mL triethyl amine (7.34 mmol, 2.2 eq.) and catalyst (5 % Pd/C, 230 mg) were added and the resulting mixture hydrogenated at 1 atm H₂ under rapid stirring for 12 h. After the TLC indicated total conversion, the catalyst was removed by filtration over Celite[®], the filtrate was evaporated and the crude product subjected to flash chromatography

IV. Experimental Section

on silica gel (hexane / ethyl acetate 1 : 1) to yield 0.84 g (2.86 mmol, 79%) of a light yellow solid.

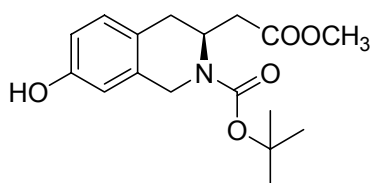
¹H-NMR (500 MHz, DMSO): δ = 12.58 (bs, -COOH), 9.25 (s, 1H, -OH), 6.97 (t, 3J = 8.9 Hz, 1H, TIC-H5), 6.58 (s, 1H, TIC-H8), 6.52 (m, 1H, TIC-H6), 4.82 (dd, 3J = 5.7 Hz, 3J = 2.8 Hz, 1H*, -CHCOOH), 4.59 (t, 3J = 5.0 Hz, 1H, -CHCOOH), 4.50 (d, 3J = 16.5 Hz, 1H*, Ar-CH(H')N), 4.43 (d, 3J = 16.5 Hz, 1H**, Ar-CH(H')N), 4.34 (d, 3J = 16.5 Hz, 1H**, Ar-CH(H')N), 4.28 (d, 3J = 16.2 Hz, 1H*, Ar-CH(H')N), 3.04-2.94 (m, 2H, ArCH₂CH), 1.45 (s, 9H*, ^tBu), 1.39 (s, 9H, ^tBu). **¹³C-NMR** (125 MHz, DMSO): δ = (172.9, 172.6), 155.8, (154.5, 154.2), (134.5, 133.7), (129.1, 128.6), (122.5, 121.9), (113.8, 113.7), (112.5, 112.3), (79.4, 79.2), (53.9, 52.2), (44.1, 43.7), (30.1, 29.8), (28.0, 27.8). **HPLC** (10-100%, 30 min): t_R = 16.99 min.

*represents one rotamer of the Boc-group

**represents the other rotamer of the Boc-group

¹³C signals with different chemical shifts in both rotamers are given in parentheses, present in ~ 1:1 ratio.

IV.3.106 Preparation of methyl (*S*)-(7-hydroxy-1-(*tert*.butyloxycarbonyl)-1,2,3,4-tetrahydroisochinolin-2-yl)acetate, **56**.



C₁₇H₂₃NO₅
Exact Mass: 321.16
Mol. Wt.: 321.37

1. Preparation of diazomethane:

A 100 mL Erlenmeyer flask was filled with 35 mL of 40% aqueous KOH solution and 50 mL of diethyl ether and cooled in an ice-salt bath to -5 - 0°C. 5.3 g *N*-methyl nitroso urea was added in portions keeping the temperature below 0°C at any time. After 1.5 h, the mixture was carefully converted into a separating funnel (with a Teflon stopcock), the layers were separated and the organic layer dried for 3 h over KOH.

2. Preparation of diazoketone

A solution of **55** (2.93 g, 10.0 mmol, 1 eq.) in 35 mL dry THF under an argon atmosphere was cooled to -15°C. After addition of TEA (2.9 mL, 20 mmol, 2 eq.) and ethyl chloroformate (1.05 mL, 11 mmol, 1.1 eq.), the colorless suspension was stirred for 0.5 h at -5°C. Subsequently, the reaction flask was opened and the freshly

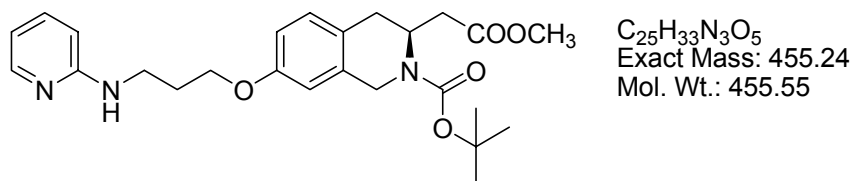
prepared diazomethane solution was added carefully via a PP pipette. The yellow suspension was stirred at $-15 - -5^{\circ}\text{C}$ for 1 h. The reaction was quenched by addition of acetic acid (0.5 mL), followed by diethyl ether and saturated NaHCO_3 solution. The layers were separated and the organic layer washed with saturated NH_4Cl solution and brine, dried with Na_2SO_4 , filtered and evaporated. The crude diazoketone was separated from the byproduct (bearing a ethyloxycarbonyl at the aromatic hydroxyl group) by column chromatography on silica gel (hexane / ethyl acetate 3 : 2, $R_f(\text{byproduct}) =$, $R_f(\text{product}) =$) to give the diazoketone as a yellow solid (350 mg, 1.1 mmol, 11%) which was immediately used in the next step.

3. Wolff- rearrangement

The diazoketone (350 mg, 1.10 mmol, 1 eq.) was dissolved in 15 mL abs. MeOH and cooled to -25°C . Silver benzoate (228 mg, 0.13 mmol, 0.12 eq.) was dissolved in triethylamine (610 μL , 4.4 mmol, 4 eq.) and added dropwise to the diazoketone. The mixture was allowed to warm to room temperature over night. After evaporation of the solvent, the residue was taken up in ethyl acetate, washed with sat. NaHCO_3 , 5% aqueous citric acid and brine, dried over Na_2SO_4 and filtered. After evaporation, the crude product was purified by column chromatography on silica gel (hexane/ethyl acetate 2 : 1) to give 215 mg (670 μmol , 61%, 7% overall yield) of a colorless solid.

$^1\text{H-NMR}$ (250 MHz, CDCl_3): $\delta = 7.07$ (bs, 1H, $-\text{OH}$), 6.94 (d, $^3J = 8.2$ Hz, 1H, TIC-*H5*), 6.70 (dd, $^3J = 8.2$ Hz, $^2J = 2.4$ Hz, 1H, TIC-*H6*), 6.67 (s, 1H, TIC-*H2*), 4.84 (m, 1H, $\text{CH-CH}_2\text{COOMe}$), 4.69 (d, $^2J = 16.9$ Hz, 1H, Ar- $\text{CH}(\text{H}')\text{N}$), 4.26 (d, $^2J = 17.2$ Hz, 1H, Ar- $\text{CH}(\text{H}')\text{N}$), 3.64 (s, 3H, $-\text{COOCH}_3$), 3.02 (dd, $^2J = 15.6$ Hz, $^3J = 5.4$ Hz, 1H, $-\text{CH}(\text{H}')\text{COOMe}$), 2.63 (dd, $^2J = 15.8$ Hz, $^3J = 2.2$ Hz, 1H, $-\text{CH}(\text{H}')\text{COOMe}$), 2.48 (dd, $^2J = 14.9$ Hz, $^3J = 7.1$ Hz, 1H, Ar- $\text{CH}(\text{H}')\text{CH}$), 2.30 (dd, $^2J = 14.5$ Hz, $^3J = 7.4$ Hz, 1H, Ar- $\text{CH}(\text{H}')\text{CH}$), 1.49 (s, 9H, NHCOO^tBu). **$^{13}\text{C-NMR}$** (62.9 MHz, DMSO): $\delta = 171.9, 155.1, 154.2, 133.5, 130.1, 123.2, 114.4, 112.7, 80.6, 51.7, 43.2, 37.1, 32.4, 28.4$. **HPLC** (10-100%, 30 min): $t_R = 16.99$ min.

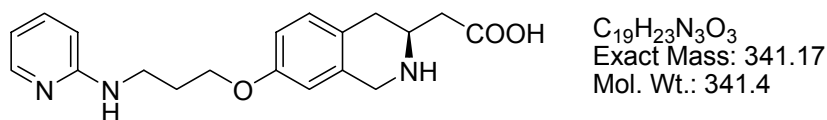
IV.3.107 Preparation of methyl (S)-(7-(3-pyridin-2-ylpropoxy)-1-(tert.butylloxycarbonyl)-1,2,3,4-tetrahydroisochinolin-2-yl) acetate, 57.



The title compound was synthesized from **56** (207 mg, 532 μ mol), **5** (162 mg, 1.06 mmol), tributyl phosphine (301 μ L, 1.22 mmol) and ADDP (308 mg, 1.22 μ mol) according to **GP2**. Purification via flash chromatography on silica gel (DCM / ethyl acetate 2 : 1) gave **57** (113 mg, 255 μ mol, 48%) as colorless foam.

1H -NMR (250 MHz, $CDCl_3$): δ = 8.04 (d, 3J = 4.8 Hz, 1H, Py-*H6*), 7.36 (t, 3J = 7.7 Hz, 1H, Py-*H4*), 6.99 (d, 3J = 8.3 Hz, 1H, TIC-*H5*), 6.71 (d, 3J = 8.3 Hz, 1H, TIC-*H6*), 6.63 (s, 1H, TIC-*H2*), 6.51 (t, 3J = 6.2 Hz, 1H, Py-*H5*), 6.37 (d, 3J = 8.4 Hz, 1H, Py-*H3*), 4.86 (m, 2H, Py-NH, $CHCH_2COOMe$), 4.69 (d, 2J = 16.1 Hz, Ar- $CH(H')N$), 4.24 (d, 2J = 17.1 Hz, Ar- $CH(H')N$), 4.02 (t, 3J = 5.8 Hz, 2H, $-CH_2OAr$), 3.62 (s, 3H, $-COOCH_3$), 3.46 (pq, J = 6.2 Hz, 2H, $PyNHCH_2-$), 3.01 (dd, 2J = 15.8 Hz, 3J = 5.3 Hz, 1H, $-CH(H')COOMe$), 2.63 (d, 2J = 15.6 Hz, 1H, $CH(H')COOMe$), 2.44 (dd, 2J = 14.5 Hz, 3J = 6.85 Hz, 1H, Ar- $CH(H')CH$), 2.26 (dd, 2J = 14.6 Hz, 3J = 7.6 Hz, 1H, Ar- $CH(H')CH$), 2.06 (m, 2H, $-CH_2CH_2CH_2-$), 1.46 (s, 9H, $NCOO^tBu$). **^{13}C -NMR** (125.1 MHz, DMSO): δ = 171.5, 158.6, 157.3, 154.4, 147.9, 137.2, 124.2, 112.6, 106.6, 80.0, 65.8, 51.5, 39.2, 32.2, 29.0, 28.3. **HPLC** (10-100%, 30 min): t_R = 17.88 min. **MS** (ESI): m/z = 456.2 $[m+H^+]^+$, 400.3 $[m+H^+-^tBu]^+$, 356.4 $[m+H^+-Boc]^+$.

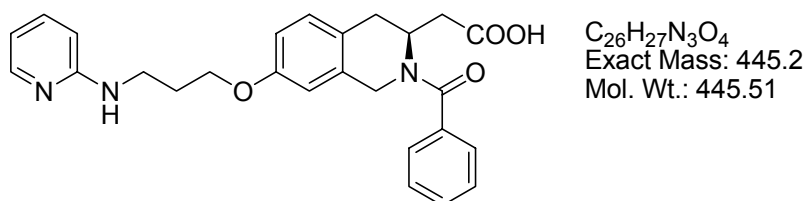
IV.3.108 Preparation of (S)-(7-(3-pyridin-2-ylpropoxy)-1-(tert.butylloxycarbonyl)-1,2,3,4-tetrahydroisochinolin-2-yl) acetic acid, 58a.



Compound **57** (37 mg, 85 μmol) was Boc-protected (dioxane / conc. hydrochloric acid 3 : 1) and the mixture evaporated to dryness. Saponification of the methyl ester with LiOH (10 mg, 417 μmol) and purification by preparative HPLC gave **58a** (4 mg, 7 μmol , 8%) as colorless solid (double TFA salt).

HPLC (10-50%, 30 min): $t_{\text{R}} = 10.97$ min. **MS** (ESI): $m/z = 342.3$ $[\text{m}+\text{H}^+]^+$, 171.7 $[\text{m}+2\text{H}^+]^{2+}$.

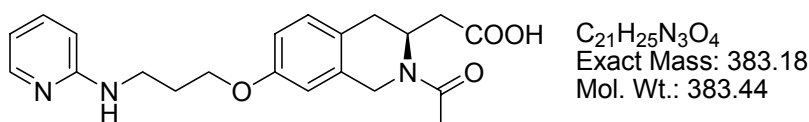
IV.3.109 Preparation of 1-benzoyl-(S)-(7-(3-pyridin-2-ylpropoxy)-1-(*tert*.butyloxycarbonyl)-1,2,3,4-tetrahydroisochinolin-2-yl) acetic acid, **58b.**



The title compound was synthesized from **57** (250 mg, 403 μmol), benzoyl chloride (13 μL , 111 μmol), NaHCO_3 (21 mg, 250 μmol) and LiOH (10 mg, 417 μmol) according to **GP8a**. Purification via preparative HPLC gave **58b** (6 mg, 11 μmol , 13%) as colorless solid (TFA salt).

$^1\text{H-NMR}$ (500 MHz, DMSO): $\delta = 8.71$ (bs, 1H, PyNH), 7.90 (m, 2H, Py-H6 + Py-H4), 7.46 (m, 4H), 7.06 (t, $^3J = 9.0$ Hz, 2H, Ph-H3,3'), 6.82 (m, 2H), 5.20 (m, 1H), 4.42 (m, 1H), 4.06 (m, 2H, $-\text{CH}_2\text{OAr}$), 3.48 (m, 2H, PyNHCH $_2$ -), 3.07 (dd, $^2J = 16.7$ Hz, $^3J = 4.9$ Hz, 1H, Ar-CH(H')) 2.63 (m 1H, Ar-CH(H')), 2.50 - 2.37 (m, 2H, $-\text{CH}_2\text{COOH}$).
HPLC (10-50%, 30 min): $t_{\text{R}} = 22.31$ min. **MS** (ESI): $m/z = 446.4$ $[\text{m}+\text{H}^+]^+$.

IV.3.110 Preparation of 1-acetyl-(S)-(7-(3-pyridin-2-ylpropoxy)-1-(*tert*.butyloxycarbonyl)-1,2,3,4-tetrahydroisochinolin-2-yl) acetic acid, **58c.**



IV. Experimental Section

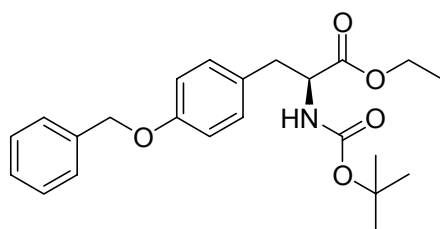
Compound **57** (38 mg, 85 μmol , 1 eq.) was firstly Boc-protected (dioxane / *conc.* hydrochloric acid 3 : 1). After 0.5 h stirring, the mixture was evaporated to dryness and the residue dissolved in 0.5 mL dioxane. NaHCO_3 (21 mg, 250 μmol , 3 eq.) and acetic acid anhydride (11 μL , 116 μmol , 1.4 eq.) were added and the mixture stirred for 0.5 h. The mixture was concentrated, and the methyl ester saponificated by LiOH (10 mg, 417 μmol) in methanol / water 3 : 1. Evaporation followed by preparative HPLC purification gave **58c** (12 mg, 30 μmol , 35%) as colorless solid (TFA salt).

$^1\text{H-NMR}$ (500 MHz, DMSO): δ = 8.71 (bs, 1H, Py-NH), 7.92 (d, 3J = 4.7 Hz, 1H, Py-H6), 7.85 (t, 3J = 7.7 Hz, 1H, Py-H4), 7.09-7.00 (m, 2H, Py-H3, TIC-H5), 6.83-6.76 (m, 3H, Py-H5, TIC-H2,6), 5.09 (d, 3J = 18.2 Hz, 1H**, TIC-CH(H')N), 5.04 (m, 1H*, CHCH₂COOH), 4.66 (d, 2J = 16.6 Hz, 1H*, Ar-CH(H')N), 4.61 (dd, 2J = 12.5 Hz, 3J = 6.2 Hz, 1H**, CHCH₂COOH), 4.42 (d, 2J = 16.6 Hz, 1H*, Ar-CH(H')N), 4.05 (m, 2H, -CH₂OAr), 3.96 (d, 2J = 18.1 Hz, 1H**, Ar-CH(H')N), 3.47 (m, 2H, -NHCH₂-), 3.03 (dd, 2J = 16.0 Hz, 3J = 5.1 Hz, 1H**, Ar-CH(H')CH), 2.85 (dd, 2J = 15.7 Hz, 3J = 4.8 Hz, 1H*, Ar-CH(H')CH), 2.73-2.36 (m, 1H*+1H**, Ar-CH(H')CH), 2.42-2.33 (m, 1H+1H*, CH(H')COOH), 2.29 (dd, 2J = 15.1 Hz, 3J = 5.4 Hz, 1H**, CH(H')COOH), 2.14 (s, 3H**, NHCOCH₃), 2.06 (s, 3H*, NHCOCH₃), 2.04 (m, 2H, CH₂CH₂CH₂). **$^{13}\text{C-NMR}$** (125.1 MHz, DMSO): δ = 172.1, (168.7*, 168.6**), 156.7, 153.1, 142.3, 136.7, (133.7*, 133.2**), (130.1**, 129.9*), (124.5*, 123.6**), (113.4*, 113.3**), 112.7, (111.7**, 111.6*), 111.5, 64.7, 48.7, (44.5*, 44.3**), 38.5, (36.4**, 36.1*), (32.1**, 31.0*), 27.6, (22.1*, 21.4**). **HPLC** (10-50%, 30 min): t_R = 16.71 min. **MS** (ESI): m/z = 384.4 [$m+\text{H}^+$]⁺.

*represents the minor rotamer of the acetyl-group

**represents the major rotamer of the acetyl-group

IV.3.111 Preparation of ethyl 2-(S)-(tert.butylloxycarbonylamino)-3-(4-benzyloxyphenyl)propionate, **59**

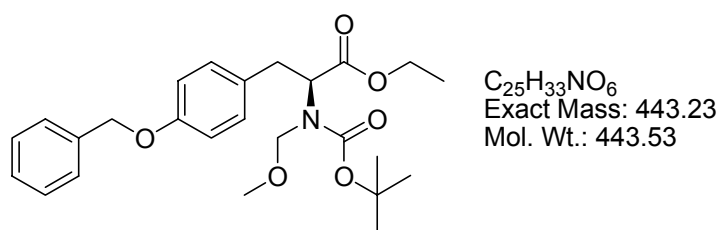


$\text{C}_{23}\text{H}_{29}\text{NO}_5$
Exact Mass: 399.2
Mol. Wt.: 399.48

H-Tyr(Bn)-OH (6.0 g, 22.0 mmol, 1 eq.) was transformed into the ethyl ester according to **GP11**, with ethanol instead of methanol. After the reaction was complete (HPLC-MS monitoring), the solution was evaporated to dryness, re-dissolved in THF and Boc-protected according to **GP6b** (Boc-anhydride: 5.28 g, 24.2 mmol, 1.1 eq.; TEA: 7.0 mL, 50.5 mmol, 2.3 eq.). The solvents were evaporated and the residue directly subjected to column chromatography on silica gel (hexane / ethyl acetate 2 : 1) to give the title compound (6.7 g, 16.5 mmol, 75% overall yield) of a colorless solid.

¹H-NMR (500 MHz, CDCl₃): δ = 7.44 - 7.31 (m, 5H, Ph-*H*), 7.06 (d, ³*J* = 7.6 Hz, 2H, Tyr-*H*3,3'), 6.91 (d, ³*J* = 7.6 Hz, 2H, Tyr-*H*2,2'), 5.04 (s, 2H, Ph-CH₂O), 5.00 (d, ³*J* = 7.3 Hz, 1H, -NHCOO^tBu), 4.53 (m, 1H, CHCOOEt), 4.16 (q, ³*J* = 7.1 Hz, 2H, CH₂CH₃), 3.06 (dd, ²*J* = 13.3 Hz, ³*J* = 6.9 Hz, 1H, Ar-CH(*H'*)-), 3.02 (m, 1H, Ar-CH(*H''*)), 1.43 (s, 9H, ^tBu), 1.23 (t, ³*J* = 7.1 Hz, 3H, -CH₂CH₃). **¹³C-NMR** (125.1 MHz, CDCl₃): δ = 171.9, 157.8, 155.0, 137.0, 130.3, 128.5, 128.3, 127.9, 127.4, 114.8, 79.7, 69.9, 61.2, 54.5, 37.5, 28.3, 14.1. **HPLC** (10-100%, 30 min): t_R = 27.55 min. **MS** (EI): m/z = 399.1 [M]⁺, 282.0, 91.0 [Bn], 57.1 [^tBu].

IV.3.112 Preparation of ethyl 2-methoxymethyl-*tert*.butyloxycarbonylamino-3-(4-benzyloxyphenyl)propionate, **60**



Compound **59** (4.19 g, 10.5 mmol, 1 eq.) was dissolved in 350 mL dry THF under an atmosphere of argon. A solution of KHMDS in THF (0.5 M, 23.2 mL, 11.6 mmol, 1.1 eq.) was added at -78°C and the mixture stirred for 10 min. After that, 8.0 mL (105 mmol, 10 eq.) MOMCl were added and stirring was continued for additional 20 h at -78°C. The mixture was poured into sat. aq. NH₄Cl solution and extracted with ethyl acetate. The organic phase was washed with sat. aq. NaHCO₃ and brine, dried over Na₂SO₄, filtered and evaporated. The residue was purified by flash column

IV. Experimental Section

chromatography (hexane / dioxane 10 : 1) to give the title compound (3.2 g, 7.25 mmol, 69%) as colorless oil.

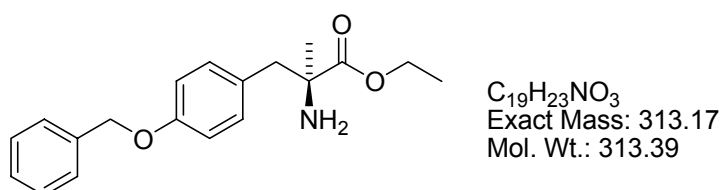
¹H-NMR (500 MHz, CDCl₃): δ = 7.43-7.30 (m, 5H, Ph-H), 7.11 (d, ³J = 8.1 Hz, 2H*, Tyr-H3,3'), 7.08 (d, ³J = 8.2 Hz, 2H**, Tyr-H3,3'), 6.89 (d, ³J = 8.4 Hz, 2H, Tyr-H2,2'), 5.04 (s, 2H, PhCH₂-), 4.73 (d, ²J = 10.8 Hz, 1H**, NCH(H')O), 4.60 (d, ²J = 11.3 Hz, 1H*, NCH(H')O), 4.25-4.15 (2m, 2H**+2H*, -COOCH₂CH₃), 4.09 (m, 1H, CHCOOEt), 4.06 (d, ²J = 10.8 Hz, 1H*, NCH(H')O), 3.89 (d, ²J = 10.9 Hz, 1H**, NCH(H')O), 3.31 (dd, ²J = 14.2 Hz, ³J = 5.2 Hz, 1H, Ar-CH(H')), 3.22 (s, 3H**, OCH₃), 3.15 (s, 3H*, OCH₃), 3.10 (dd, ²J = 13.7 Hz, ³J = 10.8 Hz, 1H, Ar-CH(H')), 1.48 (s, 9H, C(CH₃)₃), 1.29 (t, ³J = 7.0 Hz, 3H**, CH₂CH₃), 1.25 (m, 3H*, CH₂CH₃). **¹³C-NMR** (125.1 MHz, CDCl₃): δ = 171.5, (158.0**, 157.9*), 155.3, 137.5, (131.0*, 130.8**), 130.7, 129.0, 128.3, 127.9, (115.4**, 115.3*), (81.6**, 81.2*), 79.8, 70.5, 67.5, (61.7**, 61.5*), (61.3**, 60.9*), (56.3**, 55.9*), (35.9**, 34.9*), 28.7, 14.6. **HPLC** (10-100%, 30 min): t_R = 29.29 min. **MS** (EI):

* represents the minor rotamer of the Boc-group

** represents the major rotamer of the Boc-group

¹³C shifts associated with both rotamers are given in parentheses.

IV.3.113 Preparation of ethyl 2-amino-2-methyl-3-(4-benzyloxyphenyl)propionate - hydrochloride, 61

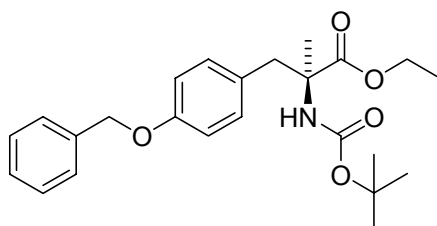


Compound **59** was dried azeotropically by double evaporation with dry toluene prior to use. A KHMDS solution in THF (0.5 M, 4.4 mL, 2.2 mmol, 1.1 eq.) was diluted with 12 mL of dry toluene. A solution of **60** (880 mg, 2 mmol, 2 eq.) in toluene (6 mL) was added to the KHMDS solution at -78°C. After stirring for 30 min, methyl iodide (630 μ L, 10 mmol, 10 eq.) was added and the resulting mixture stirred at -78°C for 15 h. The reaction mixture was poured into sat. aq. NH₄Cl solution and extracted with ethyl acetate. The organic phase was washed with sat. aq. NaHCO₃ and brine, dried over Na₂SO₄, filtered and evaporated. The residue was purified by flash column chromatography (hexane / dioxane 10 : 1). The resulting product contained impurities

resulting from Boc-cleavage. Thus, the protecting groups were cleaved with 6 M aq. HCl in DME for 3 h. The Boc- MOM cleavage was quantitative and the product could be isolated by evaporation of the solvents to give the title compound (316 mg, 906 μmol , 45% overall yield).

$^1\text{H-NMR}$ (500 MHz, CDCl_3): δ = 8.67 (d, 3H, $-\text{NH}_3^+$), 7.42 (d, 3J = 7.3 Hz, 2H, Ph-H2,2'), 7.37 (t, 3J = 7.4 Hz, 2H, Ph-H3,3'), 7.31 (t, 3J = 7.2 Hz, 1H, Ph-H4), 7.11 (d, 3J = 8.3 Hz, 2H, Tyr-H3,3'), 6.95 (d, J = 8.3 Hz, 2H, Tyr-H2,2'), 5.06 (s, 2H, PhCH₂O), 4.14 (m, 2H, $-\text{CH}_2\text{CH}_3$), 3.10 (d, 2J = 14.0 Hz, 1H, ArCH(H')C), 3.06 (d, 2J = 14.0 Hz, 1H, ArCH(H')C), 1.49 (s, 3H, NH_2CCH_3), 1.17 (t, 3J = 7.0 Hz). **$^{13}\text{C-NMR}$** (125 MHz, DMSO): δ = 170.5, 157.8, 137.0, 131.4, 128.5, 127.9, 127.7, 125.6, 114.8, 69.2, 62.1, 60.0, 41.6, 21.4, 13.9. **MS** (ESI): m/z = 314.1 $[\text{M}+\text{H}^+]^+$.

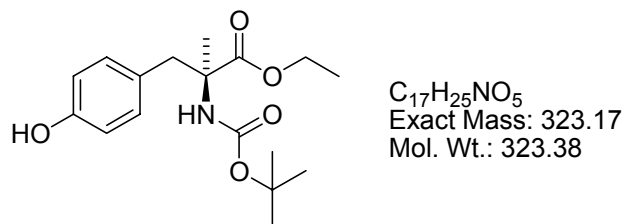
IV.3.114 Preparation of ethyl 2-(S)-(tert.butylloxycarbonylamino)-2-methyl-3-(4-benzyloxyphenyl)propionate, 62



$\text{C}_{24}\text{H}_{31}\text{NO}_5$
Exact Mass: 413.22
Mol. Wt.: 413.51

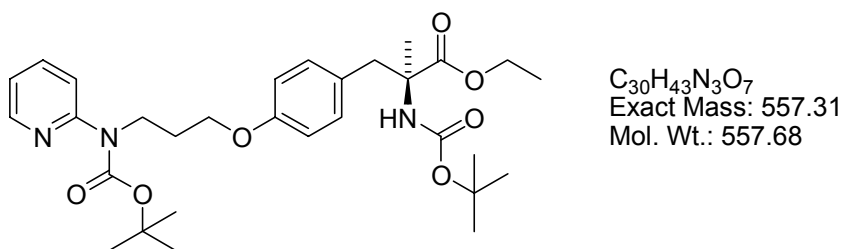
The title compound was synthesized from **61** (401 mg, 1.15 mmol, 1 eq.), Boc-anhydride (276 mg, 1.27 mmol, 1.1 eq.) and triethylamine (367 μL , 2.65 mmol, 2.3 eq.) according to **GP6b**. Purification by column chromatography on silica gel (hexane / ethyl acetate 2 : 1) gave 450 mg (1.09 mmol, 95%) of a colorless solid.

$^1\text{H-NMR}$ (500 MHz, CDCl_3): δ = 7.43 (d, J = 8.0 Hz, 2H, Ph-H2,2'), 7.38 (t, J = 7.3 Hz, 2H, Ph-H3,3'), 7.32 (t, J = 7.1 Hz, 1H, Ph-H4), 7.01 (d, J = 8.5 Hz, 2H, Tyr-H3,3'), 6.88 (d, J = 8.6 Hz, 2H, Tyr-H2,2'), 5.15 (bs, 1H, NHBoc), 5.04 (s, 2H, PhCH₂O), 4.20 (m, 2H, $-\text{CH}_2\text{CH}_3$), 3.30 (bd, 1H, ArCH(H')C), 3.15 (d, 2J = 13.6 Hz, 1H, ArCH(H')C), 1.55 (s, 3H, NHCCCH_3), 1.29 (t, 3J = 7.2 Hz, 3H, $-\text{CH}_2\text{CH}_3$). **$^{13}\text{C-NMR}$** (125 MHz, CDCl_3): δ = 174.0, 157.8, 154.3, 137.1, 131.1, 128.8, 128.5, 127.9, 127.5, 114.5, 70.0, 61.5, 60.3, 40.8, 28.4, 27.4, 23.6, 14.1. **HPLC** (10-100%, 30 min): t_R = 29.03 min. **MS** (ESI): m/z = 436.3 $[\text{m}+\text{Na}^+]^+$, 314.1 $[\text{m}+\text{H}^+-\text{Boc}]^+$.

IV.3.115 Preparation of ethyl 2-(S)-(tert.butoxycarbonylamino)-2-methyl-3-(4-hydroxyphenyl)propionate, 63

Compound **62** (438 mg, 1.06 mmol, 1 eq.) was benzyl-protected according to **GP4** (30 mg Pd / C, 50 mL MeOH, 1 atm H₂). After total conversion of the starting material, the mixture was filtered over Celite[®] and evaporated to dryness. The product could be used without further purification (Yield: 311 mg, 963 μmol, 91%).

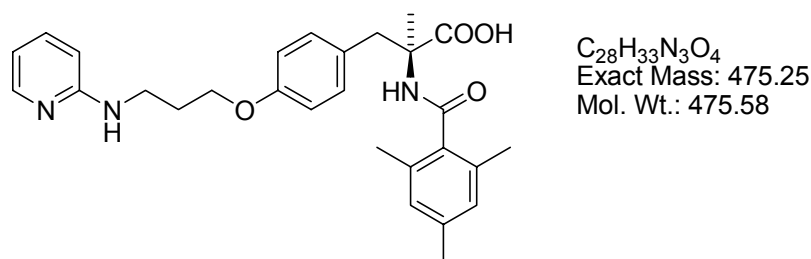
¹H-NMR (250 MHz, CDCl₃): δ = 7.11 (d, ³J = 8.5 Hz, 2H, Tyr-*H*3,3'), 6.91 (d, ³J = 8.4 Hz, 2H, Tyr-*H*2,2'), 5.33 (bs, 1H, -NH_{Boc}), 4.36 (q, ³J = 7.2 Hz, 2H, COOCH₂CH₃), 3.43-3.37 (broad d, 1H, Ar-CH(*H*')), 3.29 (d, ²J = 13.4 Hz, 1H, Ar-CH(*H*')), 1.71 (s, 3H, CCH₃), 1.65 (s, 9H, ^tBu), 1.46 (t, ³J = 7.1 Hz, 3H, -CH₂CH₃).
¹³C-NMR (125 MHz, CDCl₃): δ = 174.2, 155.2, 154.6, 131.1, 127.6, 115.1, 79.7, 61.6, 60.2, 41.0, 28.3, 23.4, 14.0. **HPLC** (10-100%, 30 min): t_R = 21.12 min. **MS** (ESI): m/z = 384.4 [m+H⁺]⁺.

IV.3.116 Preparation of ethyl 2-(S)-(tert.butylloxycarbonylamino)-2-methyl-3-(4-(3-pyridin-2-ylamino-N-(tert.butylloxycarbonyl)propoxy)phenyl)propionate, 64

The title compound was prepared from **63** (289 mg, 894 μmol, 1 eq.), **19** (338 mg, 1.34 mmol, 1.5 eq.), PBu₃ (330 mg, 1.34 mmol, 1.5 eq.) and ADDP (337 mg, 1.34 mmol, 1.5 eq.) according to **GP2**. Purification by column chromatography (hexane / ethyl acetate 8 : 2) afforded **64** (197 mg, 362 μmol, 41%) of a colorless oil.

¹H-NMR (500 MHz, CDCl₃): δ = 8.32 (dd, ³J = 4.7 Hz, ⁴J = 1.0 Hz, 1H, Py-*H*6), 7.60 - 7.56 (m, 2H, Py-*H*3,4), 6.97 (m, 1H, Py-*H*5), 6.95 (d, ³J = 8.1 Hz, 2H, Tyr-*H*3,3'), 6.72 (d, ³J = 8.0 Hz, 2H, Tyr-*H*2,2'), 5.12 (bs, 1H, -NHCOO^tBu), 4.23-4.15 (m, 2H, -COOCH₂CH₃), 4.13 (t, ³J = 7.2 Hz, 2H, -CH₂OAr), 3.97 (t, ³J = 6.2 Hz, 2H, PyNCH₂), 3.27 (d, ²J = 11.2 Hz, 1H, ArCH(*H'*)-), 3.11 (d, ²J = 13.7 Hz, 1H, ArCH(*H'*)-), 2.10 (m, 2H, -CH₂CH₂CH₂-), 1.53 (s, 3H, -C(CH₃)), 1.48 (s, 9H, ^tBu), 1.46 (s, 9H, ^tBu), 1.28 (t, ³J = 7.1 Hz, 3H, -COOCH₂CH₃). **¹³C-NMR** (125 MHz, CDCl₃): δ = 173.9, 157.9, 154.4, 154.3, 154.1, 147.5, 136.9, 130.9, 128.2, 119.8, 119.4, 114.0, 81.1, 79.3, 65.5, 61.4, 60.2, 44.1, 40.8, 28.8, 28.4, 28.2, 23.5, 14.1. **HPLC** (10-50%, 30 min): t_R = 27.19 min. **MS** (ESI): m/z = 580.1 [m+Na⁺]⁺, 458.1 [m+H⁺-Boc]⁺, 402.1 [m+H⁺-Boc-^tBu]⁺, 358.2 [m+H⁺-2Boc]⁺.

IV.3.117 Preparation of 2-(2,4,6-trimethylbenzamido)-2'-methyl-3-(4-(3-pyridin-2-ylpropoxy)phenyl)propionic acid, **65**



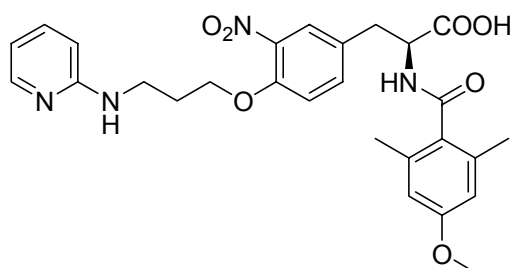
The title compound was prepared from **64** (100 mg, 180 μmol, 1 eq.) according to **GP8b** [36 mg (216 μmol, 1.2 eq.) 2,4,6-trimethylbenzoic acid, 82 mg (216 μmol, 1.2 eq.) HATU, 152 μL (0.9 mmol, 5 eq.) DIEA, 44 mg (1.8 mmol, 10 eq.) LiOH]. Purification by *reverse phase* HPLC gave 8.6 mg (15 μmol, 8%) of a colorless solid (TFA salt).

¹H-NMR (500 MHz, DMSO): δ = 12.35 (bs, 1H, -COOH), 8.67 (bs, 1H, Py-NH), 8.38 (s, 1H, -NHCOAr), 7.90 (d, ³J = 6.1 Hz, 1H, Py-*H*6), 7.85 (t, ³J = 7.8 Hz, 1H, Py-*H*4), 7.10 (d, ³J = 8.6 Hz, 2H, Tyr-*H*3,3'), 7.01 (d, ³J = 9.1 Hz, 1H, Py-*H*3), 6.87-6.81 (m, 5H, Tyr-*H*2,2'; Ar-*H*3,3'; Py-*H*5), 4.04 (t, ³J = 6.0 Hz, 2H, -CH₂OAr), 3.47 (m, 2H, PyNHCH₂-), 3.01 (d, ²J = 13.4 Hz, 1H, ArCH(*H'*)-), 2.95 (d, ²J = 13.4 Hz, ArCH(*H'*)-), 2.23 (s, 3H, Ar-CH₃), 2.22 (s, 6H, Ar(CH₃)₂), 2.04 (m, 2H, -CH₂CH₂CH₂-), 1.32 (s, 3H, C(CH₃)COOH). **¹³C-NMR** (125 MHz, DMSO): δ = 174.0, 168.5, 157.1, 142.4, 137.0, 135.0, 134.0, 131.2, 127.9, 127.7, 127.6, 113.7, 111.8, 64.6, 59.1, 42.2, 38.5, 27.6,

IV. Experimental Section

21.1, 20.5, 18.7. **HPLC** (10-50%, 30 min): $t_R = 28.13$ min. **MS** (ESI): $m/z = 476.2$ $[m+H]^+$.

IV.3.118 Preparation of (S)-3-(4-(3-(pyridin-2-ylamino)propoxy)-3-nitrophenyl)-2-(4-methoxy-2,6-dimethylbenzamido)propanoic acid, **67**.



$C_{27}H_{30}N_4O_7$
Exact Mass: 522.21
Mol. Wt.: 522.55

The title compound was prepared from the (N,O)-bis-Alloc-tyrosine **67** on (4-bromomethyl)phenoxymethyl polystyrene resin according to following procedure:

Step	Description	General procedure	HPLC (10-100%, 30 min) t_R [min]*	MS(ESI), m/z (M+H) ⁺ *
1	Resin loading	GP13	20.39	n.d.
2	O-Alloc deprotection	GP14	13.74	n.d.
3	Mitsunobu reaction with 19	GP2b	15.51	445.3
4	N-Alloc deprotection	GP23	8.89	361.6
5	Acylation with 32a	GP17	14.81	523.6
6	Cleavage from resin	GP20		

*the N-Boc-group is lost on cleavage from Wang resin.

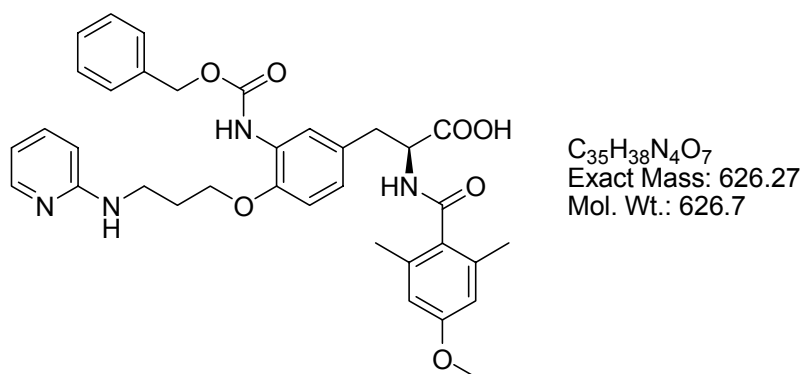
n.d. = not determined

A small amount of resin was cleaved (step 6), the rest used for the preparation of **69a-d**. The product was purified by *reverse phase* HPLC to give 3.2 mg of a light brown solid.

¹H-NMR (500 MHz, DMSO): $\delta = 13.26, 12.67$ (bs, 1H, -COOH), 8.61 (bs, 1H, Py-NH), 8.52 (d, $^3J = 8.5$ Hz, 1H, -NHCOAr), 7.93 (d, $^3J = 6.2$ Hz, 1H, Py-H6), 7.84 (t, $^3J = 7.9$ Hz, 1H, Py-H4), 7.83 (d, $^3J = 1.9$ Hz, 1H, Tyr-H3), 7.63 (dd, $^3J = 8.7$ Hz, $^4J = 2.0$ Hz, 1H, Tyr-H5), 7.34 (d, $^3J = 8.7$ Hz, 1H, Tyr-H6), 6.99 (d, $^3J = 9.0$ Hz, 1H, Py-H3), 6.83 (t, $^3J = 6.6$ Hz, 1H, Py-H5), 6.53 (s, 2H, Ar-H3,3'), 4.74-4.62 (m, 1H, -CHCOOH), 4.25 (t, $J = 5.8$ Hz, 2H, -CH₂OAr), 3.69 (m, 2H, PyNHCH₂-), 3.47 (s, 3H,

ArOCH₃), 3.20 (dd, ²J = 14.0 Hz, ³J = 3.9 Hz, 1H, ArCH(H')-), 2.87 (dd, ²J = 13.8 Hz, ³J = 11.8 Hz, 1H, ArCH(H')-), 2.15-2.01 (m, 2H, -CH₂CH₂CH₂-), 1.94 (s, 6H, Ar(CH₃)₂). ¹³C-NMR (125.1 MHz, DMSO): δ = 172.6, 169.0, 158.6, 149.9, 142.2, 138.8, 135.4, 135.2, 130.7, 130.7, 128.3, 127.9, 125.6, 115.0, 112.7, 112.2, 111.8, 66.6, 54.9, 52.9, 38.2, 34.7, 27.3, 18.6. HPLC (10-100%, 30'): t_R = 23.72 min. MS (ESI): m/z = 1045.0 [2m+H⁺]⁺, 523.3 [m+H⁺]⁺.

IV.3.119 Preparation of (S)-3-(4-(3-(pyridin-2-ylamino)propoxy)-3-(benzyloxycarbonylamino)phenyl)-2-(4-methoxy-2,6-dimethylbenzamido)propanoic acid, 68a.

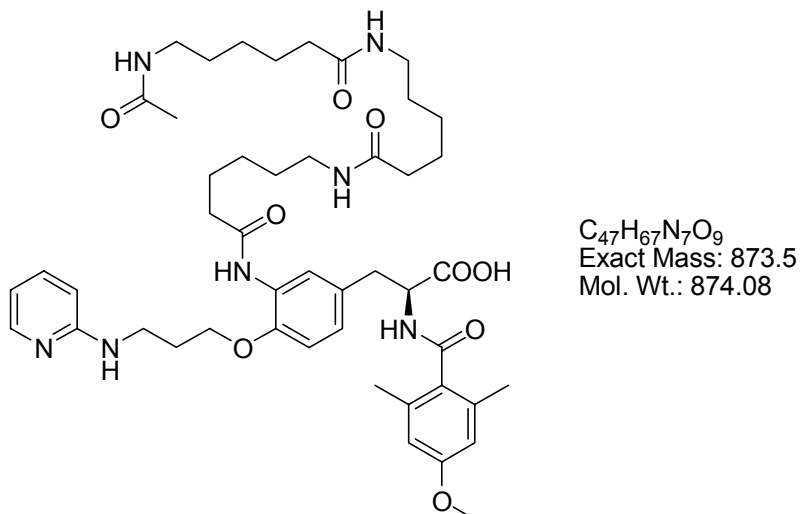


The title compound was prepared from Wang resin loaded with **67**. The nitro function was reduced according to **GP23**. The Cbz-group was introduced by treatment of the amino-functionalized resin with benzyl chloroformate (3 eq.) and DIEA (5 eq.) in DCM for 30 min. After washing of the resin with DCM (five times), the product **69a** was cleaved from the resin (**GP20**) and purified by *reverse phase* HPLC to give 5.6 mg of a light brown solid.

¹H-NMR (500 MHz, DMSO): δ = 13.26, 12.67 (bs, 1H, -COOH), 8.65 (bs, 1H, Py-NH), 8.55 (s, 1H, -NHCOOBn), 8.46 (d, ³J = 8.3 Hz, 1H, -NHCOAr), 7.89 (d, ³J = 6.0 Hz, 1H, Py-H6), 7.80 (t, ³J = 7.7 Hz, 1H, Py-H4), 7.65 (s, 1H, Tyr-H3), 7.41 (t, ³J = 7.2 Hz, 2H, Cbz-H3,3'), 7.38 (t, ³J = 7.4 Hz, 2H, Cbz-H2,2'), 7.33 (t, ³J = 7.1 Hz, 1H, Cbz-H4), 7.02-6.97 (m, 2H, Py-H3, Tyr-H5), 6.93 (d, ³J = 8.4 Hz, Tyr-H6), 6.80 (t, ³J = 6.6 Hz, 1H, Py-H5), 6.51 (s, 2H, Ar-H3,3'), 5.15 (s, 2H, Ph-CH₂O), 4.58 (ddd, ³J = 12.2 Hz, ³J = 8.3 Hz, ³J = 4.2 Hz, 1H, -CHCOOH), 4.07 (t, ³J = 5.8 Hz, 2H, -CH₂OAr), 3.70 (s, 3H, Ar-OCH₃), 3.49 (m, 2H, Py-NHCH₂-), 3.07 (dd, ²J = 13.9 Hz, ³J = 4.0 Hz, 1H, Ar-CH(H')-), 2.78 (dd, ²J = 13.8 Hz, ³J = 11.1 Hz, 1H, Ar-CH(H')-), 2.06 (m, 2H, -CH₂CH₂CH₂-), 1.97 (s, 6H, Ar(CH₃)₂). ¹³C-NMR (125.1 MHz, DMSO):

δ = 173.0, 169.0, 158.5, 153.5, 147.7, 142.2, 136.6, 135.6, 130.9, 130.0, 128.3, 127.8, 126.7, 124.7, 124.7, 112.1, 111.8, 111.7, 109.0, 65.7, 65.6, 54.9, 53.5, 38.6, 35.7, 27.4, 18.8. **HPLC** (10-100%, 30 min): t_R = 16.58 min. **MS** (ESI): m/z = 627.3 $[m+H]^+$.

IV.3.120 Preparation of 68b

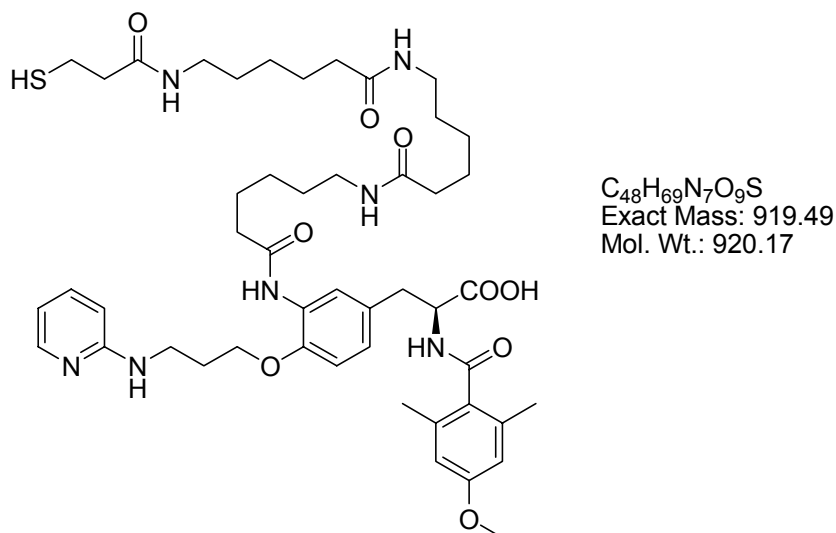


The title compound was prepared from Wang resin loaded with **67**. The nitro function was reduced according to **GP23**. The three aminohexanoic acid building blocks (Fmoc-amino hexanoic acid) were coupled according to following procedure: **GP15**, **GP14**, **GP15**, **GP14**, **GP17** and **GP14**. The free *N*-terminus was acetylated with a solution of acetic acid anhydride (3 eq.) and DIEA (5 eq.) in NMP for 30 min. After washing with NMP and DCM (five times each), the product **68b** was cleaved from the resin (**GP20**) and purified by *reverse phase* HPLC to give 4.5 mg of a colorless solid.

1H -NMR (500 MHz, DMSO): δ = 8.91 (s, 1H, Py-NH), 8.48 (d, 3J = 8.3 Hz, 1H, -NHCOAr), 7.90 (d, 3J = 5.6 Hz, Py-H6), 7.82 (s, 1H, ArNHCO-), 7.77-7.70 (m, 3H, Ahx-NHCO), 7.02-6.93 (m, 3H, Py-H3, Tyr-H5,6), 6.75 (m, 1H, Py-H5), 6.51 (s, 2H, Ar-H3,3'), 4.57 (m, 1H, -CHCOOH), 4.08 (t, 3J = 6.0 Hz, 2H, -CH₂OAr), 3.69 (s, 3H, -ArOCH₃), 3.49 (m, 2H, PyNHCH₂-), 3.06 (dd, 2J = 13.9 Hz, 3J = 3.8 Hz, 1H, ArCH(H')), 3.02-2.96 (m, 6H, Ahx-CH₂NH), 2.78 (dd, 2J = 13.7 Hz, 3J = 11.2 Hz, 1H, ArCH(H')), 2.38 (t, 3J = 7.0 Hz, 2H, 2H, Ahx-CH₂CONHAr), 2.06 (m, 2H, -CH₂CH₂CH₂OAr), 2.02 (t, 3J = 7.5 Hz, 4H, Ahx-CH₂CO), 1.98 (s, 6H, Ar(CH₃)₂), 1.77 (s, 3H, NHCOCH₃), 1.57 (m, 2H, Ahx-H), 1.46 (4H, 4H, Ahx-H), 1.40-1.32 (m, 6H, Ahx-H), 1.28 (m, 2H, Ahx-H), 1.20 (m, 4H, Ahx-H). **^{13}C -NMR** (125.1 MHz, DMSO)

δ = 173.0, 171.7, 171.7, 171.0, 169.0, 168.8, 158.5, 147.5, 135.6, 130.9, 129.9, 127.1, 124.8, 123.1, 112.1, 111.9, 111.7, 65.7, 54.8, 53.5, 38.3, 38.2, 38.1, 35.9, 35.7, 35.3, 28.9, 28.9, 28.8, 27.7, 26.0, 25.0, 24.9, 22.5, 18.8. **HPLC** (10-50%, 30 min): t_R = 22.04 min. **MS** (ESI): m/z = 896.5 $[m+Na]^+$, 874.7 $[m+H]^+$.

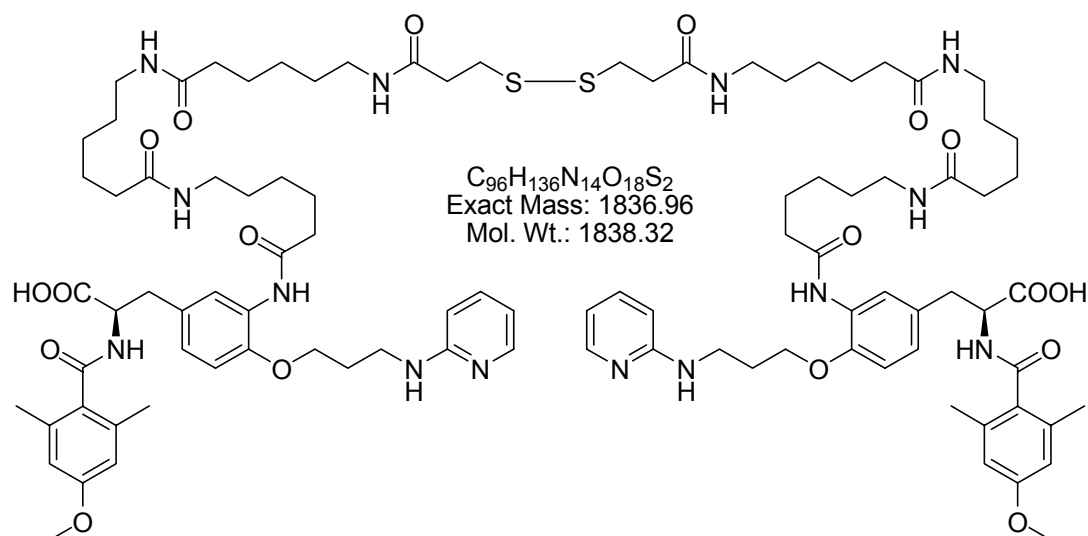
IV.3.121 Preparation of 69c



The title compound was prepared from Wang resin loaded with **67**. The nitro function was reduced according to **GP23**. The three aminohexanoic acid building blocks (Fmoc-aminohexanoic acid) were coupled according to following procedure: **GP15**, **GP14**, **GP15**, **GP14**, **GP17** and **GP14**. 3-Tritylthiopropionic acid was coupled via **GP17**, the product **69c** cleaved from the resin (**GP20**) and purified via *reverse phase* HPLC to give 8.6 mg of a light brown solid.

HPLC (10-50%, 30 min): t_R = 24.05 min. **MS** (ESI): m/z = 920.5 $[m+H]^+$.

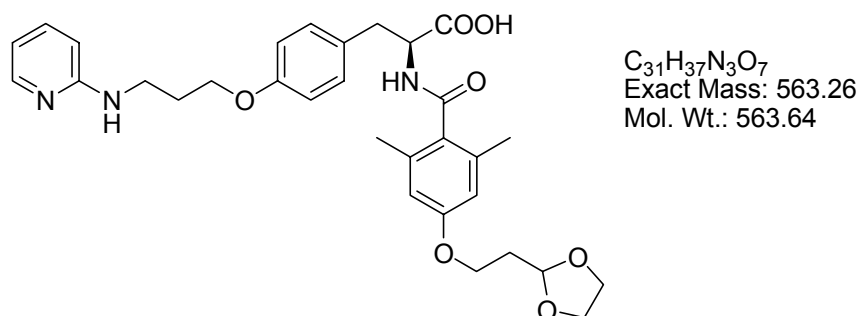
IV.3.122 Preparation of 68d



4.1 mg of **68c** (4.5 μ mol) were dissolved in 1 mL DMSO / water 7:3. The pH was adjusted to 8-9 with $NaHCO_3$ and the mixture was shaken vigorously at ambient temperature for 4 h (HPLC-monitoring). The solvents were removed at the SpeedVac and the crude product purified by *reverse phase* HPLC to give 2.5 mg (1.4 μ mol, 33%) of a light brown solid.

HPLC (10-50%, 30 min): $t_R = 27.16$ min. **MS** (ESI): $m/z = 1860.7$ [$m+Na^+$] $^+$, 1837.7 [$m+H^+$] $^+$, 942.5 [$m+2Na^+$] $^{2+}$, 930.8 [$m+Na^++H^+$] $^{2+}$, 919.8 [$m+2H^+$] $^{2+}$.

IV.3.123 Preparation of 3-(4-(3-(pyridin-2-ylamino)propoxy)phenyl)-2-(S)-(4-(2-(1,3-dioxolan-2-yl)ethoxy)-2,6-dimethylbenzamido)propanoic acid, 69.

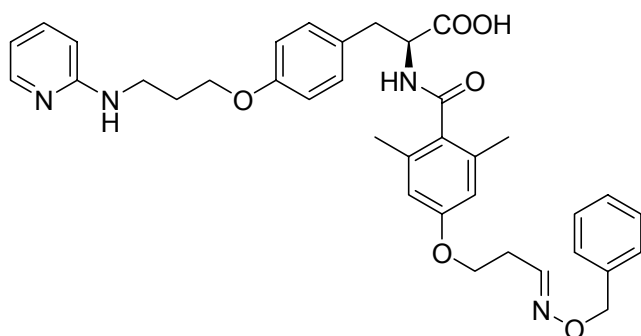


The title compound was prepared from **22b** (465 mg, 850 μ mol) following **GP8b** [**32c** (236 mg, 935 μ mol), HATU (389 mg, 1.02 mmol), DIEA (722 μ L, 4.25 mmol), LiOH

(102 mg, 4.25 mmol)]. Purification using preparative HPLC and lyophilization afforded **69** (86 mg, 153 μ mol, 18%) as TFA salt (colorless solid).

$^1\text{H-NMR}$ (500 MHz, DMSO): δ = 12.67 (bs, 1H, -COOH), 8.71 (bs, 1H, Py-NH), 8.44 (d, 3J = 8.3 Hz, 1H, -NHCOAr), 7.92 (d, 3J = 6.1 Hz, 1H, Py-H6), 7.86 (t, 3J = 7.9 Hz, 1H, Py-H4), 7.20 (d, 3J = 8.5 Hz, 2H, Tyr-H3,3'), 7.03 (d, 3J = 9.0 Hz, 1H, Py-H3), 6.85 (d, 3J = 8.6 Hz, 2H, Tyr-H2,2'), 6.82 (t, 3J = 6.5 Hz, 1H, Py-H5), 6.52 (s, 2H, Ar-H2,2'), 4.95 (t, 3J = 6.6 Hz, 1H, -CH₂CH(OCH₂)₂), 4.65-4.55 (m, 1H, -CHCOOH), 4.05 (t, 3J = 6.2 Hz, 2H, Ar-OCH₂), 4.02 (t, 3J = 6.6 Hz, 2H, -CH₂OTyr), 3.90 (m, 2H, -OCH(H')CH(H')O-), 3.78 (m, 2H, -OCH(H')CH(H')O-), 3.47 (t, 3J = 5.7 Hz, 2H, Py-NHCH₂), 3.09 (dd, 2J = 13.9 Hz, 3J = 4.0 Hz, 1H, Tyr-CH(H')), 2.79 (dd, 2J = 13.7 Hz, 3J = 11.5 Hz, 1H, TyrCH(H')), 2.04 (m, 2H, -CH₂CH₂CH₂-), 1.99 (m, 2H, ArOCH₂CH₂CH), 1.94 (s, 6H, Ar(CH₃)₂). **$^{13}\text{C-NMR}$** (125 MHz, DMSO): δ = 173.1, 169.0, 157.6, 156.9, 153.0, 142.4, 136.5, 135.6, 131.0, 130.0, 114.1, 112.9, 112.7, 111.8, 101.1, 64.7, 64.1, 63.2, 53.4, 38.5, 35.4, 33.2, 27.5, 18.7. **HPLC** (10-100%, 30 min): t_R = 14.38 min. **MS** (ESI): m/z = 564.6 [$m+\text{H}^+$]⁺.

IV.3.124 Preparation of (S)-3-(4-(3-(pyridin-2-ylamino)propoxy)phenyl)-2-(4-(3-benzyloxyiminopropoxy)-2,6-dimethylbenzamido)propanoic acid **70.**



C₃₆H₄₀N₄O₆
Exact Mass: 624.29
Mol. Wt.: 624.73

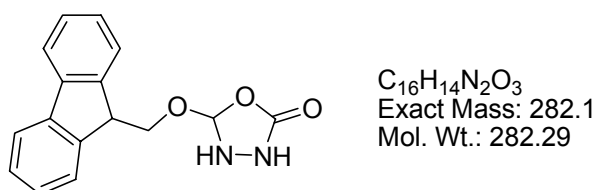
10 mg (18 μ mol, 1eq.) **69** were dissolved in 2 mL of dioxane / water 1 : 1. A catalytic amount (1 drop) of conc. hydrochloric acid was added and the resulting mixture put in a shaker at 40°C for 24 h (HPLC monitoring: t_R (Aldehyde, 10-100%, 30 min) = 13.13 min). After lyophilization, the deprotected compound and *O*-benzylhydroxylamine hydrochloride (5.8 mg, 36 μ mol, 2 eq.) were dissolved in 1 mL

IV. Experimental Section

of dry pyridine and stirred at ambient temperature for 2 h. The solvents were removed *in vacuo* and the crude product purified via *reverse phase* HPLC to give 1.2 mg (1.9 μmol , 11%) of a colorless solid.

HPLC (10-100%, 30 min): $t_R = 19.02$ min. **MS** (ESI): $m/z = 625.2$ [$m+H^+$]⁺.

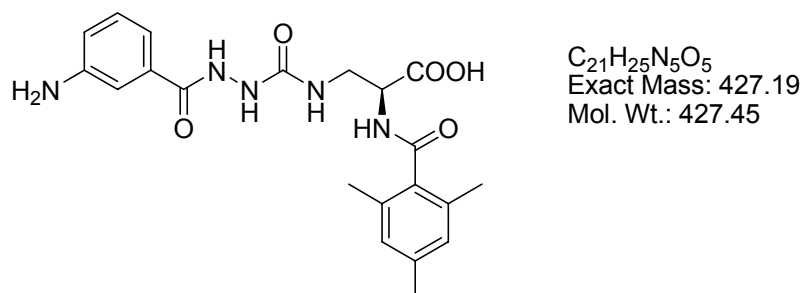
IV.3.125 Preparation of 5-(9H-fluoren-9-yloxy)-1,3,4-oxadiazolidin-2-one, 71



Fmoc-hydrazine hydrochloride (0.33 g, 1.28 mmol, 1 eq.) was suspended in 25 mL of DCM / saturated NaHCO_3 solution (1/1) in an ice-bath for five minutes under vigorous stirring. Stirring was stopped and the layers were allowed to separate for additional five minutes. 2 mL of a 1.9 M solution of phosgene in toluene (3.80 mmol, 3.0 eq.) were injected into the lower, organic phase and stirring was restarted for ten minutes. The organic layer was separated, the aqueous layer extracted twice with 10 mL DCM and the combined organic layers dried over Na_2SO_4 , filtered and the filtrate concentrated under reduced pressure. The crude product was thoughtfully dried under vacuum and used without further purification. Yield: 0.32 g (1.13 mmol, 89%) of a colorless solid.

$^1\text{H-NMR}$ (250 MHz, CDCl_3): $\delta = 7.77$ (m, 2H, Ar-H), 7.61 (m, Ar-H), 7.37 (m, 4H, Ar-H), 4.51 (t, $^3J = 7.4$ Hz, 1H, CHCH_2O), 4.40 (s, 2H, $-\text{CH}_2\text{O}$).

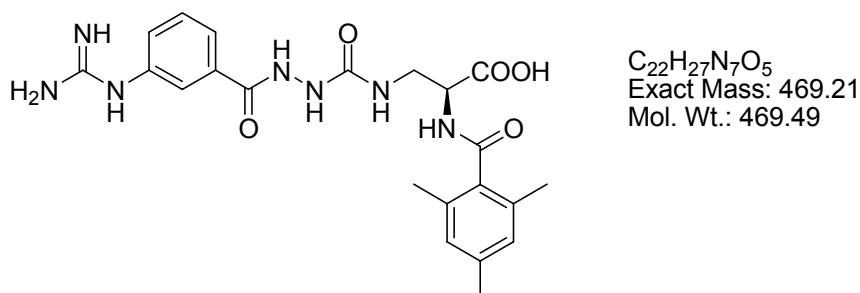
IV.3.126 Preparation of 3-[N-(N'-(3-aminobenzoyl)-hydrazino)carbonyl]amino-2-(S)-(2,4,6-trimethylbenzamido)propionic acid, 72.



TCP resin was loaded with Fmoc-Dap(Alloc)-OH (Dap = 2,3 diaminopropionic acid) according to **GP12**. After Fmoc deprotection (**GP14**), the α -amino group was acylated with mesitylene carboxylic acid (**GP17**). The side chain was deprotected according to **GP24** and the aza-glycine prepared using freshly prepared **71** (**GP25**). Fmoc deprotection (**GP14**), coupling of 3-Fmoc-aminobenzoic acid (**GP17**) and subsequent Fmoc deprotection afforded the resin loaded with **72**. A small amount was cleaved according to **GP20** (DCM / TFA / H₂O / TIPS = 47.5 / 47.5 / 2.5 / 2.5) and purified by *reverse phase* HPLC to give 1.5 mg (2.7 μ mol) of a colorless solid.

¹H-NMR (500.1 MHz, DMSO): δ = 9.99 (s, 1H, ArCONH₂), 8.39 (d, ³J = 6.6 Hz, 1H, NHMes), 8.13 (s, 1H, ArCONH₂), 7.21 (m, 1H, H-Ar), 7.19 (m, 2H, H-Ar), 6.88 (m, 1H, H-Ar), 6.83 (s, 2H, Mes-H_{3,3'}), 6.47 (bs, 1H, CONHCH₂CH), 4.36 (m, 1H, -CH₂CH), 3.60-3.55 (m, 1H, -CH(H')CH), 3.30 (m, 1H, CH(H')CH), 2.22 (s, 3H, Mes-CH₃), 2.20 (s, 6H, Mes-(CH₃)₂). **¹³C-NMR** (125 MHz, DMSO): δ = 172.7, 170.2, 167.5, 159.3, 138.1, 136.0, 134.9, 134.4, 129.7, 128.5, 54.3, 21.5, 19.7. **HPLC** (10-50%, 30 min): t_R = 14.71 min. **MS** (ESI): m/z = 1282.0 [3m+H⁺]⁺, 877.2 [2m+Na⁺]⁺, 855.1 [2m+H⁺]⁺, 428.1 [m+H⁺]⁺.

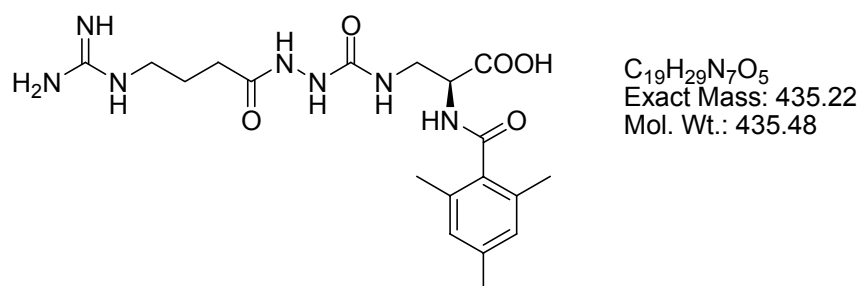
IV.3.127 Preparation of 3-[N-(N'-3-(guanidylbenzoyl)-hydrazino)carbonyl]amino-2-(S)-(2,4,6-trimethylbenzamido)propionic acid, 73.



Resin loaded with **72** was guanidylated according to **GP26**. Compound **74** was obtained by simultaneous cleavage and Boc-deprotection with DCM / TFA / H₂O / TIPS = 47.5 / 47.5 / 2.5 / 2.5 (**GP20**). The crude product was purified by *reverse phase* HPLC to give 4.8 mg (8.2 μmol) as colorless solid (TFA salt).

¹H-NMR (500 MHz, DMSO): δ = 12.69 (bs, 1H, COOH), 10.22 (s, 1H, ArCONHNH), 9.93 (s, 1H, NHAr), 8.40 (d, ³J = 6.8 Hz, 1H, -NHCOMes), 8.26 (s, 1H, NHNHCONH), 7.77 (d, ³J = 7.7 Hz, 1H, Ar-H4), 7.72 (s, 1H, Ar-H2), 7.54 (t, ³J = 7.6 Hz, 1H, Ar-H5), 7.46 (m, 3H, ^{guanidine}NH), 7.41 (d, ³J = 7.9 Hz, 1H, Ar-H6), 6.83 (s, 2H, Mes-H3,3'), 6.53 (bs, 1H, CONHCH₂CH), 4.39 (m, 1H, -CHCOOH), 3.56 (td, ²J = 12.6 Hz, ³J = 5.2 Hz, 1H, NHCH(H')CH), 3.31 (m, 1H, NHCH(H')CH), 2.23 (s, 3H, MesCH₃), 2.21 (s, 6H, Mes(CH₃)₂). **¹³C-NMR** (125.1 MHz, DMSO): δ = 171.8, 169.3, 165.4, 158.2, 155.6, 137.2, 135.5, 135.1, 134.0, 133.9, 129.7, 127.5, 125.2, 123.3, 53.1, 40.2, 39.4, 20.5, 18.7. **HPLC** (10-100%, 30 min): t_R = 15.48 min. **MS** (ESI): m/z = 939.2 [2m+H⁺]⁺, 470.2 [m+H⁺]⁺.

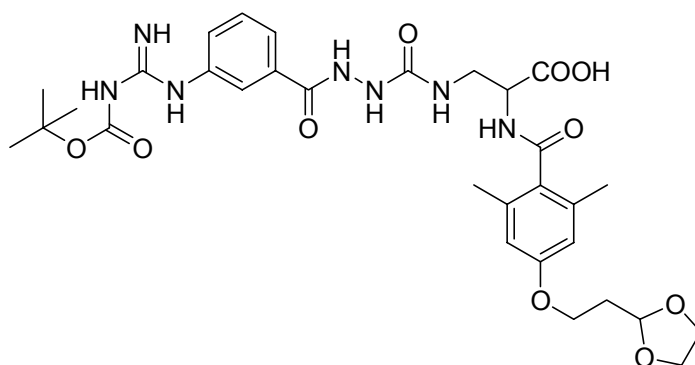
IV.3.128 Preparation of 3-[N-(N'-3-(guanidylpropylcarbonyl)-hydrazino)carbonyl]amino-2-(S)-(2,4,6-trimethylbenzamido)propionic acid, 74.



TCP resin was loaded with Fmoc-Dap(Alloc)-OH (Dap = 2, 3 diaminopropionic acid) according to **GP12**. After Fmoc deprotection (**GP14**), the α -amino group was acylated with mesitylene carboxylic acid (**GP17**). The side chain was deprotected according to **GP24** and the aza-glycine prepared using freshly prepared **71** (**GP25**). Fmoc-deprotection (**GP14**), coupling of Fmoc-GABA (GABA = γ -aminobutyric acid) (**GP15**) and subsequent Fmoc deprotection (**GP14**) gave the resin-bound free amine, which was guanylated according to **GP26**. Compound **74** was obtained by simultaneous cleavage and Boc-deprotection with DCM / TFA / H₂O / TIPS = 47.5 / 47.5 / 2.5 / 2.5 (**GP20**). The crude product was purified by *reverse phase* HPLC to give 3.8 mg (6.9 μ mol) as colorless solid (TFA salt).

¹H-NMR (500 MHz, DMSO): δ = 9.56 (s, 1H, -NHNHCONH), 8.39 (d, ³J = 7.1 Hz, 1H, NHCOMes), 8.07 (bs, 1H, -NHNHCONH), 7.56 (t, ³J = 5.6 Hz, 1H, ^{Guanidine}NHCH₂), 6.84 (s, 2H, Mes-H_{3,3'}), 6.42 (bs, 1H, CONHCH₂), 4.37 (m, 1H, CHCOOH), 3.54-3.49 (m, 1H, CH(H')CH), 3.29 (m, 1H, CH(H')CH), 3.11 (dd, ²J = 13.1 Hz, ³J = 6.7 Hz, 2H, NHCH₂), 2.23 (s, 3H, Mes-CH₃), 2.20 (s, 6H, Mes-(CH₃)₂), 2.13 (t, J = 7.24 Hz, 2H, -CH₂CH₂CON), 1.70 (m, 2H, CH₂CH₂CH₂). **¹³C-NMR** (125.1 MHz, DMSO): δ = 171.8, 171.5, 169.2, 158.2, 156.6, 137.2, 135.1, 133.8, 127.5, 53.0, 30.0, 24.3, 20.5, 18.7. **HPLC** (10-50%, 30 min): t_R = 15.27 min. **MS** (ESI): m/z = 436.2 [m+H⁺]⁺.

IV.3.129 Preparation of 3-[N-(N-(3-(bis-Boc-guanidylpropylcarbonyl)-hydrazino)carbonyl]amino-2-(S)-(2,6-trimethyl-4-(2-(1,3-dioxolan-2-yl)ethoxy)benzamido)propionic acid, **75.**



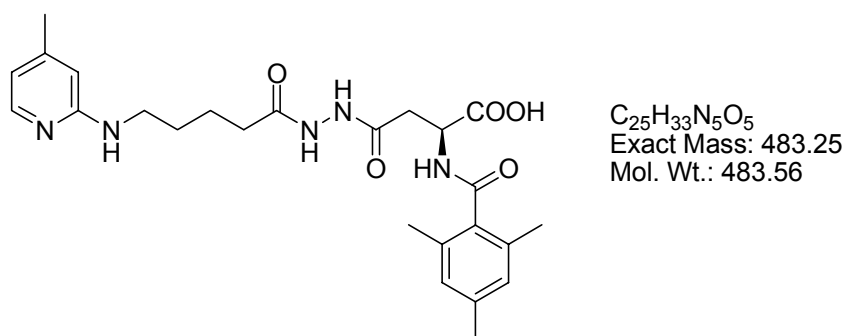
C₃₁H₄₁N₇O₁₀
Exact Mass: 671.29
Mol. Wt.: 671.7

IV. Experimental Section

TCP resin was loaded with Fmoc-Dap(Alloc)-OH (Dap = 2,3 diaminopropionic acid) according to **GP12**. After Fmoc deprotection (**GP14**), the α -amino group was acylated with **32c** (**GP17**). The side chain was deprotected according to **GP24** and the *aza*-glycine prepared using freshly prepared **71** (**GP25**). Fmoc-deprotection (**GP14**), coupling of 3-Fmoc-aminobenzoic acid (**GP15**) and subsequent Fmoc deprotection (**GP14**) gave the resin-bound free amine, which was guanidylated according to **GP26**. Compound **75** was obtained by careful cleavage under mild conditions (**GP19**) – one Boc group was lost under the specified conditions. The crude product was purified by *reverse phase* HPLC to give 0.9 mg (1.3 μ mol) as colorless solid.

HPLC (10-50%, 30 min): t_R = 25.55 min. **MS** (ESI): m/z = 672.2 $[m+H^+]^+$, 572.2 $[m+H^+-Boc]$.

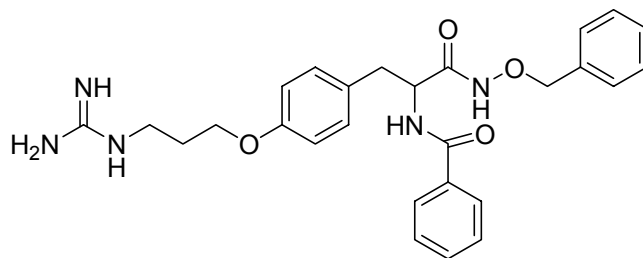
IV.3.130 Preparation of 3-(5-(4-methylpyridin-2-ylamino)pentylamidocarbamoyl)-2-(2,4,6-trimethylbenzamido)propanoic acid, **76**



TCP resin was loaded with Fmoc-Asp(OAll)-OH (α -Fmoc-aspartic acid- γ -allyl ester) according to **GP12**. After Fmoc deprotection (**GP14**), the α -amino group was acylated with mesitylene carboxylic acid (**GP17**). The side chain was deprotected according to **GP24** and coupled to Fmoc-hydrazine (**GP15**). Fmoc was removed (**GP14**) and the free amine coupled to 5-(4-methylpyridin-2-ylamino)pentanoic acid (**GP15**). Compound **76** was obtained by cleavage with DCM / TFA / H₂O / TIPS = 47.5 / 47.5 / 2.5 / 2.5 (**GP20**). The crude product was purified by *reverse phase* HPLC to give 1.0 mg (1.7 μ mol) as colorless solid (TFA salt).

HPLC (10-50%, 30 min): t_R = 19.44 min. **MS** (ESI): m/z = 484.8 $[m+H^+]^+$.

IV.3.131 Preparation of 2-(benzamido)-3-[4-(3-guanidylpropoxy)phenyl]-*N*-benzoypropionamide, 77

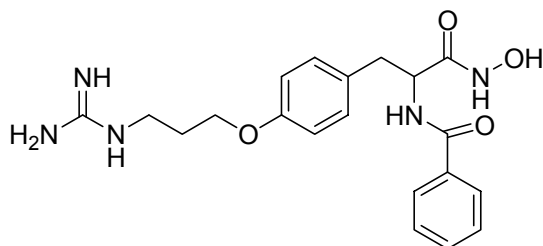


C₂₇H₃₁N₅O₄
Exact Mass: 489.24
Mol. Wt.: 489.57

O-Benzylhydroxylamine (60 mg, 488 μmol, 2 eq.), **4a** (120 mg, 241 μmol, 1 eq.), HOBT (40 mg, 289 μmol, 1.2 eq.) and TBTU (110 mg, 289 μmol, 1.2 eq.) were dissolved in 1 mL dry DMF. After addition of DIEA (205 μL, 1.21 mmol, 5 eq.), the mixture was stirred over night. The DMF was evaporated and the crude product purified by preparative HPLC to give 65 mg (108 μmol, 45%) of a light yellow solid (TFA salt)

¹H-NMR (500 MHz, DMSO): δ = 11.37 (s, 1H, *NHOBn*), 8.62 (d, ³*J* = 8.3 Hz, 1H, -*NHCOPh*), 7.83 (d, *J* = 8.3 Hz, 2H, Ph-*H2,2'*), 7.58 (bs, 1H, ^{guanidine}*NH*), 7.52 (t, ³*J* = 7.4 Hz, 1H, Ph-*H4*), 7.45 (t, ³*J* = 7.4 Hz, 2H, Ph-*H3,3'*), 7.36 (m, 5H, *Bn-H*), 7.23 (d, *J* = 8.5 Hz, 2H, Tyr-*H3,3'*), 6.83 (d, *J* = 8.6 Hz, 2H, Tyr-*H2,2'*), 4.78 (d, ²*J* = 11.0 Hz, 1H, *CONHOCH(H')*Ph), 4.79 (d, ²*J* = 11.0 Hz, 1H, *CONHOCH(H')*Ph), 4.50 (m, 1H, *CHCONO*), 3.94 (t, ³*J* = 6.1 Hz, 2H, -*CH₂OAr*), 3.24 (q, *J* = 6.6 Hz, 2H, *NHCH₂CH₂*), 2.94 (m, 2H, *Ar-CH₂-*), 1.88 (m, 2H, -*CH₂CH₂CH₂-*). **¹³C-NMR** (125.1 MHz, DMSO): δ = 210.9, 168.1, 166.1, 156.9, 156.7, 135.7, 133.8, 131.2, 130.1, 130.0, 128.8, 128.1, 128.0, 127.4, 114.0, 76.8, 64.5, 53.0, 37.8, 36.3, 28.1. **HPLC** (10-50%, 30 min): *t_R* = 25.75 min. **MS** (ESI): *m/z* = 979.4 [*2m+H*⁺]⁺, 490.5 [*m+H*⁺]⁺.

IV.3.132 Preparation of 2-(benzamido)-3-[4-(3-guanidylpropoxy)phenyl]-*N*-hydroxypropionamide, 78



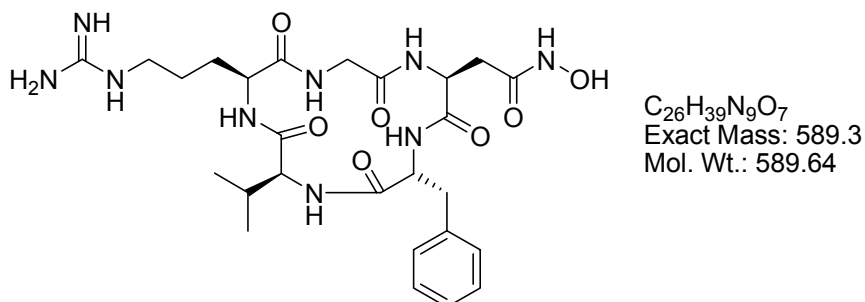
C₂₀H₂₅N₅O₄
Exact Mass: 399.19
Mol. Wt.: 399.44

IV. Experimental Section

50 mg **77** (83 μmol) was benzyle deprotected according to **GP4** (MeOH, 30 atm H_2 , 5 mg Pd/C, 1 h). The mixture was filtered, the solvent evaporated and the crude product purified by *reverse phase* HPLC to give 24 mg (58 μmol , 68%) of a colorless solid (TFA salt).

$^1\text{H-NMR}$ (500 MHz, DMSO): δ = 10.77 (s, 1H, CONHOH), 8.87 (bs, CONHOH), 8.59 (d, 3J = 8.5 Hz, 1H, -NHCOPh), 7.81 (d, J = 7.2 Hz, 2H, Ph-*H2,2'*), 7.64 (t, 3J = 5.1 Hz, 1H, ^{guanidine}NHCH₂), 7.51 (t, J = 7.3 Hz, 1H, Ph-*H4*), 7.43 (t, J = 7.5 Hz, 2H, Ph-*H3,3'*), 7.40-6.80 (bs, 2H, ^{guanidine}NH), 7.24 (d, J = 8.5 Hz, 2H, Tyr-*H3,3'*), 6.83 (d, J = 8.6 Hz, 1H, Tyr-*H2,2'*), 4.54 (m, 1H, -CHCONHOH), 3.94 (t, 3J = 6.0 Hz, 2H, -CH₂OAr), 3.24 (q, J = 6.6 Hz, 2H, NHCH₂-), 2.97-2.95 (m, 2H, Ar-CH₂CH), 1.89 (m, 2H, -CH₂CH₂CH₂-). **$^{13}\text{C-NMR}$** (125 MHz, DMSO): δ = 168.0, 166.0, 156.8, 156.7, 133.9, 131.1, 130.2, 130.0, 128.0, 127.3, 114.0, 64.4, 52.9, 37.8, 36.5, 28.1. **HPLC** (10-50%, 30 min): t_{R} = 15.74 min. **MS** (ESI): m/z = 400.2 [$m+\text{H}^+$]⁺.

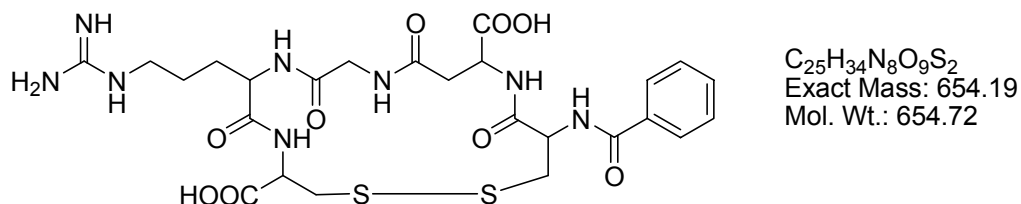
IV.3.133 Preparation of *cyclo(-Arg-Gly-Asp(NHOH)-D-Phe-Val-)*, **79**



The title compound was synthesized on solid phase (TCP-resin, 500 mg, loading 0.60 mmol / g) according to the general procedures **GP12** (loading with Fmoc-Gly-OH), **GP14** (Fmoc-deprotection) and **GP15** (Coupling). Fmoc-Asp(OAll)-OH was coupled as last amino acid, then Alloc deprotected (**GP24**), coupled to *O*-benzylhydroxylamine (**GP15**). The linear peptide was Fmoc-deprotected (**GP14**), cleaved under retention of protecting groups (**GP19**) and cyclized (**GP20**). After cyclization, the peptide was side-chain deprotected (**GP21**) and half of the deprotected peptide hydrogenated (**GP4**, DMA, 10 mg Pd/C, 25 atm H_2 , 1 h). The crude peptide was purified by *reverse phase* HPLC. Yield was 7 mg (10 μmol , 7% of total) of a colorless solid (TFA salt).

¹H-NMR (500 MHz, DMSO): δ = 10.40 (s, 1H, -CONHOH), 8.75 (bs, 1H, -CONHOH), 8.40 (dd, 2J = 7.2 Hz, 3J = 4.4 Hz, 1H, Gly-NH), 8.02 (d, 3J = 7.1 Hz, 1H, -CONH), 8.01 (d, 3J = 8.5 Hz, 1H, -CONH), 7.85 (d, 3J = 7.8 Hz, 1H, -CONH), 7.71 (d, 3J = 7.7 Hz, 1H, -CONH), 7.51 (t, 3J = 5.7 Hz, 1H, guanidineNHCH₂), 7.26-7.51 (m, 6H, -CONH + Ph-H), 4.68 (dd, J = 15.2 Hz, J = 7.4 Hz, 1H, H α), 4.53 (dd, J = 14.3 Hz, J = 7.5 Hz, 1H, H α), 4.09 (dd, J = 14.1 Hz, J = 7.8 Hz, 1H, H α), 4.03 (dd, 2J = 15.0 Hz, 3J = 7.6 Hz, 1H, Gly-H α), 3.80 (t, J = 7.4 Hz, 1H, H α), 3.37 (m, 1H, H α), 3.22 (dd, J = 14.9 Hz, Gly-H α'), 3.09 (m, 2H, Arg-H δ), 2.91 (dd, 2J = 13.4 Hz, 1H, Phe-H β), 2.82 (dd, 2J = 13.2 Hz, 3J = 5.8 Hz, 1H, Phe-H β'), 2.17 (dd, 2J = 15.0 Hz, 3J = 6.5 Hz, 1H, H β), 1.85 (m, 1H), 1.72 (m, 1H), 1.59 (m, 1H), 1.39 (m, 3H), 0.72 (d, 3J = 6.8 Hz, 3H, (CH₃)CH(CH'₃)), 0.66 (d, 3J = 6.7 Hz, 3H, (CH₃)CH(CH'₃)). **¹³C-NMR** (125 MHz, DMSO): δ = 172.1, 172.0, 171.7, 171.0, 170.4, 167.2, 157.5, 138.2, 130.0, 129.0, 127.1, 60.9, 55.0, 53.1, 49.8, 44.1, 41.2, 38.1, 34.0, 30.3, 29.1, 26.3, 20.1, 19.0. **HPLC** (10-50%, 30 min): t_R = 16.11 min. **MS** (ESI): m/z = 590.3 [m+H⁺]⁺.

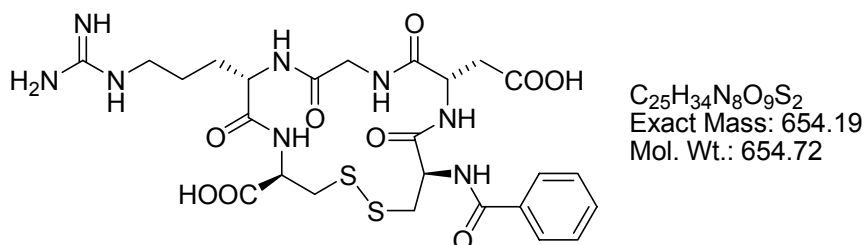
IV.3.134 Preparation of *iso*DGR2C, 80



The title compound was synthesized on solid phase (TCP-resin, 300 mg, loading 0,71 mmol / g) according to the general procedures **GP12** (loading with Fmoc-Cys(Trt)-OH), **GP14** (Fmoc-deprotection) and **GP15** (Coupling). Fmoc-Asp-O^tBu was employed as *iso*Asp-building block. The linear, Fmoc deprotected peptide H-(Cys-*iso*Asp-Gly-Arg-Cys)-TCP was benzoylated with 3 eq. benzoyl chloride and 5 eq. DIEA in NMP for 30 min. After washing with DCM (five times), the linear peptide was cleaved and deprotected (**GP20**) and precipitated in diethyl ether. Cyclization was achieved according to **GP22**, the solvents were removed and the crude peptide purified by *reverse phase* HPLC. Yield was 22 mg (29 μ mol, 14 %) of a colorless solid (TFA salt).

¹H-NMR (500 MHz, DMSO): δ = 12.91 (bs, 1H, -COOH), 8.60 (d, 3J = 9.0 Hz, 1H, *iso*Asp-NH), 8.46 (d, 3J = 8.0 Hz, 1H, Cys²-NHCOPh), 8.15 (d, 3J = 6.6 Hz, 1H, Arg-NH), 8.00 (t, 3J = 5.9 Hz, 1H, Gly-NH), 7.98 (d, 2H, Ph-H_{2,2'}), 7.89 (d, 3J = 8.0 Hz, 1H, Cys¹-NH), 7.58-7.55 (m, 2H, GuanidineNH, Ph-H₄), 7.49 (t, 2H, Ph-H_{3,3'}), 4.81 (m, 1H, *iso*Asp-H α), 4.54 (m, 2H, Cys^{1,2}-H α), 4.22 (m, 1H, Arg-H α), 4.01 (dd, 2J = 16.9 Hz, 3J = 7.1 Hz, 1H, Gly-H α), 3.64 (dd, 2J = 16.9 Hz, 3J = 4.8 Hz, Gly-H α'), 3.36 (m, 1H, *iso*Asp-H β), 3.13 (m, 2H, Arg-H δ'), 3.09 (dd, 2J = 14.3 Hz, 3J = 3.2 Hz, 1H, Cys²-H β), 2.87 (dd, 2J = 13.9 Hz, 3J = 10.8 Hz, 1H, Cys²-H β'), 2.83 (dd, 2J = 14.1 Hz, 3J = 10.9 Hz, 1H, *iso*Asp-H β'), 2.69 (dd, 2J = 13.8 Hz, 3J = 9.8 Hz, 1H, Cys¹-H β), 2.58 (dd, 2J = 13.7 Hz, 3J = 2.8 Hz, 1H, Cys¹-H β'), 1.76 (m, 1H, Arg-H β'), 1.63 (m, 1H, Arg-H β), 1.60 (m, 2H, Arg-H γ). **¹³C-NMR** (125.1 MHz, DMSO): δ = 172.0, 171.7, 171.4, 169.4, 169.3, 169.3, 166.4, 156.6, 133.8, 131.3, 128.2, 127.7, 55.1, 52.5, 50.7, 49.4, 41.5, 41.5, 40.4, 37.0, 28.6, 24.8. **HPLC** (10-50%, 30 min): t_R = 14.03 min. **MS** (ESI): m/z = 655.3 [$m+H^+$]⁺.

IV.3.135 Preparation of DGR-2C, 81



The title compound was synthesized on solid phase (TCP-resin, 300 mg, loading 0,71 mmol / g) according to the general procedures **GP12** (loading with Fmoc-Cys(Trt)-OH), **GP14** (Fmoc-deprotection) and **GP15** (Coupling). The linear, Fmoc deprotected peptide H-(Cys-Asp-Gly-Arg-Cys)-TCP was benzoylated with 3 eq. benzoyl chloride and 5 eq. DIEA in NMP for 30 min. After washing with DCM (five times), the linear peptide was cleaved and deprotected (**GP20**) and precipitated in diethyl ether. Cyclization was achieved according to **GP22**, the solvents were removed and the crude peptide purified by *reverse phase* HPLC. Yield was 9 mg (12 μ mol, 5%) of a colorless solid (TFA salt).

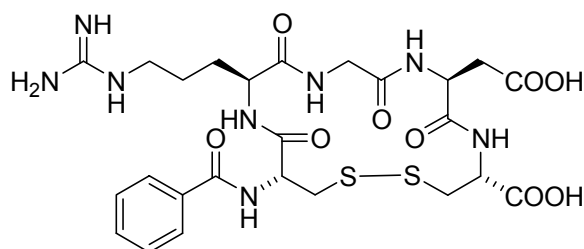
¹H-NMR (500 MHz, DMSO): δ = 8.80 (d, 3J = 7.2 Hz, 2H, -CONH), 8.16 (bs, 1H, guanidineNH), 7.90 (d, J = 7.4 Hz, 3H, Ph-H2,2'+ -CONH), 7.69 (d, 3J = 7.5 Hz, 1H, -CONH), 7.56 (t, J = 7.3 Hz, 1H, Ph-H4), 7.49 (t, J = 7.5 Hz, 2H, Ph-H3,3'), 7.30-6.90 (bs, 3H, guanidineNH), 4.58 (m, 1H, H α), 4.46 (m, 2H, H α), 4.33 (m, 1H, H α), 4.23 (dd, 2J = 16.6 Hz, 1H, Gly-H α), 3.44 (d, 2J = 16.5 Hz, 1H, Gly-H α'), 3.18-3.10 (m, 5H, H β + Arg-H δ), 2.78 (m, 1H, H β), 1.91 (m, 1H, Arg-H β), 1.64 (m, 1H, Arg-H β'), 1.51 (m, 2H, Arg-H γ). **HPLC** (10-50%, 30 min): t_R = 16.19 min. **MS** (ESI): m/z = 655.3 [m+H $^+$] $^+$.

IV.3.136 Preparation of NGR-2C, 82

The title compound was synthesized on solid phase (TCP-resin, 300 mg, loading 0,71 mmol / g) according to the general procedures **GP12** (loading with Fmoc-Cys(Trt)-OH), **GP14** (Fmoc-deprotection) and **GP15** (Coupling). The linear, Fmoc deprotected peptide H-(Cys-Asn-Gly-Arg-Cys)-TCP was benzoylated with 3 eq. benzoyl chloride and 5 eq. DIEA in NMP for 30 min. After washing with DCM (five times), the linear peptide was cleaved and deprotected (**GP20**) and precipitated in diethyl ether. Cyclization was achieved according to **GP22**, the solvents were removed and the crude peptide purified by *reverse phase* HPLC. Yield was 21 mg (27 μ mol, 13%) of a colorless solid (TFA salt), which rearranged on standing in solution to **80** and **81**.

HPLC (10-50%, 30 min): t_R = 14.96 min. **MS** (ESI): m/z = 654.3 [m+H $^+$] $^+$.

IV.3.137 Preparation of RGD-2C, 83



C₂₅H₃₄N₈O₉S₂
Exact Mass: 654.19
Mol. Wt.: 654.72

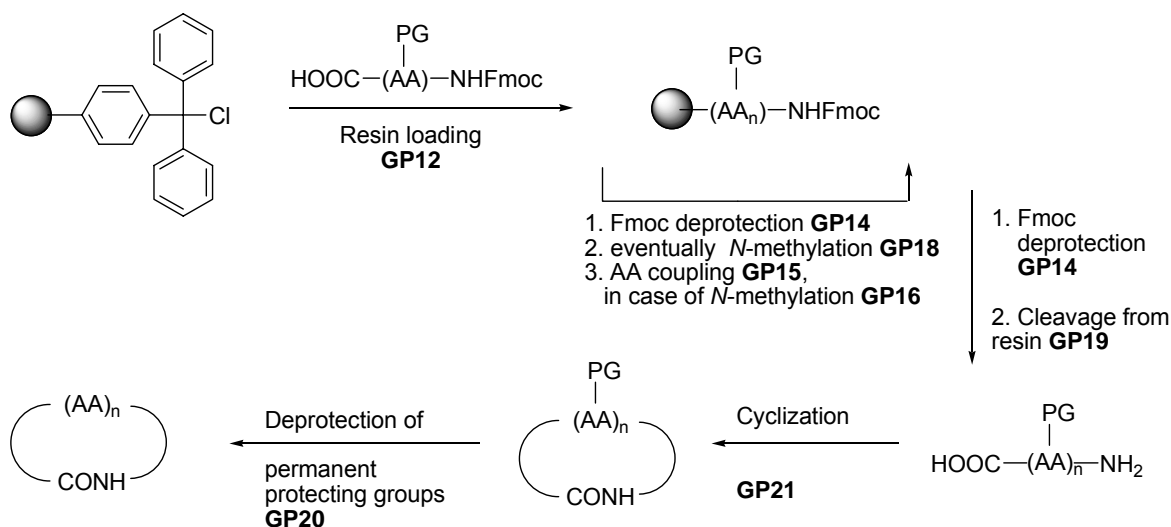
IV. Experimental Section

The title compound was synthesized on solid phase (TCP-resin, 300 mg, loading 0,71 mmol / g) according to the general procedures **GP12** (loading with Fmoc-Cys(Trt)-OH), **GP14** (Fmoc-deprotection) and **GP15** (Coupling). The linear, Fmoc deprotected peptide H-(Cys-Arg-Gly-Asp-Cys)-TCP was benzoylated with 3 eq. benzoyl chloride and 5 eq. DIEA in NMP for 30 min. After washing with DCM (five times), the linear peptide was cleaved and deprotected (**GP20**) and precipitated in diethyl ether. Cyclization was achieved according to **GP22**, the solvents were removed and the crude peptide purified by *reverse phase* HPLC. Yield was 15 mg (20 μ mol, 9%) of a colorless solid (TFA salt).

¹H-NMR (500 MHz, DMSO): δ = 8.72 (d, 3J = 7.0 Hz, 1H, PhCONH), 8.62 (bs, 1H, CONH), 8.03 (bs, 1H, CONH), 8.11 (d, 3J = 5.6 Hz, 1H, CONH), 7.88 (d, J = 7.3 Hz, 2H, Ph-*H*2,2'), 7.86 (m, 1H, CONH), 7.56 (t, 3J = 7.3 Hz, 1H, Ph-*H*4), 7.48 (t, 3J = 7.5 Hz, 2H, Ph-*H*3,3'), 7.48 (m, 1H, ^{guanidine}NH), 7.40-6.60 (bs, 3H, ^{guanidine}NH), 4.78 (m, 1H, *H* α), 4.62 (m, 1H, *H* α), 4.37 (m, 1H, *H* α), 4.29 (m, 1H, *H* α), 4.18 (dd, 2J = 16.5 Hz, 3J = 7.9 Hz, 1H, Gly-*H* α), 3.45 (dd, 2J = 16.1 Hz, 3J = 2.6 Hz, 1H, Gly-*H* α '), 3.27 (m, 1H, *H* β), 3.19-3.09 (m, 4H, *H* β , Arg-*H* δ), 2.81 (dd, 2J = 15.9 Hz, 3J = 4.9 Hz, 1H, *H* β), 1.89 (m, 1H, Arg-*H* β), 1.53-1.42 (m, 3H, Arg-*H* β ' + Arg-*H* γ).

HPLC (10-50%, 30 min): t_R = 14.51 min. **MS** (ESI): m/z = 655.3 [$m+H^+$]⁺.

IV.4 Preparation of Cyclic Peptides

Scheme IV-1. Synthesis of cyclic peptides *P1-25*.

The linear peptides were synthesized on TCP-resin (100-200 mg) according to the general procedures **GP12** (loading), **GP14** (Fmoc-deprotection), **GP15** (Coupling) and **GP19** (cleavage). First amino acid was Fmoc-D-Cys(Trt)-OH in every case. The linear, side-chain protected peptides were cyclized according to **GP21** and deprotected (**GP20**). The final deprotection step required mild conditions (47.5% TFA, 47.5% DCM, 2.5% TIPS, 2.5% water) to avoid ^tBu-alkylation of the tryptophane / cysteine. The crude peptides were purified by preparative *reverse phase* HPLC.

Table IV-1. Amino acid building blocks used for solid phase synthesis

Code	Amino acid	MW	Code	Amino acid	MW
A	Fmoc-Ala-OH	311.33	H	Fmoc-His(Trt)-OH	619.71
C	Fmoc-Cys(Trt)-OH	585.71	N	Fmoc-Gln(Trt)-OH	610.70
D	Fmoc-Asp(O ^t Bu)-OH	411.45	S	Fmoc-Ser(Trt)-OH	569.45
E	Fmoc-Glu(O ^t Bu)-OH	425.47	W	Fmoc-Trp(Boc)-OH	526.58
F	Fmoc-Phe-OH	387.43	Y	Fmoc-Tyr-OH	403.43

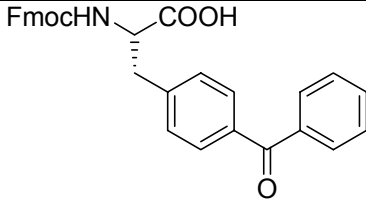
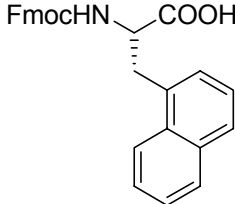
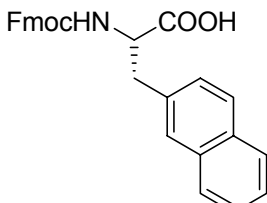
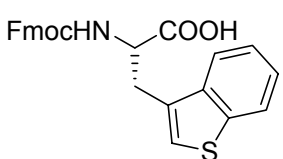
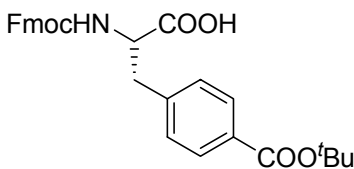
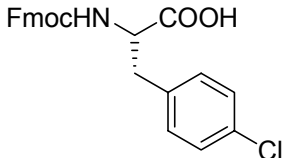
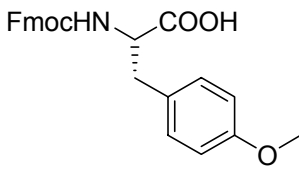
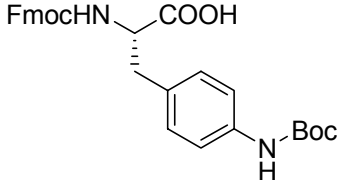
Analytical data of the prepared peptides are presented in Table IV-2.

IV. Experimental Section

Table IV-2. Analytical data of the Ala-scan peptides and the reference compounds.

Code	Sequence	ESI-MS m/z = [M+H] ⁺	HPLC t _R (10-50%), 30 min	Molecular formula	Yield [%]
P1	<i>cyclo</i> (-F-s-W-E-Y-C-)	816.4	25.55 min	C ₄₀ H ₄₅ N ₇ O ₁₀ S MW = 815.89	4.5
P2	<i>cyclo</i> (-F-S-W-E-Y-c-)	816.3	25.47 min	C ₄₀ H ₄₅ N ₇ O ₁₀ S MW = 815.89	5.8
P3	<i>cyclo</i> (-A-S-W-E-Y-c-)	740.4	24.37 min	C ₃₄ H ₄₁ N ₇ O ₁₀ S MW = 739.80	7.2
P4	<i>cyclo</i> (-F-A-W-E-Y-c-)	800.4	24.95 min	C ₄₀ H ₄₅ N ₇ O ₉ S MW = 799.89	11.3
P5	<i>cyclo</i> (-F-S-A-E-Y-c-)	701.6	25.40 min	C ₃₂ H ₄₀ N ₆ O ₁₀ S MW = 700.76	12.1
P6	<i>cyclo</i> (-F-S-W-A-Y-c-)	758.3	24.72 min	C ₃₈ H ₄₃ N ₇ O ₈ S MW = 757.86	4.3
P7	<i>cyclo</i> (-F-S-W-E-A-c-)	724.5	19.78 min	C ₃₄ H ₄₁ N ₇ O ₉ S MW = 723.8	5.1
P8	<i>cyclo</i> (-A-s-W-E-Y-C-)	740.3	17.58 min	C ₃₄ H ₄₁ N ₇ O ₁₀ S MW = 739.80	6.7
P9	<i>cyclo</i> (-F-a-W-E-Y-C-)	800.3	21.65 min	C ₄₀ H ₄₅ N ₇ O ₉ S MW = 799.89	7.7
P10	<i>cyclo</i> (-F-s-A-E-Y-C-)	701.3	17.36 min	C ₃₂ H ₄₀ N ₆ O ₁₀ S MW = 700.76	10.8
P11	<i>cyclo</i> (-F-s-W-A-Y-C-)	758.3	21.60 min	C ₃₈ H ₄₃ N ₇ O ₈ S MW = 757.86	6.1
P12	<i>cyclo</i> (-F-s-W-E-A-C-)	724.3	24.24 min	C ₃₄ H ₄₁ N ₇ O ₉ S MW = 723.80	7.4

Table IV-3. *Unnatural amino acid building blocks.*

Code	Name	Building block structure	MW
Bpa	Benzoylphenylalanine		491.53
1Na	1-Naphtylalanine		437.49
2Na	2-Naphtylalanine		437.49
Bta	Benzo[<i>b</i>]thiophenylalanine		443.51
4Cp	4-Carboxyphenylalanine		487.54
4Clp	4-Chlorophenylalanine		421.87
Mt	O-Methyltyrosine		417.45
4Ap	4-Aminophenylalanine		506.56

IV. Experimental Section

The series of compounds **P13-P25**, in which the most important amino acids of the sequence were replaced by mostly unnatural amino acids were synthesized in an analogue way (Scheme IV-1) using following building blocks (Table IV-3).

The analytical data of the prepared peptides is shown in Table IV-4.

Table IV-4. Analytical data of peptides **P13-25**.

Code	Sequence	ESI-MS m/z = [M+H ⁺] ⁺	HPLC t _R (10-50%), 30 min	Molecular formula	Yield [%]
P13	<i>cyclo</i> (-Y-S-W-E-Y-c-)	832.3		C ₄₀ H ₄₅ N ₇ O ₁₁ S MW = 831.89	2.9
P14	<i>cyclo</i> (-Bpa-S-W-E-Y-c-)	920.4	28.17 min	C ₄₇ H ₄₉ N ₇ O ₁₁ S MW = 920.00	5.4
P15	<i>cyclo</i> (-F-S-H-E-Y-c-)	767.3	19.66 min	C ₃₅ H ₄₂ N ₈ O ₁₀ S MW = 766.82	2.6
P16	<i>cyclo</i> (-F-S-1Na-E-Y-c-)	827.3	29.22 min	C ₄₂ H ₄₆ N ₆ O ₁₀ S MW = 826.91	5.8
P17	<i>cyclo</i> (-F-S-2Na-E-Y-c-)	827.4	29.16 min	C ₄₂ H ₄₆ N ₆ O ₁₀ S MW = 826.91	4.7
P18	<i>cyclo</i> (-F-S-Bta-E-Y-c-)	833.3	28.82 min	C ₄₀ H ₄₄ N ₆ O ₁₀ S ₂ MW = 832.94	3.2
P19	<i>cyclo</i> (-F-S-Bpa-E-Y-c-)	881.4	26.71 min	C ₄₅ H ₄₈ N ₆ O ₁₁ S MW = 880.96	3.5
P20	<i>cyclo</i> (-F-S-W-N-Y-c-)	815.4	24.61 min	C ₄₀ H ₄₆ N ₈ O ₉ S MW = 814.91	2.2
P21	<i>cyclo</i> (-F-S-W-D-Y-c-)	802.3	23.48 min	C ₃₉ H ₄₃ N ₇ O ₁₀ S MW = 801.86	3.6
P22	<i>cyclo</i> (-F-S-W-4Cp-Y-c-)	878.4	28.58 min	C ₄₅ H ₄₇ N ₇ O ₁₀ S MW = 877.96	3.2
P23	<i>cyclo</i> (-F-S-W-E-4Clp-c-)	835.4	32.32 min	C ₄₀ H ₄₄ ClN ₇ O ₉ S MW = 834.34	5.7
P24	<i>cyclo</i> (-F-S-W-E-Mt-c-)	830.4	29.66 min	C ₄₁ H ₄₇ N ₇ O ₁₀ S MW = 829.92	4.4
P25	<i>cyclo</i> (-F-S-W-E-4Ap-c-)	815.3	21.27 min	C ₄₀ H ₄₆ N ₈ O ₉ S MW = 814.91	3.7

The *N*-methylated peptides **P26-31** were prepared according to Scheme IV-1 starting from the amino acid prior to the *N*-methylated one. Despite the Fmoc-*N*-Me-Phe-OH, which has been synthesized before and was coupled as separate building block, all other amino acids were *N*-methylated on solid phase according to **GP18**. The following peptide coupling was performed with HOAt/HATU according to **GP16**. The analytical data is shown in Table IV-5.

Table IV-5. *N-Methyl scan of P2, MW of all peptides 829.92 (C₄₁H₄₇N₇O₁₀S).*

Code	Sequence	ESI-MS m/z = [M+H] ⁺	HPLC t _R (10-50%), 30 min	First amino acid
P26	<i>cyclo</i> (-F-S-W-E-Y-c-)	830.2	27.46 min	S
P27	<i>cyclo</i> (-F-S-W-E-Y-c-)	830.5	25.39 min	W
P28	<i>cyclo</i> (-F-S-W-E-Y-c-)	830.5	28.36 min	E
P29	<i>cyclo</i> (-F-S-W-E-Y-c-)	830.3	24.92 min	Y
P30	<i>cyclo</i> (-F-S-W-E-Y-c-)	830.4	29.20 min	c
P31	<i>cyclo</i> (-F-S-W-E-Y-c-)	830.4	24.04 min	F

IV.4.1 NMR-structure of P2

Table IV-6. *NMR of the cyclic peptide P2 (3 mg / 0.5 mL) at 300 K in d³-MeOH [Acquired on a Bruker DMX500 using a watergate pulse sequence] [213, 214a-c].*

Amino acid	chemical shifts [ppm]			
	H ^N	H ^α	H ^β	H ^γ /H ^{Ar}
Phe	8.80	4.88	3.44 / 2.78	7.26-7.25,
Ser	8.12	4.78	3.99 / 3.92	-
Trp	8.36	4.55	3.37	7.63, 7.37, 7.11, 7.06
Glu	8.02	4.17	1.59 / 1.81	1.82 / 1.91
Tyr	7.46	4.60	3.18 / 2.78	7.09, 6.73
Cys	8.48	4.09	2.64 / 2.56	-
		C ^α	C ^β	C ^γ /C ^{Ar}
Phe		55.4	37.4	
Ser		55.4	65.1	
Trp		57.4	27.4	
Glu		53.7	26.9	31.4
Tyr		55.1	39.1	
Cys		55.4	24.2	

IV. Experimental Section

Table IV-7. Restraints acquired from ROESY spectra of **P2** used in DG calculations. The distances were calibrated on the Phe-diastereotopic β -protons (1.80 Å).

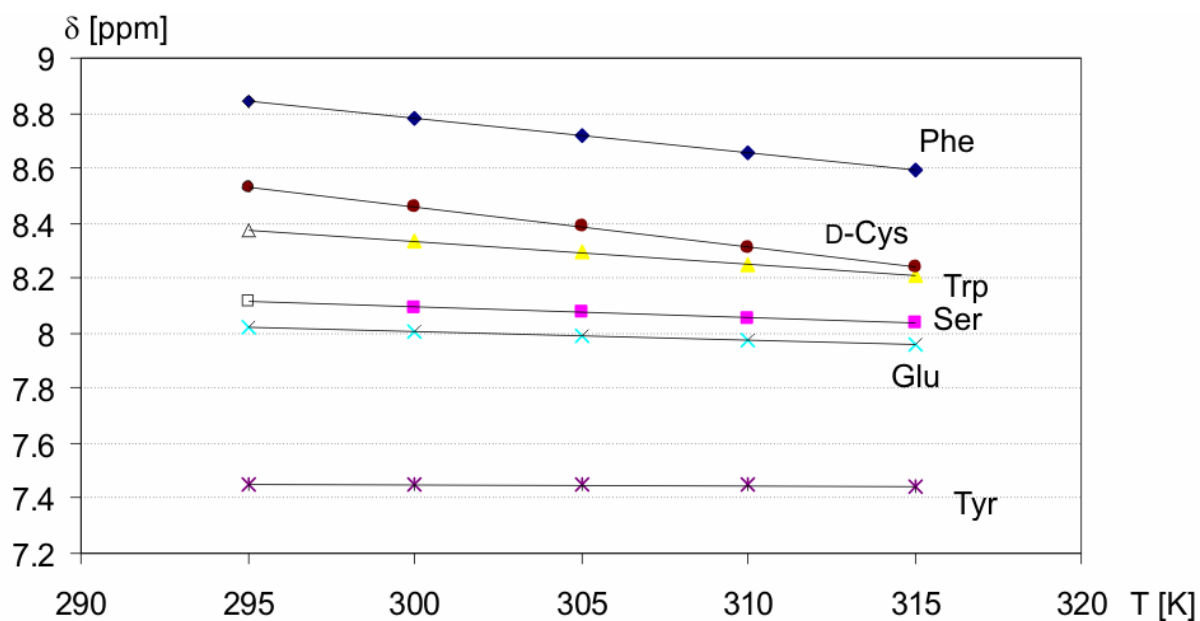
Distance [Å]					
Atom 1	Atom 2	ROE value	Min	Max	Average
Phe-H ^{β(proR)}	Phe-H ^{β(proS)}	-115.84	1.63	1.99	1.81
Phe-H ^N	Cys-H ^{α}	-61.66	1.80	2.20	2.00
Phe-H ^N	Ser-H ^N	-19.07	2.21	2.70	2.45
Ser-H ^N	Ser-H ^{α}	-13.25	2.34	2.86	2.60
Trp-H ^N	Ser-H ^{α}	-24.49	2.11	2.58	2.35
Trp-H ^N	Trp-H ^{α}	-14.96	2.29	2.80	2.55
Trp-H ^N	Trp-H ^{Ar(4)}	-12.46	2.36	2.88	2.62
Trp-H ^N	Glu-H ^N	-7.32	2.54	3.10	2.82
Glu-H ^N	Trp-H ^{α}	-3.14	3.01	3.68	3.35
Glu-H ^N	Glu-H ^{α}	-4.47	2.80	3.42	3.11
Glu-H ^N	Tyr-H ^N	-14.61	2.32	2.84	2.58
Tyr-H ^{β(proR)}	Tyr-H ^{β(proS)}	-120.21	1.61	1.97	1.79
Tyr-H ^N	Tyr-H ^{α}	-15.73	2.28	2.78	2.53
Tyr-H ^N	Glu-H ^{α}	-10.25	2.44	2.98	2.71
Cys-H ^N	Tyr-H ^{α}	-21.22	2.15	2.62	2.38
Cys-H ^N	Cys-H ^{α}	-13.44	2.34	2.86	2.60
Cys-H ^N	Tyr-H ^N	3.43	3.09	3.78	3.44

Table IV-8. Relevant couplings in the ¹H-NMR of **P2**.

Amino Acid	³ J(H ^{α} ,H ^N)	³ J(H ^{α} ,H ^{β(proR)})	³ J(H ^{α} ,H ^{β(proS)})	² J(H ^{β} ,H ^{β'})
Phe	9.3	11.3	4.3	15.1
Ser	8.5	11.3	4.5	16.0
Trp	4.1	-	-	-
Glu	8.8	-	-	-
Tyr	9.3	11.3	4.3	14.6
D-Cys	4.9	-	-	-

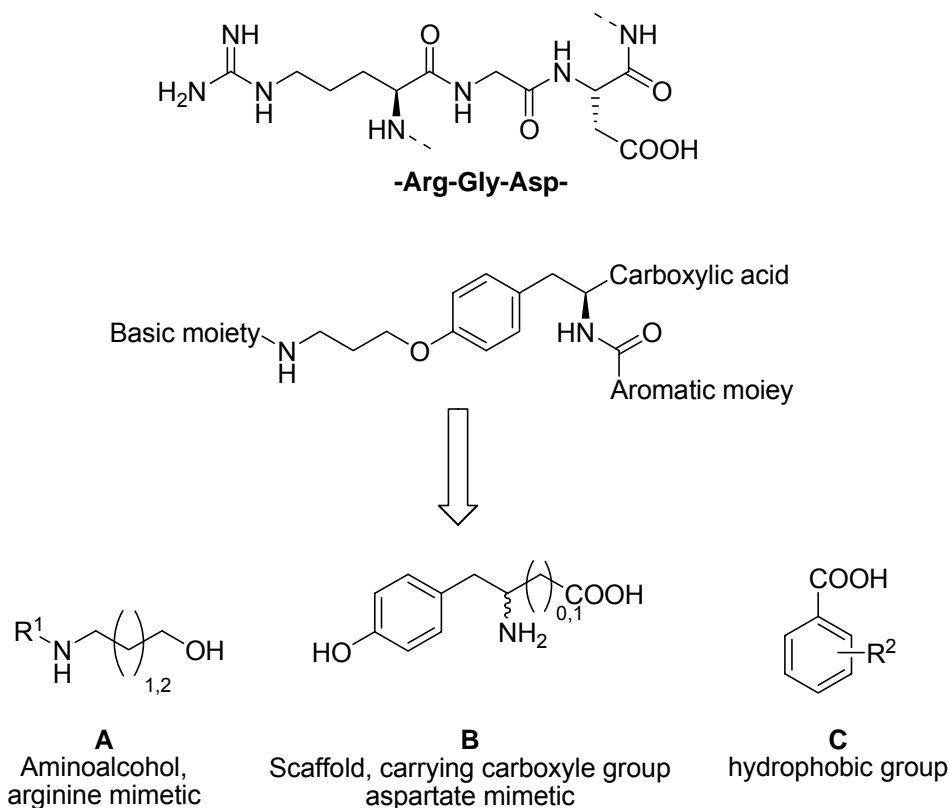
Table IV-9. Temperature dependence of H^N -signals of **P2**.

Temperatur [K]	chem. shift H^N [ppm]					
	Phe	Ser	Trp	Glu	Tyr	Cys
295	8.84447	8.11463	8.37529	8.02019	7.45102	8.53424
300	8.78294	8.09455	8.33341	8.00524	7.45017	8.46160
305	8.71756	8.07574	8.29196	7.99114	7.44803	8.38725
310	8.65346	8.05523	8.25051	7.9749	7.44718	8.31333
315	8.59193	8.03643	8.21077	7.95866	7.44632	8.24154
$d\delta / dT$ [ppb/K]	-12.7	-3.9	-8.2	-3.1	-0.2	-14.7

**Figure IV-1.** Plot of H^N -temperature coefficients of **P2** (d^3 -MeOH).

V. Summary

The scope of this work was the rational design of $\alpha 5\beta 1$ -selective integrin ligands based on a homology model which has been created in our group. The scaffold of choice was tyrosine, which has already been used successfully in the integrin field as inhibitor of $\alpha \text{IIb}\beta 3$ integrin and which provides essential features such as easy accessibility and high variability.



Scheme V-1. Design of tyrosine based integrin ligands.

The biological assays (ELISA) were performed by *Grit Zahn* at the Jerini AG, Berlin.

Comparison of the homology model of $\alpha 5\beta 1$ with the crystal structure of $\alpha \nu\beta 3$ revealed two hot spot mutations which could be utilized to induce selectivity for either $\alpha \nu\beta 3$ or $\alpha 5\beta 1$: A carboxamide bearing a 2,6-dimethyl substituted phenyl ring occupies a hydrophobic pocket in the $\alpha 5\beta 1$ integrin, which is blocked in $\alpha \nu\beta 3$ by an arginine residue. The introduction of a hydrogen bond acceptor at position 4 finally gave a sub-nanomolar binder for $\alpha 5\beta 1$ with >300 fold selectivity against $\alpha \nu\beta 3$ (**23k**).

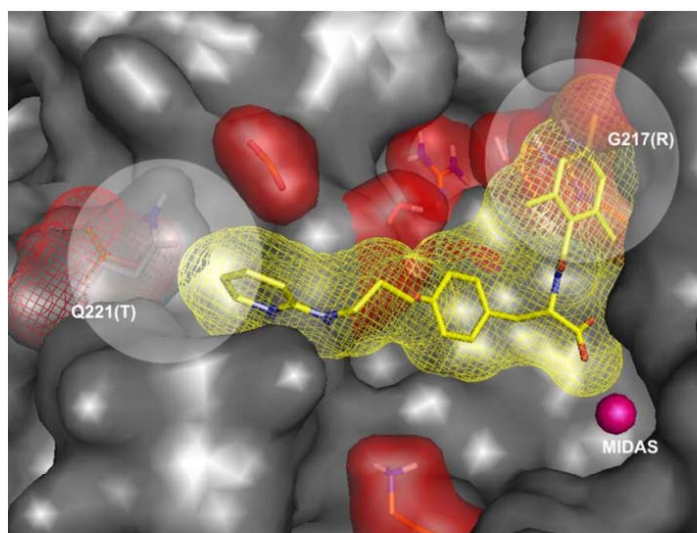
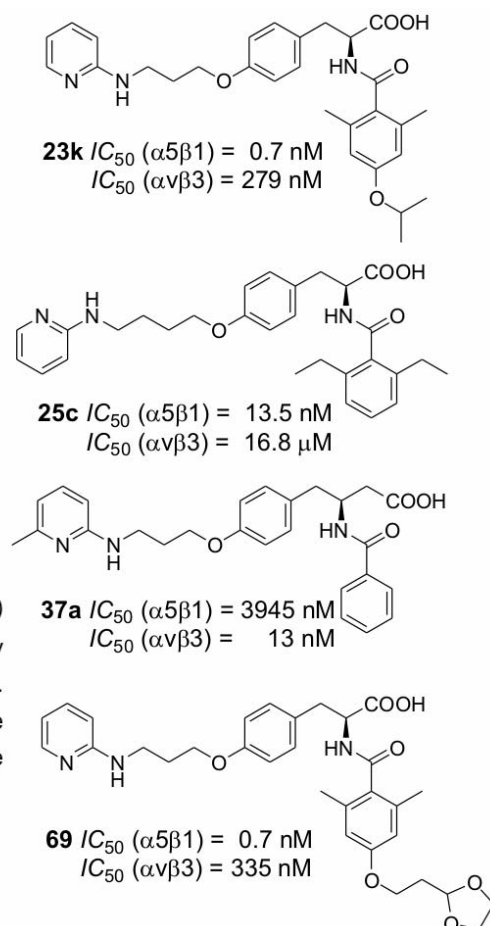
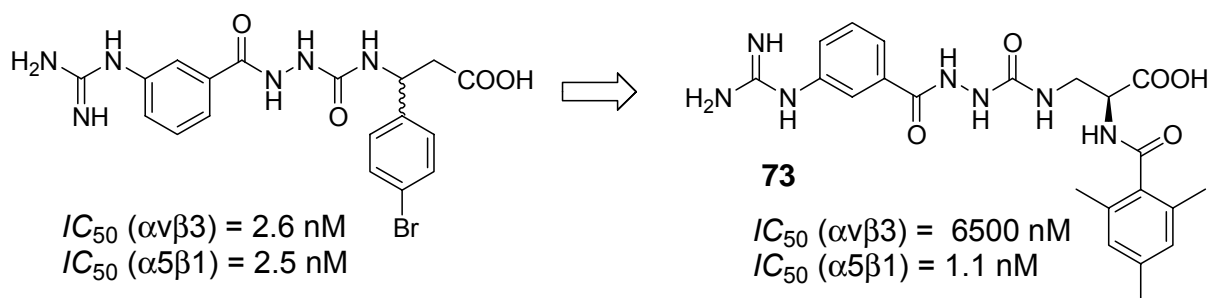


Figure V.1: Superposition of the Connolly surface of $\alpha5\beta1$ (grey) and $\alpha v\beta3$ (red). The two hot-spots important for ligand selectivity are highlighted. The MIDAS metal is shown as purple sphere. Four selected ligands with different activities and selectivities are shown on the right; compound **69** bears a protected aldehyde group as attachment point for linkers.



The switch from the α - to the longer β -tyrosine scaffold combined with a sterical more demanding aminopyridine moiety resulted in a nanomolar $\alpha v\beta3$ ligand with 300 fold selectivity against $\alpha5\beta1$ (**37a**). By careful evaluation of ligand length, basic moiety and variation of aromatic moiety, the selectivity against $\alpha v\beta3$ could be enhanced to >1000 fold (**25c**). All attempts to enhance selectivity by introduction of restraints into the tyrosine such as α -methylation and cyclization to tetrahydroisochinoline derivatives resulted in more or less inactive compounds. Furthermore, the insights obtained by the extensive SAR study of tyrosine based ligands were successfully applied on *aza*-glycine ligands, which were initially developed in our group as $\alpha v\beta3$ antagonists. Small, directed modifications of the *aza*-glycine scaffold resulted in new ligands with activities in the low nanomolar range and selectivities >6000, which make them the most selective $\alpha5\beta1$ ligands up to now (**73**).

V. Summary



Scheme V-2. Modifications of bisselective aza-glycine ligands towards highly $\alpha 5 \beta 1$ selective compounds.

In order to enable medical applications such as radiolabeling or surface coating, two approaches to attach linkers to the tyrosine scaffold were tested. The introduction of a protected aldehyde function on the aromatic moiety allowed oxime ligation of prosthetic groups under retention of both activity and selectivity (**69**). A serious issue for drug design is the bioavailability – a feature which is poor for most integrin ligands and still hampers their application as drugs. The substitution of the carboxylic moiety by a hydroxamic acid could improve the ADME parameters and may lead to orally available compounds if the receptor affinity is not affected by this modification. Preliminary studies *in vitro* demonstrate that the $\alpha v \beta 3$ affinity is not affected by hydroxamic acids. Further *in vitro* / *in vivo* studies are currently ongoing. The synthesized compounds exhibiting different selectivities on the integrins $\alpha 5 \beta 1$ and $\alpha v \beta 3$ can be used as a toolkit for the biochemical evaluation of the function of both integrins. Four ligands were used to study the role of $\alpha 5 \beta 1$ and $\alpha v \beta 3$ in the process of fibronectin fibrillogenesis in mouse fibroblasts. In experiments performed by Michael Leiss in the group of Reinhard Fässler at the Max-Planck-Institut für Biochemie, Martinsried, the ligands helped to prove the hypothesis, that fibronectin assembly can occur via a non-RGD dependent pathway mediated by $\alpha v \beta 3$. Furthermore, it could be proven for the first time that the small-molecule integrin binders serve as antagonists for their targets and are unable to trigger FAK-mediated signal transduction.

As second topic, different screening methods were used in order to optimize a cyclic hexapeptide sequence for affinity chromatography of blood coagulation factor VIII. The sequence was obtained by stepwise truncation of a linear octapeptide performed by Sebastian Knör, followed by cyclization and D-amino acid scan. The resulting two

best sequences *cyclo*(FsWEYC) (**P1**) and *cyclo*(FSWEYc) (**P2**) were subjected to an alanine scan to identify the most important residues. For the most active sequence *cyclo*(FSWEYc), a mutagenesis study with >10 variations of the amino acid side chains mostly yielded less active peptides. In contrast, an *N*-methyl scan performed on **P2** resulted in two peptides with enhanced activity. Furthermore, the solution structure of **P2** was solved using NMR, DG and MD techniques. The cyclic peptides can be used as affinity ligands for FVIII, where they should be superior compared to the linear peptide or antibodies due to their enhanced proteolytic stability and easier preparation. The solution structure may contribute to the identification of the binding epitope on FVIII and enable structure based optimization of the ligands.

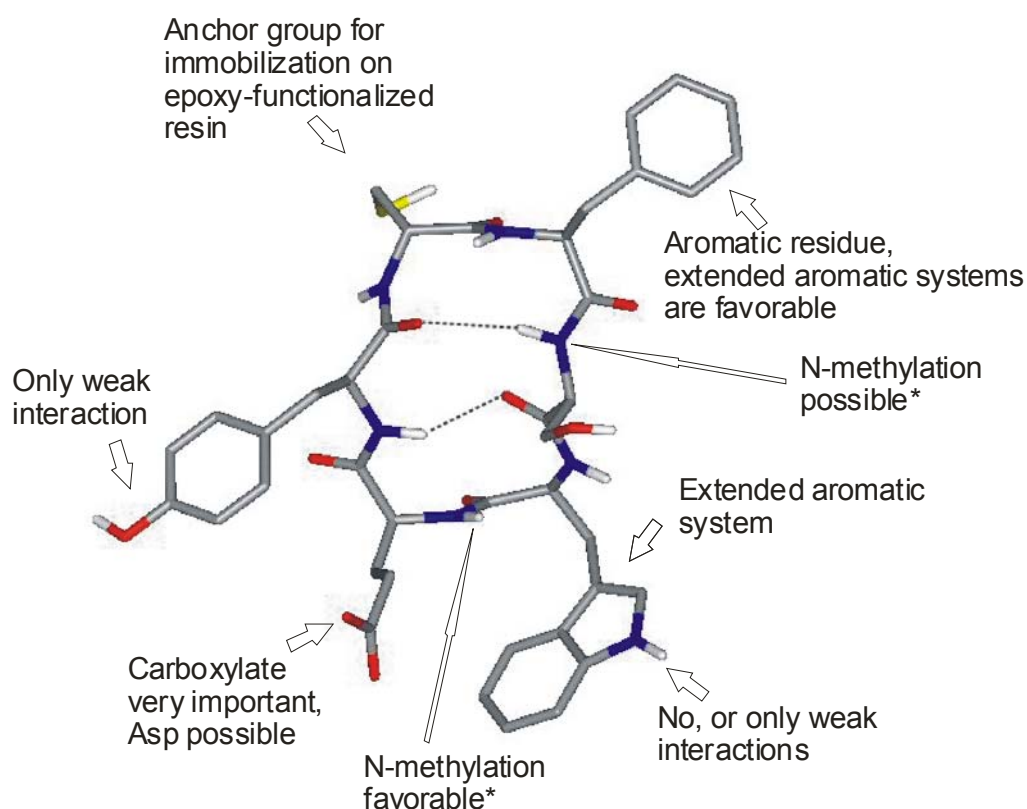


Figure V-2. Summary of pharmacophoric groups and possible modifications for the cyclic peptide *cyclo*(-FSWEYc-), **P2**.

VI. References

- [1] F. Bedürftig, *Geschichte der Apotheke Von der magischen Heilkunst zur modernen Pharmazie*, Fackelträger Verlag, Köln, **2005**.
- [2] E. Fischer, *Chem. Ber.* **1894**, 27, 2985.
- [3] P. Ehrlich, *Chem. Ber.* **1909**, 42, 17.
- [4] C. M. Dobson, *Nature* **2004**, 432, 824.
- [5] O. Sijbren, Ricardo, L.E., Sanders, J.K.M, *Curr. Opin. Chem. Biol.* **2002**, 6, 321.
- [6] R. P. Hertzberg, Pope, A.J., *Curr. Opin. Chem. Biol.* **2000**, 4, 445.
- [7] J. Drews, *Drug Disc. Today* **1998**, 3, 491.
- [8] S. S. Wang, Matsueda, R. , Matsueda, G.R., *Pept. Chem.* **1982**, 19, 37.
- [9] R. B. Merrifield, Steward, J.M., *Nature* **1965**, 207, 522.
- [10] M. D. Matteucci, M. H. Caruthers, *J. Am. Chem. Soc.* **1981**, 103, 3185.
- [11] R. L. Letsinger, J. L. Finnan, G. A. Heavner, W. B. Lunsford, *J. Am. Chem. Soc.* **1975**, 97, 3278.
- [12] P. H. Seeberger, *Chem. Comm.* **2003**, 10, 1115.
- [13] F. Darvas, G. Dorman, L. G. Puskas, A. Bucsay, L. Urge, *Med. Chem. Res.* **2004**, 13, 643.
- [14] A. R. Dongre, G. Opiteck, W. L. Cosand, S. A. Hefta, *Biopolymers* **2001**, 60, 206.
- [15] G. Schneider, U. Fechner, *Nat. Rev. Drug Discov.* **2005**, 4, 649.
- [16] G. Schneider, H. J. Böhm, *Drug Discov. Today* **2002**, 7, 64.
- [17] P. D. Lyne, *Drug Discov. Today* **2002**, 7, 1047.
- [18] A. Hillisch, L. F. Pineda, R. Hilgenfeld, *Drug Discov. Today* **2004**, 9, 659.
- [19] M. R. Arkin, J. A. Wells, *Nat. Rev. Drug Discov.* **2004**, 3, 575.
- [20] T. R. Gadek, R. S. McDowell, *Biochem. Pharmacol.* **2003**, 65, 1.
- [21] P. L. Toogood, *J. Med. Chem.* **2002**, 45, 1543.
- [22] G. Schmidt, *Top. Curr. Chem.* **1986**, 136, 109.
- [23] D. T. Krieger, *Science* **1983**, 222, 975.
- [24] A. Giannis, *Angew. Chem. Int. Ed.* **1993**, 32, 1244.
- [25] J. Gante, *Angew. Chem. Int. Ed.* **1994**, 33, 1699.
- [26] H. Kessler, *Angew. Chem. Int. Ed.* **1982**, 21, 512.

- [27] M. Gurrath, G. Müller, H. Kessler, M. Aumailley, R. Timpl, *Eur. J. Biochem.* **1992**, *210*, 911.
- [28] M. Aumailley, M. Gurrath, G. Müller, J. Calvete, R. Timpl, H. Kessler, *FEBS Lett.* **1991**, *291*, 50.
- [29a] T. Weide, A. Modlinger, H. Kessler, *Top. Curr. Chem.* **2007**, *1*.
- [29b] H. Kessler, B. Kutscher, *Liebigs Ann. Chem.* **1986**, *5*, 869.
- [29c] H. Kessler, B. Kutscher, A. Klein, *Liebigs Ann. Chem.* **1986**, *5*, 993.
- [29d] H. Kessler, B. Kutscher, *Liebigs Ann. Chem.* **1986**, *5*, 914.
- [29e] H. Kessler, R. Gratias, G. Hessler, M. Gurrath, G. Müller, *Pure & Appl. Chem.* **1996**, *68*, 1201.
- [30] R. Haubner, D. Finsinger, H. Kessler, *Angew. Chem. Int. Ed.* **1997**, *36*, 1374.
- [31] M. M. Shemyakin, Y. A. Ovchinnikov, V. T. Ivanov, *Angew. Chem. Int. Ed.* **1969**, *8*, 492.
- [32] J. Wermuth, S. L. Goodman, A. Jonczyk, H. Kessler, *J. Am. Chem. Soc.* **1997**, *119*, 1328.
- [33] H. Kessler, B. Diefenbach, D. Finsinger, A. Geyer, M. Gurrath, S. L. Goodman, G. Hölzemann, R. Haubner, A. Jonczyk, G. Müller, E. G. vonRoedern, J. Wermuth, *Lett. Pept. Sci.* **1995**, *2*, 155.
- [34] C. Gilon, M. A. Dechantsreiter, F. Burkhart, A. Friedler, H. Kessler, in *Houben-Weyl: Methods of Organic Chemistry, Vol. E 22c* (Ed.: A. F. M. Goodmann, L. Moroder, C. Toniolo), Thieme Verlag, Stuttgart, New York, **2003**, pp. 215.
- [35] R. K. Turker, M. M. Hall, M. Yamamoto, C. S. Sweet, F. M. Bumpus, *Science* **1972**, *177*, 1203.
- [36] M. A. Dechantsreiter, E. Planker, B. Marthä, E. Lohof, G. Hölzemann, A. Jonczyk, S. L. Goodman, *J. Med. Chem.* **1999**, *42*, 3033.
- [37] S. Nakanishi, A. Inoue, T. Kita, M. Nakamura, A. C. Chang, S. N. Cohen, S. Numa, *Nature* **1979**, *278*, 423.
- [38] E. J. Simon, J. M. Hiller, in *Basic Neuroscience* (Eds.: G. J. Siegel, B. W. Agranoff, R. W. Albers, P. B. Molinoff), Elsevier, Amsterdam, **1989**, p. 271.
- [39] J. Boer, D. Gottschling, A. Schuster, B. Holzmann, H. Kessler, *Angew. Chem. Int. Ed.* **2001**, *40*, 3870.
- [40] R. Hirschmann, *Angew. Chem. Int. Ed.* **1991**, *30*, 1278.

- [41] H. J. Böhm, *Nachr. Chem. Tech. Lab.* **1993**, *41*, 711.
- [42] C. Hansch, P. P. Maloney, T. Fujita, *Nature* **1962**, *194*, 178.
- [43] C. A. Lipinski, F. Lombardo, B. W. Dominy, P. J. Feeney, *Adv. Drug Deliv. Rev.* **1997**, *23*, 3.
- [44] C. A. Lipinski, F. Lombardo, B. W. Dominy, P. J. Feeney, *Adv. Drug Deliv. Rev.* **2001**, *46*, 3.
- [45] D. F. Veber, S. R. Johnson, H. Y. Cheng, B. R. Smith, K. W. Ward, K. D. Kopple, *J. Med. Chem.* **2002**, *45*, 2615.
- [46] G. C. Alghisi, C. Rüegg, *Endothelium* **2006**, *13*, 113.
- [47] R. Burke, *Int. Rev. Cytology* **1999**, *191*, 257.
- [48] M. D. Pierschbacher, E. Ruoslahti, *Nature* **1984**, *309*, 30.
- [49] R. Pytela, M. D. Pierschbacher, E. Ruoslahti, *Cell* **1985**, *40*, 191.
- [50] R. Pytela, M. D. Pierschbacher, E. Ruoslahti, *PNAS* **1985**, *82*, 5766.
- [51] E. F. Plow, T. A. Haas, L. Zhang, J. Loftus, J. W. Smith, *J. Biol. Chem.* **2000**, *275*, 21785.
- [52] C. M. Isacke, M. A. Horton, *The Adhesion Molecule Facts Book*, Academic Press, London, **2000**.
- [53] S. Suzuki, W. S. Agraves, R. Pytela, H. Arai, T. Krusius, M. D. Pierschbacher, E. Ruoslahti, *PNAS* **1986**, *83*, 8614.
- [54] J. W. Tamkun, D. W. DeSimone, D. Fonda, R. S. Patel, C. Buck, A. F. Horwitz, R. O. Hynes, *Cell* **1986**, *46*, 271.
- [55] H. Jin, J. Varner, *Brit. J. Cancer* **2004**, *90*, 561.
- [56] H. Yusuf-Makagiansar, M. E. Anderson, T. V. Yakovleva, J. S. Murray, T. J. Siahaan, *Med. Res. Rev.* **2002**, *22*, 146.
- [57] A. I. Rojas, H. Ahmed, *Criti. Rev. Oral Biol. M.* **1999**, *10*, 337.
- [58] K. J. Clemetson, J. M. Clemetson, *Cell. Mol. Life Sci.* **1998**, *54*, 502.
- [59] M. J. Humphries, *Biochem. Soc. Trans.* **2000**, *28*, 311.
- [60] M. V. Nemet, N. M. Green, P. Eason, S. S. Yamada, K. M. Yamada, *EMBO J.* **1988**, *7*.
- [61] J. P. Xiong, T. Stehle, B. Diefenbach, R. Zhang, R. Dunker, D. Scott, A. Joachimiak, S. L. Goodman, M. A. Arnaout, *Science* **2001**, *294*, 339.
- [62] J. P. Xiong, T. Stehle, R. Zhang, A. Joachimiak, M. Frech, S. L. Goodman, M. A. Arnaout, *Science* **2002**, *296*, 151.

-
- [63] P. Bork, T. Doerks, T. A. Springer, B. Snel, *Trends Biochem. Sci.* **1999**, *24*, 261.
- [64] R. C. Liddington, M. Ginsberg, *J. Cell Biol.* **2002**, *158*, 833.
- [65] J. O. Lee, P. Rieu, M. A. Arnaout, R. Liddington, *Cell* **1995**, *80*, 631.
- [66] T. Xiao, J. Takagi, B. S. Coller, J. H. Wang, T. A. Springer, *Nature* **2004**, *432*, 59.
- [67] D. F. Legler, G. Wiedle, F. P. Ross, B. A. Imhof, *J. Cell Sci.* **2001**, *114*, 1545.
- [68] A. P. Mould, M. J. Humphries, *Nature* **2004**, *432*, 27.
- [69] B. D. Adair, M. Yeager, *PNAS* **2002**, *99*, 14059.
- [70] P. E. Hughes, F. Diaz-Gonzalez, L. Leong, C. Wu, J. A. McDonald, S. J. Shattil, M. H. Ginsberg, *J. Biol. Chem.* **1996**, *271*, 6571.
- [71] R. Li, N. Mitra, H. Gratkowski, G. Vilaire, R. Litvinov, C. Nagasami, J. W. Weisel, J. D. Lear, W. F. DeGrado, J. S. Bennett, *Science* **2003**, *300*, 795.
- [72] R. Li, C. R. Babu, J. D. Lear, A. J. Wand, J. S. Bennett, W. F. DeGrado, *PNAS* **2001**, *98*, 12462.
- [73] K.-E. Gottschalk, H. Kessler, *Structure* **2004**, *12*, 1109.
- [74] D. Schneider, D. M. Engelman, *J. Biol. Chem.* **2004**, *279*, 9840.
- [75] G. Müller, M. Gurrath, H. Kessler, *J. Comp.-Aid. Mol. Des.* **1994**, *8*.
- [76] J. A. Eble, K. Kühn, *Integrin-Ligand Interaction*, Springer-Verlag, Heidelberg, **1997**.
- [77] R. Pankov, K. M. Yamada, *J. Cell Sci.* **2002**, *115*, 3861.
- [78] R. R. Potts, I. D. Campbell, *Curr. Opin. Cell Biol.* **1994**, *6*, 648.
- [79] D. F. Mosher, *Curr. Opin. Struc. Biol.* **1993**, *3*, 214.
- [80] C. Gibson, G. A. G. Sulyok, D. Hahn, S. L. Goodman, G. Hölzemann, H. Kessler, *Angew. Chem. Int. Ed.* **2001**, *40*, 165.
- [81] S. L. Goodman, G. Hölzemann, G. A. G. Sulyok, H. Kessler, *J. Med. Chem.* **2002**, *45*, 1045.
- [82] J. H. Hutchinson, W. Halczenko, K. M. Brashear, M. J. Breslin, P. J. Coleman, T. Duong le, M. Fernandez-Metzler, M. A. Gentile, J. E. Fisher, D. G. Hartman, J. R. Huff, D. B. Kimmel, C. T. Leu, R. S. Meissner, K. Merkle, R. Nagy, B. Pennypacker, J. J. Perkins, T. Prueksaritanont, G. A. Rodan, S. L. Varga, A. Wesolowski, A. E. Zartman, S. B. Rodan, M. E. Duggan, *J. Med. Chem.* **2003**, *46*.

- [83] G. D. Hartman, M. S. Egbertson, W. Halczenko, W. L. Laswell, M. E. Duggan, R. L. Smith, A. M. Naylor, P. D. Manno, R. J. Lynch, G. Zhang, C. T.-C. Chang, R. J. Gould, *J. Med. Chem.* **1992**, *35*, 4640.
- [84] J. J. Marugán, C. Manthey, B. Anaclerio, L. Lafrance, T. Lu, T. Markotan, K. A. Leonard, C. Crysler, E. Eisennagel, M. Dasgupta, B. Tomczuk, *J. Med. Chem.* **2005**, *48*, 926.
- [85] J. M. Smallheer, C. A. Weigelt, F. J. Woerner, J. S. Wells, W. F. Daneker, S. A. Mousa, R. R. Wexler, P. K. Jadhav, *Bioorg. Med. Chem. Lett.* **2004**, *14*.
- [86] E. Mutschler, G. Geisslinger, K. H.K., M. Schäfer-Korting, *Arzneimittelwirkungen: Lehrbuch der Pharmakologie und Toxikologie*, Wissenschaftliche Verlagsgesellschaft mbH, Stuttgart, **2001**.
- [87] L. Marinelli, K.-E. Gottschalk, A. Meyer, E. Novellino, H. Kessler, *J. Med. Chem.* **2004**, *47*, 4166.
- [88] A. Meyer, Technical University Munich (Munich), **2006**.
- [89] L. Marinelli, A. Meyer, D. Heckmann, A. Lavecchia, E. Novellino, H. Kessler, *J. Med. Chem.* **2005**, *48*, 4204.
- [90] J. Takagi, T. Kamata, J. Meredith, M. Puzon-McLaughlin, Y. Takada, *J. Biol. Chem.* **1997**, *272*, 19794.
- [91] T. Arndt, U. Arndt, U. Reuning, H. Kessler, *Cancer Ther. Molecular Targets in Tumor-Host Interactions* (Editor: G. F. Weber), Horizon Bioscience, Norfolk, **2005**, 93-141.
- [92] M. Karin, Y. Cao, F. R. Greten, Z.-W. Li, *Nat. Rev. Cancer* **2002**, *2*, 301.
- [93] D. A. Cheresh, D. G. Stupack, *Nat. Med.* **2002**, *8*, 193.
- [94] K. A. Reesquist, E. Ross, E. A. Koop, R. M. Wolthuis, F. J. Zwartkruis, Y. van Kooyk, M. Salmon, C. D. Buckley, J. L. Bos, *J. Cell Biol.* **2000**, *148*, 1151.
- [95] Z. Zhang, K. Vuori, H. Wang, J. C. Reed, E. Ruoslahti, *Cell* **1996**, *85*, 61.
- [96] F. Diaz-Gonzalez, J. Forsyth, B. Steiner, M. H. Ginsberg, *Mol. Biol. Cell* **1996**, *7*, 1939.
- [97] J. Folkman, *Nat. Med.* **1995**, *1*, 17.
- [98] B. Eliceiri, D. A. Cheresh, *J. Clin. Invest.* **1999**, *103*, 1227.
- [99] J. Folkman, *New Engl. J. Med.* **1971**, *285*, 1182.
- [100] J. Folkman, *Sem. Oncology* **2002**, *29*, 15.
- [101] G. C. Tucker, *Curr. Opin. Invest. Drugs* **2003**, *4*, 722.

- [102] J. S. Kerr, A. M. Slee, S. A. Mousa, *Exp. Opin. Invest. Drugs* **2002**, *11*, 1765.
- [103] D. A. Cheresh, R. C. Spiro, *J. Biol. Chem.* **1987**, *262*, 17703.
- [104] R. Haubner, R. Gratias, B. Diefenbach, S. L. Goodman, A. Jonczyk, H. Kessler, *J. Am. Chem. Soc.* **1996**, *118*, 7461.
- [105] P. C. Brooks, A. M. Montgomery, M. Rosenfeld, R. A. Reisfeld, T. Hu, G. Klier, D. A. Cheresh, *Cell* **1994**, *79*, 1157.
- [106] B. Eliceiri, R. Klemke, S. Strömblad, D. A. Cheresh, *J. Cell Biol.* **1998**, *140*, 1255.
- [107] M. Scatena, M. Almeida, M. L. Chaisson, N. Fausto, R. F. Nicosia, C. M. Giachelli, *J. Cell Biol.* **1998**, *141*, 1083.
- [108] S. Stromblad, J. C. Becker, M. Yebra, P. C. Brooks, D. A. Cheresh, *J. Clin. Invest.* **1996**, *98*, 426.
- [109] D. G. Stupack, X. S. Puente, S. Boutsaboualoy, C. M. Storgard, D. A. Cheresh, *J. Cell Biol.* **2001**, *155*, 459.
- [110] T. V. Byzova, C. K. Goldman, N. Pampori, K. A. Thomas, A. Bett, S. J. Shattil, E. F. Plow, *Mol. Cell* **2000**, *6*, 851.
- [111] B. L. Bader, H. Rayburn, D. Crowley, R. O. Hynes, *Cell* **1998**, *95*, 507.
- [112] D. Taverna, H. Moher, D. Crowley, L. Borsig, A. Vaki, R. O. Hynes, *PNAS* **2004**, *101*, 763.
- [113] L. E. Reynolds, L. Wyder, J. C. Lively, D. Taverna, S. D. Robinson, X. Huang, D. Sheppard, R. O. Hynes, K. Hodivala-Dilke, *Nat. Med.* **2002**, *8*, 27.
- [114] R. O. Hynes, *Nat. Med.* **2002**, *8*, 918.
- [115] K. O. Simon, E. M. Nutt, D. G. Abraham, G. A. Rodan, L. T. Duong, *J. Biol. Chem.* **1997**, *272*, 29380.
- [116] S. Kim, M. Bakre, H. Yin, J. A. Varner, *J. Clin. Invest.* **2002**, *110*, 933.
- [117] S. Kim, K. Bell, S. A. Mousa, J. A. Varner, *Am. J. Path.* **2000**, *156*, 1345.
- [118] S. Kim, M. Harris, J. A. Varner, *J. Biol. Chem.* **2000**, *275*, 33920.
- [119] P. H. Bolton-Maggs, K. J. Pasi, *Lancet* **2003**, *361*, 1801.
- [120] L. Stryer, *Biochemie*, Spektrum der Wissenschaft Verlagsgesellschaft mbH, Heidelberg, **1990**.
- [121] P. J. Lenting, J. A. van Mourik, K. Mertens, *Blood* **1998**, *92*, 3983.
- [122] G. A. Vehar, B. Keyt, D. Eaton, H. Rodriguez, D. P. O'Brien, F. Rotblat, H. Oppermann, R. Keck, W. I. Wood, R. N. Harkins, et al., *Nature* **1984**, *312*, 337.

- [123] W. I. Wood, D. J. Capon, C. C. Simonsen, D. L. Eaton, J. Gitschier, B. Keyt, P. H. Seeburg, D. H. Smith, P. Hollingshead, K. L. Wion, et al., *Nature* **1984**, *312*, 330.
- [124] W. Wang, Y. J. Wang, D. N. Kelner, *Int. J. Pharm.* **2003**, *259*, 1.
- [125] P. J. Fay, *Thromb. Haemost.* **1993**, *70*, 63.
- [126] J. E. Sadler, *Annu. Rev. Biochem.* **1998**, *67*, 395.
- [127] R. J. Kaufman, L. C. Wasley, A. J. Dorner, *J. Biol. Chem.* **1988**, *263*, 6352.
- [128] B. G. Boedeker, *Transfus. Med. Rev.* **1992**, *6*, 256.
- [129] H. Schwinn, M. Stadler, D. Josic, F. Bal, W. Gehringer, I. Nur, R. Schutz, *Arzneimittelforschung* **1994**, *44*, 188.
- [130] P. M. Mannucci, A. Gringeri, M. Cattaneo, *Res. Clin. Lab.* **1990**, *20*, 227.
- [131] D. Josic, H. Schwinn, M. Stadler, A. Strancar, *J. Chromatogr. B Biomed. Appl.* **1994**, *662*, 181.
- [132] T. Burnouf, M. Burnouf-Radosevich, J. J. Huart, M. Goudemand, *Vox Sang.* **1991**, *60*, 8.
- [133] E. Berntorp, *Ann. Hematol.* **1994**, *68 Suppl 3*, S35.
- [134] O. Mejan, V. Fert, M. Delezay, M. Delaage, R. Cheballah, A. Bourgois, *Thromb. Haemost.* **1988**, *59*, 364.
- [135] D. N. Fass, G. J. Knutson, J. A. Katzmann, *Blood* **1982**, *59*, 594.
- [136] K. Amatschek, R. Necina, R. Hahn, E. Schallaun, H. Schwinn, D. Josic, A. Jungbauer, *J. High. Res. Chromatogr.* **2000**, *23*, 47.
- [137] C. Henry, N. Moitessier, Y. Chapleur, *Mini Rev. Med. Chem.* **2002**, *2*, 531.
- [138] B. L. Bader, H. Rayburn, D. Crowley, R. O. Hynes, *Cell* **1998**, *95*, 507.
- [139] K. S. Kim, L. G. Qian, *Tetrahedron Lett.* **1993**, *34*, 7195.
- [140] O. Mitsunobu, M. Yamada, Mukaiyam.T, *Bull. Chem. Soc. Jap.* **1967**, *40*, 935.
- [141] O. Mitsunobu, *Synthesis* **1981**, 1.
- [142] T. Tsunoda, S. Ito, *J. Syn. Org. Chem. Jpn.* **1997**, *55*, 631.
- [143] A. Trejo, H. Arzeno, M. Browner, S. Chanda, S. Cheng, D. D. Comer, S. A. Dalrymple, P. Dunten, J. Lafargue, B. Lovejoy, J. Freire-Moar, J. Lim, J. McIntosh, J. Miller, E. Papp, D. Reuter, R. Roberts, F. Sanpablo, J. Saunders, K. Song, A. Villasenor, S. D. Warren, M. Welch, P. Weller, P. E. Whiteley, L. Zeng, D. M. Goldstein, *J. Med. Chem.* **2003**, *46*, 4702.
- [144] K. C. Lee, D. Y. Chi, *J. Org. Chem.* **1999**, *64*, 8576.
- [145] D. Yoo, J. S. Oh, D.-W. Lee, Y. G. Kim, *J. Org. Chem.* **2003**, *68*, 2979.

- [146] D. G. Batt, J. J. Petraitis, G. C. Houghton, D. P. Modi, G. A. Cain, M. H. Corjay, S. A. Mousa, P. J. Bouchard, M. S. Forsythe, P. P. Harlow, F. A. Barbera, S. M. Spitz, R. R. Wexler, P. K. Jadhav, *J. Med. Chem.* **2000**, *43*, 41.
- [147] G. Müller, M. Gurrath, H. Kessler, *J. Comp.-Aid. Mol. Des.* **1994**, *8*, 709.
- [148] M. E. Duggan, L. T. Duong, J. E. Fisher, T. G. Hamill, W. F. Hoffman, J. R. Huff, N. C. Ihle, C. T. Leu, R. M. Nagy, J. J. Perkins, S. B. Rodan, G. Wesolowski, D. B. Whitman, A. E. Zartman, G. A. Rodan, G. D. Hartman, *J. Med. Chem.* **2000**, *43*, 3736.
- [149] D. Seebach, P. E. Ciceri, M. Overhand, B. Jaun, D. Rigo, *Helv. Chim. Acta* **1996**, *79*, 2043.
- [150] J. Cesar, M. Sollner-Dolenc, *Tetrahedron Lett.* **2001**, *42*, 7099.
- [151] A. E. Zartman, L. T. Duong, C. Fernandez-Metzler, G. D. Hartman, C. T. Leu, T. Prueksaritanont, G. A. Rodan, S. B. Rodan, M. E. Duggan, R. S. Meissner, *Bioorg. Med. Chem. Lett.* **2005**, *15*, 1647.
- [152] W. H. Miller, P. J. Manley, R. D. Cousins, K. F. Erhard, D. A. Heerding, C. Kwon, S. T. Ross, J. M. Samanen, D. T. Takata, I. N. Uzinskas, C. C. K. Yuan, R. C. Haltiwanger, C. J. Gress, M. W. Lark, S. M. Hwang, I. E. James, D. J. Rieman, R. N. Willette, T. L. Yue, L. M. Azzarano, K. L. Salyers, B. R. Smith, K. W. Ward, K. O. Johanson, W. F. Huffman, *Bioorg. Med. Chem. Lett.* **2003**, *13*, 1483.
- [153] C. Dahmen, J. Auernheimer, A. Meyer, A. Enderle, S. L. Goodman, H. Kessler, *Angew. Chem. Int. Ed.* **2004**, *43*, 6649.
- [154] R. Haubner, H. J. Wester, R. Senekowitsch-Schmidtke, B. Diefenbach, G. Stöcklin, H. Kessler, M. Schwaiger, *J. Nucl. Med.* **1997**, *38*, 814.
- [155] L. Peterlin-Masic, D. Kikelj, *Tetrahedron* **2001**, *57*, 7073.
- [156] K. Verschuren, G. Toth, D. Tourwé, M. Lebl, G. Van Binst, V. J. Hruby, *Synthesis* **1992**, *5*, 458.
- [157] T. Kawabata, J. Y. Chen, H. Suzuki, K. Fuji, *Synthesis* **2005**, 1368.
- [158] T. Kawabata, S. P. Kawakami, S. Shimada, K. Fuji, *Tetrahedron* **2003**, *59*, 965.
- [159] U. Hersel, C. Dahmen, H. Kessler, *Biomaterials* **2003**, *24*, 4385.

- [160] R. Haubner, H. J. Wester, U. Reuning, R. Senekowitsch-Schmidtke, B. Diefenbach, H. Kessler, G. Stöcklin, M. Schwaiger, *J. Nucl. Med.* **1999**, *40*, 1061.
- [161] D. J. Burkhart, B. T. Kalet, M. P. Coleman, G. C. Post, T. H. Koch, *Mol. Cancer Ther.* **2004**, *3*, 1593.
- [162] J. Auernheimer, D. Zukowski, C. Dahmen, M. Kantlehner, A. Enderle, S. L. Goodman, H. Kessler, *ChemBioChem* **2005**, *6*, 2034.
- [163] R. Haubner, W. A. Weber, A. J. Beer, E. Vabuliene, D. Reim, M. Sarbia, K. F. Becker, M. Goebel, R. Hein, H. J. Wester, H. Kessler, M. Schwaiger, *PLoS Med.* **2005**, *2*, 244.
- [164] S. Biltresse, M. Attolini, G. Dive, A. Cordi, G. C. Tucker, J. Marchand-Brynaert, *Bioorg. Med. Chem.* **2004**, *12*, 5379.
- [165] D. A. Morley, *Tetrahedron Lett.* **2000**, *41*, 7405.
- [166] D. A. Morley, *Tetrahedron Lett.* **2000**, *41*, 7401.
- [167] M. Mergler, R. Nyfeler, J. Gosteli, *Tetrahedron Lett.* **1989**, *30*, 6741.
- [168] J. W. Corbett, N. R. Graciani, S. A. Mousa, W. F. DeGrado, *Bioorg. Med. Chem. Lett.* **1997**, *7*, 1371.
- [169] M. K. Schwarz, D. Tumelty, M. A. Gallop, *J. Org. Chem.* **1999**, *64*, 2219.
- [170] J. Wermuth, PhD thesis, Technical University (Munich), **1996**.
- [171] J. S. Schmitt, PhD thesis, Technical University (Munich), **1998**.
- [172] J. Gante, H. Kessler, C. Gibson, in *Houben-Weyl: Methods of Organic Chemistry, Vol. E 22c* (Ed.: A. F. M. Goodman, L. Moroder, C. Toniolo), Thieme Verlag, Stuttgart, New York, **2003**, pp. 311.
- [173] A. S. Dutta, J. S. Morley, *J. Chem. Soc. Perkin Trans. 1* **1975**, 1712.
- [174] G. A. Sulyok, C. Gibson, S. L. Goodman, G. Hölzemann, M. Wiesner, H. Kessler, *J. Med. Chem.* **2001**, *44*, 1938.
- [175] D. Craig, M. Gao, K. Schulten, V. Vogel, *Structure* **2004**, *12*, 2049.
- [176] C. Gibson, Technical University of Munich (Munich), **2000**.
- [177] T. Arndt, PhD Thesis, Technical University of Munich (Munich), **2003**.
- [178] B. Kurzak, H. Kozłowski, E. Farkas, *Coordin. Chem. Rev.* **1992**, *114*, 169.
- [179] S. S. Tam, D. H. Lee, E. Y. Wang, D. G. Munroe, C. Y. Lau, *J. Biol. Chem.* **1995**, *270*, 13948.
- [180] M. Arnold, D. A. Brown, O. Deeg, W. Errington, W. Haase, K. Herlihy, T. J. Kemp, H. Nimir, R. Werner, *Inorg. Chem.* **1998**, *37*, 2920.

- [181] N. Nishino, J. C. Powers, *Biochemistry* **1979**, *18*, 4340.
- [182] W. M. Wise, W. W. Brandt, *J. Am. Chem. Soc.* **1955**, *77*, 1058.
- [183] R. Fässler, M. Meyer, *Genes Dev.* **1995**, *9*, 1896.
- [184] C. Brakebusch, R. Grose, F. Quondamatteo, A. Ramirez, J. L. Jorcano, A. Pirro, M. Svensson, R. Herken, T. Sasaki, R. Timpl, S. Werner, R. Fässler, *Embo J.* **2000**, *19*, 3990.
- [185] A. Aszodi, E. B. Hunziker, C. Brakebusch, R. Fässler, *Genes Dev.* **2003**, *17*, 2465.
- [186] S. Gruner, M. Prostedna, V. Schulte, T. Krieg, B. Eckes, C. Brakebusch, B. Nieswandt, *Blood* **2003**, *102*, 4021.
- [187] U. H. von Andrian, B. Engelhardt, *N. Engl. J. Med.* **2003**, *348*, 68.
- [188] M. Schwander, M. Leu, M. Stumm, O. M. Dorchies, U. T. Rugg, J. Schittny, U. Müller, *Dev. Cell* **2003**, *4*, 673.
- [189] P. J. Stroeken, E. A. van Rijthoven, M. A. van der Valk, E. Roos, *Cancer Res.* **1998**, *58*, 1569.
- [190] C. Brakebusch, K. Wennerberg, H. W. Krell, U. H. Weidle, A. Sallmyr, S. Johansson, R. Fässler, *Oncogene* **1999**, *18*, 3852.
- [191] C. Brakebusch, R. Fässler, *Cancer Metastasis Rev.* **2005**, *24*, 403.
- [192] S. Takahashi, M. Leiss, M. Moser, T. Ohashi, D. Heckmann, A. Pfeifer, J. Takagi, H. Kessler, H. P. Erickson, R. Fässler, *J. Biol. Chem.* **2007**, *submitted*.
- [193] F. Curnis, R. Longhi, L. Crippa, A. Cattaneo, E. Dondossola, A. Bachi, A. Corti, *J. Biol. Chem.* **2006**, *281*, 36466.
- [194] J. Najbauer, J. Orpizewski, D. W. Aswad, *Biochemistry* **1996**, *35*, 5183.
- [195] M. V. Paranandi, A. W. Guzzetta, W. S. Hancock, D. W. Aswad, *J. Biol. Chem.* **1994**, *269*, 243.
- [196] N. E. Robinson, A. B. Robinson, *PNAS* **2001**, *98*, 944.
- [197] K. J. Reissner, D. W. Aswad, *Cell. Mol. Life Sci.* **2003**, *60*, 1281.
- [198] P. Di Matteo, F. Curnis, R. Longhi, G. Colombo, A. Sacchi, L. Crippa, M. P. Protti, M. Ponzoni, S. Toma, A. Corti, *Mol. Immunol.* **2006**, *43*, 1509.
- [199] N. E. Robinson, Z. W. Robinson, B. R. Robinson, A. L. Robinson, J. A. Robinson, M. L. Robinson, A. B. Robinson, *J. Pept. Res.* **2004**, *63*, 426.
- [200] A. Tonelli, *Biopolymers* **1976**, *15*, 1615.

- [201] R. H. Mazur, P. A. James, D. A. Tyner, E. A. Hallinan, J. H. Sanner, R. Schulze, *J. Med. Chem.* **1980**, *23*, 758.
- [202] H. Kessler, J. Chatterjee, E. Biron, V. J. Hruby, C. Gilon, D. Hoyer, D. Mierke, *J. Pept. Sci.* **2006**, *12*, 94.
- [203] P. Manavalan, F. A. Momany, *Biopolymers* **1980**, *19*, 1943.
- [204] E. Biron, H. Kessler, *J. Org. Chem.* **2005**, *70*, 5183.
- [205] R. M. Freidinger, J. S. Hinkle, D. S. Perlow, B. H. Arison, *J. Org. Chem.* **1983**, *48*, 77.
- [206] E. Biron, J. Chatterjee, H. Kessler, *Biopolymers* **2005**, *80*, 522.
- [207] J. Chatterjee, D. Mierke, H. Kessler, *J. Am. Chem. Soc.* **2006**, *128*, 15164.
- [208] G. Cardillo, L. Gentilucci, A. Tolomelli, C. Tomasini, *J. Org. Chem.* **1998**, *63*, 2351.
- [209] K. Barlos, D. Gatos, J. Kallitsis, G. Papaphotiu, P. Sotiriu, W. Q. Yao, W. Schäfer, *Tetrahedron Lett.* **1989**, *30*, 3943.
- [210] L. A. Carpino, G. Y. Han, *J. Org. Chem.* **1972**, *37*, 3404.
- [211] R. Knorr, A. Trzeciak, W. Bannwarth, D. Gillessen, *Tetrahedron Lett.* **1989**, *30*, 1927.
- [212] L. A. Carpino, *J. Am. Chem. Soc.* **1993**, *115*, 4397.
- [213] M. Liu, X. Mao, C. He, H. Huang, J. K. Nicholson, J. C. Lindon, *J. Magn. Reson.* **1998**, *132*, 125.
- [214a] A. G. Palmer III, J. Cavanagh, P. E. Wright, M. Rance, *J. Magn. Reson.* **1991**, *93*, 151.
- [214b] L. E. Kay, P. Keifer, T. Saarinen, *J. Am. Chem. Soc.* **1992**, *114*, 10663.
- [214c] J. Schleucher, M. Schwendinger, M. Sattler, P. Schmidt, O. Schedletsky, S. J. Glaser, O. W. Sorensen, C. Griesinger, *J. Biomol. NMR*, **1994**, *4*, 301.

CURRICULUM VITAE

Persönliche Daten

Name: Dominik Heckmann
Geburtsdatum / Geburtsort: 12.07.1977, 68519 Viernheim
Adresse (Universität): Institut für Organische Chemie und Biochemie,
Lehrstuhl II, Technische Universität München,
Lichtenbergstraße 4, D-85747 Garching

Adresse (privat): Belgradstraße 66a, 80804 München
Telephon / Fax: +49-89-289-13324 / +49-89-289-13210
Mobil: +49-160-1892692
E-mail: dominik.heckmann@ch.tum.de

Ausbildung

Sep. 1983 – Jul. 1987 Besuch der Pestalozzi Grundschule Weinheim
Aug. 1987 – Jul. 1996 Besuch des Werner-Heisenberg Gymnasiums
Weinheim
Jul. 1996 Allgemeinen Hochschulreife, Note 1.5
Sep. 1996 – Aug. 1997 Zivildienst im mobilen sozialen Dienst bei der Caritas
Weinheim
Okt. 1997 – Jul. 2002 Studium der Chemie an der Ruprecht-Kars- Universität
Heidelberg
Aug. 2002 – Mrz. 2003 Diplomarbeit unter der Betreuung von
Prof. G. Helmchen über die „Synthese beider
Enantiomeren einer Vorstufe des Isoprostaglandins A₂“
Apr. 2003 Diplom mit der Note 1.0
Seit Jul. 2003 Promotion an der TU Muenchen unter der Betreuung
von Prof. H. Kessler über die „Synthese selektiver
Liganden für das $\alpha 5\beta 1$ Integrin und die Entwicklung
zyklischer Peptide als Affinitätsliganden zur Reinigung
von Faktor VIII“

Praktika

Jul. 2001 – Sep. 2001 Bayer AG, Pharma-Forschungszentrum Wuppertal

Auslandsaufenthalt

Okt. 2000 – Apr. 2001 ERASMUS – Austauschprogramm mit der University of Bristol, UK

Publikationen

D. Heckmann, H. Kessler,
Design and Chemical Synthesis of Integrin Ligands
Methods in Enzymology **2007**, accepted.

D. Heckmann, A. Meyer, L. Marinelli, G. Zahn, R. Stragies, H. Kessler,
Probing Integrin Selectivity: Rational Design of Highly Active and Selective Ligands for the $\alpha 5\beta 1$ and $\alpha v\beta 3$ Integrin Receptor,
Angew. Chemie Int. Ed. **2007** online DOI: 10.1002/ange.200700008.

L. Marinelli, A. Meyer, D. Heckmann, A. Lavecchia, E. Novellino, H. Kessler,
Ligand Binding Analysis for Human $\alpha 5\beta 1$ Integrin Antagonists, *J. Med. Chem.* **2005**, 48(13), 4204-4207.

B. Luy, K. Kobzar, S. Knör, J. Furrer, D. Heckmann, H. Kessler.
Orientational Properties of Stretched Polystyrene Gels in Organic Solvents and the suppression of their residual 1H-NMR signals, *J. Am. Chem. Soc.* **2005**, 127(17), 6459-6465.

C. J. Freudenberger, S. Knör, K. Kobzar, D. Heckmann, T. Paululat, H. Kessler, B. Luy
Stretched poly(vinyl acetate) gels as NMR alignment media for the measurement of residual dipolar couplings in polar organic solvents, *Angew. Chemie Int. Ed.* **2005**, 44(3), 423-426.

Konferenzen

Sep. 2004 3rd International and 28th European Peptide Symposium, Prague, Tschechische Republik
Posterpräsentation: "Linear and Cyclic Peptides as Affinity Ligands for Factor VIII Purification"

Feb. 2006 50th Annual Meeting of the Society of Thrombosis and Haemostasis Research, Basel, Schweiz.
Posterpräsentation: "Linear and Cyclic Peptides as Affinity Ligands for Factor VIII Purification"

Mrz. 2007 8th German Peptide Symposium, Heidelberg
Posterpräsentation: "Rational Design of Selective $\alpha 5\beta 1/\alpha v\beta 3$ Integrin Ligands"

